



HAL
open science

Treatment of complex effluents and emerging contaminants by a compact Process coupling wet aiox oxidation with a biofilm reactor

Dan Feng

► **To cite this version:**

Dan Feng. Treatment of complex effluents and emerging contaminants by a compact Process coupling wet aiox oxidation with a biofilm reactor. Chemical and Process Engineering. Ecole Centrale Marseille, 2019. English. NNT : 2019ECDM0010 . tel-03042625

HAL Id: tel-03042625

<https://theses.hal.science/tel-03042625>

Submitted on 7 Dec 2020

HAL is a multi-disciplinary open access archive for the deposit and dissemination of scientific research documents, whether they are published or not. The documents may come from teaching and research institutions in France or abroad, or from public or private research centers.

L'archive ouverte pluridisciplinaire **HAL**, est destinée au dépôt et à la diffusion de documents scientifiques de niveau recherche, publiés ou non, émanant des établissements d'enseignement et de recherche français ou étrangers, des laboratoires publics ou privés.

**Laboratoire de Mécanique, Modélisation et Procédés Propres
UMR CNRS 7340**

École Doctorale – Sciences de l’environnement

ED251

N° attribué par la bibliothèque:

THÈSE DE DOCTORAT

pour obtenir le grade de

**DOCTEUR de l’ÉCOLE CENTRALE de MARSEILLE et AIX-MARSEILLE
UNIVERSITÉ**

Spécialité: Génie des procédés

TITRE DE LA THÈSE

**Traitement d’effluents complexes et de polluants
émergents par couplage d’un procédé d’OVH et d’un
procédé biologique**

Par

FENG Dan

**Directeur de thèse : BOUTIN Olivier
Co-directrice de thèse : SORIC Audrey**

Présentée le 6 Décembre 2019

devant le jury composé de :

M. Juan GARCIA SERNA	Professeur, Valladolid Université	Rapporteur
M. Jean Marc CHOUBERT	Directeur de Recherche, IRSTEA	Rapporteur
M. Eric SCHAER	Professeur, ENSIC	Examineur
Mme Laure MALLERET	Maître de conférences, Aix Marseille Université	Examinatrice
M. Olivier BOUTIN	Professeur, Aix Marseille Université	Directeur de thèse
Mme Audrey SORIC	Maître de conférences, Ecole Centrale Marseille	Co-directrice de thèse

Contents

<i>List of figures</i>	1
<i>List of tables</i>	5
<i>Abbreviations</i>	7
<i>Introduction</i>	11
Chapter 1 Bibliographical study.....	17
1.1 Background.....	19
1.1.1 Overview of emerging contaminants	19
1.1.2 Overview of glyphosate	22
1.2 Occurrence, behavior, and fate of glyphosate in aqueous environment	24
1.3 Treatment technology for glyphosate from environment	27
1.3.1 Adsorption.....	27
1.3.2 Filtration.....	28
1.3.3 Biological treatment.....	29
1.3.4 Advanced oxidation processes (AOPs).....	34
1.4 Wet air oxidation	41
1.4.1 WAO for single organic compounds treatment.....	42
1.4.2 WAO for real industrial wastewater treatment	42
1.4.3 Reaction mechanisms.....	44
1.4.4 Reaction kinetics for WAO.....	44
1.4.5 Mass transfer for WAO.....	46
1.5 Microfluidic device.....	47
1.6 Coupled advanced oxidation technology and biological treatment to treat emerging contaminants.....	48
1.7 Conclusions	52
Chapter 2 Bubble characterization and gas-liquid interfacial area in two phase gas-liquid system in bubble column at low Reynolds number and high temperature and pressure	55
2.1 Introduction	57
2.2 Experimental methods	62
2.2.1 Experimental setup.....	62
2.2.2 Data analysis	65
2.3 Results and discussion	66
2.3.1 Effect of superficial gas velocity.....	66
2.3.2 Effect of superficial liquid velocity.....	69

2.3.3	Effect of pressure	71
2.3.4	Effect of temperature	73
2.3.5	Effect of different liquid and gas phase	74
2.3.6	The correlation for average bubble size and gas holdup.....	76
2.4	Conclusion.....	78
Chapter 3	Kinetic study of glyphosate degradation by a wet air oxidation process.....	81
3.1	Introduction	83
3.2	Materials and methods.....	85
3.2.1	Chemicals.....	85
3.2.2	Experimental procedure	86
3.2.3	Analytical methods	87
3.3	Results and discussion	88
3.3.1	Glyphosate degradation.....	88
3.3.2	Kinetic modeling.....	90
3.3.3	Formation of byproducts.....	92
3.3.4	Proposed degradation pathway	95
3.4	Conclusions	96
Chapter 4	Oxidation of glyphosate by wet air oxidation using a microfluidic device	99
4.1	Introduction	101
4.2	Materials and methods.....	103
4.2.1	Chemicals.....	103
4.2.2	Microreactor fabrication.....	103
4.2.3	Evaluation of glyphosate degradation.....	104
4.2.4	Analytical methods	105
4.3	Results and discussion	106
4.3.1	Glyphosate degradation.....	106
4.3.2	TOC and COD reduction	108
4.3.3	The formation of byproducts.....	108
4.3.4	Modelling.....	109
4.4	Conclusions	110
Chapter 5	Acclimation of aerobic activated sludge to glyphosate biodegradation: experimental study and kinetics modelling	115
	Abstract.....	117
5.1	Introduction	117

5.2	Materials and methods.....	119
5.2.1	Chemicals.....	119
5.2.2	Acclimation process of activated sludge.....	119
5.2.3	Compared experiments between acclimated and non-acclimated sludge	120
5.2.4	Analytical methods	120
5.3	Results and discussion	123
5.3.1	Bacteria activity validation during acclimation process	123
5.3.2	Removal efficiency of glyphosate and TOC during acclimation process	125
5.3.3	Validation of the acclimation performances compared to fresh activated sludge.....	125
5.3.4	Kinetics of glyphosate biodegradation.....	127
5.4	Conclusion.....	132
Chapter 6	The removal of glyphosate from wastewater by a compact process combining wet air oxidation and biological treatment	135
6.1	Introduction	137
6.2	Materials and methods.....	139
6.2.1	Materials.....	139
6.2.2	Experimental set-up for WAO process	139
6.2.3	Experimental set-up for biological treatment process.....	140
6.2.4	Analytical procedures	141
6.3	Results and discussion	143
6.3.1	WAO pretreatment.....	143
6.3.2	Biological process	144
6.3.3	Combination of WAO and biological process	147
6.3.4	Identification and quantification of by-products.....	147
6.3.5	The degradation pathway of glyphosate	151
6.4	Conclusions	151
Chapter 7	Conclusions and Perspectives.....	153
7.1	Conclusions	155
7.2	Perspectives	156
References	157
<i>Annexe</i>	179

List of figures

Fig. 1.1 Schematic pathways for emerging contaminants from sources to receptors (Lapworth et al., 2012)	20
Fig. 1.2 The structure of glyphosate	22
Fig. 1.3 Inhibition process of shikimate acid pathway and inhibition role of glyphosate (Helander et al., 2012)	23
Fig. 1.4 Glyphosate use worldwide from 1994 to 2015 (in million kilograms) (from: “Glyphosate Market Share, Size - Industry Trends Report 2024,” n.d., “Glyphosate use worldwide 1994-2014 Statistic,” n.d.; “Glyphosate Market Analysis, Size, Share and Forecasts - 2022 MarketsandMarkets,” n.d.).....	24
Fig. 1.5 Glyphosate accumulation and transport in the environment (from Helander et al., 2012) ..	25
Fig. 1.6 Biodegradation pathways of glyphosate in microorganisms (Zhan et al., 2018).	30
Fig. 1.7 The possible oxidation pathway of glyphosate under different processes. Information based on (Barrett and McBride, 2005; Chen et al., 2007; Muneer and Boxall, 2008; Balci et al., 2009; Echavia et al., 2009; Manassero et al., 2010; Lan et al., 2013; Xing et al., 2018; Yang et al., 2018)	39
Fig. 1.8 Generalized lumped kinetic model (GLKM) for WAO of organic compounds (Li et al., 1991)	46
Fig. 2.1 Schematic diagram of experimental setup. 1 – gas tank; 2 – syringe used for liquid; 3 – liquid pump; 4 – gas pump; 5 – liquid purge; 6 – gas purge; 7 – liquid coil; 8 – gas coil; 9 – oven; 10 – bubble column; 11 – gas sparger; 12 – buffer tank; 13 – pressure limiter; 14 – liquid outlet; 15 – monitor; 16 – camera; 17 – lamp.	63
Fig. 2.2 Photograph (a) N ₂ -H ₂ O system, $U_G=0.083 \text{ cm.s}^{-1}$, $U_L=0.022 \text{ cm.s}^{-1}$, $T=373\text{K}$, $P=10\text{MPa}$; (b) N ₂ -H ₂ O system, $U_G=0.276 \text{ cm.s}^{-1}$, $U_L=0.022 \text{ cm.s}^{-1}$, $T=373\text{K}$, $P=10\text{MPa}$; (c) N ₂ -ethanol/water mixture system, $U_G=0.083 \text{ cm.s}^{-1}$, $U_L=0.022 \text{ cm.s}^{-1}$, $T=373\text{K}$, $P=10\text{MPa}$	66
Fig. 2.3 Bubble number distribution and number fraction under various superficial gas velocity and at $T=373\text{K}$, $P=10\text{MPa}$ and $U_L=0.022 \text{ cm.s}^{-1}$	67
Fig. 2.4 Bubble mean Sauter diameter (d_{32}), gas holdup (ϵ) and interfacial area (a) under various superficial gas velocity and pressure at $T=373\text{K}$ and $U_L=0.022\text{cm.s}^{-1}$	68
Fig. 2.5 Bubble mean Sauter diameter along the location of the column under various superficial gas velocity and pressure at $T=373\text{K}$ and $U_L=0.022\text{cm.s}^{-1}$	68
Fig. 2.6 Bubble number distribution along the location of the column under various superficial gas velocity at $T=373\text{K}$ and $P=10\text{Mpa}$	69

Fig. 2.7 Bubble number distribution and number fraction under various superficial liquid velocity at P=10MPa, T=373K and $U_G = 0.138\text{cm.s}^{-1}$	70
Fig. 2.8 Bubble mean Sauter diameter (d_{32}), gas holdup (ϵ) and interfacial area (a) under various superficial liquid velocity and temperature at P=10MPa and $U_G = 0.138\text{cm.s}^{-1}$	71
Fig. 2.9 Bubble number distribution and number fraction under different pressure at T=373K and $U_L = 0.022\text{cm.s}^{-1}$	71
Fig. 2.10 Bubble number distribution along the location of the column under three pressures at T=373 K, $U_G = 0.276\text{cm.s}^{-1}$ and $U_L = 0.022\text{cm.s}^{-1}$	72
Fig. 2.11 Bubble number distribution and number fraction under different temperature at P=10MPa and $U_G = 0.138\text{cm.s}^{-1}$	73
Fig. 2.12 Bubble number distribution and number fraction distribution under various liquid and gas phase at P=10MPa, T=373K, $U_L = 0.022\text{cm.s}^{-1}$ and $U_G = 0.138-0.276\text{cm.s}^{-1}$	74
Fig. 2.13 Bubble mean Sauter diameter (d_{32}), gas holdup (ϵ) and interfacial area (a) under various liquid and gas phase at P=10MPa, T=373K, $U_L = 0.022\text{cm.s}^{-1}$ and $U_G = 0.138-0.276\text{cm.s}^{-1}$	76
Fig. 2.14 Comparison of the Sauter mean diameter (left) and gas holdup (right) prediction with experimental data	78
Fig. 3.1 Schematic diagram of WAO setup using the batch reactor. 1 – air bottle; 2 – nitrogen bottle; 3 – gas purge; 4 – bursting disk; 5 – liquid injection; 6 – gas purge; 7 – stir; 8 – cooling water inlet; 9 – compressed air; 10 – cooling water outlet; 11 – heater; 12 – liquid sampling	86
Fig. 3.2 Effect of temperature on the glyphosate and TOC removal at 15 MPa.....	89
Fig. 3.3 Arrhenius plot for glyphosate oxidation	91
Fig. 3.4 Experimental and simulated concentration of glyphosate and generated AMPA concentration during the experimental process: (1) ■: Experimental glyphosate concentration at 423 K; (2) ●: Experimental glyphosate concentration at 473 K; (3) ▲: Experimental glyphosate concentration at 523 K; (4) Solid line (—): Simulated glyphosate concentration at 423 K (5) Dash line (---): Simulated glyphosate concentration at 473 K; (6) Dot line (···): Simulated glyphosate concentration at 523 K; (7) □: Experimental generated AMPA concentration at 423 K; (8) ○: Experimental generated AMPA concentration at 473 K; (9) △: Experimental generated AMPA concentration at 523 K.	92
Fig. 3.5 Glyphosate destruction, AMPA yield and P mass balance during oxidation process: (1) ■: glyphosate destruction; (2) ●: AMPA yield; (3) ▲: P mass balance	93
Fig. 3.6 AMPA degradation by WAO process under 523 K.	94
Fig. 3.7 The formation of glyoxylic acid in WAO degradation of glyphosate.	94
Fig. 3.8 A proposed degradation pathway of glyphosate by WAO process	96

Fig. 4.1 Schematic diagram of microreactor system. 1 – gas tank; 2 – syringe used for liquid; 3 – liquid pump; 4 – gas pump; 5 – liquid purge; 6 – gas purge; 7 – liquid coil; 8 – gas coil; 9 – oven; 10 – microfluidic device; 11 – liquid outlet;.....	104
Fig. 4.2 Effect of residence time on glyphosate removal through comparison between experiments and modeling results at 473 and 523 K.....	106
Fig. 4.3 Effect of residence time on pH values at 473 and 523 K.	107
Fig. 4.4 Effect of residence time on TOC and COD reduction at 473 and 523 K.	108
Fig. 4.5 AMPA yield and P mass balance under different residence time at 473 and 523 K.....	109
Fig. 5.1 MLSS concentration profile along the acclimation process	123
Fig. 5.2 pH values (a) and the removal efficiency of TOC (b) and glyphosate (c) with time in the third stage of the acclimation process: (1) □ 200 mg.L ⁻¹ glyphosate + 426 mg. L ⁻¹ glucose; (2) ○ 500 mg. L ⁻¹ glyphosate + 266 mg. L ⁻¹ glucose; (3) △ 1000 mg. L ⁻¹ glyphosate.....	124
Fig. 5.3 The removal efficiency of glyphosate (left) and TOC (right) with time: (1) ■ acclimated activated sludge at 500 mg.L ⁻¹ glyphosate; (2) ● non-acclimated activated sludge at 500 mg.L ⁻¹ glyphosate; (3) □ acclimated activated sludge at 1000 mg.L ⁻¹ glyphosate; (4) ○ non-acclimated activated sludge at 1000 mg.L ⁻¹ glyphosate.....	126
Fig. 5.4 Glyphosate and AMPA concentration and TOC reduction under three initial glyphosate concentration: (a) 200 mg.L ⁻¹ ; (b) 500 mg.L ⁻¹ ; (c) 1000 mg.L ⁻¹	128
Fig. 5.5 Time evolution of glyphosate concentration using Monod model and comparison with experimental data	130
Fig. 5.6 Proposed biodegradation pathway of glyphosate	132
Fig. 6.1 Schematic diagram of WAO setup using the batch reactor. 1 – air bottle; 2 – nitrogen bottle; 3 – gas purge; 4 – bursting disk; 5 – liquid injection; 6 – gas purge; 7 – stir; 8 – cooling water inlet; 9 – compressed air; 10 – cooling water outlet; 11 – heater; 12 – liquid sampling	140
Fig. 6.2 A proposed degradation pathway of glyphosate by the integrated WAO-biological treatment	151

List of tables

Table 1.1 Adverse effects of emerging contaminants (Bolong et al., 2009).....	21
Table 1.2 Chemical and physical properties of glyphosate	22
Table 1.3 Glyphosate occurrence and concentration in surface or groundwater samples in several countries in North America, South America, and Europe (Van Bruggen et al., 2018)	26
Table 1.4 Glyphosate concentration in industrial wastewater	27
Table 1.5 Removal of glyphosate from aqueous environment by adsorption	28
Table 1.6 Glyphosate-degrading microorganisms reported in the literature	31
Table 1.7 Some AOPs process reported to be used for glyphosate treatment	35
Table 1.8 Available literature studies on the treatment of single compounds by WAO process.....	43
Table 1.9 Summary of literature on WAO of real industrial wastewater	44
Table 1.10 Global kinetic models for WAO of organic compounds	44
Table 1.11 Integrated AOPs-biological systems for the treatment of various contaminants.....	50
Table 1.12 Integrated WAO-biological systems for the treatment of various contaminants.....	52
Table 2.1 Available literature studies on bubble characteristics in bubble column reactors	58
Table 2.2 Physical properties of liquid and gas phases at different pressures and temperatures (“Thermophysical properties of fluid systems,” n.d.).....	64
Table 2.3 Dimensionless number for this study.....	77
Table 2.4 Comparison of Sauter mean diameter and gas holdup correlation between Kanaris et al. (2018) and this study.....	77
Table 3.1 Available studies on the treatment of organic pollutants by WAO process	85
Table 3.2 Estimations of rate constant, pre-exponential factor and activation energy for glyphosate oxidation.....	91
Table 3.3 Concentration of by-products of glyphosate in the WAO process under three temperature after 30 min	95
Table 4.1 Operating conditions for glyphosate degradation	104
Table 5.1 Composition of medium used for acclimating activated sludge.....	119
Table 5.2 The change of MLSS and pH values in the acclimated activated sludge and non-acclimated activated sludge after 24 h at various glyphosate concentration.....	125
Table 5.3 Glyphosate removal efficiency by acclimated and non-acclimated sludge at two initial glyphosate after 24 h.....	127
Table 5.4 OUR in the kinetics process under different initial glyphosate concentration	129
Table 5.5 The concentration of possible byproducts of glyphosate before and after 24 h treatment	131
Table 6.1 Operation conditions for glyphosate degradation by the compact process.....	141

Table 6.2 Glyphosate, TOC and COD removal efficiency for each treatment and the combine process	145
Table 6.3 The change of MLSS and pH values for glyphosate degradation in the biological treatment after WAO pretreatment.....	146
Table 6.4 The concentration and yield of AMPA after WAO pretreatment.....	147
Table 6.5 The concentration of byproducts of glyphosate after the treatment of the combined process.	150

Abbreviations

<i>a</i>	Gas-liquid interfacial area
<i>a</i> ₁ - <i>a</i> ₆	Parameters used in Eq. 2-8
AMPA	Aminomethylphosphonic acid
AOPs	Advanced oxidation processes
<i>Ar</i>	Archimedes number ($= gD^3\rho_L^2/\mu_L^2$)
<i>b</i> ₁ - <i>b</i> ₆	Parameters used in Eq. 2-9
BOD	Biochemical oxygen demand
COD	Chemical oxygen demand
<i>D</i>	Column diameter (m)
DAS	Dewatered alum sludge
DDT	Dichloro-diphenyl-trichloroethane
DEA	diethanolamine
DSA [®]	dimensionally stable anode
DO	Dissolved oxygen (mg.L ⁻¹)
<i>d</i> ₃₂	Sauter diameter (m)
<i>d</i> _{<i>b,i</i>}	equivalent bubble diameter defined in Eq. 2-1 (m)
<i>d</i> _{<i>b,max</i>}	maximum bubble diameter (m)
<i>d</i> _{<i>b,min</i>}	minimum bubble diameter (m)
<i>d</i> _{<i>b,eq</i>}	equivalent mean bubble diameter (m)
<i>d</i> _{<i>b,i</i>}	initial bubble diameter at class <i>i</i> (m)
<i>d</i> _{<i>b,i+1</i>}	final bubble diameter at class <i>i</i> (m)
<i>d</i> _p	Sparger column (m)
<i>Ea</i>	Activation energy
<i>Eo</i>	Eötvös number ($= gD^2\rho_L/\sigma_L$)
<i>Fr</i>	Froude number ($= U_G^2/gD$)
<i>g</i>	Gravitational constant (m.s ⁻²)
GC	Wastewater treatment
GLKM	Generalized lumped kinetic model
HCN	Hydrocyanic acid
IARC	International Agency for Research on Cancer
IC	Inorganic carbon concentration (mg.L ⁻¹)
<i>K</i>	Rate constant
<i>k</i> ₀	Pre-exponential factor
<i>K</i> _{<i>i</i>}	Inhibition coefficient
<i>K</i> _{<i>s</i>}	Half-saturation constant
<i>k</i> _L <i>a</i>	Mass transfer coefficient
LAS	Liquid alum sludge
LC-MS	Liquid chromatography-mass spectrometry
MLSS	Mixed liquor suspended solid (g.L ⁻¹)
<i>m, n</i>	Partial order
<i>Mo</i>	Morton number ($= g\mu_L^4/\rho_L\sigma_L^3$)

N	Number of bubble class
n_i	Bubble number of each class (mol)
$n_{O_2,total}^0$	The initial amount of oxygen injected into the reactor (mol)
$n_{O_2,total}^0$	Oxygen amount at t time (mol)
$n_{O_2,d}^t$	The amount of oxygen dissolved in the liquid phase at t time (mol)
$n_{O_2,G}^t$	The amount of oxygen dissolved in the gas phase at t time (mol)
Oh	Ohnesorge number ($= \frac{\mu_L}{\sqrt{\rho_L \sigma_L D}}$)
OUR	Oxygen uptake rate ($\text{mgO}_2 \cdot \text{L}^{-1} \cdot \text{min}^{-1}$)
OUR_{en}	Endogenous oxygen uptake rate ($\text{mgO}_2 \cdot \text{L}^{-1} \cdot \text{min}^{-1}$)
OUR_{ex}	Exogenous oxygen uptake rate ($\text{mgO}_2 \cdot \text{L}^{-1} \cdot \text{min}^{-1}$)
P	Total pressure (MPa)
P_{O_2}	Partial oxygen pressure (MPa)
Q_{inf}	Flow rate of the influent ($\text{mL} \cdot \text{min}^{-1}$)
Q_{eff}	Flow rate of the effluent ($\text{mL} \cdot \text{min}^{-1}$)
PDMS	Polydimethylsiloxane
PMMA	Polymethyl-methacrylate
PP	Polypropylene
R	Gas constant ($8.314 \text{ J} \cdot \text{mol}^{-1} \cdot \text{K}^{-1}$)
Re	Reynolds number ($= \frac{\rho_L U_G D}{\mu_L}$)
RT	Residence time
S	Sample size
$t_{1/2}$	Half-life (h)
T	Temperature (K)
TC	Total carbon concentration ($\text{mg} \cdot \text{L}^{-1}$)
TNT	2,4,6-Trinitrotoluene
TOC	Total organic carbon concentration ($\text{mg} \cdot \text{L}^{-1}$)
U_G	Superficial gas velocity ($\text{cm} \cdot \text{s}^{-1}$)
U_L	Superficial liquid velocity ($\text{cm} \cdot \text{s}^{-1}$)
$V_{b,i}$	Bubble volume at each class (m^3)
V_c	Column volume (m^3)
V_G	The gas phase volume (L)
V_L	The liquid phase volume (L)
V_m	The total internal volume of the microchannel
WAO	Wet air oxidation
WHO	World Health Organization
WWT	Wastewater treatment
We	Weber number ($= \frac{\rho_L U_G^2 D}{\sigma_L}$)
Y	Yield coefficient
$Y_{S/O}$	Yield of substrate on oxygen
Z	Oxygen compressibility factor
ε	Gas holdup
μ	Specific growth rate (h^{-1})

μ_m	Maximum specific cell growth rate (h^{-1})
μ_L	liquid viscosity ($\text{kg} \cdot (\text{m s})^{-1}$)
ρ_L	liquid density ($\text{kg} \cdot \text{m}^{-3}$)
σ	Standard deviations
σ_L	liquid surface tension ($\text{N} \cdot \text{m}^{-1}$)
ξ	The extent of reaction

Introduction

Wastewater treatment (WWT), from domestic or industrial origin, is becoming more and more difficult due to the presence of many molecules hard to remove, especially for emerging contaminants. Emerging contaminants have been reported to cause adverse ecological or human health effects; thus, it is necessary to remove them from the environment.

Many technologies can be used to treat emerging contaminants, such as filtration, adsorption, biological process and advanced oxidation processes (AOPs). In order to enhance the overall efficiency of the pollutants degradation, it seems interesting to combine the advantages of several processes. This work is included in a project aiming at the development of a combination of an oxidation process, to increase the biodegradability, and a biological process. The general objective is also to treat principally effluent for the industry, at different scales, and hence to have at the end a compact process. The compactness for oxidation is to use wet air oxidation conditions (high pressure, high temperature) in a microfluidic system, in order to decrease the constraint of pressure and temperature. The compactness for biological process is to develop a packed bed biological reactor. Moreover, in order to take profit of the high temperature at the exit of the wet air oxidation step, it is envisaged to use thermophilic bacteria.

This thesis is part of this global process, and proposes to study part of the system developed in this project. More precisely, the oxidation part will be developed in a microfluidic system, and the effluent will be then tested in a classical biological treatment. In order to study this process combination, it is necessary to choose a model molecule.

Among emerging contaminants, glyphosate, a most widely used herbicide in the world, is chosen as the research object due to its frequently both use in France and China. The application of glyphosate has achieved up to over 850 thousand tons, among these 25% used in Europe and 35% used in China and India. In 2017, the French government rejected a European Commission decision to reapprove the use of glyphosate for five years and planned to ban the product within three years. However, it is reported to be impossible to find an alternative for these short time which is both economically viable and environmental friendly. Due to the intensive use of glyphosate, it has frequently been detected in the aqueous environment and could cause harmful effects to the plant, animal and human health. Conventional methods (adsorption, filtration, and biological treatment) and advanced oxidation processes (AOPs) have been applied to treat glyphosate-containing wastewater. The conventional methods generally need post-treatment (adsorption or filtration) or a long residence time (biological treatment). AOPs tend to be difficult for complete chemical mineralization of glyphosate due to the formation of the oxidation intermediates. Thus, a more effective, safe and affordable technology is needed to degrade glyphosate from aqueous environment. The combination of WAO and biological

processes is a promising treatment technology for organic compounds with high degradation and mineralization efficiency, considering environmental and economic advantages.

Consequently, the aim of this thesis is to develop a new effective treatment for glyphosate from wastewater by a combined system coupling WAO and biological treatment at laboratory scale. To evaluate the combined process, it is necessary to study step by step the WAO process, the biological process and then the combination. Therefore, the manuscript is mainly composed of seven parts:

Chapter 1 focuses on the bibliographic study. An overview of emerging contaminants, especially glyphosate is presented, including its occurrence and behavior in the Environment. Different treatments for glyphosate from wastewater are discussed in terms of their advantages and disadvantages, as well as the influencing parameters and possible degradation pathways. Meanwhile, the application, reaction mechanisms, reactions kinetics and mass transfer of WAO for organic contaminants are reviewed. Then, a review of combine processes coupling AOPs and biological treatment used for organic compounds is presented. Finally, a short overview on the current research status of microfluidic device is shown.

In Chapter 2, in order to evaluate the mass transfer for WAO process, a bubble column was used to investigate bubble hydrodynamic, including bubble size distribution and gas-liquid interfacial area as a function of gas and liquid superficial velocity, pressure, temperature and different gases (N_2 and He) and liquids (water and ethanol/water mixture) mixtures. Two correlations for bubble average size and gas holdup were proposed in order to predict mass transfer phenomena in WAO process.

Chapter 3 focused on the kinetics of glyphosate degradation via WAO process in a batch reactor. A first-order equation was used to fit experimental data. The possible intermediates of the reaction and main end products of glyphosate degradation were identified and quantified in the aim of proposing a degradation scheme of glyphosate oxidation.

Chapter 4 is concerned with microfluidic devices used for WAO process to treat glyphosate-containing wastewater. The effects of residence time and temperature were discussed through comparing the reduction of glyphosate, total organic carbon (TOC) and chemical oxygen demand (COD). Experimental data were well fitted with a first-order kinetics model.

In Chapter 5, an acclimation process for activated sludge was performed in order to improve glyphosate biodegradation. Removal kinetics and oxygen uptake rate were investigated. Meanwhile, a possible biodegradation pathway of glyphosate by acclimated activated sludge was proposed.

In Chapter 6, the degradation of glyphosate by an integrated WAO-biological treatment process was investigated. Glyphosate, TOC and COD removal for each process and then combined process

were studied. A possible degradation pathway of glyphosate by the combined process was finally proposed.

Finally, the main conclusions achieved in the present thesis were summarized at the end of the document as well as the perspectives of the work.

This thesis is a compilation of several articles, submitted or to be submitted.

Chapter 1: the bibliographical study. It has been submitted to “Water research” by 18 July, 2019 (Dan FENG, Audrey SORIC, Olivier BOUTIN*) in a shorter version: “Treatment technologies and degradation pathways of glyphosate: A critical review.” The version submitted is given in annex 1.

Chapter 2: “Bubble characterization and gas-liquid interfacial area in two phase gas-liquid system in bubble column at low Reynolds number and high temperature and pressure”. It has been published in “Chemical Engineering Research and Design” (Dan FENG, Jean-Henry FERRASSE, Audrey SORIC, Olivier BOUTIN*. Volume 144, April 2019, Pages 95-106. DOI: <https://doi.org/10.1016/j.cherd.2019.02.001>).

Chapter 3: “Kinetic study of glyphosate degradation by a wet air oxidation process”. It has been submitted to “Chemosphere” by 20 August, 2019 (Dan FENG, Laure MALLERET, Audrey SORIC, Olivier BOUTIN*).

Chapter 5: “Acclimation of aerobic activated sludge degrading glyphosate and its biodegradation kinetics”. It will be submitted to “Bioresource Technology” (Dan FENG, Laure MALLERET, Guillaume CHIAVASSA, Olivier BOUTIN, Audrey SORIC*).

The other chapters will be submitted to other journals.

In this manuscript, in order to be clear and avoid some repetitions, all the references are given once at the end of the manuscript.

Chapter 1 Bibliographical study

1.1 Background

1.1.1 Overview of emerging contaminants

Wastewater treatment (WWT) is a severe worldwide problem, which urgently requires different and effective proposals. Liquid aqueous wastes, from domestic or industrial origin, are becoming more and more complex for their treatment, due to the presence of many molecules difficult to remove, especially in case of emerging contaminants. They are defined as natural or synthetic chemicals which are not commonly found in the environment but has potential to enter the Environment and are known or suspected to ecological or human health effects (Geissen et al., 2015). Emerging contaminants include many types of contaminants such as pesticides and herbicides, pharmaceuticals, personal care products, plasticizers, fragrances, flame retardants, hormones, nanoparticles, water treatment by-products, surfactants and so on (Sauvé and Desrosiers, 2014). Since 2016, more than 1,000 emerging contaminants have been listed to be present in the European aquatic environment (“Emerging substances | NORMAN,” n.d.). Emerging contaminants are currently not included in routine monitoring programs at the European level and their behavior, fate and (eco)toxicological effects are often not well known (Geissen et al., 2015). Due to the rapid increase of use in industry, agriculture, transport, and urbanization, these compounds are entering the Environment with increasing levels as hazardous wastes and nonbiodegradable substances (Gavrilescu et al., 2015; Lei et al., 2015). These compounds can be released to the Environment from a lot of sources and pathways (Fig. 1.1): industrial effluents (e.g. manufacturing plants, food processing plants, hospitals), domestic effluents, wastewater treatment plants from urban or industrial areas, combined sewage-storm-water overflows, waste disposal sites (landfill, industrial impoundments, farm waste lagoons), septic tanks and agricultural runoff (Lapworth et al., 2012).

Due to their persistence in the environment, these chemicals can lead to bioaccumulation and biomagnification through food/drink intake in living organisms (Poynton and Vulpe, 2009). These compounds can cause endocrine disruption by mimicking, blocking or also disrupting the function of hormones. In addition, some chemicals have risks of carcinogenicity, mutagenicity, and teratogenicity (Bolong et al., 2009). Some of the selected emerging contaminants and their adverse effects are shown in Table 1.1 (Bolong et al., 2009).

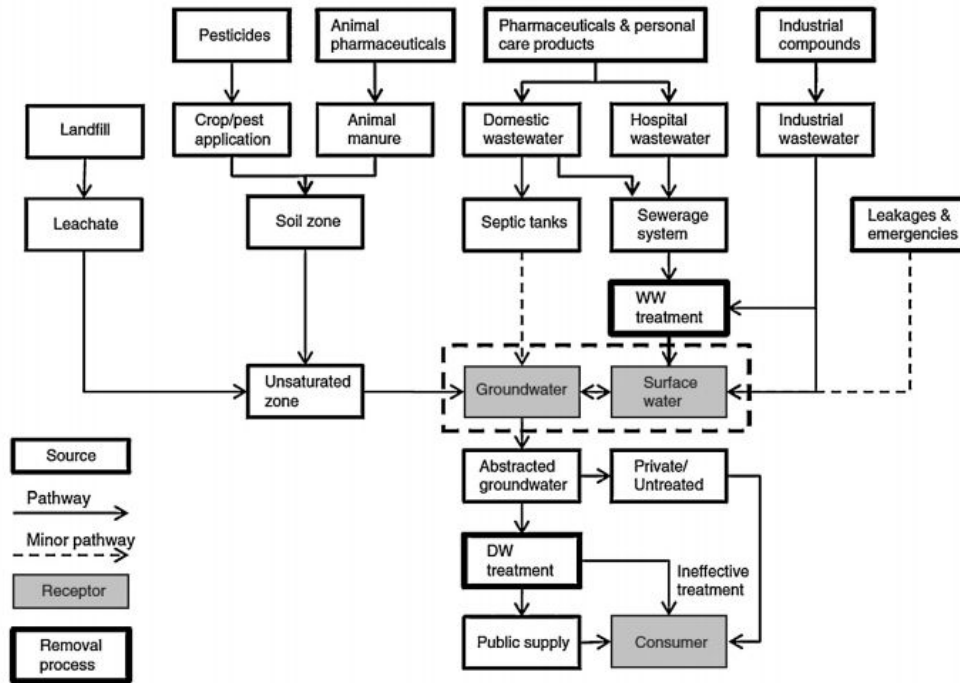


Fig. 1.1 Schematic pathways for emerging contaminants from sources to receptors (Lapworth et al., 2012)

Among these emerging contaminants, due to the development of modern agriculture, the use of pesticides has significantly increased productivity. Many pesticides remain partitioned in the aqueous Environment due to their relatively high-water solubility. Currently, pesticides and their metabolites are often detected in water sources and wastewater effluents at high concentrations (Postle et al., 2004; Lapworth and Goody, 2006; Gavrilescu et al., 2015). It has been reported that pesticides have significant chronic health effects, including neurological effects, diabetes, fetal diseases, respiratory diseases, neurological effects, cancer, and genetic disorders. Effectively removing pesticides from the aqueous environment has been a research hotspot. Thus, in this work, glyphosate which is the most widely used pesticide in the world has been chosen as a model molecule to study the removal efficiency by a compact process coupling wet air oxidation and biological processes.

Table 1.1 Adverse effects of emerging contaminants (Bolong et al., 2009)

Emerging contaminants	Adverse effects
Pesticides	Dichloro-diphenyl-trichloroethane (DDT): an insecticide which causes hormonal effect (shinning of eggshells, damage male reproductivity and behavioral changes) (Colborn, 1995) Lindane: an organochlorine pesticide which leads to vitellogenin and zona radiate (eggshell protein) in liver cells of Atlantic Salmon (Celius et al., 1999) Prochloraz: a fungicide that can affect pituitary weight (McKinney and Waller, 1994) Propiconazole: a fungicide that influences steroid metabolism (McKinney and Waller, 1994) Tridemorph: a fungicide that can cause cystic ovaries (McKinney and Waller, 1994)
Bisphenol A—used in epoxy resin and polycarbonate plastics (in food and drink packaging)	Estrogenic effects in rats and hormonal effects (Dodds and Lawson, 1938) which increase breast cancer risk in human (Krishnan et al., 1993)
Butylated Hydroxyanisole — used as a food antioxidant	Estrogenic to breast cancer cells, rainbow trout estrogen receptor and stimulates human estrogen receptor (Jobling et al., 1995)
Alkylphenols (ie nonylphenol)—used in detergents	Mimicking estrogen and disturbing reproduction by increasing the number of eggs produced by Minnos and vitellogenin levels (ENDS, 1999)
Phthalates—used as plasticizers in plastic, PVC baby toys, flooring	Exposure to high levels reported to cause miscarriage and pregnancy complication (IEH, 1995)
Polychlorinated biphenyls — used in electrical equipment (capacitors and transformers)	The metabolites able to mimic estradiol (female hormone) (Jacobson and Jacobson, 1997) and cause carcinogenic (IEH, 1995). Exposure was reported to cause delayed brain development and IQ decrease in children (Routledge et al., 1998)
Estrone and 17- β estradiol (steroidal estrogens) and 17- α ethynylestradiol (synthetic contraceptive) — contained in contraceptive pills	Cause feminization which observed for fish in sewage treatment (Witte, 1998). The discharge causes mimicking estrogen/hormone effect to non-target.
Antibiotics (such as penicillin, sulfonamides, tetracyclines)	Shown to cause resistance among bacterial pathogens (Witte, 1998), that lead to altered microbial community structure in nature and affect higher food chain (Daughton and Ternes, 1999)
Fragrances (musk)	Musk ambrette may damage the nervous system (KIRSCHNER, 1997)
Preservatives, i.e., parabens (alkyl-phdroxybenzoate) — used for anti-microbiological preservatives in cosmetics, toiletries and even foods	Shows weak estrogenic activity (Routledge et al., 1998)
Disinfectants/antiseptics, i.e., triclosan — used in toothpaste, handsoaps, acne cream	Found in the receiving waters (Okumura and Nishikawa, 1996), that cause toxic, biocide (kill microorganism) and also cause bacteria resistance development towards triclosan (McMurry et al., 1998)

1.1.2 Overview of glyphosate

Glyphosate (N-(phosphonomethyl)glycine, $C_3H_8NO_5P$, Fig. 1.2, Table 1.2) is a nonselective broad-spectrum herbicide used in agriculture to control many annual and perennial weeds (Waiman et al., 2012). Glyphosate is the most extensively used herbicide in agricultural, forestry and urban setting in the world, due to its high ability to control weeds and its low toxicity (da Silva et al., 2011; Zhang et al., 2011). Glyphosate is a biosynthesis inhibitor of essential aromatic amino acids, resulting in various metabolic disorders, which include the deregulation of the shikimate pathway and the suspension of protein synthesis, leading to general metabolic disruption and the plant death (Oliveira et al., 2012). Glyphosate interrupts aromatic amino acid biosynthesis in plants through inhibiting the enzymes 5-enolpyruvylshikimate-3-phosphate synthase or 3-deoxy-D-arabino-heptulosonate-7-phosphate synthase, which is a precursor for aromatic amino acids, ultimately hormones, vitamins and other important metabolites for plants (Kataoka et al., 1996). The mechanism of inhibition effect which has been reported is that the binding site for glyphosate overlaps closely with the binding site of shikimate 3-phosphate (Helander et al., 2012) (Fig. 1.3).

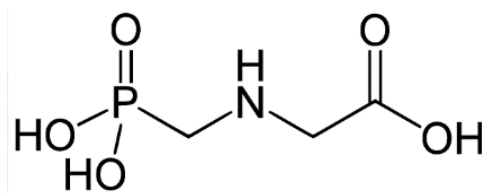


Fig. 1.2 The structure of glyphosate

Table 1.2 Chemical and physical properties of glyphosate

Properties	Values	Units
Molecular weight	169.07	$g \cdot mol^{-1}$
Physical state	White solid	-
Odor	Odorless	-
Density	1.704	$g \cdot cm^{-3}$
pKa	0.78 (first proton phosphonate group) 2.29 (proton of the carboxyl group) 5.96 (second phosphonate proton) 10.98 (proton of the amino group)	-
Melting point	184.5	$^{\circ}C$
Boiling point	187	$^{\circ}C$
Solubility (20 $^{\circ}C$)	1.01	$g \text{ glyphosate}/100 \text{ mL H}_2\text{O}$

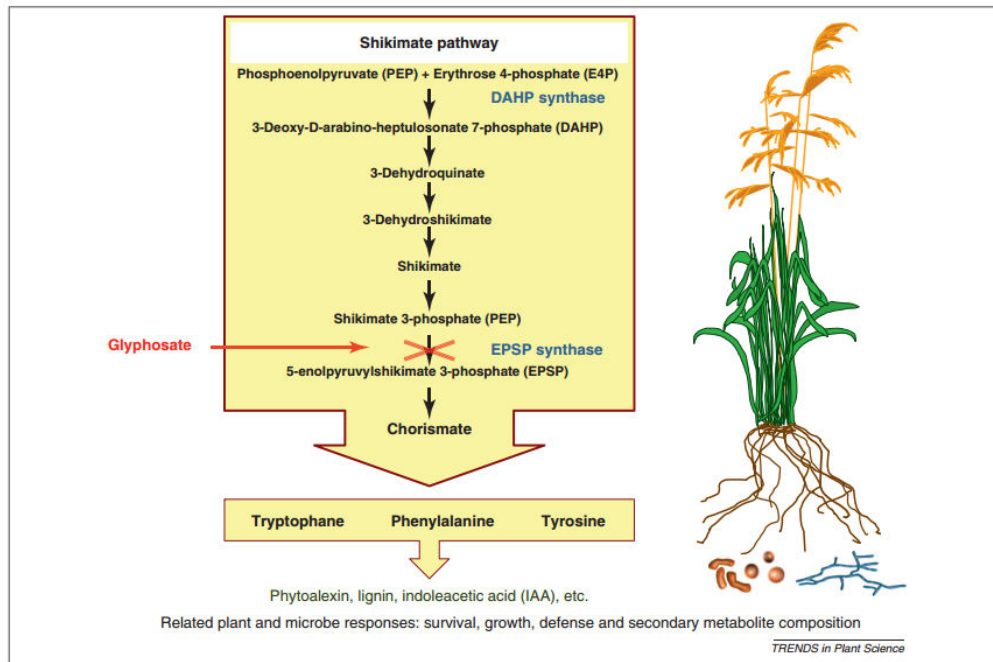


Fig. 1.3 Inhibition process of shikimate acid pathway and inhibition role of glyphosate (Helander et al., 2012)

Glyphosate is available in various chemical forms, such as ammonium salt, diammonium salt, isopropylamine salt, dimethylammonium salt, and potassium salt (Benbrook, 2016; Gillezeau et al., 2019). Glyphosate mixed with other chemicals known as “inert ingredients” constitutes glyphosate-based herbicides (Benbrook, 2016; Gillezeau et al., 2019). Fig. 1.4 shows the glyphosate use worldwide from 1994 to 2015 and by regions in 2014 (available from: “Glyphosate Market Share, Size - Industry Trends Report 2024,” n.d., “Glyphosate use worldwide 1994-2014 | Statistic,” n.d.; “Glyphosate Market Analysis, Size, Share and Forecasts - 2022 | MarketsandMarkets,” n.d.). Generally, glyphosate-based herbicides are used in the preparation of soils for sowing and in crop areas with its sprayed applications from 6.7 to 8.9 kg.ha⁻¹ and from 0.53 to 1.0 kg.ha⁻¹, respectively (Giesy et al., 2000; Benbrook, 2016; Villamar-Ayala et al., 2019). These herbicides are also used to control annual perennial species (agriculture), invasive vegetation (forestry), and aquatic algae (aquaculture) during the post-harvest activities with the applications up to 0.84 kg.ha⁻¹ of its acid equivalent (active ingredient) (Giesy et al., 2000; Duke and Powles, 2008; Villamar-Ayala et al., 2019).

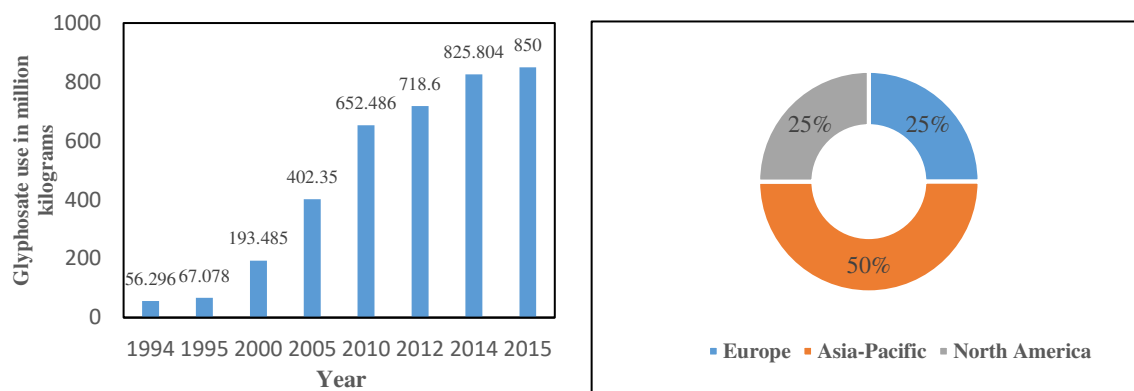


Fig. 1.4 Glyphosate use worldwide from 1994 to 2015 (in million kilograms) (from: “Glyphosate Market Share, Size - Industry Trends Report 2024,” n.d., “Glyphosate use worldwide 1994-2014 | Statistic,” n.d.; “Glyphosate Market Analysis, Size, Share and Forecasts - 2022 | MarketsandMarkets,” n.d.)

Due to the intensive use and accumulation of glyphosate in the environment, some harmful effects of glyphosate have been reported for plant, animal and human health. Glyphosate weakened plant system, decreased photosynthesis and caused cell damage (Huber et al., 2005; Gomes et al., 2016; Van Bruggen et al., 2018). Authors reported that glyphosate suppressed the acetylcholinesterase activity, disturbed the metabolism and may cause DNA or liver damage both for terrestrial and aquatic animals (Menéndez-Helman et al., 2012; Sandrini et al., 2013; Kwiatkowska et al., 2014, 2017; Mesnage et al., 2015; Cattani et al., 2017). Although humans are not a direct target for glyphosate, humans could contact glyphosate due to occupational exposure by agricultural practices (Acquavella et al., 2004; Paz-y-Miño et al., 2007) or through the food chain (Wigfield and Lanouette, 1990; McQueen et al., 2012). Glyphosate has been reported to cause cell and DNA damage and endocrine disruption to humans (Richard et al., 2005; Paz-y-Miño et al., 2007; Benachour and Séralini, 2009; Mesnage et al., 2015). In 2015, the International Agency for Research on Cancer (IARC) classified glyphosate as “probably carcinogenic to humans”, while authors disagree on this conclusion which require further research (Andreotti et al., 2018). Numerous studies and reviews have been reported on the adverse effects of glyphosate and glyphosate-based formulations on plants, animals and human (Tsui and Chu, 2003; Vendrell et al., 2009; Vera et al., 2010; Kier and Kirkland, 2013; Tarazona et al., 2017). Acute toxicity tests show that the 96-hour LD₅₀ of glyphosate ranged from 2.3 to 150 mg.L⁻¹ for different fish species (Armiliato et al., 2014; Sandun et al., 2015; Rodrigues et al., 2017; Vajargah et al., 2018). Therefore, glyphosate removal from the environment is a priority and needs to be addressed promptly.

1.2 Occurrence, behavior, and fate of glyphosate in aqueous environment

Glyphosate containing herbicides may contaminate the environment after application. Fig. 1.5 (Helander et al., 2012) shows glyphosate accumulation and transport in the environment. First, through air spraying, glyphosate can directly enter atmosphere environment, with concentration in air

up to 0.48 g.L^{-1} (Helander et al., 2012; Villamar-Ayala et al., 2019). Then, through wind or rain, glyphosate reaches the target organisms by foliar contact or the soil (Villamar-Ayala et al., 2019). In the target plant, glyphosate is first absorbed by foliage and then translocated to the shoots and roots via the phloem (Helander et al., 2012). Without degradation in the plant, large root systems of some weeds transport glyphosate into deep soil layers (Laitinen et al., 2007; Helander et al., 2012). A part of glyphosate which enters the soil through rain, wind or transportation by root of the plant may stay at the soil surface. Glyphosate can be adsorbed to organic matter and clay of soils, resulting in its accumulation in soils over time (Cassigneul et al., 2016; Okada et al., 2016; Sidoli et al., 2016; Van Bruggen et al., 2018). As glyphosate possesses three polar functional groups (amino, carboxyl and phosphonate groups), it can be strongly adsorbed by soil minerals (Borggaard and Gimsing, 2008). Glyphosate mobility in the soil depends on the adsorption and desorption processes which related to soil characteristics and other environmental conditions (Helander et al., 2012; Villamar-Ayala et al., 2019). Microbial degradation is the most important transformation process to determine the persistence of glyphosate in the soil (Aparicio et al., 2013a). Glyphosate can be degraded to aminomethylphosphonic acid (AMPA) or sarcosine as primary metabolite under aerobic and anaerobic conditions by the microflora in the soil/sediment (Ermakova et al., 2010; Aparicio et al., 2013). The AMPA pathway is the main microbial process, whereas the sarcosine pathway is only found in pure microbial culture (Vereecken, 2005; Villamar-Ayala et al., 2019). Glyphosate has been reported to have a soil half-life between 2 and 215 days (Battaglin et al., 2014; Maqueda et al., 2017). Due to the runoff, such as rain and erosion, glyphosate and AMPA can be transferred into surface water (Wang et al., 2016; Maqueda et al., 2017; Rendon-von Osten and Dzul-Caamal, 2017).

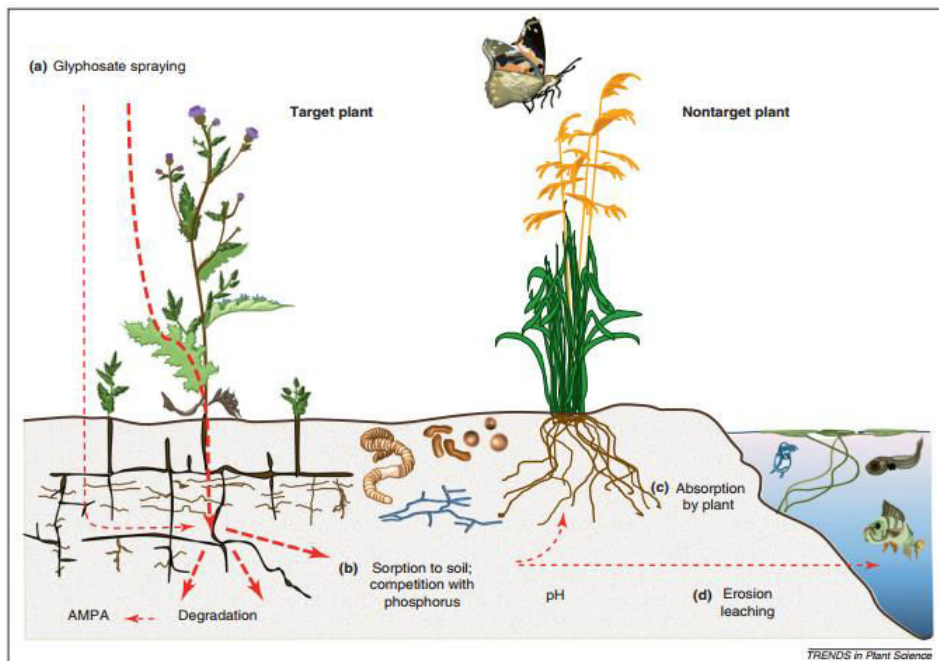


Fig. 1.5 Glyphosate accumulation and transport in the environment (from Helander et al., 2012)

Glyphosate is highly water soluble and can be mobile in aqueous environment (Veiga et al., 2001). The mobility of AMPA is found 1.6 to 4.0 times higher than glyphosate (Coupe et al., 2012; Villamar-Ayala et al., 2019). Thus, glyphosate and AMPA are frequently detected in surface or groundwater (Table 1.3). Table 1.3 shows that glyphosate has been detected in river water and stream water with the concentration range of 2-430 $\mu\text{g.L}^{-1}$ in the USA, which is at higher levels than in Europe. In areas of the USA, genetically modified glyphosate-resistant crops are grown, thus glyphosate and AMPA occur widely in soil, surface, and groundwater (Battaglin et al., 2014). However, in Europe, growing genetically modified crops is not allowed yet, which makes glyphosate to be detected in various water sources at lower levels (Van Bruggen et al., 2018). It is also reported that glyphosate can be detected in air and rain during the crop growing season and in water from spring snowmelt (Battaglin et al., 2009, 2014; Chang et al., 2011). Ultimately, glyphosate enters to the seawater with high persistence (Mercurio et al., 2014; Van Bruggen et al., 2018).

Table 1.3 Glyphosate occurrence and concentration in surface or groundwater samples in several countries in North America, South America, and Europe (Van Bruggen et al., 2018)

Country	Date	Glyphosate occurrence and concentrations	Refer.
Canada	2002	22% of samples positive, up to 6.07 $\mu\text{g.L}^{-1}$	(Humphries et al., 2005)
US (Midwest)	2002	36% of stream samples positive, up to 8.7 $\mu\text{g.L}^{-1}$	(Battaglin et al., 2005)
US (Midwest)	2013	44% of steam samples positive, up to 27.8 $\mu\text{g.L}^{-1}$	(Mahler et al., 2017)
US (Washington, Maryland, Iowa, Wyoming)	2005-2006	All streams positive, up to 328 $\mu\text{g.L}^{-1}$	(Battaglin et al., 2009)
US (Iowa, Indiana, Mississippi)	2004-2008	Most rivers positive, up to 430 $\mu\text{g.L}^{-1}$ after a storm	(Coupe et al., 2012)
Mexico	2015	All groundwater samples positive, up to 1.42 $\mu\text{g.L}^{-1}$	(Rendon-von Osten and Dzul-Caamal, 2017)
Argentina	2012	35% of surface water samples positive, 0.1-7.6 $\mu\text{g.L}^{-1}$	(Aparicio et al., 2013a)
Germany	1998	Few positive samples in two tributaries to the Ruhr river, up to 0.59 $\mu\text{g.L}^{-1}$	(Skark et al., 1998)
Switzerland	2016	Most stream water samples, up to 2.1 $\mu\text{g.L}^{-1}$	(Poiger et al., 2017)
Spain	2007-2010	41% positive groundwater samples, up to 2.5 $\mu\text{g.L}^{-1}$	(Sanchís et al., 2012)
Hungary	2010-2011	Most river and groundwater samples positive, up to 0.001 $\mu\text{g.L}^{-1}$	(Mörtl et al., 2013)
Denmark	1999-2009	25% of surface water samples positive, up to 31 $\mu\text{g.L}^{-1}$, 4% of groundwater samples positive, up to 0.67 $\mu\text{g.L}^{-1}$	(Rosenbom, 2010)
France	2003-2004	91% of stream samples positive, up to 165 $\mu\text{g.L}^{-1}$	(Villeneuve et al., 2011)

Moreover, Birch et al. (2011) reported that glyphosate and AMPA were found in samples of sewage and storm water overflows with the concentration of 0.043-1.3 $\mu\text{g.L}^{-1}$ and 0.06-1.3 $\mu\text{g.L}^{-1}$, respectively. Rendon-von Osten and Dzul-Caamal (2017) found that even in the bottled drinking water, glyphosate concentration could achieve up to 0.79 $\mu\text{g.L}^{-1}$ which exceeded the acceptable limits for human consumption in the European Union (0.1 $\mu\text{g.L}^{-1}$) (“Emerging substances | NORMAN,”

n.d.). Currently, glyphosate is in the list of the U.S. national primary drinking water contaminants with a maximum contaminant level goal of 0.7 mg.L^{-1} (Songa et al., 2009).

Table 1.4 Glyphosate concentration in industrial wastewater

References	Sampling point	Glyphosate concentration
(Heitkamp et al., 1992)	Glyphosate production wastewater	$500\text{-}2000 \text{ mg.L}^{-1}$
(Manassero et al., 2010)	Rinsing herbicide containers	$50.7\text{-}76.05 \text{ mg.L}^{-1}$
(Zhang et al., 2011)	Zhejiang Wynca Chemical Industry Group Co., Ltd. (China)	258 mg.L^{-1}
(Zhou et al., 2014)	Xinan Chemical Plant (Zhejiang, China)	1% wt
(Xing et al., 2017)	Jiangsu Good Harvest-Weien agrochemical Ind. Co. Ltd.; Jiema Chemical Ind. Co. Ltd.; Guangan Ind. Co. Ltd. (China)	$213\text{-}2560 \text{ mg.L}^{-1}$

Glyphosate contaminants the environment from various sources: agricultural runoff, chemical spill as well as industrial effluents (Baylis, 2000; Botta et al., 2009). Three major industrial synthesis methods were used for glyphosate production: hydrocyanic acid (HCN), diethanolamine (DEA) and glycine process. All of these processes have a large amount of industrial wastewater and other environmental pollution (Zhou et al., 2012). To obtain 1 ton of glyphosate, about 5-6 tons of crystallized mother liquid is generated with ~ 1% glyphosate, 1-4% formaldehyde (HCHO) and other byproducts (Xing et al., 2018). Most of glyphosate is recovered from the mother liquor through nanofiltration (Song et al., 2013), while $200\text{-}3000 \text{ mg.L}^{-1}$ glyphosate remains in the nanofiltration permeate wastewater in China (Xing et al., 2018). It has also been reported that glyphosate concentration in industrial effluents could achieve up to $2,560 \text{ mg.L}^{-1}$ (Table 1.4). Therefore, it is necessary to effectively remove glyphosate residue from industrial wastewater to lower its environmental impact.

1.3 Treatment technology for glyphosate from environment

Conventional methods, such as adsorption, filtration, and biological treatment have been applied to treat glyphosate-containing wastewater. Moreover, AOPs, such as photolysis oxidation, Fenton oxidation, electrochemical oxidation, and ozonation oxidation, have been proposed as alternative technologies for glyphosate-containing wastewater (Villamar-Ayala et al., 2019). All these technologies are described in detail below.

1.3.1 Adsorption

Currently, adsorption is widely used in large-scale biochemical and purification for wastewater treatment due to simple design, non-toxic and low-cost adsorbents and high efficiency (Mayakaduwa et al., 2016). Several materials have been used as adsorbents for glyphosate adsorptive removal, such as activated carbon, biochar, water industrial residues, clay substances, resin, biopolymers, polyvinylpyrrolidone (PVP) capped silver nanocubes, etc. (Table 1.5). Table 1.5 shows that activated carbon, biochar or resin used as adsorbents could achieve higher removal efficiency and higher

maximum adsorption capacity of glyphosate. Recently, biochar has drawn more attention because of its low cost and highly aromatic and porous structure, which contributes high removal efficiency of biochar (Zhang et al., 2013). However, with this process, disposal of the residue after adsorption remains a problem which needs to be further studied (Mayakaduwa et al., 2016).

Table 1.5 Removal of glyphosate from aqueous environment by adsorption

Refer.	Adsorbent	Initial glyphosate concentration (mg.L ⁻¹)	Marks
(Villa et al., 1999)	Hydrotalcites and organo-hydrotalcites	5-25	Adsorption capacity: 1-4 µg.g ⁻¹
(Li et al., 2005)	MgAl-layered double hydroxides	169	Maximum adsorption capacity: 184 mg.L ⁻¹
(Nourouzi et al., 2010)	Activated carbon	5-100	Maximum adsorption capacity: 48.4 mg.g ⁻¹
(Hu et al., 2011)	Dewatered alum sludge (DAS) and liquid alum sludge (LAS)	50-100 for DAS; 200-500 for LAS	Removal efficiency: 65.4%-91.6% For DAS; 64.7%-97.4% for LAS Maximum adsorption capacity: 85.9 mg.g ⁻¹ for DAS; 113.6 mg.g ⁻¹ for LAS
(Salman et al., 2012)	Palm oil fronds activated carbon	25-250	Maximum adsorption capacity: 104.2 mg.g ⁻¹
(Chen et al., 2016)	Resin D301	1% mass fraction	Maximum adsorption capacity: 400-833.33 mg.g ⁻¹ mg.g ⁻¹
(Herath et al., 2016)	Rice husk derived engineered biochar	0-100	Maximum removal: 82.0%; maximum adsorption capacity: 123.03 mg.g ⁻¹
(Mayakaduwa et al., 2016)	Woody biochar	20	Maximum adsorption capacity: 44 mg.g ⁻¹
(Jia et al., 2017)	Resin-supported double valent nano-sized hydroxyl iron oxide	400	Maximum adsorption capacity: 401.12 mg.g ⁻¹
(Rissouli et al., 2017)	Chitin and chitosan	1-30	Maximum adsorption capacity: 14.04 mg.g ⁻¹ for chitin and 35.08 mg.g ⁻¹ for chitosan
(Sarkar and Das, 2017)	PVP capped silver nanocubes	100	No data for glyphosate removal efficiency

1.3.2 Filtration

Bank filtration process can achieve up to 95% and 87% of glyphosate and AMPA removal efficiency, respectively (Jönsson et al., 2013). Xie et al. (2010) reported that a high glyphosate removal of 95.5% was obtained by nanofiltration using a Desal-5 DK membrane from neutralization liquor produced by the glycine-dimethylphosphit process. Schoonenberg Kegel et al. (2010) obtained a glyphosate removal efficiency of >99% by a technology equipped with reverse osmosis and subsequently activated carbon filtration. Saitúa et al. (2012) observed that more than 85% of glyphosate could be removed by nanofiltration for the initial glyphosate concentration up to 250 mg.L⁻¹, depending on pressure and pH value. Liu et al. (2012) reported that nanofiltration separation of glyphosate from wastewater using a GE Osmonic DK membrane could achieve a high glyphosate removal efficiency. Although high glyphosate removal potentially achieved by filtration, the removal rate is likely to be highly dependent on physicochemical conditions. Large scale production of water by these methods is expensive, which is unable to commonly used in practice and unlikely to be adopted for the treatment of organic compounds (Jönsson et al., 2013).

1.3.3 Biological treatment

Biodegradation of organic compounds is known as an effective and eco-friendly method to remove organic pollutants from the aqueous environment (Zhan et al., 2018). Various micro-organism, including bacteria and fungi, have been reported to use glyphosate as a sole carbon, nitrogen, and/or phosphorus source. Table 1.6 shows that the microorganisms responsible for glyphosate biodegradation are mainly bacteria, only little fungi strains have been reported. Among these microorganisms, most species use glyphosate as sole phosphorus source. Some exceptions use glyphosate as nitrogen or carbon source.

To assess glyphosate-degradation performance of microorganisms, it is necessary to optimize culture conditions, including culture temperature, initial pH, glyphosate concentration, inoculated biomass and incubation time (Zhan et al., 2018). The culture conditions most used for glyphosate-degrading microorganism are a temperature of 25-37°C, a pH of 6-7.5 and aerobic medium. Only Obojska et al. (2002) observed a thermophilic bacteria, *Geobacillus caldxylosilyticus* T20, which could achieve more than 65% of glyphosate removal at 60°C with initial glyphosate concentration of 1 mM. Kryuchkova et al. (2014) found a facultative anaerobic strain, *Enterobacter cloacae* K7, which could utilize glyphosate as sole phosphorus source and obtain 40% degradation with glyphosate initial concentration of 5 mM.

Two major degradation pathways have been identified in glyphosate-degrading microorganisms (Fig. 1.6). One pathway is glyphosate converted to stoichiometric quantities of AMPA and glyoxylate through the cleavage of C-N bond by the enzyme glyphosate oxidoreductase (Zhan et al., 2018). Glyoxylate usually enters the tricarboxylic acid cycle as a convenient energy substrate for most glyphosate-degrading bacteria (Sviridov et al., 2015). Three pathways exist for AMPA: (i) AMPA releases to the Environment (Jacob, 1988; Lerbs et al., 1990); (ii) AMPA is further metabolized to methylamine and phosphate, catalyzed by C-P lyase (Pipke et al., 1987; Jacob, 1988; Pipke and Amrhein, 1988); (iii) AMPA is first metabolized to phosphonoformaldehyde by transaminase and then transformed to phosphate and formaldehyde for further metabolism by phosphonate (Sviridov et al., 2014).

The second degradation pathway is glyphosate metabolized to phosphate and sarcosine through the direct cleavage of the C-P bond, catalyzed by C-P lyase (Firdous et al., 2017). Sarcosine can be used as growth nutrient (carbon and nitrogen source) for microorganism and is further metabolized to glycine and formaldehyde by sarcosine-oxidase (Borggaard and Gimsing, 2008). Glycine is further metabolized by microorganism and formaldehyde enters the tetrahydrofolate-directed pathway of single-carbon transfers to produce CO₂ and NH₄⁺ (Borggaard and Gimsing, 2008). Some reports

indicate that AMPA and sarcosine pathways simultaneously exist in some bacteria, such as *Bacillus cereus* CB4, *Ochrobacterium anthropic* GPK3, and *Pseudomonas* sp. LBr (Jacob, 1988; Fan et al., 2012; Sviridov et al., 2012). The AMPA pathway is not generally subjected to P_i (inorganic phosphorus) concentration, however, glyphosate conversion to sarcosine strongly depends on the concentrations of exogenous and endogenous P_i , which rarely occurs in natural environments (Sviridov et al., 2015) due to C-P lyase activity generally induced under phosphate starvation condition (Borggaard and Gimsing, 2008; Sviridov et al., 2015).

At least, another degradation pathway was observed in *Achromobacter* sp. Kg16 which utilized glyphosate as sole phosphorus source, resulting in production of acetylglyphosate (Shushkova et al., 2016). However, *Achromobacter* sp. Kg16 is not able to further utilize acetylglyphosate as a phosphorus source, causing its poor growth. Although the glyphosate biodegradation has been extensively studied, the precise degradation mechanism and pathways are still not known.

Most studies reported have focused on the glyphosate biodegradation by pure culture of bacteria. Little research on glyphosate biodegradation was carried on mixed culture. Hallas and Adams (1992) reported glyphosate removal from wastewater effluent discharged from an activated sludge process in lab columns and found that more than 90% of glyphosate degradation was achieved for an initial concentration of 50 mg.L⁻¹. Nourouzi et al. (2010) reported that 99.5% of glyphosate (300 mg.L⁻¹) was converted to AMPA and 2% of AMPA was degraded to further metabolites by mixed bacteria isolated from oil palm plantation soil. The mixed cultures are more likely able to completely degrade contaminants, compared to pure culture due to the various enzymes available in mixed culture (Barbeau et al., 1997; Nourouzi et al., 2012). Moreover, due to the high requirements of pure culture, mixed culture processes are more suitable for industrial applications.

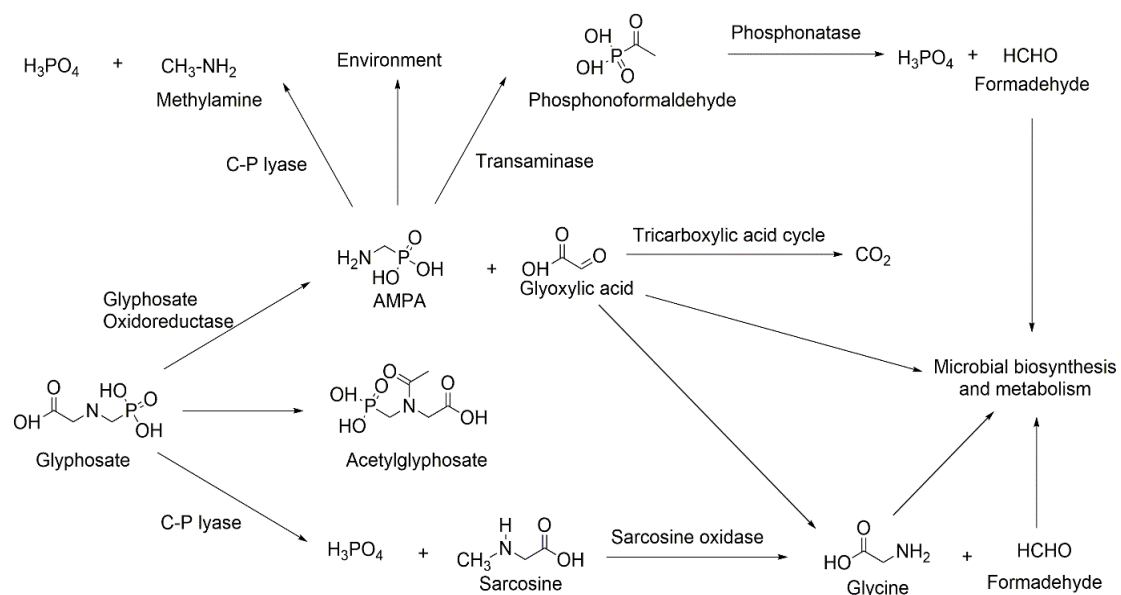


Fig. 1.6 Biodegradation pathways of glyphosate in microorganisms (Zhan et al., 2018).

Table 1.6 Glyphosate-degrading microorganisms reported in the literature

Microorganism	Source	Source type for glyphosate used	Culture conditions	Type of degradation pathway	Comments	References
Bacteria						
<i>Acetobacter</i> sp.	Glyphosate-contaminated rice field	Carbon or phosphorus source	30°C; aerobic	Not shown	Bacteria could tolerate up to 250 mg.ml ⁻¹ glyphosate	(Moneke et al., 2010)
<i>Achromobacter</i> sp. Kg 16	Glyphosate-contaminated soil	Sole phosphorus source	28-30°C; pH: 6.0-7.5; aerobic	Acetylgliphosate pathway	A new pathway of glyphosate utilization: acetylation	(Shushkova et al., 2016)
<i>Achromobacter</i> sp. LW9	Activated sludge from glyphosate process waste stream	Sole carbon source	28°C; pH: 7; aerobic	AMPA pathway	100% glyphosate (0.1%, w/v) transformation to AMPA	(McAuliffe et al., 1990)
<i>Achromobacter</i> sp. MPK 7A	Glyphosate-contaminated soil	Sole phosphorus source	28-30°C; pH: 7; aerobic	Sarcosine pathway	About 60% glyphosate (500 mg.L ⁻¹) removal	(Ermakova et al., 2017)
<i>Achromobacter</i> sp. MPS 12A	Alkylphosphonates-contaminated soil	Sole phosphorus source	28°C; pH: 6.5-7.5; aerobic	Sarcosine pathway	Glyphosate consumption: 124 µmol g ⁻¹ biomass	(Sviridov et al., 2012)
<i>Agrobacterium radiobacter</i>	Sludge from waste treatment plant	Sole phosphorus source	30°C; pH:7; aerobic	Sarcosine pathway	No data for glyphosate removal efficiency	(Wackett et al., 1987)
<i>Alcaligenes</i> sp. GL	Non-axenic cultures of the cyanobacterium <i>Anacystis nidulans</i>	Sole phosphorus source	28°C; pH:7.5; aerobic	Sarcosine pathway	50-80% glyphosate (5 mM) removal	(Lerbs et al., 1990)
<i>Arthrobacter atrocyaneus</i> ATCC 13752	Collection of microorganisms and cell cultures, Germany	Sole phosphorus source	Room temperature; pH: 7.2; aerobic	AMPA pathway	Capable of degrading glyphosate without previous culture selection	(Pipke and Amrhein, 1988)
<i>Arthrobacter</i> sp. GLP-1	Mixture culture with <i>Klebsiella pneumoniae</i>	Sole phosphorus source	Room temperature; pH: 7; aerobic	Sarcosine pathway	Capable of degrading glyphosate without previous culture selection	(Pipke et al., 1987)
<i>Bacillus cereus</i> CB4	Glyphosate-contaminated soil	Sole phosphorus source	35°C; pH: 6; aerobic	Both AMPA and sarcosine pathway	94.47% degradation (6 g.L ⁻¹) in 5 days	(Fan et al., 2012)
<i>Bacillus cereus</i> 6 P	Glyphosate-exposed orange plantation site	Sole phosphorus source	28°C; pH: 7; aerobic	Not shown	37.7% glyphosate (1 mM) removal	(Acosta-Cortés et al., 2019)
<i>Bacillus subtilis</i> Bs-15	Rhizospheric soil of a pepper plant	Carbon and phosphorus source	35°C; pH: 8; aerobic	Not shown	65% glyphosate removal	(Yu et al., 2015)
<i>Burkholderia vietnamiensis</i> AO5-12 and <i>Burkholderia</i> sp. AO5-13	Glyphosate contaminated sites in Malaysia	Sole phosphorus source	30°C; pH: 6; aerobic	Not shown	91% and 74% glyphosate (50 mg.L ⁻¹) degradation for AQ5-12 and AQ5-13, respectively	(Manogaran et al., 2017)
<i>Comamonas odontotermitis</i> P2	Glyphosate-contaminated soil in Australia	Carbon and phosphorus source	29.9°C; pH: 7.4; aerobic	Not shown	Complete degradation (1.5 g.L ⁻¹) within 104 h	(Firdous et al., 2017)

<i>Enterobacter cloacae</i> K7	Rhizoplane of various plants in Russia	Sole phosphorus source	30-37°C; pH: 6.8-7; Facultative anaerobe	Sarcosine pathway	40% glyphosate (5 mM) degradation	(Kryuchkova et al., 2014)
<i>Flavobacterium</i> sp. GD1	Monsanto activated sludge	Sole phosphorus source	25°C; pH: 6.8-7; aerobic	AMPA pathway	Complete degradation of glyphosate (0.02%)	(Balthazor and Hallas, 1986)
<i>Geobacillus caldoxylosilyticus</i> T20	Central heating system water	Sole phosphorus source	60°C; pH: 7; aerobic	AMPA pathway	>65% glyphosate (1 mM) removal	(Obojska et al., 2002)
<i>Ochrobacterium anthropic</i> GPK3	Glyphosate-contaminated soil	Sole phosphorus source	28°C; pH: 6.5-7.5; aerobic	Both AMPA and sarcosine pathway	Glyphosate consumption: 283.8 μ mol g ⁻¹ biomass	(Sviridov et al., 2012)
<i>Ochrobactrum intermedium</i> Sq20	Glyphosate-contaminated soil	Sole carbon source	Room temperature; pH 7; aerobic	Sarcosine pathway	Complete degradation (500 mg.L ⁻¹) within 4 days	(Firdous et al., 2018)
<i>Ochrobactrum</i> sp. GDOS	Soil	Sole phosphorus source	30°C; pH: 7; aerobic	AMPA pathway	Complete degradation (3 mM) within 60 h	(Hadi et al., 2013)
<i>P.fluorescens</i>	Glyphosate-contaminated rice field	Carbon or phosphorus source	30°C; aerobic	Not shown	Bacteria could tolerate up to 250 mg/ml glyphosate	(Moneke et al., 2010)
<i>Pseudomonas pseudomallei</i> 22	Soil	Sole phosphorus source	28°C; aerobic	AMPA pathway (putative)	50% glyphosate (170 mg.L ⁻¹) degradation in 40 h	(Peñaloza-Vazquez et al., 1995)
<i>Pseudomonas</i> sp. 4ASW	Glyphosate-contaminated soil	Sole phosphorus source	29°C; pH: 7.2; aerobic	Sarcosine pathway	100% glyphosate (0.25 mM) removal	(Dick and Quinn, 1995)
<i>Pseudomonas</i> sp. GLC11	Mutant of <i>Pseudomonas</i> sp. PAO1 on selective medium	Sole phosphorus source	37°C; pH: 7; aerobic	Sarcosine pathway	Capable of tolerating up to 125 mM glyphosate	(Selvapandiyan and Bhatnagar, 1994)
<i>Pseudomonas</i> sp. LBr	A glyphosate process waste stream	Sole phosphorus source	Room temperature; pH: 7; aerobic	Both AMPA and sarcosine pathway	Capable of eliminating 20 mM glyphosate from growth medium	(Jacob, 1988)
<i>Pseudomonas</i> sp. PG2982	<i>Pseudomonas aeruginosa</i> -ATCC 9027	Sole phosphorus source	Room temperature; aerobic	Sarcosine pathway	No data for glyphosate removal efficiency	(Kishore and Jacob, 1987)
<i>Pseudomonas</i> spp. strains GA07, GA09 and GC04	Glyphosate-contaminated soil in China	Sole carbon source	33°C; pH: 7; aerobic	Both AMPA and sarcosine pathways	Glyphosate (500 mg.L ⁻¹) removal: 53.6%-80.8%	(Zhao et al., 2015)
<i>Rhizobiaeae meliloti</i> 1021	Spontaneous mutation of a wild-type strain	Sole phosphorus source	28-32°C; pH: 7; aerobic	Sarcosine pathway	50% glyphosate (0.5 mM) removal	(Liu et al., 1991)
<i>Salinicoccus</i> spp.	Qom Hoze-Soltan Lake in Iran	Sole carbon source	Salt concentration: 5%-10%; 30°C; pH: 6.5-8.2; aerobic	Not shown	The native halophilic isolates could biodegrade glyphosate	(Sharifi et al., 2015)
<i>Streptomyces</i> sp. StC	Activated sludge from a municipal sewage treatment plant	Sole phosphorus, nitrogen or nitrogen and phosphorus source	28°C; pH: 7.2; aerobic	Sarcosine pathway	60% degradation (10 mM) within 10 days	(Obojska et al., 1999)

Fungi						
<i>Aspergillus niger</i>	Soil	Sole phosphorus source	28°C; pH: 6; aerobic	AMPA pathway	No data for removal efficiency	(Krzyśko-Lupicka et al., 1997)
<i>Aspergillus oryzae</i> sp. A-F02	Sludge in an aeration tank of a glyphosate manufacture	Sole carbon source	30°C; pH: 7.5; aerobic	Not shown	86.82% degradation (1000 mg.L ⁻¹) within 7 days	(Wu et al., 2010)
<i>Fusarium oxysporum</i>	Sugar cane	Sole phosphorus source	30°C; pH: 6; aerobic	Not shown	41% glyphosate (50 mg.L ⁻¹) removal	(Castro et al., 2007)
<i>Penicillium chrysogenum</i>	Soil	Sole nitrogen source	Dark at 28 (±1) °C; pH:7.0; aerobic	AMPA pathway (putatively)	40% degradation (5 mM) after 15 days	(Klimek et al., 2001)
<i>Penicillium notanum</i>	Spontaneous growth on hydroxyfluorenyl-9-phosphate	Sole phosphorus source	28°C; pH: 7.2; aerobic	AMPA pathway	Capable to degrade glyphosate at sublethal doses (<0.5 mM)	(Bujacz et al., 1995)
<i>Scopulariopsis sp.</i>	Soil	Sole phosphorus source	28°C; pH: 6; aerobic	AMPA pathway	No data for removal efficiency	(Krzyśko-Lupicka et al., 1997)
<i>Trichoderma harzianum</i>	Soil	Sole phosphorus source	28°C; pH: 6; aerobic	AMPA pathway	No data for removal efficiency	(Krzyśko-Lupicka et al., 1997)

1.3.4 Advanced oxidation processes (AOPs)

AOPs are promising technologies, which have been widely used for the treatment of toxic, recalcitrant organic compounds in water (Divyapriya et al., 2016), including photolysis, ozonation, Fenton, electro-oxidation, wet air oxidation (WAO) and supercritical water oxidation. The mechanism in AOPs system is to oxidize organic contaminants to CO₂, H₂O and inorganic ions due to the generation of hydroxyl radical ($\cdot\text{OH}$), hydrogen peroxide (H₂O₂), and superoxide (O₂ \cdot^-) in the system (Malato et al., 2002; Manassero et al., 2010). The hydroxyl radical ($\cdot\text{OH}$) is a non-selective, strong oxidant (2.8 V oxidation potential), which can act very fast on a wide range of organic compounds (Mota et al., 2008; Divyapriya et al., 2016). Compared to conventional treatment, AOPs can non-selective completely mineralized pollutants without chemical or biological sludge production.

AOPs could be an alternative technology to effectively treat glyphosate at a short time compared to physical (adsorption and filtration) and biological treatment. Recently, single or combined AOPs have been reported to treat glyphosate-containing wastewater, such as photolysis oxidation, Fenton oxidation, electrochemical oxidation, ozonation oxidation, and combined oxidation process. Table 1.7 summarizes some AOPs process used for glyphosate treatment.

Table 1.7 shows that photolysis-based oxidation can lead to high glyphosate removal efficiency up to 99.8% at low concentration (less than 50 mg.L⁻¹) and the use of photocatalyst improve the photodegradation of glyphosate. TiO₂ is the common used heterogeneous photocatalyst for glyphosate photocatalytic degradation because of its stability, non-toxic and low cost (Echavia et al., 2009). In order to improve the photocatalytic activity of TiO₂, several attempts have been reported, such as non-metal doping (Echavia et al., 2009), metal doping (Xue et al., 2011) and metal and non-metal codoping (Lin et al., 2012). Although complete glyphosate removal has achieved (Echavia et al., 2009), while, the mineralization efficiency is not high (less than 74%). Meanwhile, the preparation processes for modified TiO₂ are generally complicated, resulting in an increase of the cost. In order to decrease the cost, the combination of hydrogen processes and UV radiation (H₂O₂/UV) has been reported to treat glyphosate with higher concentration (up to 91.26 mg.L⁻¹) compared to photocatalytic degradation, which is a simple and convenient process (Manassero et al., 2010; Junges et al., 2013; Vidal et al., 2015; López et al., 2018). H₂O₂/UV process induced a good degradation of glyphosate (>70%), but it requires a long treatment time (more than 5 h). Meanwhile, due to the high cost of electricity associated with using energy-consuming UV lamps (Echavia et al., 2009), the disposal of catalysts and difficulties to control the conditions (Zhan et al., 2018) hamper the development of these photolysis-based processes at large scale application (Tran et al., 2017).

Table 1.7 Some AOPs process reported to be used for glyphosate treatment

Refer.	Type	Conditions	Glyphosate concentration (mg.L ⁻¹)	Remarks
(Chen et al., 2007)	Photodegradation	T: 22°C; pH: 3.5-6; illumination time: 3 h; the presence of Fe ³⁺ and C ₂ O ₄ ²⁻	5.0	Maximum degradation efficiency: 63.2%
(Chen and Liu, 2007)	Photocatalytic degradation	Catalyst: TiO ₂ ; T: 30°C; pH: 2-12; illumination time: 0.5-3.5 h	0.042	Maximum degradation efficiency: 92.0%
(Echavia et al., 2009)	Photocatalytic degradation	Catalyst: TiO ₂ immobilized on silica gel; T: 22 °C ; illumination time: 2 h	16.9	Glyphosate conversion: 100%; TOC conversion: 74%
(Yang et al., 2018)	Photocatalytic degradation	Catalyst: Goethite or magnetite; T: 20 °C ; pH: 3-9; illumination time: 2 h	10	Maximum glyphosate removal: 92.0% for goethite and 99.3% for magnetite
(Manassero et al., 2010)	H ₂ O ₂ /UV	T: 25°C; pH : 3.5-10; illumination time : 5 h	27.04-91.26	Maximum glyphosate conversion: 70%; TOC conversion: 29%
(Junges et al., 2013)	H ₂ O ₂ /UV	T: 20°C; pH: 5.2; illumination time: 2-6 h	50	Maximum glyphosate conversions: 90%; TOC conversion: 70%
(Liao et al., 2009)	Fenton	T: 90°C; pH: 3-4; reaction time: 2 h; n(H ₂ O ₂)/n(Fe ²⁺)=4:1	-	TP removal: 95.7%; COD removal: 62.9%
(Zhang et al., 2011)	Adsorption-Fenton	Adsorbent: nano-tungsten/D201 resin; pH: 2-4	258	Maximum glyphosate degradation: 60.5%
(Balci et al., 2009)	Electro-Fenton	Mn ²⁺ as catalyst; T: 23±2°C; pH: 3; anode: Pt cylindrical mesh; cathode: carbon felt; electrolyte: 0.05 M Na ₂ SO ₄ ; current: 100 mA	16.9	Complete glyphosate removal at 3 h; 82% TOC reduction in 5 h
(Lan et al., 2016)	Electro-Fenton	room temperature; pH 3-6; anode: RuO ₂ /Ti mesh; cathode: activated carbon fiber; electrolyte: 0.1 M Na ₂ SO ₄ ; current: 0.12-0.36 A	16.9-253.5	85% glyphosate removal after 2 h; 72% COD removal in 6 h
(Huston and Pignatello, 1999)	Photo-Fenton	T: 25°C; pH: 2.8; reaction time: 2 h; H ₂ O ₂ : 0.01 M; Fe ³⁺ : 5.0×10 ⁻⁵ M; UV irradiation: 300-400 nm	0.034	TOC removal: 35.0%
(Souza et al., 2013)	Photo-Fenton	T: 40±2°C; pH 2.8±0.2; reaction time: 2; H ₂ O ₂ : 10.3 M; Fe ²⁺ /Fe ³⁺ : 0.27 M; oxalate: 1.3 M; UV irradiation: 320-400 nm	100	Complete glyphosate removal; TOC removal: 74.4%
(Aquino Neto and de Andrade, 2009)	Electrochemical oxidation	Anode: RuO ₂ and IrO ₂ DSA [®] ; T: 25±1°C; pH: 3; current density: 50 mA cm ⁻² ; electrolyte: Na ₂ SO ₄	1000	Highest glyphosate and TOC removal: 65% and 43%, respectively after 12 h
(Lan et al., 2013)	Electrochemical oxidation	Anode: RuO ₂ and IrO ₂ DSA [®] ; room temperature; pH: 5.0; current density: 10 mA.cm ⁻² ; MnO ₂ dosage: 0.25 mM; reaction time: 2 h; electrolyte: Na ₂ SO ₄	16.9	40% and 80% glyphosate removal for electrochemical and electro-MnO ₂ process
(Kukurina et al., 2014)	Electrochemical oxidation	Anode: PbO ₂ ; room temperature; current density: 0.12 A.cm ⁻² ; reaction time: 4 h; electrolyte: H ₂ SO ₄	16.9	Completely glyphosate mineralization

(Rubí-Juárez et al., 2016)	et	Electrochemical oxidation	Anode: Born doped diamond; room temperature; natural pH; current density: 10-100 mA.cm ⁻² ; electrolyte: Na ₂ CO ₃ , Na ₂ SO ₄ , NaCl	100	Complete glyphosate mineralization in NaCl media
(Speth, 1993)		O ₃	Gas flowrate: 0.62 L.min ⁻¹ ; O ₃ : 1.0-2.9 mg.L ⁻¹	0.8-1	Complete glyphosate degradation
(Assalin et al., 2009)	et al.,	O ₃	O ₃ : 14 mg.L ⁻¹ ; pH: 6.5 and 10; reaction time: 30 min	42.275	97.5% TOC reduction
(Jönsson et al., 2013)	et al.,	O ₃ /H ₂ O ₂	T: 15°C; O ₃ : 0.5 and 1.0 mg.L ⁻¹ ; H ₂ O ₂ : 0.5 and 1.0 mg.L ⁻¹	0.00259-0.00365	>99% glyphosate and >85% AMPA removal
(Barrett and McBride, 2005)	and	Manganese oxidation	Room temperature; pH: 5.0-7.0; Mn ²⁺ : 0.5 mM; electrolyte: NaNO ₃	10.5	71% glyphosate and 47% AMPA degradation

Fenton based oxidation (Table 1.7) has been reported to be a successful technology for glyphosate treatment, which has the advantages of simple operation, no mass transfer limitation and easy implementation as a stand-alone or hybrid system and easy integration in existing water treatment processes (Chen et al., 2007; Bokare and Choi, 2014). 95.7% and 62.9% removal of total phosphate and chemical oxygen demand (COD), respectively, have been achieved by conventional Fenton process (Liao et al., 2009). However, several drawbacks exist in conventional Fenton process: the continuous loss of oxidants and iron ions, the formation of solid sludge and the high costs and risks associated with handling, transportation and storage of reagents (Zhang et al., 2019). In order to overcome these shortcomings, Fenton process is improved to form various optimized Fenton processes for glyphosate treatment, i.e. electro-Fenton (Balci et al., 2009; Lan et al., 2016) and photo-Fenton processes (Huston and Pignatello, 1999; Souza et al., 2013). Electro-Fenton process overcomes the limitations of the accumulation of iron sludge and the high costs and risks related to the handling, transportation, and storage of reagents. Photo-Fenton process can reduce iron sludge production (Zhang et al., 2019). Electro-Fenton and photo-Fenton processes have both reported to achieve complete glyphosate removal and good mineralization at low concentration (Balci et al., 2009; Souza et al., 2013). However, electro-Fenton consumes extensive anode (Aramyan, 2017; Zhang et al., 2019). Photo-Fenton process faces several challenges, such as short working life span, high energy consumption and economic costs (Aramyan, 2017; Zhang et al., 2019). Moreover, Fenton based process needs an acidic reaction condition (usual pH at 2-4). This consumes a lot of acid along with high cost due to extra electrical energy (UV lamp). Thus, Fenton-based processes are generally used in a synthetic and low concentration glyphosate wastewater rather than real wastewater from the glyphosate production (Huston and Pignatello, 1999; Balci et al., 2009; Liao et al., 2009; Souza et al., 2013).

Electrochemical oxidation is one of the cleanest technologies to effectively degrade glyphosate compared to other AOPs (Villamar-Ayala et al., 2019), with high energy efficiency and easy operations (Sirés et al., 2014). And electrochemical oxidation has been reported to treat effluents with wider glyphosate concentration ranging from 16.9 to 1000 mg.L⁻¹, compared to other AOPs. Complete glyphosate mineralization has been achieved by electrochemical oxidation at glyphosate concentration less than 100 mg.L⁻¹ (Kukurina et al., 2014; Rubí-Juárez et al., 2016). Even when the initial glyphosate concentration up to 1000 mg.L⁻¹, high mineralization (91%) was also obtained by Aquino Neto and De Andrade (2009), on PuO₂ and IrO₂ dimensionally stable anode (DSA[®]). PbO₂, boron doped diamond (BDD) and Ti/PbO₂ have been also used as anode for electrochemical oxidation of glyphosate (Kukurina et al., 2014; Rubí-Juárez et al., 2016; Farinos and Ruotolo, 2017; Tran et al., 2017). Electrochemical degradation could be affected by several parameters: pH, glyphosate initial

concentration, supporting electrolyte nature and concentration, electronic composition, electrolysis and current density (Aquino Neto and de Andrade, 2009; Aquino Neto and De Andrade, 2009; Moreira et al., 2017). However, some drawbacks exist during electrochemical oxidation process: the high costs related to the electrical supply, the addition of electrolytes required due to the low conductance of wastewaters and the loss of activity and the short lifetime of electrode by fouling due to the deposition of organic compounds on the surface of electrode (Sirés et al., 2014). More research should be studied to overcome these disadvantages.

Compared to other AOPs, ozonation oxidation can effectively treat glyphosate-containing wastewater at a shortest time under low concentration. Complete glyphosate degradation and 97.5% mineralization have been obtained by Speth (1993) and Assalin et al. (2009), respectively. Both high removal efficiencies of glyphosate (>99%) and AMPA (85%) were achieved with simultaneous use of O₃ and H₂O₂ under a short reaction time (Jönsson et al., 2013). However, it is generally applied to treat glyphosate-containing wastewater at low concentration rather than real glyphosate industrial wastewater. Furthermore, there are several drawbacks for ozonation which hinders its application into practice: (1) ozone is unstable under normal conditions; (2) due to its low solubility in water, special mixing techniques are needed; (3) ozone water treatment is much expensive due to the high service and maintenance; (4) high toxicity and chemical hazards; (5) harmful disinfection by-products maybe generate (Rice, 1996).

In addition, Barrett and McBride (2005) obtained 71% and 47% of glyphosate and AMPA removal efficiency by Manganese oxidation, respectively. Zhang et al. (2011) combined adsorption treatment and Fenton oxidation using the nano-metal/resin complexes as the adsorbent to treat the industrial wastewater containing glyphosate. They found that the maximum degradation rate of glyphosate (258 mg.L⁻¹) was enhanced up to 60.5%. Xing et al. (2018) reported that 100% glyphosate removal and over 93% organic phosphorus removal for real glyphosate wastewater (containing 200-3000 mg.L⁻¹ glyphosate) was achieved by catalytic wet oxidation using modified activated carbon as a catalyst in a co-current upflow fixed bed reactor, which could be a potential method for glyphosate-containing wastewater treatment.

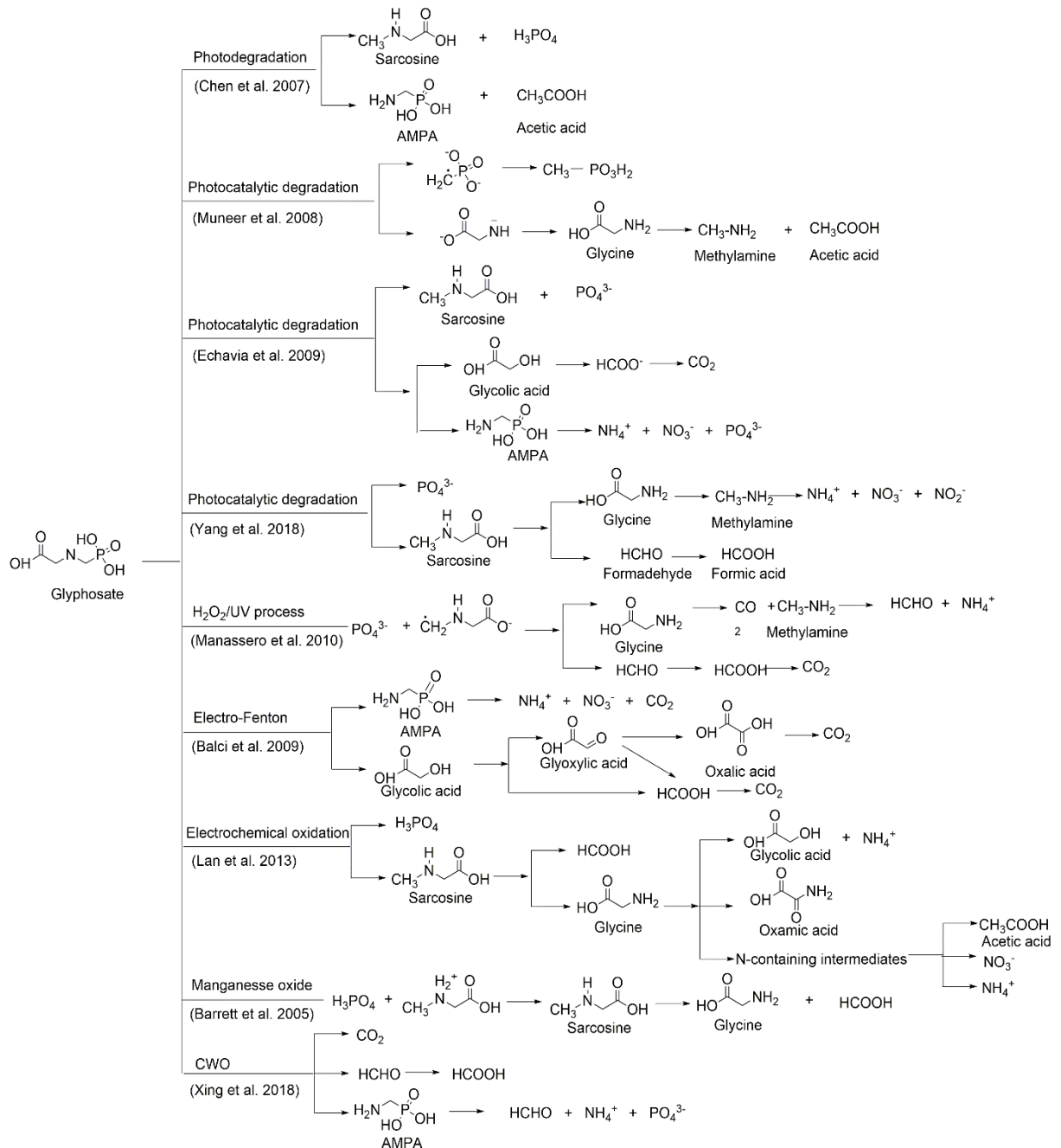


Fig. 1.7 The possible oxidation pathway of glyphosate under different processes. Information based on (Barrett and McBride, 2005; Chen et al., 2007; Muneer and Boxall, 2008; Balci et al., 2009; Echavia et al., 2009; Manassero et al., 2010; Lan et al., 2013; Xing et al., 2018; Yang et al., 2018)

Meanwhile, Fig. 1.7 summarizes the possible oxidation pathway of glyphosate under different AOPs reported in the literature. It shows that glyphosate oxidation process generally follows two mechanisms related to the cleavage of C-P and C-N bonds attributed to hydroxyl radicals. In the first case, glyphosate is attacked by hydroxyl radicals to yield sarcosine and PO₄³⁻ and to generate AMPA and glycolic acid in the second case. The two mechanisms can exist alone or together during glyphosate oxidation process. The glyphosate photo-degradation are often related to the both AMPA and sarcosine pathways, however, only sarcosine pathway during glyphosate photo-degradation is presented by Yang et al. (2018) on goethite and magnetite. This is because the formation of Fe-O-P

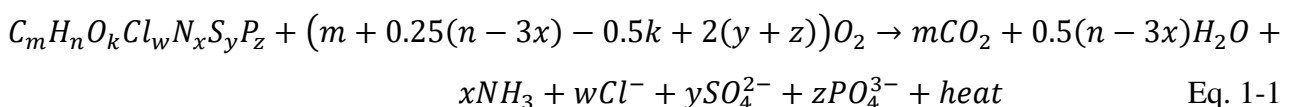
bond in the presence of iron oxide would change the electron density distribution around the phosphorus center of glyphosate, and potentially induce the C-P bond more assailable to reactive oxygen species generated in goethite and magnetite suspension under UV irradiation (Yang et al., 2018). Besides, a few studies have proved the direct generation of glycine at high pH without the generation of sarcosine in TiO₂/UV process (Muneer and Boxall, 2008; Manassero et al., 2010). The mechanism for this phenomenon is still unclear and further research is needed. The single sarcosine pathway is also been reported in the electrochemical and Manganese oxidation of glyphosate (Barrett and McBride, 2005; Lan et al., 2013), whereas, the single AMPA pathway is found in electro-Fenton and CWO process of glyphosate (Balci et al., 2009; Xing et al., 2018). Sarcosine could be further oxidized to glycine, formaldehyde or formic acid. Glycine could be transferred to methylamine, formaldehyde, and NH₄⁺. AMPA may be further converted to formaldehyde, NH₄⁺, NO₃⁻ and PO₄³⁻ through the cleavage of C-P bond. Other small molecules organic compounds may also exist in the glyphosate oxidation processes, such as acetic acid and glycolic acid. Even though the possible oxidation pathways of glyphosate have been abundantly reported, the precise mechanisms are still unknown which is needed further studies.

In conclusion, adsorption and filtration can't transfer glyphosate to other products nor reduce its toxicity, causing that post-treatment may be needed. The conventional biological processes is a friendly and low-cost glyphosate treatment technology, however, these processes generally require a long residence time. Furthermore, industrial wastewater emitted from glyphosate-manufacturing factory is characteristic of high COD, strong toxicity, poor biodegradability and complicated constituents, which can't be effectively treated directly using biological treatment (Xing et al., 2017). AOPs takes advantages of degrading glyphosate with high reaction rate and efficiency at low concentration. However, the main disadvantages for AOPs are their high treatment cost caused by the high consumption of electrical energy for devices, such as UV lamps, heater, and ozonizers, and long processing times and AOPs tend to be difficult for complete chemical mineralization of glyphosate due to the formation of the oxidation intermediates during treatment. Thus, to develop a more effective, safe and affordable technology to degrade glyphosate is necessary. Recently, combining AOPs and biological processes has been a promising treatment technology for organic compounds, considering environmental and economic advantages (Mantzavinos and Kalogerakis, 2005). The toxic and/or non-biodegradable effluent is first treated by AOPs during a short time to generate easily biodegradable intermediates which can be completely degraded by a subsequent biological treatment (Azabou et al., 2010). Among different AOPs, wet air oxidation (WAO) is a very promising technology to treat organic contaminants due to its fast reaction rate and high efficiency (Chakchouk et al., 1994; Lin and Chuang, 1994; Kaçar et al., 2003; Suarez-Ojeda et al., 2005). It is reported that

the compact process coupling WAO and biological treatment shows high degradation efficiency for various organic compounds or effluents, such as polyethylene glycol (Mantzavinos et al., 1997), substituted phenols (Suarez-Ojeda et al., 2007), deltamethrin (Lafi and Al-Qodah, 2006), Afyon alcaloide factory's wastewater (Kaçar et al., 2003), olive mill wastewaters (Chakchouk et al., 1994). However, no information regards the application of the combined WAO and biological processes to treat glyphosate-containing wastewater.

1.4 Wet air oxidation

Wet air oxidation (WAO) is an attractive treatment for waste streams containing organic compounds which are too dilute to incinerate and too concentrated for biological treatment (Luck, 1999), which was first proposed by Zimmermann (1954). WAO process is defined to oxidize organic compounds into carbon dioxide and water or less toxic intermediates at elevated temperatures and pressure by using oxygen or air as oxidants (Mishra et al., 1995; Luck, 1999; Debellefontaine and Foussard, 2000). Typical conditions for WAO process are 398-573 K for temperature, 0.5-20 MPa for a total pressure, 15-120 min for residence times and 10-150 g.L⁻¹ for the preferred COD load (Debellefontaine and Foussard, 2000; Lefèvre et al., 2011a, 2011b; Lefevre et al., 2012). The elevated temperature enhances the solubility of oxygen in aqueous solutions and the elevated pressure is to keep water in the liquid state and provide a strong driving force for gas-liquid transfer and oxygen solubility (Mishra et al., 1995). The oxygen used for WAO reactions is provided by air bubbled through the liquid phase in the reactor (Joglekar et al., 1991). WAO is one of the few processes which do not transfer contaminants from one form to another, but really make it disappear (Debellefontaine et al., 1996). Organic carbon is oxidized to small acid chains and CO₂; organic nitrogen is converted to ammonia, nitrite, or elemental nitrogen; sulfur is turned to sulfuric acid or sulfates; phosphorus and chlorine are transferred to phosphate and hydrochloric acid, respectively (Mishra et al., 1995; Debellefontaine and Foussard, 2000). Therefore, the general element balance for the WAO process can be described by Eq. 1-1 with the heat value about 435 kJ (mol O₂ reacted)⁻¹ (Debellefontaine and Foussard, 2000):



The oxidation degree mainly depends on temperature, oxygen partial pressure, reaction time, and the oxidizability of the contaminants under consideration. The previous researches have reported WAO process used for single organic compounds or real wastewater.

1.4.1 WAO for single organic compounds treatment

Table 1.8 summarize available literature studies on the treatment of single organic compounds by WAO process. It depicts that WAO process could achieve high degradation efficiency (more than 80%) to treat carboxylic acids, phenolics and dyes at a short time (always less than 2 h). However, the complete mineralization cannot always be achieved by WAO process for these compounds due to the high TOC or COD remaining, which need to be further treated to meet the discharge standard. Many studies have reported that the biodegradability of effluents treated by WAO process is improved, which could be easily treated by a following biological treatment (Patterson et al., 2002; Kaçar et al., 2003; Suárez-Ojeda et al., 2008). Among these organic compounds, phenolic substances have attracted more attention due to their toxicity and frequency of industrial wastewaters. However, there is no information reported on the glyphosate degradation by WAO process.

1.4.2 WAO for real industrial wastewater treatment

Many researches have focused on the feasibility of WAO process to treat real wastewater. Some studies on the real industrial wastewater treatment by WAO process are summarized in Table 1.9. It can be seen that WAO process has been applied to treat many kinds of wastewater, such as emulsified waster, 2,4,6-Trinitrotoluene (TNT) red wastewater, chemical wastewater, desizing wastewater, paper mills wastewater, Afyon alcaloide factory's wastewater, and pesticide wastewater. These wastewaters generally belong to the typical high concentration of hardly biodegradable wastewater. WAO process could achieve high COD or TOC removal for these wastewaters, while complete COD or TOC reduction couldn't always be achieved. Therefore, the effluent quality cannot meet the discharge standards. However, the biodegradability of the wastewater is greatly improved after WAO treatment, thus providing good conditions for further biological treatment (Luan et al., 2017). For instance, Lei et al. (2000) investigated the WAO of desizing wastewater from the textile industry and found that BOD₅/COD was increased from 0.05 to 0.8, indicating that the biochemical nature of effluent was greatly enhanced.

Table 1.8 Available literature studies on the treatment of single compounds by WAO process

Refer.	Pollutants	Conditions	Remarks
Carboxylic acids			
(Shende and Levec, 2000)	Acrylic acid	$T=523-563$ K, $P_{O_2}=3.0-5.5$ MPa	78% TOC reduction (3 MPa, 563K, 2 h)
(Shende and Levec, 1999)	Formic acid	$T=513-542$ K, $P_{O_2}=0.8-2$ MPa	90% formic acid removal (0.8 MPa, 542 K, 2 h)
(Shende and Mahajani, 1997)	Formic acid	$T=423-513$ K, $P_{O_2}=0.345-1.38$ MPa	95% COD reduction (0.69 MPa, 513 K, 20 min)
(Shende and Mahajani, 1994)	Glyoxalic acid	$T=393-518$ K, $P_{O_2}=0.345-1.38$ MPa	About 95% COD reduction (0.690 MPa, 473 K, 100 min)
(Shende and Levec, 1999)	3-hydroxypropionic acid	$T=523-583$ K, $P_{O_2}=1-4.5$ MPa	99.9% 3-hydroxypropionic acid removal (1 MPa, 573 K, 1 h)
(Shende and Levec, 2000)	Muconic acid	$T=513-533$ K, $P_{O_2}=2.0-4.0$ MPa	72.7% of TOC removal (2 MPa, 533 K, 2 h)
(Day et al., 1973)	Propionic acid	$T=505-561$ K, $P_{O_2}=1.72-5.17$ MPa	55% TOC removal (3.45 MPa, 533 K, 100 min)
(Shende and Levec, 1999)	Oxalic acid	$T=493-523$ K, $P_{O_2}=0.8-2.2$ MPa	72% TOC reduction (1.5 MPa, 493 K, 2 h)
Phenolic compounds			
(Pruden and Le, 1976)	Phenol	$T=473-523$ K, $P_{O_2}=5-15$ MPa	99% phenol removal (15 MPa, 523 K, 15 min)
(Willms et al., 1987)	Phenol	$T=415-439$ K, $P=13.8$ MPa	100% phenol degradation (439 K, 2.5 ks)
(Joglekar et al., 1991)	Phenol	$T=423-453$ K, $P_{O_2}=0.3-1.5$ MPa	~ 99.9% phenol and ~ 90% COD removal (0.5 MPa, 453 K, 2 h)
(Lin and Chuang, 1994a)	Phenol	$T=423-573$ K, $P_{O_2}=10.3$ MPa	100% COD reduction (573 K, 1 h)
(Kolaczowski et al., 1997)	Phenol	$T=473$ K, $P=3.0$ MPa	95% phenol destruction (30 min)
(Wu et al., 2001)	Phenol	$T=423-473$ K	85% TOC removal (473 K, 80 min)
(Vicente et al., 2002)	Phenol	$T=443-493$ K, $P_{O_2}=5.10-10.15$ MPa	Complete phenol degradation (10.15 MPa, 493 K, 10 min)
Lefèvre et al. (2011)	Phenol	$T=423-573$ K, $P=30$ MPa	Complete phenol removal (573 K, 10 min)
Minière et al. (2017)	Phenol	$T=523$ K, $P=30$ MPa	97% phenol removal and 84% TOC reduction (15 min)
(Chang et al., 1995)	2-chlorophenol	$T=483$ K, $P_{O_2}=3.55$ MPa	99% 2-chlorophenol removal (1 h)
(Baillod et al., 1982)	2-chlorophenol	$T=477-533$ K, $P_{O_2}=0.34$ MPa	~ 80% TOC reduction (533 K, 1 h)
(Wilhelmi and Knopp, 1979)	2-chlorophenol	$T=548$ and 593 K	94.96% 2-chlorophenol degradation (548 K)
(Wilhelmi and Knopp, 1979)	4-nitrophenol	$T=548$ and 593 K	99.6% 4-nitrophenol removal (548 K)
(Wilhelmi and Knopp, 1979)	pentachlorophenol	$T=548$ and 593 K	81.96% pentachlorophenol reduction (548 K)
(Imamura, 1999)	<i>o</i> -cresol	$T=493$ K, $P_{O_2}=3$ MPa	78% TOC and 86% COD reduction (2 h)
(Misra et al., 1993)	<i>p</i> -cresol	$T=423-498$ K, $P_{O_2}=0.69-1.34$ MPa	54.95% COD destruction (498 K, 2 h)
Dyes			
(Minière et al., 2018)	Acid orange 7	$T=473-573$ K, $P=30$ MPa	Complete acid orange 7 degradation and 87% TOC removal
(Hu et al., 2001)	Acid red 97 dye	$T=423$ and 473 K	80% TOC removal
(Zhou and He, 2007)	Azo dye and cationic red X-GRL	$T=393-453$ K, $P_{O_2}=0.5-1.5$ MPa	35.4% COD removal
(Lei et al., 2007)	Azo dye cationic red X-GRL	$T=333-453$ K, $P_{O_2}=0-1.2$ MPa	92% dye degradation
(Chen et al., 1999)	Reactive dyes	$T=423$ K	70% TOC reduction

Table 1.9 Summary of literature on WAO of real industrial wastewater

Refer.	Type of real wastewater	Conditions	Remarks
(Tang et al., 2000)	Emulsified wastewater	$T=493$ K	86.4% COD reduction
(Zeng et al., 2004)	Emulsified wastewater	$T=493$ K	TOC removal up to 82.1%
(Lu et al., 2007)	TNT red wastewater	$T=473$ K, $P_{O_2}=4$ MPa	98.10% COD reduction
(Hao et al., 1993)	TNT red wastewater	$T=613$ K, $P_{O_2}=0.8$ MPa	77% TOC removal and 91% COD reduction
(Hao et al., 1994)	TNT red wastewater	$T=498$ K, $P_{O_2}=3$ MPa	71.3% COD removal
(Lin and Ho, 1997)	Chemical wastewater	$T=513-533$ K, $P_{O_2}=2.0-4.0$ MPa	50% COD destruction
(Lei et al., 2000)	Desizing wastewater	$T=423-563$ K, $P_{O_2}=0.375-2.25$ MPa	77% TOC removal and 91% COD reduction
(Verenich et al., 2000)	Paper mills wastewater	$T=403-473$ K, $P_{O_2}=1$ MPa	80% of TOC and COD reduction
(Kaçar et al., 2003)	Afyon alcaolide factory's wastewater	$T=418$ K, $P=0.56$ MPa	33.2% COD removal
(Zhang et al., 2007)	Pesticide wastewater	$T=553$ K, $P_{O_2}=4.2$ MPa	98% COD destruction

P_{O_2} : partial oxygen pressure; P : total pressure

1.4.3 Reaction mechanisms

Reaction mechanisms and pathways for WAO process are not clear even for a pure organic compound due to the very complicated routes and the formation of various intermediates (Luan et al., 2017). Generally, the final molecules are short-chain organic compounds, such as acetic acid (Day et al., 1973; Mantzavinos et al., 1997). However, it has been proposed that WAO occurs mostly via a chain reaction mechanism in which hydroxyl, oxygen, hydroperoxyl and organic hydroperoxyl free radicals actively participate (Kolaczowski et al., 1999). The reaction mechanisms for WAO process consist in several free radical reactions, such as initiation, propagation, and termination of free radical (Mantzavinos et al., 1997; Patterson et al., 2002; Robert et al., 2002; Bhargava et al., 2006;). A direct experimental evidence of the presence of free-radical intermediates was obtained by Robert et al. (2002) in the WAO of cellulose using electron spin resonance spectroscopy coupled to a spin trapping technique. Moreover, several methods have provided indirect experimental evidence: (1) co-oxidation, which involves the oxidation of an organic compound by free radical intermediates produced from another organic compound (Mantzavinos et al., 1996; Birchmeier et al., 2000; Raffainer and Rudolf von Rohr, 2001; Tardio et al., 2004); (2) to hinder the free radical reactions using inhibitors, such as *tert*-butyl alcohol (Stöffler and Luft, 1999; Vaidya and Mahajani, 2002); (3) to use a free radical promoter like hydrogen peroxide (Chang et al., 1995).

1.4.4 Reaction kinetics for WAO

WAO reactions for organic compounds have been extensively studied in laboratory batch reactors for kinetic purposes under a wide range of temperatures and pressures. The global reaction kinetic model is useful to understand the reaction mechanisms for pure compounds, while it is not sufficient for real wastewaters which contains a mixture of organic compounds. More detailed kinetic models are required for WAO of real wastewaters to describe the reaction rate. Thus, the reaction rate

has to be expressed by lumped parameters, such as TOC and COD (Luan et al., 2017), which could be as a verification of the generation of intermediates during WAO process.

Table 1.10 Global kinetic models for WAO of organic compounds

Refer.	Pollutants	Conditions	Activation energy (kJ.mol ⁻¹)	Pollutants order	Oxygen order
(Foussard Jean-Noël et al., 1989)	Acetic acid	$T=543-593$ K, $P=2.0-20$ MPa	167.7	1.0	0.37
(Shende and Mahajani, 1997)	Formic acid	$T=423-513$ K, $P_{O_2}=0.35-1.38$ MPa	121.3 ^a	1.0	0.86
(Shende and Levec, 1999)	3-hydropropionic acid	$T=523-583$ K, $P_{O_2}=1-4.5$ MPa	135	1.0	0.5
(Foussard Jean-Noël et al., 1989)	Oxalic acid	$T=500-561$ K, $P=2.0-20$ MPa	133.8	1.0	0.31
(Shende and Mahajani, 1994)	Oxalic acid	$T=498-518$ K, $P_{O_2}=0.69-1.03$ MPa	129.4 ^a	1.0	0.32
(Pruden and Le, 1976)	Phenol	$T=473-523$ K, $P=5-15$ MPa	45.2	1	1
(Helling et al., 1981)	Phenol	$T=458-503$ K, $P_{O_2}=10.4-15.6$ MPa	33.1	1	0
(Harris et al., 1983)	Phenol	$T=448-493$ K, $P_{O_2}=9.3$ MPa	93.3	1	0
(Joglekar et al., 1991)	Phenol	$T=423-453$ K, $P_{O_2}=0.3-1.1$ MPa	50 ^c	1	1
(Kolaczowski et al., 1999)	Phenol	$T=418-483$ K, $P=2.0-4.5$ MPa	92 148 ^a	1	1.07
(Day et al., 1973)	Propionic acid	$T=505-561$ K, $P_{O_2}=1.72-5.17$ MPa	135	1.43	0.39
(Merchant, 1992)	Propionic acid	$T=523-548$ K	139	1.0	0.0
(Shende and Levec, 1999)	Propionic acid	$T=523-583$ K, $P_{O_2}=1-4.5$ MPa	150 158 ^b	1.0 1.0	0.5 0.61
(Suárez-Ojeda et al., 2007)	Sodium dodecylbenzene sulfonate	$T=453-493$ K, $P_{O_2}=1.5$ MPa	77.3 ^c 74.7 ^d	-	0

^abase on COD concentration. ^bbased on TOC concentration. ^cFirst step. ^dSecond step.

Kinetic data for WAO of organic compounds is summarized in Table 1.10. In most case, a first-order reaction was obtained with respect to the concentration of organic compounds and between zero and one for oxygen. These studies have resulted in a range of values for global kinetic constants with activation energy from 33.1 to 167.7 kJ.mol⁻¹ for different organic compounds. The activation energies with respect to the concentration of organic compounds were smaller than that for TOC or COD concentration (Kolaczowski et al., 1999; Shende and Levec, 1999). Moreover, the activation energies for carboxylic acids were higher than those for organic compounds possessing a lower oxygen content, among them, acetic acid with the highest activation energy of 167.7 kJ.mol⁻¹.

Nevertheless, during WAO process, organic compounds could first degrade to low molecular weight compounds and finally to lower molecular weight carboxylic acids, which is difficult to be further oxidized (Mishra et al., 1995; Shende and Mahajani, 1997). Thus, the oxidation of these acids to carbon dioxide and water often becomes the rate-controlling step in the overall wet oxidation process (Shende and Mahajani, 1997). The global rate of WAO depends on the formation of final

products as well as on the rates of formation and destruction of the intermediates (Debellefontaine and Foussard, 2000). Therefore, Li et al. (1991) proposed a generalized lumped kinetic model (GLKM) based on a simplified reaction scheme with acetic acid as a rate-limiting intermediate (Fig. 1.8). Lump “A” includes parent organics and unstable intermediates, lump “B” contains the refractory intermediates represented chiefly by acetic acid and lump “C” represents end products. k_1 , k_2 , and k_3 , are apparent constants for the chemical reaction rates, which depend on reaction temperature and dissolved oxygen concentration. The GLKM has been applied to evaluate the experimental kinetic in several literature (Jin et al., 2004; López et al., 1999).

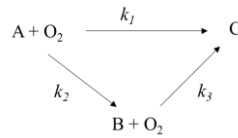


Fig. 1.8 Generalized lumped kinetic model (GLKM) for WAO of organic compounds (Li et al., 1991)

1.4.5 Mass transfer for WAO

WAO process is a heterogeneous reaction and consists of two steps occurring in the overall WAO process: (1) a physical stage, involving oxygen transfer from the gas phase to the liquid phase; (2) a chemical stage, which involves the chemical reaction between the organic compounds and the transferred oxygen or an active species generated from oxygen (Bhargava et al., 2006). Generally, the mass transfer of oxygen across the gas-liquid phase boundary is considered as the combination of resistances between gas and liquid phases, where diffusional resistance is assumed to be concentrated in a thin film either side of the interface (Kolaczowski et al., 1999). Due to the low solubility of oxygen in water, the transport of oxygen in the liquid phase is much slower than that in the gas phase. Thus, the gas phase resistance can be ignored, while the liquid film resistance controls the mass transfer (Pruden and Le, 1976; Kolaczowski et al., 1999).

The overall volumetric gas-liquid mass transfer coefficient ($k_L a$) is represented by the following equation:

$$r_m = k_L a (C_{O_2}^* - C_{O_2,L}) \quad \text{Eq. 1-2}$$

where r_m is the oxygen mass transfer rate, k_L is the liquid mass transfer coefficient, a is the gas-liquid interfacial area, $C_{O_2}^*$ is the saturation oxygen concentration (solubility), and $C_{O_2,L}$ is the oxygen concentration in the bulk liquid.

The oxygen solubility ($C_{O_2}^*$) is enhanced with the increase of the temperature and oxygen partial pressure, which provides a strong driving force for the mass transfer (Kolaczowski et al., 1999; Bhargava et al., 2006). $k_L a$ is affected by operating conditions, such as reactor geometry, temperature,

pressure, gas flowrate and liquid characteristics (Bhargava et al., 2006; Kastánek et al., 1993; Kolaczowski et al., 1999; Shah et al., 1982). In order to achieve minimal limitations of mass transfer for the design of WAO reactor, several aspects should be considered: bubble diameter, gas holdup, gas-liquid interfacial area, liquid mass transfer coefficient, the reactor geometry and the material of construction (Kastánek et al., 1993; Bhargava et al., 2006; Shah et al., 1982; Leonard et al., 2019, 2015).

The smaller size of bubbles in the reactor will be the larger area available for mass transfer (Kolaczowski et al., 1999). The bubble size in the reactor is influenced by sparger type, flow regime, the properties of liquid phase and operation conditions (Kolaczowski et al., 1999). Moreover, for WAO reactor, a large liquid hold-up with sufficient interfacial area is required to avoid mass transfer limitations (Kolaczowski et al., 1999). Gas holdup is defined as the ratio of gas volume to total fluid volume, which determines the extent of interfacial area used for mass transfer (Kastánek et al., 1993). Gas holdup depends on superficial gas velocity and rises the velocity of the bubble (Bhargava et al., 2006; Leonard et al., 2015). Generally, gas holdup increases with the increase of superficial gas velocity (Clark, 1990; Wilkinson et al., 1992; Stegeman et al., 1996; Luo et al., 1999; Lau et al., 2004; Behkish et al., 2007). However, the capital and operating cost will increase accordingly due to the increased pumping requirement (Bhargava et al., 2006). The rise velocity of the bubble is linked to bubble size and liquid characteristics. The smaller bubbles have a slower rise velocity, resulting in a bigger area for mass transfer (Behkish et al., 2007).

Thus, in the design of WAO process for glyphosate, it is necessary to study the effects of temperature and pressure, reaction kinetics and mass transfer.

1.5 Microfluidic device

Microfluidic technology is emerging as a new platform which could manipulate small volumes of fluids in a microchannel network with micro-scale dimensions (Meng et al., 2013). Microfluidic devices have a considerable impact on the fields of drug development and biomedical diagnostics and are also widely applied in the food and chemical industries. The initial uses of microfluidic devices were high throughput screening in microanalytical chemistry (Yi et al., 2014), biological analysis of proteins and cells (Tu et al., 2010), reaction kinetics and mechanisms studies (Sandel et al., 2012; Yao et al., 2015). The diminutive scale of the flow channels in microfluidic systems increases the surface to volume ration, resulting in providing many advantages for their applications (Lee et al., 2011). Microfluidic devices have high mass and heat transfer capabilities, and the contact time, size and shape of the interface between fluids can be easily and precisely controlled (Licklider and Kuhr, 1994; Yao et al., 2015). Furthermore, since the small volume capacity of microfluidic systems greatly

reduces the materials required to optimize reaction conditions, it can be effective to develop more sophisticated continuous flow reaction on increasingly complex molecular targets (Yao et al., 2015).

Microfluidic devices used for chemical reactions have reported to have high yields and conversions and offer better control on mass and heat transfer within the reaction (Suryawanshi et al., 2018), which allows better thermal control if unit operation. It is easy to scale up, scale down or modularize the processes (Scialdone et al., 2010).

In the recent years, microfluidic reactors have been increasingly employed to wastewater treatment over conventional macroscale reactors (Lei et al., 2010; Han et al., 2013; Jayamohan et al., 2016). This is because conventional macroscale reactors have many technical challenges, such as mass transfer limitations, energy consumption, poor management, etc. (Scialdone et al., 2011; Jayamohan et al., 2016; Pérez et al., 2017). The use of microfluidic reactor has the potential to reduce these limitations due to its large surface to volume ratio, smaller diffusion distance, large mass transfer efficiency and easy to control (Scialdone et al., 2011; Jayamohan et al., 2016). The microfluidic devices have been used to photodegradation (Yamada et al., 2010; Yoon et al., 2011; Eskandarloo et al., 2015), electrochemical oxidation (Scialdone et al., 2010, 2011; Pérez et al., 2017) and electro-Fenton oxidation (Scialdone et al., 2013) of organic pollutants to obtain high removal efficiency and reduce mass transfer limitations. Since one of the rate-limiting steps in WAO process is mass transfer of oxygen from the gas phase to the liquid phase due to its low solubility in water (Pruden and Le, 1976; Kolaczowski et al., 1999), WAO performance can be enhanced by the increase of the gas-liquid oxygen mass transfer rate. Therefore, microfluidic device used for WAO process will be a very promising method for the treatment of glyphosate-containing wastewater due to its high mass transfer efficiency. Microfluidic devices can be made in a range of materials, such as stainless steel, ceramics, polydimethylsiloxane (PDMS), polymethyl-methacrylate (PMMA), glass, and silicon, depending on its application (Yao et al., 2015; Das and Srivastava, 2016). Among these, stainless steel microfluidic devices can be operated at high temperature and pressure, which can be potential device for continuous WAO process.

1.6 Coupled advanced oxidation technology and biological treatment to treat emerging contaminants

Wastewater produced in many industrial processes usually contains very complex and toxic organic compounds, which often requires severe remediation treatments (Mantzavinos et al., 1997; Suarez-Ojeda et al., 2007). At present, the various treatment technologies available to treat a variety of polluted aqueous streams are AOPs (UV irradiation, ozonation, wet air oxidation, Fenton, etc.), physical treatment (adsorption, filtration, reverse osmosis, etc.), biological treatment, etc. However,

the biological treatment cannot always give satisfactory results for many industrial wastewaters, because many organic compounds generated from the chemical and related industries are inhibitory, toxic or resistant to biological treatment (Mantzavinos et al., 1999; Suárez-Ojeda et al., 2007). Furthermore, AOPs might become extremely cost-intensive in order to obtain complete destruction of organic compounds. Marco et al. (1997) reported that the investment cost for chemical processes may be 5-20 times higher than biological processes due to the generation of intermediates formed during AOPs treatment which is refractory to be further totally oxidized (Mantzavinos et al., 1999). Due to the combination of both economic and environmental advantages, the coupling of AOPs as pretreatment with biological treatment is a promising technology for complete oxidation of organic compounds (Al Momani et al., 2004; Kotsou et al., 2004; Azabou et al., 2010). The main idea of coupling is to first treat the toxic and/or non-biodegradable effluent by AOPs to generate intermediated which are fully biodegradable, thus achieving the possibility of subsequent biological treatment for the complete degradation of organic compounds (Azabou et al., 2010). Table 1.11 summarizes some integrated AOPs-biological systems for the treatment of various contaminants.

This survey spans treatment problems ranging from single organic contaminant to highly specialized industrial wastewater by different methods to combine AOPs and biological process. The AOPs include UV irradiation, photocatalytic oxidation, Fenton, ozonation, electrochemical oxidation or the combined processes, while biological treatments include pure and mixed, aerobic and anaerobic, acclimated and non-acclimated cultures. Integration of AOPs and biological processes can provide high degradation and mineralization efficiency and environmentally friendly treatment for wastewaters containing a pure organic compound, mixed contaminants or real wastewater which are not readily biodegradable. Most studies on wastewater treatment by combined processes refer to laboratory and pilot scale tests.

In combined AOPs and biological treatment, it is necessary to consider the characteristics of each individual treatment (Oller et al., 2011), such as AOPs type, chemical oxidation capacity (Jones et al., 1985; Lee and Carberry, 1992), the formation of intermediates (Trgovcich et al., 1983; Wang, 1992), choice of biological agent, comparison of different cultures (Lee and Carberry, 1992), comparison of acclimated and non-acclimated culture (Hu and Yu, 1994).

Table 1.11 Integrated AOPs-biological systems for the treatment of various contaminants.

Refer.	Target contaminants	AOPs type	Biological treatment	Remarks
(Torres et al., 2003)	5-amino-6-methyl-2-benzimidazolone (AMBI)	Electrochemical oxidation	Fixed bed biological reactor	100% AMBI degradation; complete mineralization of solution pre-treated.
(Pariante et al., 2008)	Benzoic acid	Photo-Fenton process	Activated biosystem	77% COD reduction
(Stockinger et al., 1995)	Chloro and nitro aromatic wastewater	O ₃	Activated biosystem	Total mineralization of chloro and nitro aromatics
(Al Momani et al., 2004)	2,4-dichlorophenol	Photo-Fenton process	Biological sequencing batch reactor	Complete 2,4-dichlorophenol removal and 70% TOC reduction
(Chen et al., 2009)	di-(2-ethylhexyl) phthalate (DEHP)	Photo-Fenton process	Fixed bed reactor	Complete mineralization; BOD ₅ /COD ratio increased from 0.19 to 0.45
(Park et al., 2001)	Dimethyl sulphoxide	Fenton process	Activated sludge biotreatment	90% TOC removal; BOD ₅ /COD ratio increased from 0.035 to 0.87
(Toor and Mohseni, 2007)	Disinfection byproducts (DBPs)	UV/H ₂ O ₂	Biological activated carbon treatment	43% and 52% reduction for DBPs and TOC, respectively
(Yongrui et al., 2015)	Hydrolyzed polyacrylamide	Fenton oxidation	Anaerobic baffled reactor	Maximum COD and hydrolyzed polyacrylamide removal of 94.61% and 91.06%, respectively
(Lafi and Al-Qodah, 2006)	Pesticides effluents	O ₃ ; O ₃ /UV	Acclimated activated-sludge system	Complete removal of pesticide; >95% COD removal
(Amat et al., 2003)	Phenolic pollutants	O ₃	Activated sludge biotreatment	50% COD removal; biodegradability increased 10 times
(Nadarajah et al., 2002)	Polycyclic aromatic hydrocarbons	Fenton process	A mixed bacteria culture	80-85% of polycyclic aromatic hydrocarbons removal
(Rafin et al., 2009)	Polycyclic aromatic hydrocarbon benzo[a]pyrene	Fenton process	<i>Fusarium solani</i>	25% benzo[a]pyrene degradation
(Bijan and Mohseni, 2008)	Paper mill wastewater	Ozonation (membrane treatment)	pre-Activated biosystem	40-50% complete mineralization of organic compounds
(Ballesteros Martín et al., 2009)	Pesticide mixture	Photo-Fenton process	Activated-sludge batch reactor	Complete removal of pesticide
(Badawy et al., 2009)	Olive mill wastewater	Photo-Fenton process	BOD	87%, 84% and 97.44% of COD, TOC, lignin removal; BOD ₅ /COD increased from 0.19 to 0.8
(Lafi et al., 2009)	Olive mill wastewater	UV/O ₃	Batch aerobic biological system	91% COD removal
(El-Gohary et al., 2009)	Olive mill wastewater	Wet hydrogen peroxide catalytic oxidation	Upflow anaerobic sludge blanket reactor	77% COD removal and 71% TOC removal
(Azabou et al., 2010)	Olive mill wastewater	Wet hydrogen peroxide catalytic oxidation	Anaerobic digestion treatment	The combined treatment enhanced the yield of biogas production.
(Wang et al., 2008)	Surfactant wastewater containing abundant sulfate	Fenton process	Immobilized biomass reactor	94% and 99% of COD and linear alkylbenzene sulfonate removal, respectively
(Kotsou et al., 2004)	Table olive processing wastewater	Fenton process	<i>Aspergillus niger</i>	70% COD removal and 41% total phenolic compounds reduction
(Yan et al., 2010)	Trihalomethanes precursor	Ozonation	Biological activated granular carbon filtration	38% of dissolved organic compounds removal

The AOPs type used in integrated AOPs-biological treatment schemes will determine the oxidation intermediates and thus affect the subsequent biodegradability of the reaction products and the overall effectiveness of the combined system (Scott and Ollis, 1995). With respect to the choice of AOPs type, the appropriate biological process is dependent on the characteristics of the wastewater

and the goal of the treatment (Scott and Ollis, 1995). Table 1.11 shows that pure cultures used for biological treatment in the integrated processes are effective to reduce the concentration of the target compounds. Complete mineralization is generally not achieved, resulting in the accumulation of intermediates and possibly requiring the addition of post-treatment. The mixed cultures represent higher efficiency for organic compounds removal by the combined processes. And an interesting aspect of the biological processes for the combined treatment is the effect of acclimation on the degradation ability (Scott and Ollis, 1995). The acclimation process to the substrate for microorganisms is necessary to maximize the degradation efficiency of specific compounds. This is accomplished by increasing the concentration of substrate over a period of time to achieve the growth of culture which could use the substrate as a carbon, nitrogen, phosphorus or nutrient source (Scott and Ollis, 1995).

The evaluation of the performance of integrated AOPs and biological process depends on the purpose of the treatment, but normally the independent optimization of each AOPs and biological step is required. In order to find the optimal operating conditions for the combined process, it is important to measure the efficiencies of the individual AOPs and biological efficiencies. Thus, several analytical parameters should be monitored during each step for the combined treatment. For AOPs, the parameters generally measured are TOC, COD, the concentration of target compounds and intermediates, and complete oxidation of heteroatoms released (N, P, Cl, etc.) as inorganic species (NH_4^+ , NO_3^- , PO_4^{3-} , Cl^- , etc.) (Oller et al., 2011). It is also important to perform biodegradability tests to ensure the AOP effluent to be successfully treated by the following biological treatment. The biodegradability assessment can be monitored by analysis of general parameters (COD, BOD, dissolved organic carbon), calculation of BOD_5/COD ratio, or oxygen uptake rate (OUR) (Oller et al., 2011). BOD has been used in many studies (Kaçar et al., 2003; Park et al., 2001; Scott and Ollis, 1995). However, BOD measurement has limitations, including the requirement for a suitably active microbial inoculum and the lack of stoichiometric validity over the entire period of the test (Scott and Ollis, 1997). OUR is a rapid alternative method to BOD biodegradability test. The OUR by activated sludge in the presence of organic compounds can be compared to endogenous biomass respiration in a short period of time. This method has been used to assess the biodegradability of chloro- and nitro-aromatic containing wastewaters, phenolic wastewater, textile wastewater, landfill leachate wastewater, etc., treated by AOPs (Stockinger et al., 1995; Amat et al., 2003; Arslan-Alaton et al., 2005; Rubalcaba et al., 2007; Goi et al., 2009). During the biological treatment, it is necessary to analyze several parameters, such as biomass concentration, TOC, COD, pH and dissolved oxygen, etc.

In previous studies, most literature reported on UV irradiation, photocatalysis, ozonation, Fenton, as well as various combination of these process as chemical pretreatment, while relative few studies on WAO as a pretreatment step. Some studies on the treatment of various contaminants by combined WAO with biological treatments are summarized in Table 1.12 It shows that to combine WAO process with activated sludge system is a promising technology to treat organic compound to achieve almost complete mineralization.

Table 1.12 Integrated WAO-biological systems for the treatment of various contaminants.

Refer.	Target contaminants	WAO conditions	Biological treatment	Remarks
(Minière et al., 2017)	Phenol	$T=423-573$ K, $P=30$ MPa	Packed-bed biofilm reactor	99% and 97% phenol and TOC removal, respectively
(Lin and Chuang, 1994a)	Phenolic wastewater	$T=423-573$ K; air flow: 1-1.5 L.min ⁻¹	Acclimated activated sludge system	>99% COD removal
(Suárez-Ojeda et al., 2008)	Substituted phenols	$T=488-538$ K, $P_{O_2}=0.2-0.9$ MPa	Activated sludge biosystem	>86% TOC abatement; maximum readily biodegradable COD fraction: 24% for phenol
(Suarez-Ojeda et al., 2007)	<i>o</i> -cresol	$T=433$ K, $P_{O_2}=0.2$ MPa; catalyst: activated carbon	Activated sludge biosystem	98% COD removal
(Kaçar et al., 2003)	Afyon alcaloide factory wastewater	$T=423$ K, $P_{O_2}=0.65$ MPa	BOD	BOD5/COD ratio increasing from 0.15 to above 0.5
(Patterson et al., 2002)	Linear alkylbenzene sulfonates	$T=453-513$ K, $P_{O_2}=1.5$ MPa	A mixed bacterial culture	Maximum TOC removal: 93.8%; maximum COD reduction: 91.7%
(Otal et al., 1997)	Polyethylene glycol	$T=423$ K, $P_{O_2}=3$ MPa	Continuous fermentation system	93.5% TOC removal
(Kang et al., 2011)	Wastewater from Vitamin B ₆ production	$T=483-543$ K, catalyst: CuO/Al ₂ O ₃	Anaerobic/aerobic biological process	99.3% COD reduction

1.7 Conclusions

The treatment of wastewater containing emerging contaminants is a severe worldwide problem, which requires effective proposals. Glyphosate, as a typical emerging contaminants, has been frequently detected in the aqueous environment, which could cause several adverse effects to plants, animals and humans. Plenty of treatment technologies have been used to remove glyphosate from wastewater. Post-treatment is needed for physical treatment, long residence time is required for biological treatment and incomplete mineralization exists for AOPs.

Bibliographical study shows that it is necessary to find a more effective and safer method to treat glyphosate-containing wastewater. The integrated WAO-biological systems have been reported to be an effective method to treat organic compounds. WAO process as a pretreatment could enhance the biodegradability of effluent which could be successfully treated by the following biological treatment. Thus, in this thesis, a compact process coupling WAO process and biological treatment was developed to treat glyphosate-containing wastewater in order to improve the removal and mineralization efficiency of glyphosate. In order to evaluate the performance of the compact process, the efficiencies of glyphosate degradation by individual WAO and biological process should be studied. Since the oxidation of pollutants by WAO process is controlled by two steps: mass transfer of oxygen from the gas phase to the liquid phase; reaction between pollutants and the dissolved oxygen. Thus, it is necessary to predict and improve the mass transfer efficiency and study the reaction kinetics of glyphosate by WAO process. Microfluidic device is a promising method to reduce the mass transfer limitation and then increase the performance of WAO process, due to its large surface to volume ratio, high mass transfer efficiency, high conversion, and easy control. Moreover, in order to know the degradation mechanisms for glyphosate by the integrated WAO-biological treatment, it is necessary to study the degradation pathways of glyphosate by the compact process.

Thus, main objectives of this thesis are:

- (1) Investigating bubble characteristics under WAO conditions in order to predict mass transfer;
- (2) Elucidating glyphosate degradation by WAO process or biological treatment, as well as its degradation pathways;
- (3) Setting up a microfluidic device for WAO process to treat glyphosate-containing wastewater
- (4) Validating a compact process coupling WAO with biological treatment in order to increase the degradation and mineralization efficiencies of glyphosate from wastewater;
- (5) Proposing a degradation pathway of glyphosate by the compact process;

Therefore, in order to evaluate the performance of the combined process, it is necessary to study the efficiencies of the individual WAO and biological process. For WAO process under high temperature and pressure, the overall oxidation of pollutants is controlled by two steps: mass transfer of oxygen from gas to liquid phase; reaction between pollutants and dissolved oxygen. Thus, in order to design and optimize WAO process, it is necessary to predict the mass transfer efficiency. Due to the low oxygen solubility in water, mass transfer is controlled by gas-liquid transfer, which is significantly affected by bubble properties and a function of specific interfacial area. Thus, to optimize the WAO process on the mass transfer phenomena, it is essential to know the bubble characterization and interfacial area in WAO process at different operating conditions. Bubble

column, a good gas-liquid operation, which has been frequently used to evaluate bubble characteristics and interfacial area due to its simplicity, low operation cost, high thermal stability and high energy efficiency, can be a promising method to predict mass transfer for WAO process. Thus, in next chapter, a small bubble column at laboratory scale was used to study the bubble characteristics and interfacial area under WAO conditions in order to predict the mass transfer of WAO process and scale-up WAO process.

Chapter 2 Bubble characterization and gas-liquid interfacial area in two phase gas-liquid system in bubble column at low Reynolds number and high temperature and pressure

This chapter has been published in the journal “Chemical Engineering Research and Design” (Volume 144, April 2019, Pages 95-106, DOI: 10.1016/j.cherd.2019.02.001).

Abstract

Bubbles hydrodynamic in gas liquid contactor, including bubble size distribution, bubble size and gas-liquid interfacial area, was evaluated as a function of superficial gas velocity, superficial liquid velocity, temperature, pressure and different gases (N₂ and He) and liquids (water and ethanol/water mixture) phases. The results showed that with the increase of superficial gas velocity, the bubble size distribution shifted from smaller- to larger-size bubble and the Sauter mean diameter, the gas holdup and the interfacial area generally increased due to the increase of coalescence. The effect of superficial liquid velocity on bubble characteristics was not significant. Pressure and temperature showed slight influence on gas holdup and interfacial area. The bubble characteristics were not significantly influenced by the type of gas phase, but mainly affected by the liquid composition. Correlations to predict Sauter mean bubble diameter and the gas holdup are developed using Kanaris correlation and in good agreement with experimental results.

Keywords: Bubble column; bubble size distribution; gas holdup; interfacial area; wet air oxidation

2.1 Introduction

Bubble columns are widely used in many industrial gas-liquid operations (*e.g.* wet air oxidation, gas/liquid reactions, fermentations, agitation by gas injection) in chemical and biochemical industries due to their simple construction, no mechanically moving parts, low operating cost, high thermal stability, high-energy efficiency and good mass transfer capabilities (Kanaris et al., 2018). Most research for bubble columns focused on ambient conditions, while many industrial bubble columns are operated at extreme conditions with high temperatures and pressures (Pohorecki et al., 2001 ; Léonard, 2015). Among the different processes operated in bubble columns, Wet Air Oxidation (WAO) is for instance widely recognized as one of the most efficient technology for wastewater treatment with high pollutant removal efficiency and less toxic by-products (Barge and Vaidya, 2018). WAO accomplishes oxidation at high temperature (up to 325°C) and high pressure (up to 30MPa) (Leonard et al., 2015). To design and optimize WAO processes, it is necessary to predict the mass transfer efficiency in the bubble column. However, in the literature, almost no papers reported bubble columns studies under WAO conditions. Only few research have been carried out at temperatures over 373K or at pressure over 3MPa in air-water or oxygen-water systems (Clark, 1990; Wilkinson et al., 1992; Luo et al., 1999; Pohorecki et al., 2001; Lau et al., 2004; Jin et al., 2014). Consequently, this article proposes an experimental focus on bubbles characterisation in WAO process conditions and can be obviously used in any gas liquid contactor working in these conditions.

Table 2.1 Available literature studies on bubble characteristics in bubble column reactors

Reference	System	Conditions	Remarks
(Akita and Yoshida, 1973)	$D=0.15\text{m}$, $H=4\text{m}$ Air-H ₂ O, glycol, carbon tetrachloride, methanol	P : 0.1MPa; T : 293K; U_G : up to 0.33m.s ⁻¹	d_{32} decreased with U_G
(Clark, 1990)	$D=0.075\text{m}$, $H=3\text{m}$ N ₂ , H ₂ -H ₂ O, CH ₃ OH	P : 2.5-10MPa; T : 293-453 K; U_G : 0.002-0.055m.s ⁻¹ ; U_L : 0.0014m.s ⁻¹	ε_G increased with U_G and P
(Oyevaar et al., 1991)	$D=0.081\text{ m}$, $H=0.081$ and 0.81 m N ₂ , CO ₂ -water, diethanolamine	P : 1-8.0 MPa; T : 298 K U_G : 0.01-0.1 m/s	ε_G increased with P ; the increase of a with increasing P was larger for higher U_G ;
(Wilkinson et al., 1992)	$D=0.158\text{m}$, $H=1.5\text{m}$ N ₂ -H ₂ O, n-Heptane, Mono-ethylene glycol	P : 0.1-2.0MPa; T : 293-313K; U_G : 0.002-0.055m.s ⁻¹ ; U_L : 0.11m.s ⁻¹	ε_G increased with U_G and P
(Wilkinson et al., 1994)	$D=0.158\text{ m}$, $H=1.5\text{ m}$ He, N ₂ , Ar, CO ₂ , SF ₆ -water, n-Heptane, Mono-ethylene glycol, Na ₂ SO ₃	P : 0.1-0.8 MPa; T : 293 K; U_G : up to 0.2 m/s	ε_G increased with P ; volumetric mass transfer coefficient increased with P at high U_G ; while no effect of P at low U_G
(Stegeman et al., 1996)	$D=0.156\text{ m}$, $H=0.64\text{ m}$ N ₂ , CO ₂ -water, diethanolamine	P : 0.1-6.6 MPa; T : 298 K U_G : up to 0.06 m/s	ε_G increased with U_G ; a increased with P and moderately affected by U_G
(Lin et al., 1998)	$D=0.0508$ - 0.1016 m , $H=0.8$ - 1.58 m N ₂ -Paratherm NF	P : up to 20 MPa; T : 300-351 K; U_G : 0.02-0.08 m/s	ε_G increased with P and T ; Maximum stable bubble size decreased with T and P
(Luo et al., 1999)	$D=0.102\text{m}$, $H=1.37\text{m}$ N ₂ -Paratherm NF	P : 0.1-5.6MPa; T : 301 and 351K; U_G : up to 0.4m.s ⁻¹	ε_G increased with U_G and P ; Smaller bubble size at high pressure; Maximum bubble size increased with U_G , but decreased with P
(Pohorecki et al., 1999)	$D=0.304\text{ m}$, $H=3.99\text{ m}$ N ₂ -H ₂ O	P : 0.1-1.1 MPa; T : 303-433°C; U_G : 0.002-0.055 m/s; U_L : up to 0.02 m/s	d_{32} slightly with U_G ; No influence of P and T on d_{32} and ε_G
(Pohorecki et al., 2001)	$D=0.3\text{ m}$, $H=4\text{ m}$ N ₂ -cyclohexane	P : 0.2-1.1 MPa; T : 303-433 K; U_G : 0.002-0.055 m/s; U_L : 0.14 cm/s	No effect of P and T on d_{32} ; no effect of P on ε_G ; ε_G increased with T ; a increased with T
(Schäfer et al., 2002)	$D=0.54\text{ m}$, $H=0.475\text{ m}$ N ₂ -H ₂ O, cyclohexane, Na ₂ SO ₄ solution	P : up to 5 MPa; T : up to 448 K; U_G : up to 0.37 cm/s	d_{32} decreased with P ; d_{32} increased along the height of column; Effect of T on d_{32}
(Maalej et al., 2003)	$D=0.046\text{ m}$, $H=0.25\text{ m}$ N ₂ , CO ₂ -NaOH, Na ₂ CO ₃ /NaHCO ₃	P : up to 5 MPa; T : 293 K; U_G : up to 0.03 m/s; U_L : 0.067 m/s	a increased with P
(Lau et al., 2004)	$D=0.0508\text{m}$ and 0.1016m N ₂ , air-Paratherm NF	P : up to 4.24MPa; T : up to 365K; U_G : up to 0.4m.s ⁻¹ ; U_L : 0.08-0.89cm.s ⁻¹	ε_G increased with U_G , T and P , but slightly decreased with U_L ; a increased with P and T ;
(Chaumat et al., 2005)	$D=0.2\text{m}$, $H=1.6\text{m}$ N ₂ , CO ₂ -H ₂ O, cyclohexane	P : atmospheric pressure; T : 293K; U_G : up to 0.14m.s ⁻¹ ; U_L : up to 0.08m.s ⁻¹	ε_G increased with U_G , but slightly decreased with U_L ; ε_G was slightly greater in cyclohexane than in H ₂ O

Chapter 2: Bubble characterization and gas liquid interfacial area in two phase gas-liquid system in bubble column at low Reynolds number and high temperature and pressure

(Sehabiague et al., 2005)	$D=0.3$ m, $H=3$ m N ₂ , He-Fischer-Tropsch	P : 0.17-3.0 MPa; T : 298-453 K	ε_G and mass transfer parameters increased with U_G , P and T
(Majumder et al., 2006)	$D=0.05$ m, $H=1.6$ m Air-H ₂ O	P : atmospheric pressure; T : 302K; U_G : 0.17-1.358cm.s ⁻¹ ; U_L : 7.07-14.14cm.s ⁻¹	d_{32} increased with U_G , but decreased with U_L ; a increased with U_L
(Behkish et al., 2007)	$D=0.29$ m, $H=3$ m N ₂ , He-Isopar-M	P : 0.67-3MPa; T : 300-473K; U_G : 0.07-0.39m.s ⁻¹	ε_G increased with U_G , and T ; Effect of P on ε_G ; d_{32} decreased with P ; Effect of T on d_{32} ; $d_{32}(\text{N}_2) > d_{32}(\text{He})$
(Baz-Rodríguez et al., 2014)	$D=0.095$ m, $H=1.2$ m O ₂ -H ₂ O, NaCl, MgCl ₂ , CaCl ₂	P : atmospheric pressure; T : 303 K; U_G : 0.0005-0.0197 m/s	a increased with U_G ;
(Jin et al., 2014)	$D=0.1$ m, $H=1.25$ m H ₂ , CO, CO ₂ -Paraffin	P : 1.0-3.0MPa; T : 293-473K; U_G : 0.03-0.1m.s ⁻¹	a increased with U_G , P and T
(Kanaris et al., 2018)	$D=0.05$ m, $H=0.35$ m Air, CO ₂ , He-H ₂ O, aqueous glycerine (40% v/v)	P : atmospheric pressure; T : ambient temperature; U_G : 0-0.064m.s ⁻¹	ε_G increased with U_G ; d_{32} was not considerably affected by gas type but mainly affected by liquid type
(Mohagheghian and Elbing, 2018)	$D=0.063$ -0.102m, $H=0.61$ -1.22m Air-H ₂ O	P : up to 0.6MPa; T : 293 -295K; U_G : 0.14-5.5cm.s ⁻¹ ; U_L : up to 0.08	d_{32} decreased with U_G

In all above processes, bubble size distribution and gas holdup are important design parameters, which have been often used to define the gas-liquid interfacial area available for mass transfer (Akita and Yoshida, 1974; Stegeman et al., 1996; Pohorecki et al., 2001; Majumder et al., 2006; Kanaris et al., 2018). The operation of bubble columns can be affected by several parameters. Gas and liquid superficial velocities, temperature, pressure, liquid-phase viscosity, density and surface tension have been indicated to affect the formation and stability of the gas bubbles and then the hydrodynamic and mass transfer behaviour in the bubble column reactors (Behkish et al., 2007).

Table 2.1 summarizes available literature studies on the influence of operation parameters on bubble characteristics in bubble columns. Many research reported that with the increase of gas superficial velocity, the gas holdup enhanced, inducing an increase in bubbles number, turbulence and collision frequency, resulting in the increase of bubble size (Clark, 1990; Wilkinson et al., 1992; Luo et al., 1999; Lau et al., 2004; Majumder et al., 2006; Behkish et al., 2007; Kanaris et al., 2018). However, Mohagheghiana and Elbing (2018) and Akita and Yoshida (1974) both observed a decrease in Sauter mean diameter of bubbles with increasing gas superficial velocity. Majumder et al. (2006) indicated that in an air-water system, bubble size decreased with increasing liquid superficial velocity, due to bubble breakup. Chaumat et al. (2005) indicated that in a cyclohexane/N₂-CO₂ system, gas holdup decreased by increasing the liquid superficial velocity. For an air-water system, Schäfer et al. (2002) reported a significant decrease of bubble size when increasing the pressure up to 5MPa at ambient temperature with different types of spargers in the homogeneous regime, while a plateau for the effect of pressure on bubble size has been observed by some authors (Chilekar, 2007; Hashemi et al., 2009; Chilekar et al., 2010; Kumar et al., 2012; Pjontek et al., 2014). Moreover, it is commonly observed by many authors that a pressure increase results in an increase of gas holdup (Therning and Rasmuson, 2001; Urseanu et al., 2003; Maalej et al., 2003; Hashemi et al., 2009; Chilekar et al., 2010; Kumar et al., 2012; Pjontek et al., 2014), which is attributed to the increase of gas density, the reduction of the bubble size, and the increase of bubble number density (Behkish et al., 2007). Generally, with the increase of temperature, bubble diameter decreases and gas holdup increases (Lau et al., 2004; Behkish et al., 2007; Hashemi et al., 2009), while no effect (Pohorecki et al., 1999) or even negative effect (Deckwer et al., 1980; Grover et al., 1986; Yang et al., 2001) of temperature on gas holdup have been reported. Lin et al. (1998) reported a decrease of the maximum stable bubble size of N₂ in Paratherm NF fluid with temperature due to a combined effect of the decrease of surface tension and liquid viscosity. Several publications also revealed that gas holdup increased with the reduction of liquid viscosity and surface tension (Kawase et al., 1992; Wilkinson et al., 1992). Apart from pressure and temperature, physical properties of the phases can also play a role in the bubble

characteristics. This influence will be tested using different gases and liquids, allowing significant variations of the phases properties.

For the design and scale-up of bubble column reactors for industrial processes, the knowledge of mass transfer between gas-liquid contacting systems is required. In many gas-liquid systems, the mass transfer rate is controlled by volumetric mass transfer coefficient, which is a function of specific interfacial area (Majumder et al., 2006). Thus, it is essential to study the interfacial phenomena in the gas-liquid system at different operating conditions. In recent years, most research focused on mass transfer characteristics in bubble columns at atmospheric conditions, few data obtained on volumetric mass transfer coefficient and interfacial area at high pressure and high temperature (Jin et al., 2014). Pohorecki et al. (1999) and Baz-Rodríguez et al. (2014) reported that with the increase of the superficial gas velocity, the interfacial area increased. Chaumat et al. (2005) found that the local interfacial area decreased with superficial liquid velocity in different liquid-gas phase with cyclohexane or water as liquid phase and N₂ or CO₂ as gas phase. Oyevaar and Westerterp (1991) observed a positive influence of pressure on the interfacial areas at pressure up to 8MPa in a mechanically stirred gas-liquid reactor and a bubble column, consistent with Stegeman et al. (1996). Sehabiague et al. (2005) reported that volumetric mass transfer coefficient values and gas holdup increased with the increase of the pressure, operating temperature and superficial gas velocity in a slurry bubble column under the range of pressure 0.17-3.0MPa and the range of temperature 298-453K. However, at low superficial gas velocity ($U_G < 3\text{cm}\cdot\text{s}^{-1}$), no effect of pressure on mass transfer was observed for pressure between 0.1-0.8MPa (Wilkinson et al., 1994) and a decrease of the values with pressure was reported by Maalej et al. (2003). Furthermore, most research point out that the interfacial area values seems to increase with the increase of temperature (Pohorecki et al., 2001; Jin et al., 2014). Nevertheless, it was also reported that the interfacial area increased with increasing superficial gas velocity and pressure, while decreased with the increase of the temperature (Lau et al., 2004). All this literature analysis is summed up in Table 2.1

Therefore, the objective of this study is to investigate the effect of gas and liquid superficial velocity, pressure (10-20MPa), temperature (373-473K) on bubble size distribution and interfacial area. In order to evaluate these effects in very different conditions, the physical properties of the phases must be changed on a large range. For that purpose, different liquid-gas systems (water-N₂ system, water-He system, ethanol/water mixture-N₂ system and ethanol/water mixture-He system) has been used.

2.2 Experimental methods

2.2.1 Experimental setup

Fig. 2.1 shows a schematic diagram of the bubble column used in this study (Top Industrie, France). The system consists of a vertical column, liquid and gas supplying equipment, two piston pumps used for gas and liquid, a liquid exhaust reservoir, an oven, a buffer tank and a pressure limiter. The bubble column, made of sapphire, has an internal diameter of 1cm and an outer diameter of 2.4cm with 0.7cm thick wall. The height and the total volume of the bubble column are 10cm and 8mL, respectively. The column is intended to operate at pressures up to 20MPa and temperatures up to 473K. The liquid pump is a volumetric piston pump, with a total volume of 53mL, delivering a liquid flowrate up to 16 mL.min⁻¹. In this study, the liquid flow rate was set at 1, 3 and 5 mL.min⁻¹ (i.e. liquid superficial velocity of 0.022, 0.066 and 0.122 cm.s⁻¹ respectively). These values are coherent with those used in industrial bubble columns and allow enough time to reach the steady state regarding the volume of the pump reservoir. The precision on the flow rate is 0.3%. The purity of N₂ and He are both higher than 99% (supplied by Air Liquid). The gas pump is also a volumetric piston pump with total volume of 52mL and maximum flow rate of 22mL.min⁻¹. In this study, 1-10mL.min⁻¹ of gas flow rate was used to obtain gas superficial velocity of 0.028-0.276 cm.s⁻¹. The gas phase is injected through a nozzle with an average pore size of 80µm. The temperature of both fluids is controlled in the oven, a vitreous oven with a volume of 32 L (Memmert). The temperature of the oven is controlled up to ±0.1°C. A pressure limiter (TESCOM) is used for pressure regulation, controlled by the user through a pressure sensor. A buffer tank is placed before pressure reduction to avoid large rises or declines of pressure or non-negligible pressure oscillations in the bubble column during the passage from the liquid to the gas through the pressure limiter. A camera is used to record the bubbles behaviour in the column with a 19MPixel resolution, equipped with a 69mm macro lens with fixed focal length (Canon EOS M®). The accuracy of diameter measurement with a photo is ±38µm (corresponding to 2 Pixels).

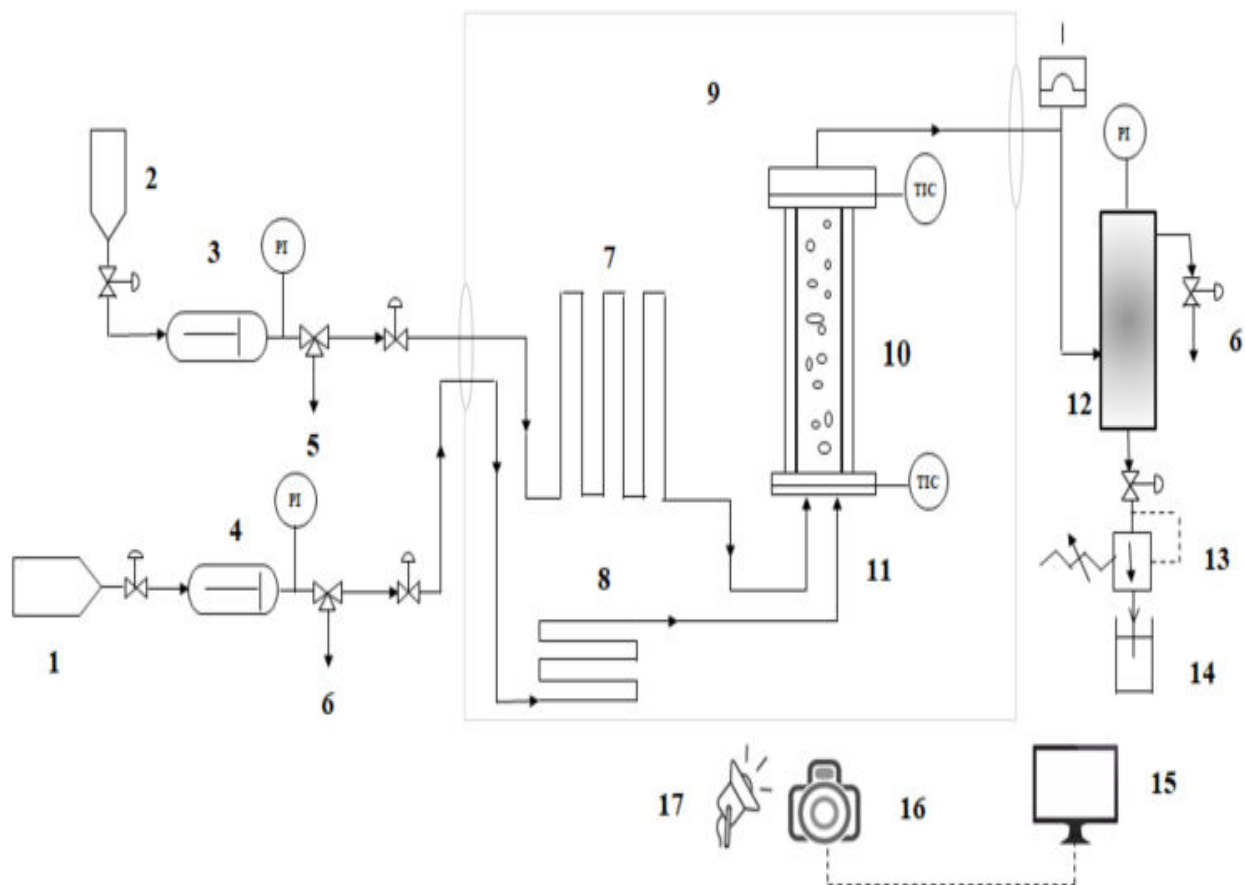


Fig. 2.1 Schematic diagram of experimental setup. 1 – gas tank; 2 – syringe used for liquid; 3 – liquid pump; 4 – gas pump; 5 – liquid purge; 6 – gas purge; 7 – liquid coil; 8 – gas coil; 9 – oven; 10 – bubble column; 11 – gas sparger; 12 – buffer tank; 13 – pressure limiter; 14 – liquid outlet; 15 – monitor; 16 – camera; 17 – lamp.

In this study, N_2 or He and water or ethanol/water mixture are used as the gas and liquid phase respectively. The operating variables are shown in Table 2.2. With the increase of pressure, the density of gas phase significantly increases, while the effect on liquid properties, gas viscosity and dimensionless numbers are independent. As temperature increases, gas and liquid density, liquid viscosity, liquid surface tension, Oh number and Mo number all decrease, whereas Ar and Eo number increase.

Chapter 2: Bubble characterization and gas liquid interfacial area in two phase gas-liquid system in bubble column at low Reynolds number and high temperature and pressure

Table 2.2 Physical properties of liquid and gas phases at different pressures and temperatures (“Thermophysical properties of fluid systems,” n.d.)

Conditions		Liquid phase					Gas phase		Dimensionless number			
Liquid phase	Gas phase	T (K)	P (MPa)	Density (g.mL ⁻¹)	Viscosity (μ Pa.s)	Surface tension (mN.m ⁻¹)	Density (g.mL ⁻¹)	Viscosity (μ Pa.s)	Ar	Eo	Mo	Oh
H ₂ O	N ₂	373	10	0.963	284.4	58.9	0.087	22.6	31978	16	3.3E-11	3.8E-4
			15	0.965	285.7	58.9	0.128	23.5	31960	16	3.3E-11	3.8E-4
			20	0.967	287.1	58.9	0.166	24.6	31943	16	3.4E-11	3.8E-4
H ₂ O	N ₂	423	10	0.922	184.9	48.7	0.077	24.4	45096	18	1.1E-11	2.8E-4
			15	0.925	186.1	48.7	0.112	25.2	45087	19	1.1E-11	2.8E-4
			20	0.928	187.3	48.7	0.145	26.0	45082	19	1.1E-11	2.8E-4
H ₂ O	N ₂	473	10	0.871	136.4	37.7	0.068	26.2	54539	23	7.3E-12	2.4E-4
			15	0.875	137.6	37.7	0.100	26.8	54561	23	7.5E-12	2.4E-4
			20	0.877	138.8	37.7	0.130	27.5	54341	23	7.8E-12	2.4E-4
H ₂ O	He	373	10	0.963	284.4	58.9	0.012	23.2	31978	16	3.3E-11	3.4E-4
Ethanol/wa-ter mixture (1:1, v/v)	N ₂	373	10	0.796	448.0	31.3	0.087	22.6	13869	24	1.6E-09	9.0E-4
	He						0.012	23.4	13869	24	1.6E-09	9.0E-4

2.2.2 Data analysis

2.2.2.1 Bubble size determination

In this study, bubble size distribution of the liquid-gas mixture was obtained by photographic method. The shapes of the bubbles were considered ellipsoidal. Under these conditions, the maximum and minimum axis of the ellipse were measured. Then an equivalent spherical bubble diameter was calculated by the following equation (Majumder et al., 2006):

$$d_{b,i} = \sqrt[3]{d_{b,max}^2 d_{b,min}} \quad \text{Eq. 2-1}$$

where $d_{b,max}$ and $d_{b,min}$ are the maximum and minimum diameter of bubbles. The bubble size distribute

ons were obtained by sorting the equivalent diameters of the bubbles into different uniform classes. The minimum number of bubble diameter classes required for the construction of the size distribution, N , was calculated using Sturges' rule (Sturges, 1926) given by:

$$N = 1 + \log_2 S \quad \text{Eq. 2-2}$$

S is the sample size. In this study, the number of classes used for the construction of the bubble distributions is 10, with equal intervals. Furthermore, the column is divided into three vertical stages (0-3.3, 3.3-6.6 and 6.6-10cm) to evaluate the effect of the height along the column on the bubble sizes. For the consistency of the experiments, measurements of all bubbles in the column were performed with several pictures for each operating condition. Then the Sauter mean diameter (d_{32}) was calculated as follows (Eq. 2-3):

$$d_{32} = \frac{\sum_i^N n_i d_{b,i}^3}{\sum_i^N n_i d_{b,i}^2} \quad \text{Eq. 2-3}$$

where n_i is the bubble number for each class.

2.2.2.2 Gas holdup measurement

Gas holdup in a bubble column is defined as the fraction of the gas phase volume occupied in the total volume of two- or three-phases mixture (Tang and Heindel, 2006).

$$\varepsilon_G = \frac{\sum n_i V_{b,i}}{V_c} \quad \text{Eq. 2-4}$$

$$V_{b,i} = \frac{4}{3} \pi \left(\frac{d_{b,eq}}{2} \right)^3 \quad \text{Eq. 2-5}$$

$$d_{b,eq} = \frac{d_i + d_{i+1}}{2} \quad \text{Eq. 2-6}$$

where $V_{b,i}$ and V_c are the bubbles volume at each class and the volume of the column, respectively; $d_{b,eq}$ is the equivalent mean diameter at each class; d_i and d_{i+1} are initial diameter and final diameter at class i .

2.2.2.3 Calculation of gas-liquid interfacial area

Gas-liquid interfacial area (a) was calculated using the Sauter diameter by following equation (Eq. 2-7) (Maceiras et al., 2010):

$$a = \frac{6\varepsilon_G}{d_{32}(1-\varepsilon_G)} \quad \text{Eq. 2-7}$$

2.3 Results and discussion

The dominant parameter controlling bubbles dispersion state is the dynamic size variation of the bubbles due to the local bubble coalescence and breakup. It is however difficult to make an accurate evaluation of these two phenomena. Therefore, global variation of bubble size has been evaluated. Bubbles' characteristics (bubble size, gas holdup and interfacial area) are evaluated through the direct video visualization of bubbles under three pressure and temperature and different gas and liquid superficial velocity conditions. Three examples are shown in Fig. 2.2.

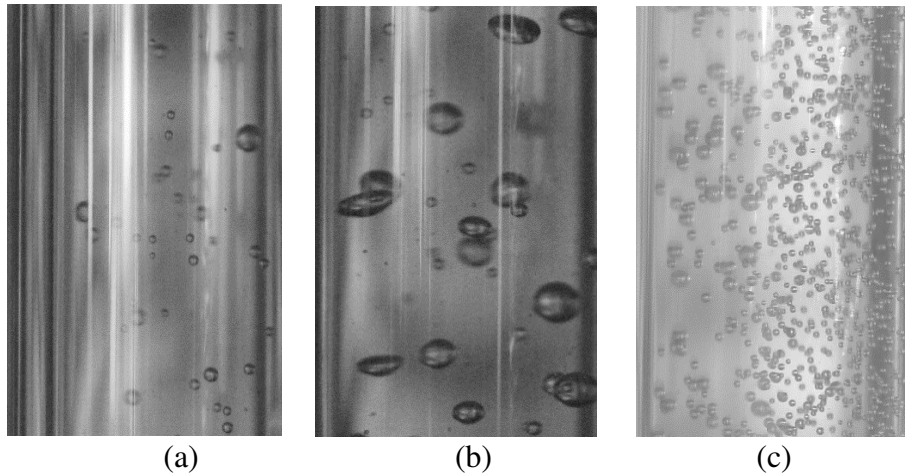


Fig. 2.2 Photograph (a) N₂-H₂O system, $U_G=0.083 \text{ cm.s}^{-1}$, $U_L=0.022 \text{ cm.s}^{-1}$, $T=373\text{K}$, $P=10\text{MPa}$; (b) N₂-H₂O system, $U_G=0.276 \text{ cm.s}^{-1}$, $U_L=0.022 \text{ cm.s}^{-1}$, $T=373\text{K}$, $P=10\text{MPa}$; (c) N₂-ethanol/water mixture system, $U_G=0.083 \text{ cm.s}^{-1}$, $U_L=0.022 \text{ cm.s}^{-1}$, $T=373\text{K}$, $P=10\text{MPa}$

2.3.1 Effect of superficial gas velocity

As an example of raw data, the bubble number distribution and number fraction distribution under various superficial gas velocity and pressure at the temperature of 373K and the superficial

liquid velocity of 0.022 cm.s^{-1} is presented in Fig. 2.3. The width of the distribution increases with the increase of the superficial gas velocity, which is in good agreement with the previous studies (Lin et al., 1998; Mouza et al., 2005; Ramezani et al., 2012). The trends can be due to the increase of coalescence and breakup by the increase of superficial gas velocity, resulting in the growth of collision frequency (Ramezani et al., 2012). The bubble number fraction distribution under all conditions follows the same lognormal distribution trend. At 373K and 10MPa, the bubble size distribution shifts from smaller- to larger-size bubbles and the dominant bubble size shifts from 0.45 to 0.75mm, with the increase of superficial gas velocity.

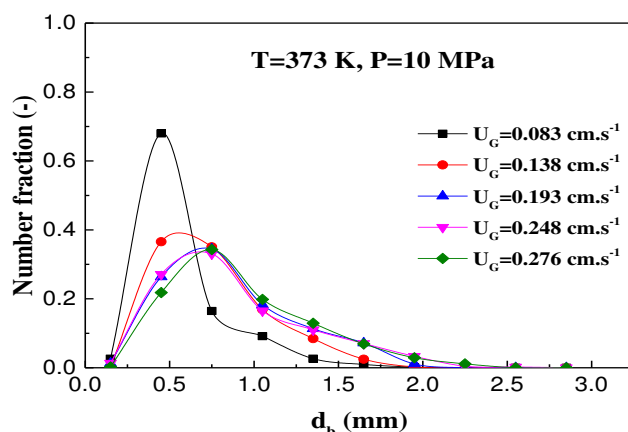


Fig. 2.3 Bubble number distribution and number fraction under various superficial gas velocity and at $T=373\text{K}$, $P=10\text{MPa}$ and $U_L=0.022 \text{ cm.s}^{-1}$

Fig. 2.4 shows the effect of superficial gas velocity on bubble average diameter, gas holdup and interfacial area. With the increase of superficial gas velocity, the Sauter mean bubble diameter and gas holdup increase. In Fig. 2.2, the bubble diameter at $U_G=0.276 \text{ cm.s}^{-1}$ is higher than at $U_G=0.083 \text{ cm.s}^{-1}$. This is in agreement with previous results (Hashemi et al., 2009; Li et al., 2018; Pjontek et al., 2014). This may be due to the superficial gas velocity increase, leading to more bubbles formation and the increase of the rate of coalescence, and the formation of bigger bubbles. The larger bubbles rise faster than smaller bubbles, thus the liquid resistance decreases, leading to the increase of average bubble size and gas holdup. Nevertheless, an opposite trend was also observed by other authors (Pohorecki et al., 2001; Shahrouz Mohagheghian and Brian Elbing, 2018), due to the complex role of superficial gas velocity on modifying bubble formation processes and liquid circulation (Mohagheghian and Elbing, 2018).

Chapter 2: Bubble characterization and gas liquid interfacial area in two phase gas-liquid system in bubble column at low Reynolds number and high temperature and pressure

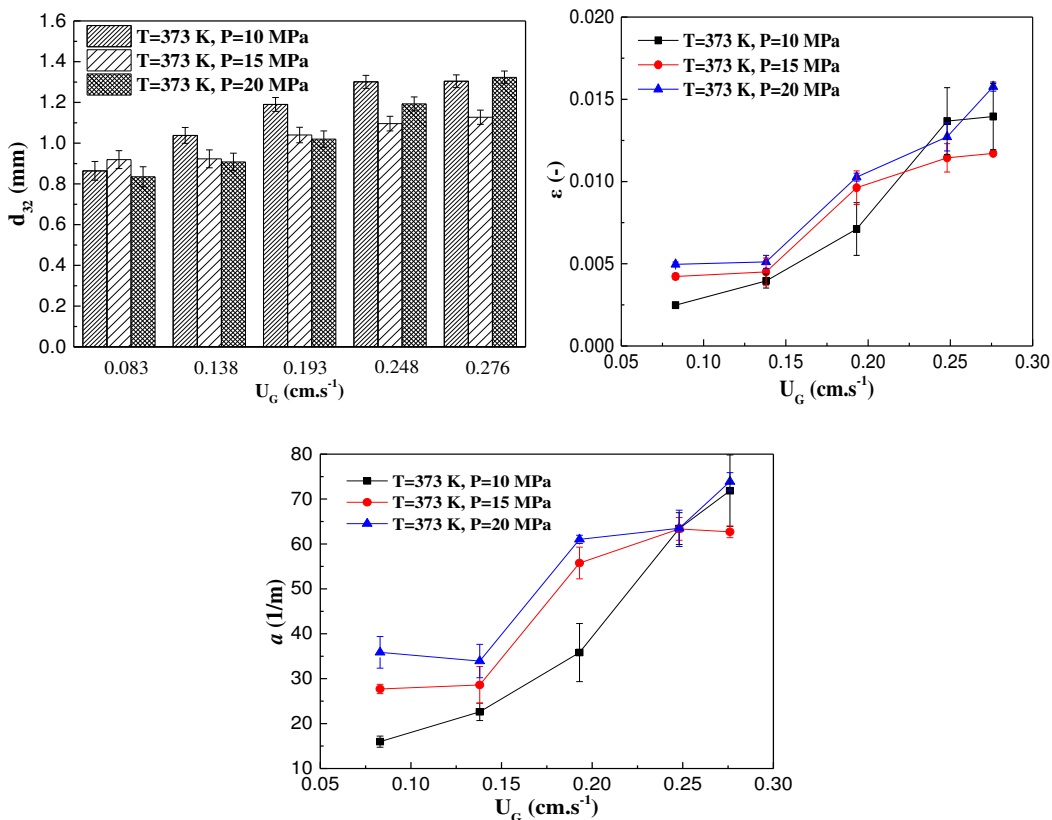


Fig. 2.4 Bubble mean Sauter diameter (d_{32}), gas holdup (ϵ) and interfacial area (a) under various superficial gas velocity and pressure at $T=373K$ and $U_L = 0.022cm.s^{-1}$

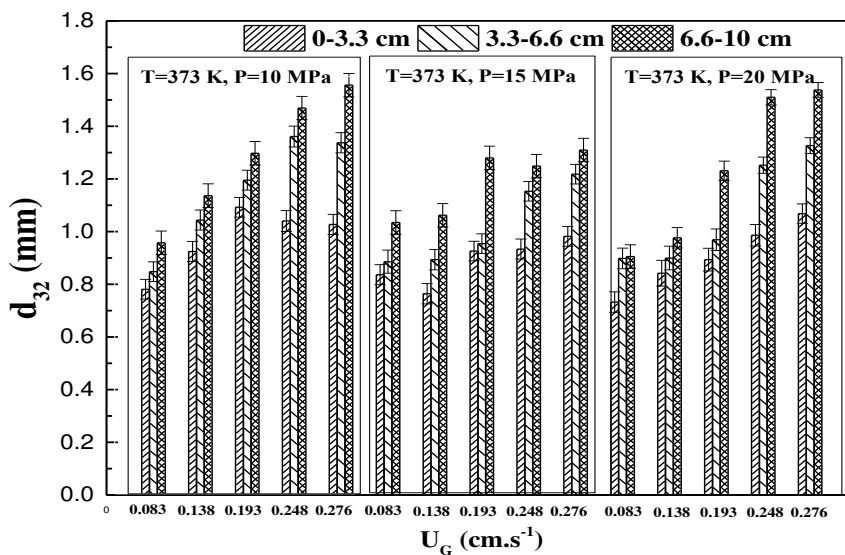


Fig. 2.5 Bubble mean Sauter diameter along the location of the column under various superficial gas velocity and pressure at $T=373K$ and $U_L = 0.022cm.s^{-1}$

The interfacial area calculated by Eq. 2-7 is shown in Fig. 2.4, which is related to the Sauter mean diameter and the liquid volume. It shows that the interfacial area is generally observed to be higher at higher superficial gas velocity. The similar observation has been reported by Jin et al. (2014).

This can be attributed to the increase of the bubble passage frequency and gas holdup with superficial gas velocity. The mean Sauter diameters are also obtained in three axial locations (0-3.3, 3.3-6.6 and 6.6-10cm) from the bottom of the column (Fig. 2.5).

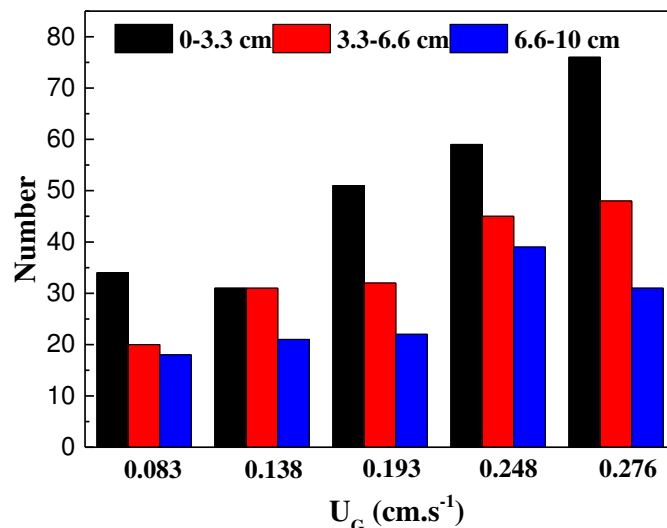


Fig. 2.6 Bubble number distribution along the location of the column under various superficial gas velocity at T=373K and P=10MPa

The mean Sauter diameter increases with the increase distance from the bottom of the column due to the coalescence of smallest bubbles, which is in good agreement with the results reported by Majumder et al. (2006). This trend is due to the coalesced bubbles went up due to their buoyancy and accumulated along the column from the bottom to the top (Majumder et al., 2006), which is presented on Fig. 2.6. For each gas superficial velocity, the bubble number decreases along the height from the bottom to the top of the column, indicating the increase of coalescence. However, Pohorecki et al. (2001) observed no changes of Sauter mean diameter along the column axis in the N₂-cyclohexane system, which was attributed to the dynamic equilibrium between coalescence and redispersion processes in the column. Luo et al. (1999) revealed that the effect of the column height was insignificant for the column height above 1-3m and the ratio of the column height to the diameter larger than 5.

2.3.2 Effect of superficial liquid velocity

The effects of superficial liquid velocity on bubble hydrodynamic in the column are shown in Fig. 2.7 and Fig. 2.8. Fig. 2.7 shows that with the superficial liquid velocity enhancement, the total bubble number little increases, and the influence of superficial liquid velocity on bubble size distribution is insignificant. Moreover, as shown in Fig. 2.8, the effect of superficial liquid velocity on the bubble average diameter is not significant. This figure also shows that under the temperature

range 373K-423K, superficial liquid velocity displays insignificant effect on gas holdup and interfacial area, indicating that under low superficial liquid velocity conditions (superficial liquid velocity less than 1cm.s^{-1}), the liquid-phase motion has little effect on bubble characteristics. This trend is consistent with previous literature results (Akita and Yoshida, 1974; Wilkinson et al., 1992). Higher superficial liquid velocity increases the kinetic energy, the turbulence intensity, bubble-bubble interaction and bubble velocity, which reduces gas holdup (Lau et al., 2004). However, the increase of superficial liquid velocity raises bubble breakup at the distributor and thus increases gas holdup attributed to higher bubble residence times in the column (Pjontek et al., 2014). Thus, the slight increase in gas holdup is dominated by the effect of superficial liquid velocity on bubble residence time. Shah et al. (2012) has indicated that the gas holdup is more affected by the superficial gas velocity rather than the liquid velocity. Furthermore, the interfacial area increases with the increase of superficial liquid velocity, while the variation of interfacial area is small due to the marginal effect of the superficial liquid velocity on the gas holdup and bubble size for the range studied. Lau et al. (2004) observed a similar observation in the air-Paratherm system under lower pressures (up to 4.24MPa) and lower temperatures (up to 365 K) with the superficial gas and liquid velocity varying up to 40 and 0.89cm.s^{-1} . While under the temperature of 473K, gas holdup and interfacial area increases with superficial liquid velocity. The reason for this trend needs to be further studied.

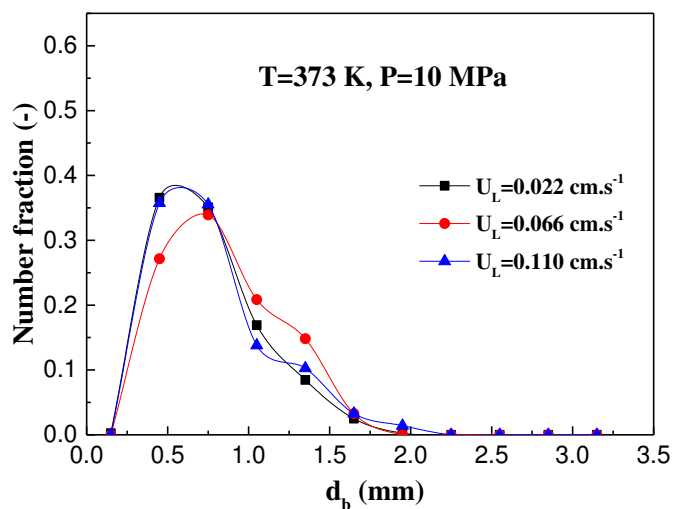


Fig. 2.7 Bubble number distribution and number fraction under various superficial liquid velocity at $P=10\text{MPa}$, $T=373\text{K}$ and $U_G = 0.138\text{cm.s}^{-1}$

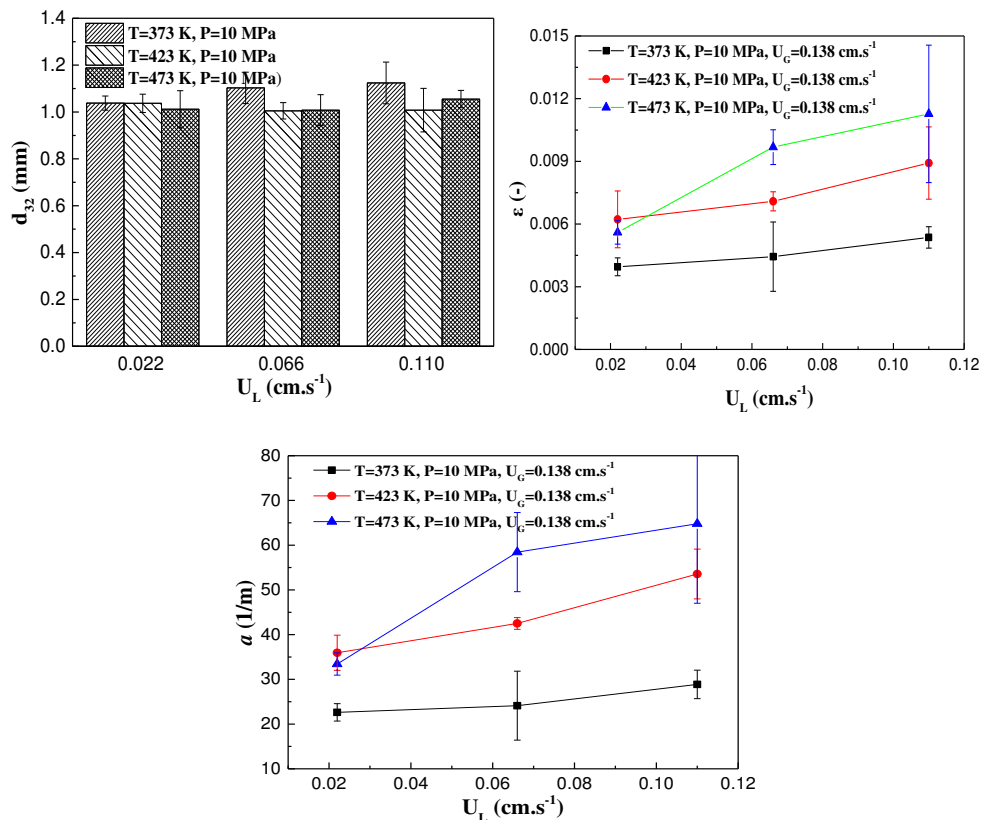


Fig. 2.8 Bubble mean Sauter diameter (d_{32}), gas holdup (ϵ) and interfacial area (a) under various superficial liquid velocity and temperature at $P=10\text{MPa}$ and $U_G=0.138\text{cm.s}^{-1}$

2.3.3 Effect of pressure

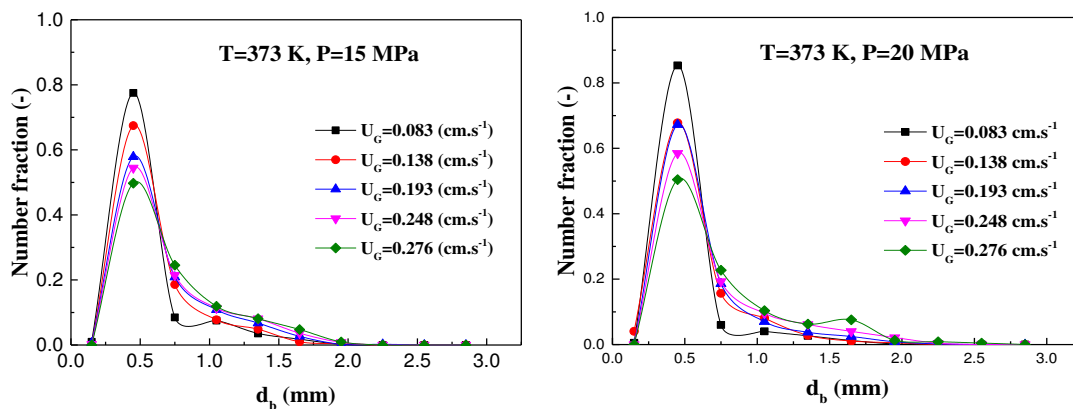


Fig. 2.9 Bubble number distribution and number fraction under different pressure at $T=373\text{K}$ and $U_L=0.022\text{cm.s}^{-1}$

Fig. 2.3 and Fig. 2.9 demonstrate the effects of pressure on bubble size distribution at 373K. Fig. 2.3 and Fig. 2.9 show that with the increase of pressure, the bubble number increases and the bubble-size distribution shifts from large to smaller size distribution. Similar results were observed by other

researchers (Lin et al., 1998). When the pressure increased from 10 to 20MPa, the dominant bubble size shifts from 0.75 to 0.45mm.

The effect of pressure on bubble average diameter is complex, but generally, with the pressure ranging from 10 to 15MPa, most of bubble mean diameters decrease (Fig. 2.4). The increase of pressure results in an increase in bubble breakage due to the increase of gas density with pressure, caused by the larger gas inertia in the fluctuating bubble. Fig. 2.10 shows that the bubble number along the location of the column always increases with the pressure, indicating the increase in bubble breakage. Increased pressure enhances the momentum of the gas jets, enforcing turbulence and decreasing initial bubble size and maximum stable bubble size (Schäfer et al., 2002). Moreover, the effect of pressure on surface tension is not significant and hence surface tension has an almost negligible influence on bubble coalescence (Schäfer et al., 2002). Thus, the mean bubble size decreases with increasing pressure from 10 to 15MPa. Nevertheless, with the pressure further increased to 20MPa, the pressure effect on the Sauter mean diameter is more noticeable at high gas velocity ($\geq 0.248 \text{ cm.s}^{-1}$) and slightly effect at low gas velocity. This similar phenomenon was observed by other research (Lau et al., 2004) in the air-Paratherm system with the pressure up to 4.24MPa. The more pronounced effect of the pressure at high gas velocities is may be due to the stronger bubble coalescence at high gas velocities.

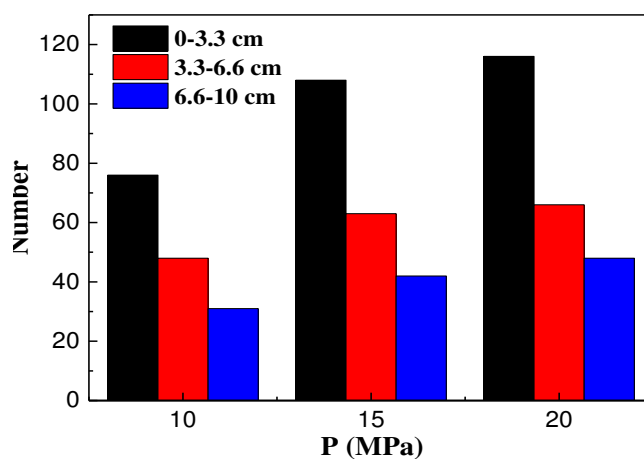


Fig. 2.10 Bubble number distribution along the location of the column under three pressures at $T=373 \text{ K}$, $U_G=0.276 \text{ cm.s}^{-1}$ and $U_L=0.022 \text{ cm.s}^{-1}$

Fig. 2.4 also shows that the gas holdup is almost independent of pressure in the studied range. Behkish et al. (2007) also reported that under high pressure from 1.7 to 3MPa, the increase of gas holdup for He and N₂ in Isopar-M/Alumina system were both insignificant. However, at the pressure below 1.7MPa, the gas holdup increased with the pressure. Under low pressure, large-size and less-dense bubbles are formed and the gas momentum enhances, which increases the rate of bubbles

rupture, resulting in the increase of the gas holdup of small gas bubbles. Moreover, the increase in gas density with pressure increases the kinetic energy, leading to the increase of the collision energy which promotes the bubbles rupture (Inga and Morsi, 1999). Whereas under high pressure, the small-size and dense bubbles exist and the increasing gas momentum are not enough to rupture the small and dense gas bubbles, thus the increase of gas holdup becomes insignificant (Behkish et al., 2007). Inga and Morsi (1999) also observed the similar results: gas holdup increased under low pressures and gradually levelled off under high pressure, attributed to the balance between coalescence and the gas bubbles rupture. As shown in Fig. 2.4, interfacial area generally increases with the pressure ranging from 10 to 20MPa. This increasing trend is partly attributed to the relative extent to which the gas holdup slightly increases with increasing pressure and partly attributed to the reduction in bubble size with the increase of the pressure (Wilkinson et al., 1991).

2.3.4 Effect of temperature

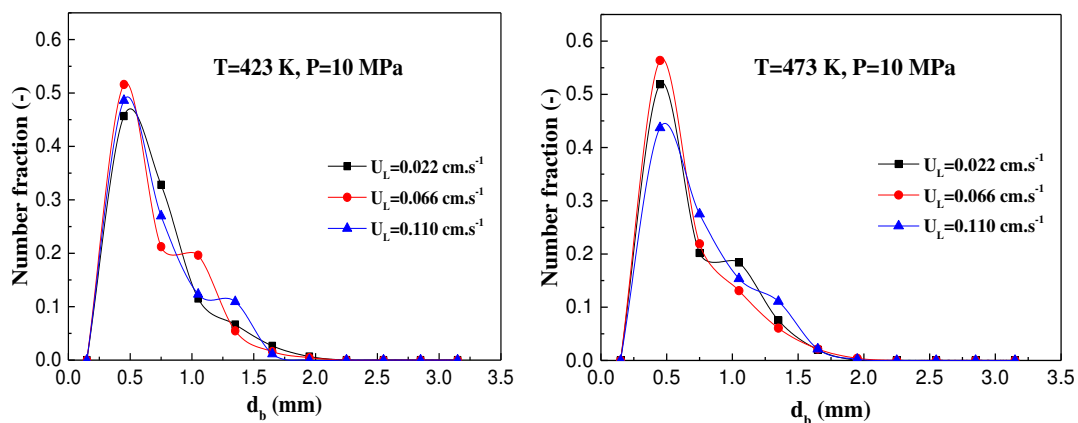


Fig. 2.11 Bubble number distribution and number fraction under different temperature at $P=10\text{MPa}$ and $U_G=0.138\text{cm.s}^{-1}$

Fig. 2.7, Fig. 2.8 and Fig. 2.11 show the effects of temperature on bubble hydrodynamics. As shown in Fig. 2.7 and Fig. 2.11, with the increase of temperature, the bubble number increases and the bubble size distribution shifts from larger- to smaller size distribution. Fig. 2.8 shows a little decrease on bubble average diameter with the increase of temperature, while the effect is insignificant, like the observation by Pohorecki et al. (2001). For set pressure and superficial gas velocity, gas holdup presents a small increase with increasing temperature. This general trend is due to the dominant role of associated reduction in surface tension and liquid viscosity, leading to a smaller average bubble diameter and a narrower bubble size distribution. With the decrease of liquid surface tension with temperature, the cohesive forces for maintaining gas bubbles in a spherical shape reduces and subsequently the increase of the gas momentum, leading to the rupture of large gas bubbles into

smaller bubbles, hence the gas holdup increases (Behkish et al., 2007). Increasing temperature can decrease gas density, which increases the bubble size and decreases gas holdup. Furthermore, it has been reported that with the decrease of liquid viscosity, the bubble rise velocity increased, which led to a reduction of bubble residence time and subsequently reduced the gas holdup (Deng et al., 2010). As reported by Pohorecki et al. (2001), the influence of the surface tension on the gas holdup was considerably higher than that of the liquid viscosity. In this study, all the values of Oh number, which relates the viscous forces to inertial and surface tension forces, are small (less than 1), indicating a higher influence of the surface tension than viscosity. Therefore, the small gas holdup increases when increasing temperature is probably mainly due to the influence of the surface tension (Leonard et al., 2018). The data in Fig. 2.8 also shows that as the temperature ranges from 373 to 473K, the interfacial area generally increases due to the slight decrease of bubble size and the increase of gas holdup.

2.3.5 Effect of different liquid and gas phase

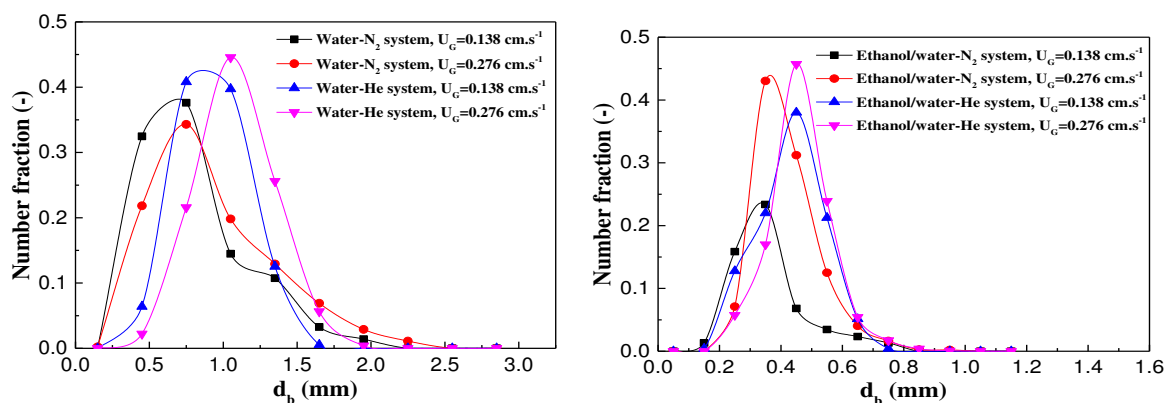


Fig. 2.12 Bubble number distribution and number fraction distribution under various liquid and gas phase at $P=10\text{MPa}$, $T=373\text{K}$, $U_L=0.022\text{cm.s}^{-1}$ and $U_G=0.138-0.276\text{cm.s}^{-1}$

The effects of different liquid and gas phase are also evaluated (Fig. 2.12 and Fig. 2.13). As shown in Fig. 2.12, the bubble number in ethanol/water mixture system is much more than that in the water system, which is also presented in Fig. 2.2 (c). The bubble size distributions are log-normal while the He gas with low density exhibits an observable effect on the bubble distribution curve, which can be attributed to lower momentum force for the low density He gas. Moreover, with the gas velocity increase from 0.138 to 0.276cm.s^{-1} , the bubble size distribution for the four systems (water- N_2 , water-He, ethanol/water mixture- N_2 and ethanol/water-He) all become wider and the shifts from small to larger-size bubble, as presented in section 2.3.1.

It is observed on Fig. 2.13 that the mean Sauter diameter, gas holdup and interfacial area are slightly affected by the type of gas employed, but significantly affected by the liquid phase, in

agreement with Kanaris et al. (2018) (Kanaris et al., 2018). The Sauter mean diameters of He in water and ethanol/water mixture are generally slight higher than those of N₂ under similar operating conditions (Fig. 2.13), which is in agreement with literature findings (Behkish et al., 2007). This behaviour may be due to the lower density of He than N₂ under the same operating conditions shown in Table 2.2: He is expected to form larger gas bubbles compared with N₂ (Behkish et al., 2007). It is also shown that the Sauter mean diameter in the system using ethanol/water mixture as liquid phase are much smaller than the system using water as liquid phase. That is because the coalescence of bubbles is strongly influenced by the composition of the liquid phase, which is reduced for the mixture liquids in comparison to pure liquids. The liquid mixture can cause coalescence inhibition (Lehr et al., 2002). Pjontek et al. (2014) also found a significant reduction in bubble size with the addition of ethanol in water when comparing to water, which was attributed to the shear stresses acting on the bubbles due to liquid and gas passing through the gas distributor, which increased bubble breakup. Furthermore, as viscosity increases, the drag force increases, leading to the formation of smaller bubbles (Kazakis et al., 2008). Thus, in ethanol/water mixture system, coalescence inhibition and shear stresses through the distribution leads to a bubble size reduction.

Many researchers observed that with increasing gas density, gas holdup increases, attributing this behaviour to a lower momentum force for the lower density gas in the primary bubble formation at the gas distributor (Hecht Kristin et al., 2015; Kanaris et al., 2018). In this study, the effects of gas phase with different gas density on gas holdup are complex. Fig. 2.13 shows that in the ethanol/water mixture system, the gas holdup for He is a little bigger than for N₂, while in the water system, the effects of gas phases are different at different superficial gas velocity. The reason for this phenomenon needs to be further studied. At the superficial gas velocity of 0.276 cm.s⁻¹, the gas holdup in ethanol/water system with the higher viscosity is smaller than the water system, which is similar to the results in the literature (Deng et al., 2010; Besagni et al., 2018; Ojha and Al-Dahhan, 2018). This behaviour is mainly due to reduced bubble interaction resulting from reduced turbulence and mixing at higher viscosities (Deng et al., 2010; Ojha and Al-Dahhan, 2018). With the superficial gas velocity at 0.138 cm.s⁻¹, the gas holdup are close in the water and in the ethanol/water mixture, which is similar to Fransolet et al. (2005) . Wu et al. (2013) found that with an increase in liquid viscosity, the gas holdup in carboxyl methyl cellulose-water solution first increased and reached a maximum, and then decreased. The reason for the complex effect of liquid phase on gas holdup has been attributed to “dual effect of viscosity” on gas holdup (Besagni et al., 2018). Furthermore, Fig. 2.13 also shows that the interfacial area for ethanol/water mixture is bigger than water, which is opposite to Ojha et al. (2018) and Wu et al. (2013).

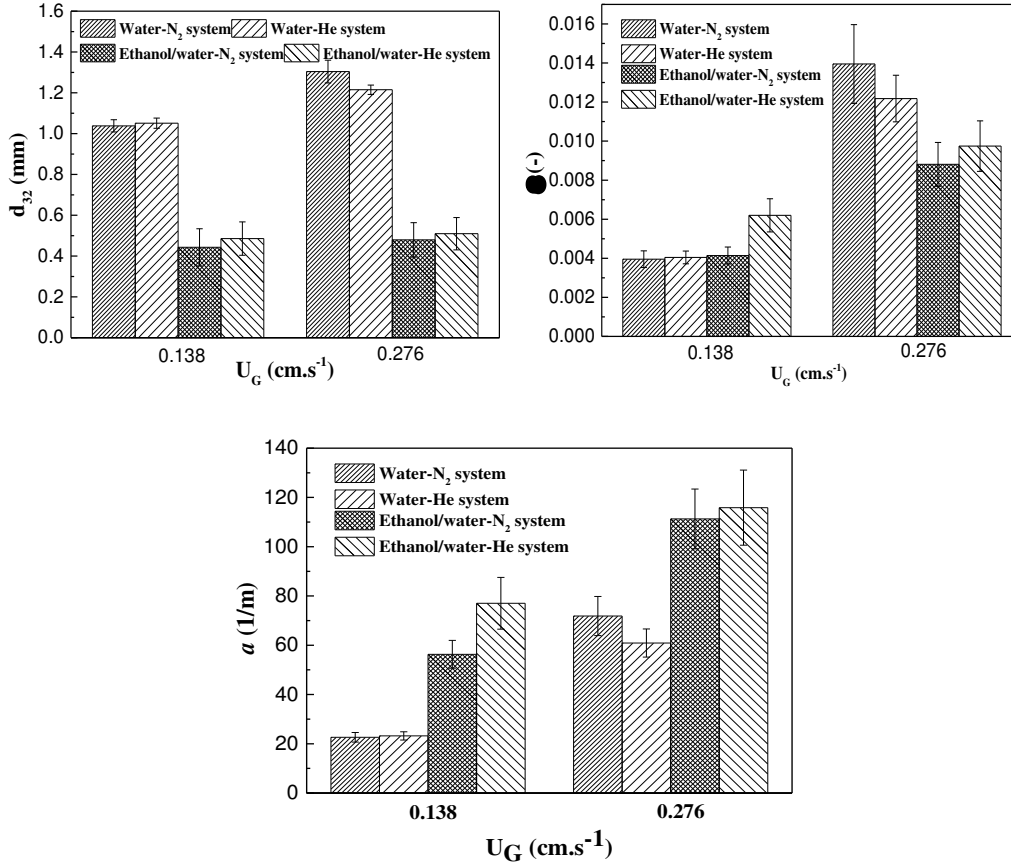


Fig. 2.13 Bubble mean Sauter diameter (d_{32}), gas holdup (ϵ) and interfacial area (a) under various liquid and gas phase at $P=10\text{MPa}$, $T=373\text{K}$, $U_L=0.022\text{cm.s}^{-1}$ and $U_G=0.138-0.276\text{cm.s}^{-1}$

2.3.6 The correlation for average bubble size and gas holdup

Possible factors affecting the average bubble size and the gas holdup are the column diameter, the diameter of gas inlet orifice, superficial gas velocity, kinematic viscosity, liquid density and surface tension (Akita and Yoshida, 1973). Kanaris et al. (2018) proposed a correlation for predicting the average bubble size and the gas holdup based on dimensionless numbers with general form:

$$\frac{d_{32}}{D} = a_1 \left[We^{a_2} Re^{a_3} Fr^{a_4} \left(\frac{d_p}{D} \right)^{a_5} \right]^{a_6} \quad \text{Eq. 2-8}$$

$$\epsilon_G = b_1 \left[Eo^{b_2} Ar^{b_3} Fr^{b_4} \left(\frac{d_p}{D} \right)^{b_5} \right]^{b_6} \quad \text{Eq. 2-9}$$

Values of a_1 to a_6 , b_1 to b_6 are determined from the experiment data. We , Re , Eo , Ar and Fr are the dimensionless Weber, Reynolds, Eötvös, Archimedes and Froude number respectively (Table 2.3). The effect of gas velocity can be taken into account by defining Fr , We and Re number and the effect of the physical properties (viscosity, density and surface tension) of the liquid phase can be included in We , Re , Ar , and Eo numbers (Maceiras et al., 2010).

Table 2.3 Dimensionless number for this study

System	T (K)	P (MPa)	U_G (cm/s)	We	Re	Fr	Ar	Eo
H ₂ O-N ₂	373	10	0.083	0.000113	28	7.02E-06	31978	16.0
			0.138	0.000311	46	1.94E-05	31978	16.0
			0.193	0.000609	65	3.80E-05	31978	16.0
			0.248	0.001005	83	6.27E-05	31978	16.0
			0.276	0.001245	93	7.77E-05	31978	16.0
	373	15	0.083	0.000113	28	7.02E-06	31961	16.1
			0.138	0.000312	46	1.94E-05	31961	16.1
			0.193	0.000610	65	3.80E-05	31961	16.1
			0.248	0.001007	83	6.27E-05	31961	16.1
			0.276	0.001248	93	7.77E-05	31961	16.1
	373	20	0.083	0.000313	27	7.02E-06	31944	16.1
			0.138	0.000313	46	1.94E-05	31944	16.1
			0.193	0.000611	65	3.80E-05	31944	16.1
			0.248	0.001010	83	6.27E-05	31944	16.1
			0.276	0.001250	92	7.77E-05	31944	16.1
423	10	0.138	0.000360	683	1.94E-05	45096	18.6	
473	10	0.138	0.000440	88	1.94E-05	54539	22.7	
H ₂ O-He	373	10	0.138	0.000311	4.7	1.94E-05	31979	16.0
			0.276	0.001245	93	7.77E-05	31979	16.0
Ethanol/H ₂ O-N ₂	373	10	0.138	0.00485	24	1.94E-05	13870	25.0
			0.276	0.001938	49	7.77E-05	13870	25.0
Ethanol/H ₂ O-He	373	10	0.138	0.00485	24	1.94E-05	13870	25.0
			0.276	0.001938	49	7.77E-05	13870	25.0

In this study, the values of the constants a_1 - a_6 and b_1 - b_6 have been adjusted through changing one parameter with fixing other parameters in order to find the optimal curves. The new correlation Sauter mean diameter and gas holdup are formulated and compared with Kanaris et al. (2018) which is shown in Table 2.4.

Table 2.4 Comparison of Sauter mean diameter and gas holdup correlation between Kanaris et al. (2018) and this study

Authors	Diameter correlation	Gas holdup correlation
(Kanaris et al., 2018)	$\frac{d_{32}}{D} = 0.9 \left[We^{0.95} Re^{0.40} Fr^{0.47} \left(\frac{d_p}{D} \right)^{0.55} \right]^{0.51}$	$\varepsilon_G = 0.020 \left[Eo^{3.5} Ar^{0.015} Fr^{0.300} \left(\frac{d_p}{D} \right)^{1.10} \right]^{2.62}$
In this study	$\frac{d_{32}}{D} = 0.35 \left[We^{0.95} Re^{0.40} Fr^{0.47} \left(\frac{d_p}{D} \right)^{0.55} \right]^{0.09}$	$\varepsilon_G = 0.13 \left[Eo^{0.64} Ar^{0.85} Fr^{1.77} \left(\frac{d_p}{D} \right)^{0.02} \right]^{0.36}$

Table 2.4 showed that the exponents (a_2 - a_5) of We , Re , Fr and d_p/D for Sauter diameter correlation in this study is the same with Kanaris et al (2018), while a_1 and a_6 are different. b_1 - b_6 for gas holdup correlation in this research are all different with Kanaris et al (2018), which may be due to the different operation conditions between this study with Kanaris et al. (2018). The correlations for Sauter mean diameter and gas holdup in this study are plotted in Fig. 2.14. The data are in good agreement ($\pm 15\%$ for Sauter mean diameter and $\pm 20\%$ for gas holdup) with the corresponding

experimental data. Thus, the two correlations are suitable for predicting the bubble average diameter and gas holdup for the bubble column under the WAO operation.

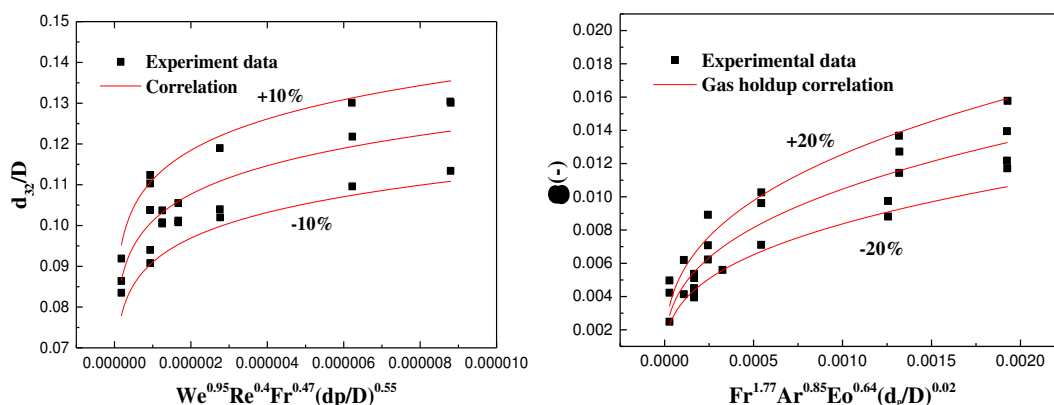


Fig. 2.14 Comparison of the Sauter mean diameter (left) and gas holdup (right) prediction with experimental data

2.4 Conclusion

The bubble size distribution, the Sauter mean diameter, the gas holdup and the interfacial area were determined in a bubble column under wet air oxidation conditions with a wide range of gas and liquid superficial velocities, pressure, temperature and different liquid and gas phases. With the increase of superficial gas velocity, the bubble size distribution shifted from small-to- larger size bubble and the Sauter mean diameter, the gas holdup and the interfacial area generally increased due to the increase of coalescence with superficial gas velocity. The bubble size enhanced with the increasing height from the bottom to the top of the column due to coalescence. The effect of superficial liquid velocity on bubble characteristics was not significant. Increasing pressure and temperature resulted in bubble size distribution shifting from larger-to-smaller size bubble. The effect of pressure on the Sauter mean diameter was complex to determine. A marginal decrease in the Sauter mean diameter was found with the increase of temperature. Pressure and temperature slightly affected the gas holdup and the interfacial area. Moreover, bubble characteristics were not considerably affected by the type of the gas phase, but mainly influenced by the liquid phase. Parameters for Kanaris correlation(ref) were given for the prediction of the bubble mean Sauter diameter and gas holdup for the bubble column under high pressure and high temperature in subcritical water conditions. For a unique set of parameters, this correlation was in good agreement with all experimental data (10% for diameter, 20% for gas hold-up). The correlations may be recommended to scale-up the system for gas liquid contactors working at high pressure and temperature, as WAO for instance.

Wet air oxidation (WAO) is a promising method to convert organic pollutants to CO₂ and H₂O and less toxic oxidation intermediates using oxygen or air as the oxidizing agent at high temperature and pressure. As described in Chapter 1, the overall oxidation of glyphosate by WAO process is controlled by mass transfer of oxygen from gas to liquid phase followed by the reaction between glyphosate and dissolved oxygen. In order to evaluate the performance of WAO process for glyphosate degradation, these two steps should be studied. In Chapter 2, the bubble characteristics, including bubble size distribution, gas holdup and gas-liquid interfacial area have been investigated under WAO conditions and two correlations for bubble mean diameter and gas holdup were proposed in order to predict the mass transfer for WAO process. Then, in next chapter, the oxidation kinetics of glyphosate by WAO process under different temperatures was studied. Furthermore, to understand the reaction mechanisms involved for glyphosate oxidation by WAO process, byproducts evaluation and degradation pathway were also evaluated.

***Chapter 3 Kinetic study of glyphosate degradation by a wet air
oxidation process***

This chapter has been submitted to “Chemosphere” by 20 August 2019.

Abstract

Glyphosate is the most widely used herbicide in the world against perennial and annual weeds. It has been reported to be an emerging contaminant, and its degradation in different wastewater treatment processes must be studied. For that purpose, the kinetics of wet air oxidation (WAO) of glyphosate was studied in an autoclave reactor at a temperature range of 423-523 K and under the total pressure of 15 MPa. Oxidation reactions obeyed a first-order kinetics with respect to glyphosate concentration. The activation energy for glyphosate oxidation was found to be equal to 68.44 kJ.mol⁻¹. Furthermore, the possible reaction intermediates and main end products of glyphosate degradation in WAO process were identified and quantified using UV-vis spectrophotometry and liquid chromatography coupled to mass spectrometry. A possible degradation pathway for glyphosate oxidation were proposed.

Keyword: Glyphosate; wet air oxidation; kinetics; emerging contaminant

3.1 Introduction

Glyphosate (*N*-(phosphonomethyl)glycine), a synthetic phosphonate compound, is a broad-spectrum, post-emergence and non-selective organophosphate herbicide (Manassero et al., 2010; Gill et al., 2017). Glyphosate is the most widely used herbicides in the world against perennial and annual weeds and the active ingredient of Roundup (Baylis, 2000; Chen and Liu, 2007). Due to the numerous use of glyphosate, it has been reported to be widely detected in aquatic environment with potential toxicity to non-target aquatic life (Guilherme et al., 2010; Sandy et al., 2013). Therefore, it has attracted much attention in recent years in order to avoid further risks and effectively avoid glyphosate in the environment.

Various conventional methods have been applied to treat glyphosate-containing wastewater, such as precipitation, membrane filtration, adsorption and biodegradation (Xie et al., 2010; Liu et al., 2013; Herath et al., 2016; Firdous et al., 2017). However, these processes may cause secondary pollution (Wang et al., 2016). Biological treatment generally needs a long residence time to obtain high glyphosate removal efficiency. Thus, more efficient technology for glyphosate degradation is needed to be developed. In this work, the conditions to use wet air oxidation (WAO) as an efficient process are studied. This process would be more dedicated to treat effluents from the pesticides industry, or other types of effluents with rather high pollutants concentration, before their release in the environment.

WAO oxidizes organic pollutants at high temperature and pressure through the generation of

active oxygen species, such as hydroxyl radicals. It has been proven to be a potential treatment technology for wastewaters containing a high content of organic contaminants or toxic pollutants which direct biological treatment is unfeasible (Levec and Pintar, 2007). Typical conditions of WAO are 398-573 K for temperature and 0.5-20 MPa for pressure (Kolaczowski et al., 1999; Luck, 1999; Debellefontaine and Foussard, 2000; Lefèvre et al., 2011a, 2011b; Lefevre et al., 2012). By using oxygen or air as the oxidizing agent, WAO method can effectively convert organic pollutants to CO₂ and H₂O and less toxic oxidation intermediates up to short chain acids (Joglekar et al., 1991; Mishra et al., 1995; Luck, 1999; Hu et al., 2001). Under high temperatures and pressures, the solubility of oxygen is enhanced in aqueous solutions, which provides a strong driving force for oxidation (Demirel and Kayan, 2012). For industrial applications, the design of bubble columns working at high pressure and high temperature has been deeply studied (Leonard et al., 2015, 2019; Feng et al., 2019).

Table 3.1 summarizes available studies on the treatment of pollutants by WAO process. It is shown that WAO technology could achieve high organic compound and total organic carbon (TOC) removals. The performance of WAO can be affected by mainly three parameters: temperature, oxygen pressure (and overall pressure) and reaction time. With the increase of temperature, the removal efficiency of organic compounds generally increased (Joglekar et al., 1991; Mantzavinos et al., 1996; Thomsen, 1998; García-Molina et al., 2007; Lei et al., 2007; Lefèvre et al., 2011). For instance, the removal of 4-chlorophenol ranged from 1.1% to 99.5% with the temperature increasing from 423 to 463 K (García-Molina et al., 2007). The partial pressure of oxygen is the part of the driving force for mass transfer, thus the removal efficiency increases with the increase of oxygen amount (Joglekar et al., 1991; Mantzavinos et al., 1996; Thomsen, 1998; Lei et al., 2007). However, if the stoichiometric quantity of oxygen is achieved, the oxygen partial pressure is not a significant factor for organic compounds degradation (Lei et al., 2007; Kim and Ihm, 2011). With increasing reaction time, more free radicals are generated, which promotes the degradation rate (Shende and Levec, 1999; Lefèvre et al., 2011a; Demirel and Kayan, 2012). Although WAO technology has been frequently used for the treatment of organic pollutants, most studies focused on phenolic compounds. Little literature study the degradation of glyphosate via WAO technology. Only Xing et al. (2018) reported that 100% glyphosate removal and over 93% organic phosphorus removal for real glyphosate wastewater (containing 200-3000 mg.L⁻¹ glyphosate) were achieved by catalytic wet oxidation using modified activated carbon as a catalyst in a co-current upflow fixed bed reactor at 383-403 K and under 1.0 MPa with the residence time of 4.8 h. There is no literature focused on the kinetics of glyphosate oxidation by WAO technology, which is necessary for the design of WAO reactor.

Table 3.1 Available studies on the treatment of organic pollutants by WAO process

Reference	Pollutants	Conditions	Remarks
(Joglekar et al., 1991)	Phenol (200 mg.L ⁻¹)	$T=423-453$ K; $P_{O_2}=0.3-1.5$ MPa	99.9% phenol removal; 90% COD reduction; E_a : 12.4-201 kJ.mol ⁻¹
(Mantzavinos et al., 1996)	Polyethylene glycol (1 g.L ⁻¹)	$T=383-513$ K; $P_{O_2}=2-3$ MPa; reaction time: 240 min	100% polyethylene glycol removal; 20% TOC removal
(Thomsen, 1998)	Quinolone (poly nuclear aromatics, 25-250 mg.L ⁻¹)	$T=493-553$ K; $P=5.8-7.6$ MPa	99% quinoline removal; 30-50% TOC reduction
(Shende and Levec, 1999)	3-hydroxypropionic (3-HPA, 330 mg.L ⁻¹) and propionic acid (PA, 1000 mg.L ⁻¹)	$T=523-583$ K; $P_{O_2}=1-4.5$ MPa; reaction time: 1-3 h	99.9% 3-HPA removal and 95% HP removal; E_a : 135 kJ.mol ⁻¹ for 3-HPA and 158 kJ.mol ⁻¹ for PA
(García-Molina et al., 2007)	4-chlorophenol (500, 1000 mg.L ⁻¹)	$T=423-463$ K; $P_{O_2}=0.5-1.5$ MPa; reaction time: 90 min	4-chlorophenol removal: 1.1%-99.5%; TOC removal: 1.56%-74.1%
(Lei et al., 2007)	Cationic red X-GRL (dye, 2 g.L ⁻¹)	$T=333-453$ K; $P_{O_2}=0-1.2$ MPa; reaction time: 60 min	Dye removal: 4%-92%; E_a : 39.9 kJ.mol ⁻¹
(Lefèvre et al., 2011a)	Phenol (8.94 g.L ⁻¹)	$T=423-573$ K; $P=20, 30$ MPa; reaction time: 15-60 min	100% phenol removal; 90% TOC reduction; E_a : 77±8 kJ.mol ⁻¹
(Demirel and Kayan, 2012)	AR 271 (azo dye)	$T=373-523$ K; $P_{O_2}=3.0-5.0$ MPa; reaction time: 30-90 min	TOC removal: 80.30%
(Minière et al., 2017)	Phenol (9.3 g.L ⁻¹)	$T=523$ K; $P=30$ MPa; reaction time: 15 min	97% phenol removal; 84% TOC removal

Several research shows two possible oxidation pathways of glyphosate under other oxidation processes, such as photodegradation (Chen et al., 2007a; Echavia et al., 2009), Manganese oxidation (Barrett and McBride, 2005) and H₂O₂/UV oxidation (Manassero et al., 2010): (1) glyphosate transfers to aminomethylphosphonic acid (AMPA) through the cleavage of C-N bond; (2) glyphosate converts to sarcosine through the direct cleavage of C-P bond. AMPA may be further oxidized to methylamine, formaldehyde, NH₄⁺, NO₃⁻ and PO₄³⁻. Sarcosine could be further oxidized to glycine, formaldehyde and NH₄⁺. The study on oxidation pathway of glyphosate by WAO process is rare. Only Xing et al. (2018) proposed the AMPA pathways for glyphosate degradation by catalytic wet oxidation.

Therefore, the main goal of this work is to investigate the glyphosate degradation by WAO process under temperature range of 423-523 K and pressure of 15 MPa. The kinetics of glyphosate degradation by WAO process is studied. The oxidation kinetics is provided with respect to the glyphosate concentration. A kinetic model is determined to represent the experimental data for glyphosate. A possible oxidation pathway of glyphosate by WAO process is proposed.

3.2 Materials and methods

3.2.1 Chemicals

Glyphosate was purchased from Leap Labchem Co., Limited, China with the purity of >95%. AMPA and glyoxylic acid were obtained from Sigma-Aldrich (Saint Quentin Fallavier, France). Aqueous

stock solutions (1 g.L^{-1}) were prepared in polypropylene (PP) bottles, as well as standards and injection solutions. All other chemicals and solvents used were also obtained from Sigma-Aldrich. The synthetic air (purity >99.999%) used as oxidant was brought from Air Liquid, France.

3.2.2 Experimental procedure

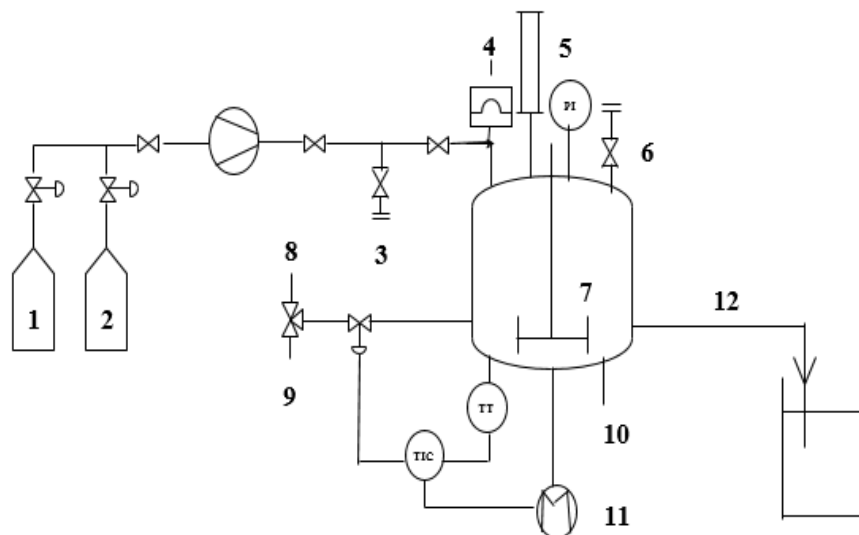


Fig. 3.1 Schematic diagram of WAO setup using the batch reactor. 1 – air bottle; 2 – nitrogen bottle; 3 – gas purge; 4 – bursting disk; 5 – liquid injection; 6 – gas purge; 7 – stir; 8 – cooling water inlet; 9 – compressed air; 10 – cooling water outlet; 11 – heater; 12 – liquid sampling

In order to study the kinetics of glyphosate degradation, the experiments were conducted in a batch reactor (Top Industrie, France). The experimental apparatus for WAO in the batch reactor is shown schematically in Fig. 3.1. The autoclave with internal volume of 202 mL has maximum pressure and temperature of 30 MPa and 623 K, respectively. The temperature in the reactor is regulated by a hot (electric power)/cold (double jacket with air or water) regulating system. The stirring device is a rushton type mixer with 8 blades, with a hollow shaft allowing a recirculation of the gas phase into the liquid phase. Experimentally, the reactor was first pressurized with an amount of nitrogen, which was estimated from thermodynamic calculations using the Soave-Redlich-Kwong equation of state (Lefèvre et al., 2011b), in order to reach desired final pressure and temperature. To evaluate the influence of the temperature on glyphosate oxidation by WAO process, reactions with an initial glyphosate concentration of 1 g.L^{-1} were conducted at three temperature (423, 473 and 523 K). This concentration of glyphosate is in the range of glyphosate concentration which was detected in the industrial wastewater (Heitkamp et al., 1992; Xing et al., 2017). The initial pressure of nitrogen was 7.78, 6 and 2.15 MPa with respect to the temperature of 423, 473 and 523 K, respectively. 120 mL glyphosate solution was injected into the reactor and then the reactor was isolated. When the set temperature was reached, the air was injected into the reactor to achieve the required pressure of 15

MPa and the reaction began ($t=0$). An excess of oxygen of 70% in comparison to the stoichiometry was fixed at the beginning of the reaction for each tested temperature, i.e. air ratio of 1.7 (Lefèvre et al. 2011a, 2011b), The agitation speed was set at 1000 rpm, which could permit to overcome the limitations for mass transfer (Lefèvre et al., 2011a). The samples were collected at regular intervals for glyphosate and TOC concentration analysis. The experiments at 473 and 523 K with a reaction time of 15 and 30 min were repeated for three times in order to obtain the standard error.

3.2.3 Analytical methods

pH was determined by pH meter (HACH Sension+ PH3). TOC concentration was calculated from the difference between total carbon (TC) concentration and inorganic carbon (IC) concentration measured by a TOC-L SHIMADZU analyzer.

The possible organic intermediates of glyphosate degradation which have reported in the literature are aminomethylphosphonic acid (AMPA), glyoxylic acid, sarcosine and formaldehyde (HCHO) (Chen and Liu, 2007; Aquino Neto and de Andrade, 2009; Balci et al., 2009; Echavia et al., 2009; Lan et al., 2013; Xing et al., 2018). The detection of sarcosine was performed by a specific test kit with enzyme (Biovision kit Sarcosine, K636-100) with the maximum of absorption wavelength (λ) of 570 nm. HCHO is measured by UV-vis spectrophotometry by Spectroquant[®] test kit (1.14678.0001, Merck Chemicals) at $\lambda=565$ nm.

The concentrations of glyphosate and two possible byproducts, AMPA and glyoxylic acid were determined by LC/MS analysis. LC/MS analyses were performed using an Agilent 1290 Infinity system coupled to an Agilent 6530 Q-TOF tandem mass spectrometer equipped with an Agilent jet stream (AJS) ion source. Instrument control, data analysis and processing were performed using Mass Hunter workstation software B4.00. The analysis method was adapted from Yoshioka et al. (2011). Briefly, 1 μ L of sample was injected and separation was performed by using an Obelisc N column (150 mm x 2.1 mm I.D, 5 μ m) distributed by SIELC Technologies (Interchim, Montluçon, France). The mobile phase was composed of acetonitrile/water (20/80, v/v) acidified with 0.1% formic at a flow rate of 0.2 mL.min⁻¹. The column was kept at 40°C in the column oven. Mass calibration was first performed pre-acquisition using ESI-L low concentration tuning mix, provided by Agilent technologies. Mass correction was performed by continuous calibration with hexakis (1H, 1H, 3H, tetrafluoropropoxy) phosphazine and purine at m/z 922.0098 and m/z 121.0509 amu. After LC separation, the solution was introduced into the atmospheric pressure ionization source and ionized by electrospray in negative ion mode (ESI-) leading to the formation of the $[M - H]^-$ ions of the analytes. Source parameters were set as follows: fragmentor 140 V, capillary 3000 V, skimmer 65 V,

and nitrogen was used as the drying (350°C, 10 L.min⁻¹), nebulizing (30 psi) and sheath (350°C, 8 L.min⁻¹) gas. Scanning was performed from m/z 50 to 1000 amu with 10 038 transients per spectrum.

For quantification of the three targeted analytes, Extracted Ion Current (EIC) chromatograms were used. Retention times, mass of deprotonated molecules and EIC target molecular weight ranges shown between brackets were as follows: glyoxylic acid (3.400 min, 72.9943 amu, [72.8-73.2 amu]), AMPA (3.695 min, 110.0032 amu, [109.8-110.2 amu]) and glyphosate (7.455 min, 168.0111 amu, [167.8-168.2amu]). The quantification of glyphosate, AMPA and glyoxylic acid concentrations were based on linear regression ($R^2 > 0.999$) obtained by injecting standard solutions containing the three analytes with concentrations ranging from 5-200 µg.mL⁻¹. Instrumental QC was performed by regular analyses of solvent blanks and random injection of standards. Measured values were not deviating more than 15% from the theoretical values. A rough estimation of the concentrations of other phosphorylated by-products identified was performed by using the linear curve obtained for AMPA.

A screening of by-products was performed by working in Total Ion Current (TIC) MS mode in order to determine molecular ions m/z. The chromatograms and their mass spectra were inspected for transformation products known from the literature and for unknown compounds. It should be underlined that none of the degradation products were detected in the blank and standard. The elemental compositions were further calculated, the maximum deviation was set to 10 ppm and C, H, N, O, P were selected as possible present elements.

PO₄³⁻, NH₄⁺ and NO₃⁻ are reported as possible inorganic degradation by-products of glyphosate (Aquino Neto and de Andrade, 2009; Manassero et al., 2010; Lan et al., 2013; Ndjeri et al., 2013). PO₄³⁻ was quantified by UV-vis spectroscopy through using Spectroquant[®] test kit (1.00798.0001, Merck Chemicals) at λ=690 nm. NH₄⁺ was detected by UV-vis spectrophotometry through using Spectroquant[®] test kit (1.14752.0001, Merck Chemicals) at λ=690 nm. NO₃⁻ was measured by UV-vis spectroscopy (Spectroquant[®] test kit 1.09713.0001, Merck Chemicals) with λ=340 nm.

3.3 Results and discussion

3.3.1 Glyphosate degradation

In order to check the possible thermal degradation of glyphosate under the three temperatures, the glyphosate concentrations were measured when the required temperature was achieved and before oxygen injection. Different thermal degradation of glyphosate under the three temperatures were found. The glyphosate concentration after thermal degradation ranged from 1000 to 915.56, 754.00 and 459.00 mg.L⁻¹, in correspondence with TOC decreasing from 213 to 210.5, 178.1 and 159.3 mg.L⁻¹ under the temperature of 423, 473 and 523 K, respectively. Thus, the initial concentrations of

glyphosate and TOC for oxidation under the three temperatures were revised to the concentration after thermal degradation.

The experimental results of glyphosate removal with time under three temperature is shown in Fig. 3.2. At 523 K, during the first 5 min of reaction, the temperature in the cell increased up to 2 to 3°C due to exothermicity. It then stabilized at 523 K thanks to the regulation system. The reaction temperature has a major effect on the reduction of glyphosate. The glyphosate removal was seen to significantly increase with an increase in temperature from 423 to 523 K. At 523 K, completed glyphosate removal was obtained after 30 min. However, the reduction of glyphosate was of 87.6% and 21.4% after 60 min at 473 and 423 K, respectively. Furthermore, the results show that glyphosate is degraded rather quickly at 473 and 523 K, while slowly at 423 K, indicating that there seems to be a threshold between 423 and 473 K due to the significant gap in terms of degradation.

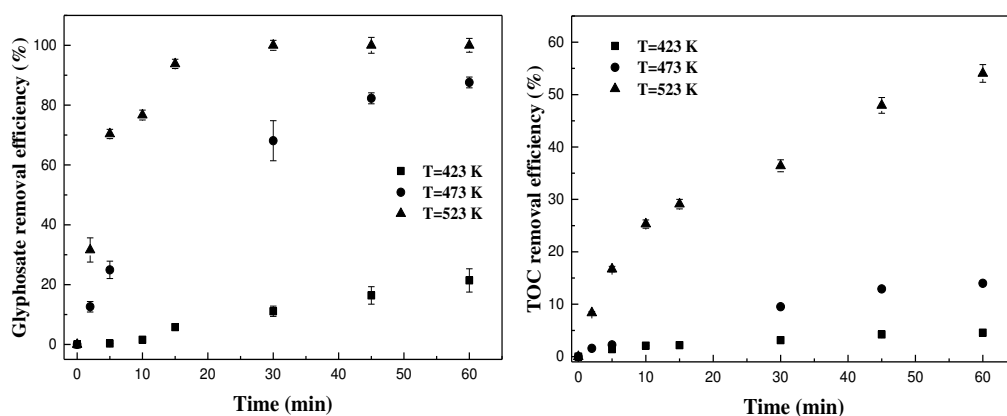


Fig. 3.2 Effect of temperature on the glyphosate and TOC removal at 15 MPa

As some intermediate products appeared during the oxidation of glyphosate to carbon dioxide, it would be convenient for WAO design purposes to present its lumped parameter, i.e., TOC. The effect of temperature of the TOC removal is shown in Fig. 3.2. During the reaction time, the TOC decreased following the same pattern with glyphosate concentration. For instance, after 60 min, the TOC removal was 4.5%, 14% and 54% at 423, 473 and 523 K, respectively. Furthermore, at the same reaction time, the TOC reduction was smaller than glyphosate removal. This was attributed to the formation of low-molecular weight and refractory intermediates, which remained in the solution and were not oxidized (Mishra et al., 1995; Vicente et al., 2002), especially at the temperature below 473 K. Between 473 and 523 K, there is a considerable performance gap for TOC abatement, indicating that the intermediates of glyphosate are more degradable at 523 K than at 473 K.

Regarding reaction intermediates, the formation of oxidation by-products of glyphosate in WAO process was confirmed by pH of the effluent. During the glyphosate oxidation by WAO process, the

pH increased from 2.5 to 2.6, 3.0 and 4.1 after 60 min at 423, 473 and 523 K, respectively. The increase of pH after oxidation was also found by Xing et al. (2018). The higher pH value was obtained when working at higher temperature, indicating a faster elimination of glyphosate and its intermediates. This trend is opposite to other literatures for other compounds which found a pH decrease with the increasing temperature caused by the formation of organic acids as reaction intermediates (García-Molina et al., 2007; Suárez-Ojeda et al., 2007). This is possibly due to the generation of PO_4^{3-} during glyphosate oxidation as confirmed by UV-vis spectrometry. For instance, the concentration of PO_4^{3-} ranged from 5.9 to 99.8 mg.L^{-1} with the temperature increasing from 423 to 523 K after 30 min. PO_4^{3-} presents alkaline in aqueous solution, causing the increase of pH.

3.3.2 Kinetic modeling

The global kinetic model tested take into account the concentration of organic compound and oxygen concentration, which has been validated by other authors for WAO of organic compounds and different wastewaters (Li et al., 1991; Rivas et al., 1998; Shende and Levec, 1999; Lefèvre et al., 2011). The resulting mass balance in the batch reactor is given through Eq. 3-1.

$$r = -\frac{dC}{dt} = kC^n C_{O_2}^m \quad \text{Eq. 3-1}$$

where C is the concentration of organic compound (mg.L^{-1}); C_{O_2} is the concentration of oxygen dissolved in the liquid phase; n and m are the partial orders; k is the rate constant, which depends on Arrhenius equation (Eq. 3-2).

$$k = k_o e^{-E_a/RT} \quad \text{Eq. 3-2}$$

where k_o is the pre-exponential factor; E_a is the activation energy for the reaction (kJ.mol^{-1}); R is the gas constant ($8.314 \text{ J.mol}^{-1}.\text{K}^{-1}$) and T is the temperature (K). k_o and E_a can be obtained through a linear regression between $\ln k$ and $1/T$.

It is reported that if an excess oxygen was maintained at a constant partial pressure in the reactor, the zero order respects to the oxygen and the oxygen terms may be assumed as a constant (Li et al., 1991; Kolaczowski et al., 1999; García-Molina et al., 2007; Suárez-Ojeda et al., 2007). In this study, the air ratio is 1.7, which oxygen is in excess. Thus, the Eq. 3-1 can be transferred to Eq. 3-3.

$$r = -\frac{dC}{dt} = kC \quad \text{Eq. 3-3}$$

In this study, C represents the concentration of glyphosate or TOC.

Table 3.2 shows the first-order kinetic reaction fits well the glyphosate degradation. The apparent reaction constants of these reactions are presented in Table 3.2. It indicates that glyphosate degradation rate increases significantly with an increased in temperature, which is similar to the literature (Lin et al., 1996; Lei et al., 2007). Furthermore, the apparent reaction constants are found to well agree with the Arrhenius equation (Fig. 3.3) with R^2 of 0.999. The activation energy for glyphosate oxidation was estimated through Arrhenius equation to be $68.44 \text{ kJ.mol}^{-1}$, which is in the upper range of those found in the literature using WAO process to treat other organic compounds ($33.1\text{-}77.8 \text{ kJ.mol}^{-1}$) (Pruden and Le, 1976; Helling et al., 1981; Joglekar et al., 1991; Suárez-Ojeda et al., 2007; Lefèvre et al., 2011a). This value is less than some small molecules organic compounds, such as acetic acid ($167.7 \text{ kJ.mol}^{-1}$), formic acid ($121.3 \text{ kJ.mol}^{-1}$), oxalic acid ($129.4\text{-}133.8 \text{ kJ.mol}^{-1}$) (Foussard Jean-Noël et al., 1989; Shende and Mahajani, 1994, 1997). For most WAO process, organic compounds are inclined to oxidize to these small molecules instead of CO_2 and H_2O (Lei et al., 2007). In this study, the low activation energy indicates that glyphosate is more likely to be oxidized to various intermediates.

Table 3.2 Estimations of rate constant, pre-exponential factor and activation energy for glyphosate oxidation

T (K)	k ($\text{mmol.L}^{-1}.\text{min}^{-1}$)	R^2	k_0 ($\text{mol.L}^{-1}.\text{min}^{-1}$)	E_a (kJ.mol^{-1})
423	0.0042	0.991		
473	0.035	0.995	1212.26	68.44
523	0.17	0.954		

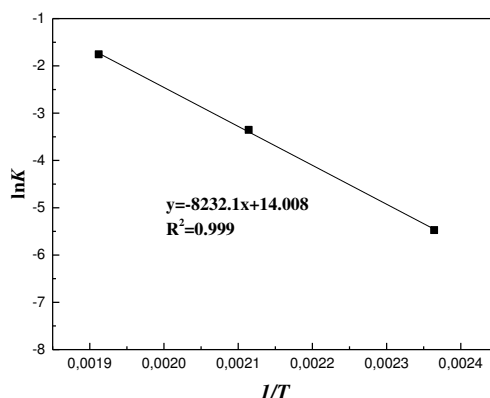


Fig. 3.3 Arrhenius plot for glyphosate oxidation

A comparison of the experimental oxidation results for glyphosate concentration with those calculated from the kinetic models is presented in Fig. 3.4 as a parity plot. It can be seen that for the three temperatures studied, the models show a good fit to the experimental points.

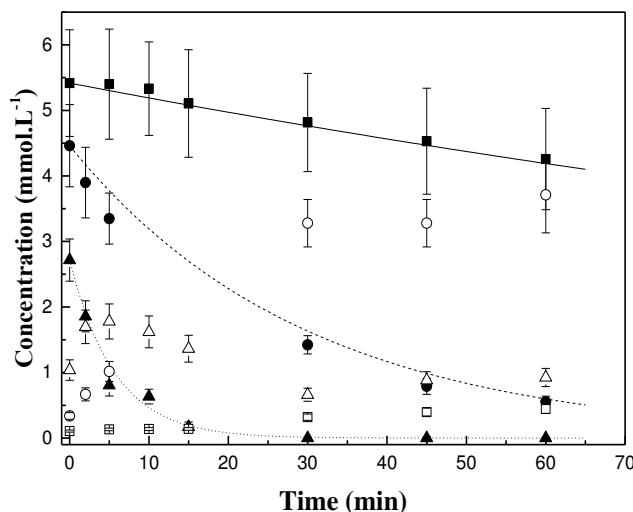


Fig. 3.4 Experimental and simulated concentration of glyphosate and generated AMPA concentration during the experimental process: (1) ■: Experimental glyphosate concentration at 423 K; (2) ●: Experimental glyphosate concentration at 473 K; (3) ▲: Experimental glyphosate concentration at 523 K; (4) Solid line (—): Simulated glyphosate concentration at 423 K (5) Dash line (---): Simulated glyphosate concentration at 473 K; (6) Dot line (···): Simulated glyphosate concentration at 523 K; (7) □: Experimental generated AMPA concentration at 423 K; (8) ○: Experimental generated AMPA concentration at 473 K; (9) △: Experimental generated AMPA concentration at 523 K.

3.3.3 Formation of byproducts

To further understand the reaction mechanisms involved for glyphosate oxidation by WAO process, byproduct evaluation is required. Due to the complex variety of oxidation products, it is difficult to identify and quantify all the intermediates. However, some major stable oxidation products were measured and the possible degradation pathway of glyphosate via WO was proposed. Some oxidation by-products of glyphosate in WAO process were confirmed by LC-MS and UV-vis spectrophotometry. Sarcosine was not detected in the samples by UV-vis spectrophotometer. AMPA, a degradation product of glyphosate which is the most frequently detected in water, soil and oxidation treatments (Chen and Liu, 2007; Assalin et al., 2009; Echavia et al., 2009; Xing et al., 2018), was also detected in our study by LC-MS analysis with the m/z of 110.0032 amu. The concentrations of AMPA generated under three temperatures are shown in Fig. 3.4. It shows that at 423 K, low removal of glyphosate is obtained and little AMPA is formed; at 473 K, high removal of glyphosate and almost all glyphosate are transformed into AMPA; complete glyphosate degradation is achieved and generated AMPA is degraded into other byproducts with time at 523 K.

To further understand the relationship between glyphosate destruction and AMPA formation, glyphosate destruction, AMPA yield and P mass balance (described as the ratio of the sum of the final transformation products quantified to the quantity of glyphosate removed) are calculated by following equations:

$$\text{Glyphosate destruction (\%)} = \frac{n_{GLY}^0 - n_{GLY}^t}{n_{GLY}^0} \times 100 \quad \text{Eq. 3-4}$$

$$\text{AMPA yield (\%)} = \frac{n_{AMPA}}{n_{GLY}^0} \times 100 \quad \text{Eq. 3-5}$$

$$\text{P mass balance (\%)} = \frac{n_{byproducts}}{n_{GLY}^0 - n_{GLY}^t} \times 100 \quad \text{Eq. 3-6}$$

where n_{GLY}^0 is the glyphosate initial molar concentration; n_{GLY}^t is the glyphosate molar concentration at time t ; n_{AMPA} is the AMPA molar concentration at time t ; $n_{byproducts}$ is the sum of the final transformation products (just described by AMPA in this study).

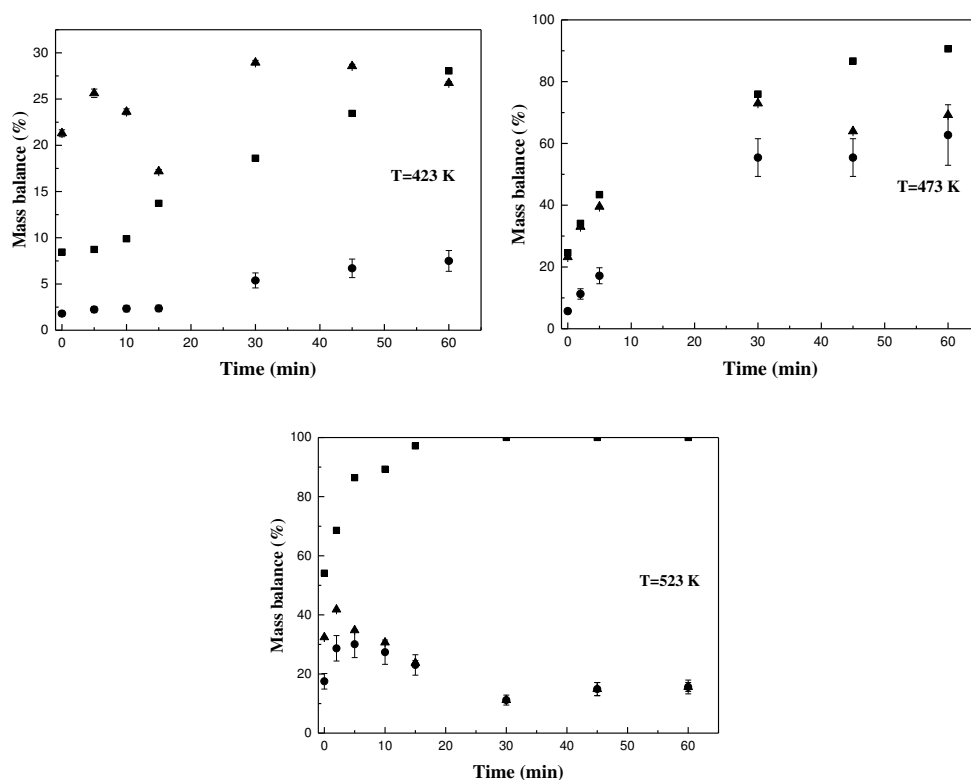


Fig. 3.5 Glyphosate destruction, AMPA yield and P mass balance during oxidation process: (1) ■: glyphosate destruction; (2) ●: AMPA yield; (3) ▲: P mass balance

The results of glyphosate destruction, AMPA yield and P mass balance during glyphosate oxidation process under three temperatures are shown in Fig. 3.5. In order to keep the constant of the initial P mass, the initial glyphosate concentration of 1000 mg.L^{-1} is used for all calculations. Fig. 3.5 shows that AMPA yield increases with respect to the increase of glyphosate destruction at 423 and 473 K, while first increases then decreases at 523 K. This indicates that AMPA is the primary products of glyphosate and can be further oxidized at high temperature. Moreover, the P mass balance are always higher than AMPA yield, indicating the formation of other byproducts.

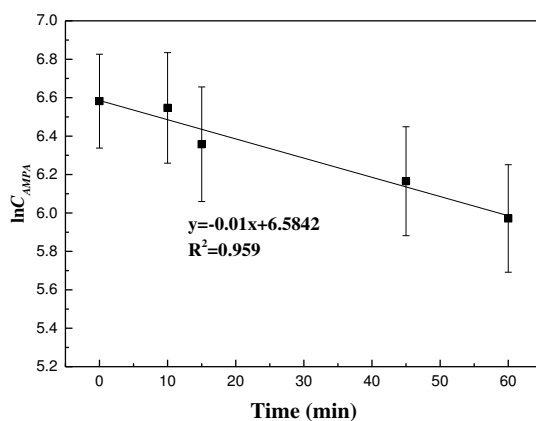


Fig. 3.6 AMPA degradation by WAO process under 523 K.

Furthermore, in order to further confirmation of the degradation of AMPA at 523 K, some kinetic experiments of AMPA oxidation by WAO process were conducted using the same experimental procedure of glyphosate described in section 3.2.2, with the initial AMPA concentration of 658 mg.L⁻¹ in consistent with the same molar of initial glyphosate of 1 g.L⁻¹. The rate constant of AMPA oxidation by WAO process is 0.01 min⁻¹ with the half-life of 69.3 min (Fig. 3.6). After 60 min, the removal efficiency of AMPA is 45.7%, which is lower than glyphosate destruction at same conditions, indicating that AMPA was much more resistant to oxidation than glyphosate, which is consistent with Xing et al. (2018).

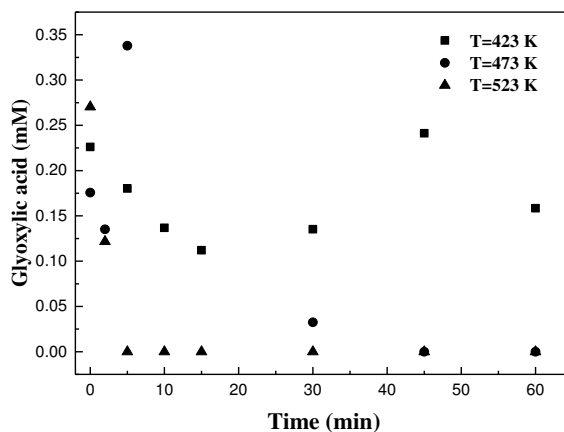


Fig. 3.7 The formation of glyoxylic acid in WAO degradation of glyphosate.

The LC-MS analysis also revealed the presence of glyoxylic acid with m/z of 72.9943 amu. Fig. 3.7 shows the formation of glyoxylic acid during WAO degradation of glyphosate. The low concentration of glyoxylic acid is always found at 423 K, while at 473 and 523 K, its concentration first increases and then decreases until disappearing, especially. This decrease is especially very fast at 523 K. This is probably due to its quick further oxidation at high temperature. It has reported that

glyoxylic acid can be further oxidized into formic acid (HCOOH) and finally mineralized into CO₂ (Balci et al., 2009; Echavia et al., 2009).

Table 3.3 Concentration of by-products of glyphosate in the WAO process under three temperature after 30 min

<i>T</i> (K)	AMPA (mg.L ⁻¹)	PO ₄ ³⁻ (mg.L ⁻¹)	NH ₄ ⁺ (mg.L ⁻¹)	NO ₃ ⁻ (mg.L ⁻¹)	HCHO (mg.L ⁻¹)
423	35.37	5.9	-	2.7	3.15
473	364.00	41.1	-	2.5	42.25
523	73.43	99.8	9.2	2.6	35.45

Table 3.3 shows the concentration of other byproducts of glyphosate in the WAO process under three temperatures after 30 min, such as PO₄³⁻, NH₄⁺, NO₃⁻, and HCHO. It indicates that the concentration of PO₄³⁻ increases with reaction time, while not consistent with the destruction of glyphosate, implying that PO₄³⁻ was not transferred directly from glyphosate, but from AMPA. As for the element of N in AMPA, NH₄⁺ (Aquino Neto and de Andrade, 2009; Echavia et al., 2009; Ndjeri et al., 2013; Xing et al., 2018), which is frequently reported as one of the final mineralization product of AMPA, only existed at 523 K. And the mass in NH₄⁺ was not equal to that in AMPA degraded, indicating that other intermediate exists before AMPA degrading to NH₄⁺. From previous literatures (Annett et al., 2014; Fu et al., 2017), methylamine (CH₃NH₂) has been reported as the intermediate during the degradation of AMPA to NH₄⁺. Thus, the presence of methylamine is possible. It was not measured in this study. The concentrations of NO₃⁻ under three temperatures are almost the same and equal to the initial glyphosate solutions, indicating that NO₃⁻ is not the final mineralization product of glyphosate. Furthermore, the HCHO concentration significantly increases with the reaction temperature increasing from 423 K and 473 K. As for each mole of glyphosate decomposed, the yield of AMPA and HCHO is not equivalent, indicating that glyphosate was not directly degraded into HCHO. The concentration of HCHO is approximately the same as PO₄³⁻. This equality could indicate that HCHO and PO₄³⁻ are directly formed from the oxidation of AMPA, in consistent with Xing et al. (2018). When the temperature further increased to 523 K, the concentration of HCHO decreased, indicating that HCHO can be further oxidized to other byproducts at higher temperature, generally to HCOOH and finally mineralized into CO₂ (Manassero et al., 2010; Xing et al., 2018; Yang et al., 2018).

3.3.4 Proposed degradation pathway

A degradation pathway of glyphosate in WAO process (Fig. 3.8) was proposed taking into account the evaluation of major intermediates and end products based on experimental data. Previous studies have reported that glyphosate oxidation often follows two mechanisms which are related to the cleavage of C-N and C-P

bonds to generate AMPA or sarcosine, respectively (Barrett and McBride, 2005; Manassero et al., 2010; Paudel et al., 2015; Yang et al., 2018). In this work, the existence of AMPA and glyoxylic acid and the absence of sarcosine indicates that glyphosate degradation by WAO process followed the mechanism of C-N bond cleavage. First, the C-N bond of glyphosate promoted by $\cdot\text{OH}$ attack broken to yield AMPA, and glyoxylic acid. Glyoxylic acid was transferred into HCOOH . Then C-P bond cleavage of AMPA generated PO_4^{3-} , HCHO and methylamine (CH_3NH_2). Methylamine was further oxidized into NH_4^+ and HCHO . WAO conditions also involved the oxidation of HCHO into HCOOH , and further into CO_2 and H_2O .

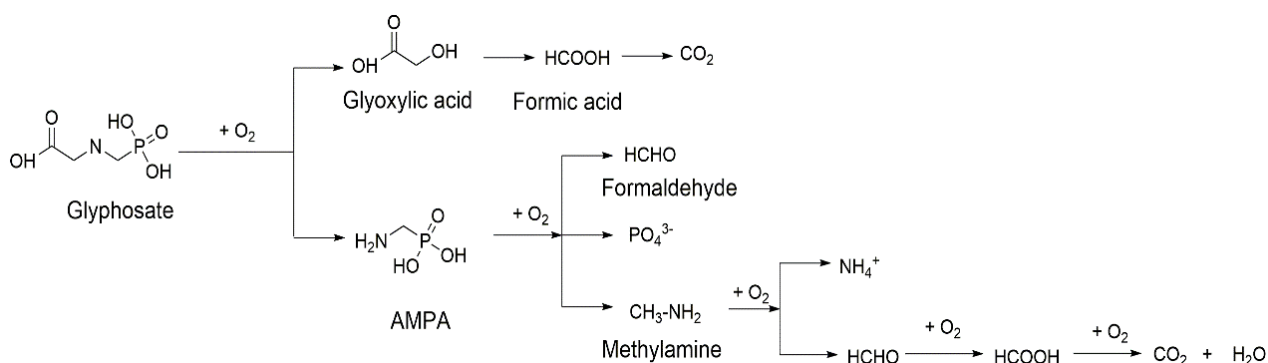


Fig. 3.8 A proposed degradation pathway of glyphosate by WAO process

3.4 Conclusions

WAO process was proved to be an effective technique to treat effluents containing glyphosate since destruction of the target compound and TOC were obtained at 523 K and 15 MPa with the complete glyphosate removal and 54% of TOC reduction after 60 min, respectively. The glyphosate oxidation obeyed first-order kinetics with respect to glyphosate concentration. The degradation rate was faster when increasing the operation temperature. The activation energy was $68.44 \text{ kJ}\cdot\text{mol}^{-1}$. Some possible by-products of glyphosate in WAO process were identified and a degradation pathway was proposed. This study presented a kinetic scheme which can be easily implemented in a WAO process simulation in order to obtain a first evaluation of the process functioning. Further work to consider the kinetic scheme with byproducts of glyphosate should be studied to have more accurate information on WAO process.

In Chapter 3, the kinetics of glyphosate oxidation by WAO process has been studied in a batch reactor under different temperatures and the results showed that the oxidation reactions were well fitted by a first-order kinetic model. Due to the existence of mass transfer limitation in WAO process, as described in Chapter 1, it is interesting to find a method to improve mass transfer for WAO process. Microfluidic devices have been increasingly applied to advanced oxidation process (AOPs) for wastewater treatment, such as electrochemical oxidation and photocatalytic oxidation, due to their inherent advantages, such as large surface to volume ratio and high mass transfer efficiency, which can be a promising technology for WAO process. Thus, in the next chapter, a microfluidic device was used for WAO process for glyphosate degradation in order to improve mass transfer efficiency of WAO process. In this chapter, the effects of temperature and residence time were evaluated, as well as the formation of byproducts. Furthermore, the experimental data has been simulated through using the first-order model from the kinetic studies in Chapter 3.

***Chapter 4 Oxidation of glyphosate by wet air oxidation using a
microfluidic device***

Abstract

A novel microfluidic device was developed, and its performance used for wet air oxidation (WAO) process to degrade glyphosate, an emerging contaminant, was systematically studied. The effects of temperature and residence time on performance of microfluidic device were studied with the range of 473-523 K and 30-90 min, respectively. Glyphosate degradation efficiency increased with an increase of temperature and residence time. Almost complete glyphosate degradation and 74.14% and 84.15% of TOC and COD reduction, respectively, have been obtained at 523 K with the residence time of 90 min. First-order kinetic model has been used to fit the experimental data.

Keyword: Microfluidic device; wet air oxidation; glyphosate; residence time; hydrodynamic model.

4.1 Introduction

Wastewater treatment is a big concern and serious challenge in the world, due to the increasing complex of pollutants (Jayamohan et al., 2015). High-efficiency and low-cost water remediation technologies are needed. Conventional wastewater treatment methods, such as coagulation and adsorption, merely concentrate the contaminants by converting them into other phases (Chong et al., 2010; Jayamohan et al., 2016). Other conventional technologies, such as sedimentation, filtration, chemical and membrane methods are expensive and potentially cause toxic secondary pollutants (Shannon et al., 2008; Jayamohan et al., 2016). Advanced Oxidation Processes (AOPs) are promising methods for wastewater treatments, which could solve some of the issues related to the conventional wastewater treatment technologies, through the oxidation of pollutants by the generation of transitory highly reactive oxygen species. Single or combined AOPs have been used to treat wastewater with high efficiency, including photocatalysis oxidation, Fenton oxidation, electrochemical oxidation, ozonation oxidation, wet air oxidation, etc. But the efficiency of AOPs is still limited to many technical challenges, such as mass transfer limitations, energy consumption, poor managements, etc. (Scialdone et al., 2011; Jayamohan et al., 2016; Pérez et al., 2017). The use of microfluidic device has the potential to reduce these limitations.

Microfluidic device, coming from miniaturization of data-processing devices and information technology, has been applied in various areas in our daily life, such as food industry, pharmaceutical products, biological analysis of proteins and cells, and industrial chemistry for the production of millions of chemicals (Scialdone et al., 2011). Microfluidic device used for chemical reactions can benefit superior heat and mass transfer, high product yield selectivity and purity, easy to control

contact time between fluids, improved safety, and quite easy to scale up, scale down, and modularization of the processes (Scialdone et al., 2010, 2011; Yao et al., 2015).

Recently, microfluidic devices used for AOPs have been increasingly applied to wastewater treatment. Electrochemical microfluidic devices have been reported for the treatment of wastewaters contaminated by organic pollutants with high degradation and mineralization efficiency and high current efficiencies under short treatment times, such as oxalic acid (Scialdone et al., 2010), formic acid (Scialdone et al., 2011), clopyralid (Pérez et al., 2017), 1,1,2,2-tetrachloroethane, etc. (Scialdone et al., 2012). Microfluidic devices used for electrochemical oxidation of organic compounds benefit lower cell voltages and without supporting electrolyte and improve mass transport of pollutants to electrodes surfaces (Scialdone et al., 2010, 2011). Microfluidic devices used for electrochemical processes were also employed for preparative purposes (Paddon et al., 2006), monitoring flow velocities in microfluidic channels (Amatore et al., 2006, 2009), or evaluating chemical-physical parameters such as diffusion coefficients and kinetic rate constants (Thompson et al., 2005; Amatore et al., 2006; Scialdone et al., 2011).

Microfluidic devices also show great potential for photocatalytic applications for wastewater treatment due to their inherent advantages, such as large surface to volume ratio, high mass transfer efficiency, smaller diffusion distance, uniform irradiation over the whole catalytic surface (Han et al., 2013; Corbel et al., 2014; Jayamohan et al., 2015, 2016; Das and Srivastava, 2016). During the past years, microfluidic photocatalytic reactors have been reported to show improved photocatalytic efficiency compared to the conventional reactors, such as slurry reactors (Gorges et al., 2004; Han et al., 2013; Jayamohan et al., 2015, 2016). Furthermore, since microfluidic devices with very small channel dimensions which could provide uniform exposure of light and resolve the immobilization of catalyst, a number of researchers have carried out photocatalytic degradation of pollutants within microfluidic devices, such as phenol (Zhang et al., 2013), 4-chlorophenol (Gorges et al., 2004), terephthalic acid (Eskandarloo et al., 2015), methylene blue (Han et al., 2013; Ramos et al., 2014), methyl orange (Shen et al., 2015), etc.

Among AOPs, wet air oxidation (WAO) is a very effective technology to treat wastewater containing a high content of recalcitrant compounds, which oxidizes organic contaminants at high temperature and pressure by using oxygen or air as the oxidizing agent (Joglekar et al., 1991; Mishra et al., 1995; Luck, 1999; Hu et al., 2001). Typical conditions used for WAO process is the temperature of 398-573 K for temperature and 0.5-20 MPa for pressure (Kolaczowski et al., 1999; Luck, 1999; Debellefontaine and Foussard, 2000; Lefèvre et al., 2011a, 2011b; Lefevre et al., 2012). The WAO process not only depends on the kinetic reactions but also on the transfer between phases (Bhargava

et al., 2006). It has been reported that the rate-limiting step in the WAO process is the mass transfer of oxygen from the gas phase to the liquid phase due to its low solubility in water (Pruden and Le, 1976; Kolaczowski et al., 1999). The WAO performance for wastewater treatment can be enhanced by increasing the gas-liquid mass transfer rate of oxygen. Thus, it will be a very promising technology for wastewater treatment through using microfluidic devices for WAO process owing to its high mass transfer efficiency. The use of microfluidic devices for pollutants treatment are mostly focused on photodegradation and electrochemical oxidation, while no information has been reported for WAO process.

Therefore, in this work, we first report the use of a microfluidic devices for WAO process for the degradation of organic contaminants. Glyphosate, a most widely used herbicide, was chosen model organic compound. The effects of the residence time were evaluated.

4.2 Materials and methods

4.2.1 Chemicals

Glyphosate was purchased from Leap Labchem Co., Limited, China (purity >95%). Aminomethylphosphonic acid (AMPA) and sarcosine was obtained from Sigma-Aldrich (Saint Quentin Fallavier, France). Aqueous stock solutions (1000 mg.L⁻¹) were prepared in polypropylene bottles, as well as standards and injection solutions. The synthetic air (purity>99.999%) used as oxidant was purchased from Air Liquid, France.

4.2.2 Microreactor fabrication

Fig. 4.1 depicts a schematic diagram of the microreaction system in this study (Top Industrie, France). This system consists of several parts, including a stainless-steel pipe with microchannels as microreactor, liquid and gas supplying equipment, two piston pumps for gas and liquid, an oven and a liquid exhaust reservoir. The microchannels has an internal diameter of 1.6 mm and an outer diameter of 3.2 mm. The length of the stainless-steel pipe is 5 or 10 m in order to obtain different residence time. The liquid and gas pump are both a volumetric piston pump, with a minimum flowrate both of 0.005 mL.min⁻¹ and a total volume of 52 and 53 mL, respectively. A vitreous oven (Memmert) with a volume of 32 L is used to control the temperature of the system. The valves outside the oven is used to adjust the pressure of the system.

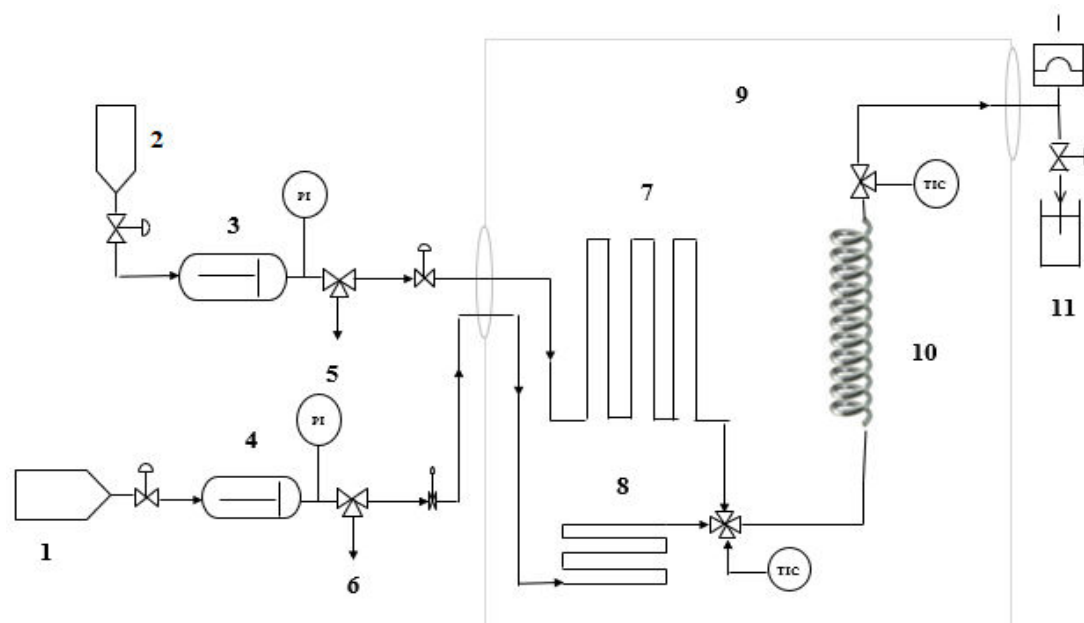


Fig. 4.1 Schematic diagram of microreactor system. 1 – gas tank; 2 – syringe used for liquid; 3 – liquid pump; 4 – gas pump; 5 – liquid purge; 6 – gas purge; 7 – liquid coil; 8 – gas coil; 9 – oven; 10 – microfluidic device; 11 – liquid outlet;

4.2.3 Evaluation of glyphosate degradation

In a typical experiment run, 1 g.L⁻¹ aqueous solution of glyphosate was injected through the liquid pump into the microfluidic device to achieve the required pressure of 15 MPa at the flow rate of 0.3 and 0.2 mL.min⁻¹. When the setup temperature (473 and 523 K) was achieved, the air was injected into the microfluidic device through the gas pump with the flow rate of 0.035 and 0.025 mL.min⁻¹ with respect to liquid flowrate and the length of microchannel in order to obtain the air ratio of 1.7 and the residence time of 30, 45, 60, 90 min, respectively. Then the reaction began, set as zero time ($t=0$). After the residence time, the samples were collected for glyphosate, TOC and chemical oxygen demand (COD) concentration analysis. At the end of experiments, the reactor was depressed and cooled down. The conditions selected for the glyphosate degradation in WAO process using a microfluidic device are summarized in Table 4.1.

Table 4.1 Operating conditions for glyphosate degradation

Parameters	Unit	Values
Glyphosate concentration	g.L ⁻¹	1
Pressure	MPa	15
Temperature	K	473, 523
Air factor	-	1.7
Residence time	min	30, 45, 60, 90

4.2.4 Analytical methods

pH values of the samples before and after reaction were determined by using a pH meter (HACH Sension+PH3). TOC concentration was calculated from the difference between total carbon (TC) concentration and inorganic carbon (IC) concentration which were measured by a TOC-L SHIMADZU analyzer. COD concentration was measured by COD Cell Test C4/25 (1.14541.0001, Merck Chemicals) using UV-vis spectrophotometry (photoLab® 6600 UV-VIS) at the maximum wavelength of 605 nm.

The glyphosate concentration was determined by liquid chromatography/mass spectrometry technique (LC/MS) using an Agilent 1290 Infinity system coupled to an Agilent 6530 Q-TOF tandem mass spectrometer equipped with an Agilent jet stream (AJS) ion source. Instrument control, data analysis and processing were performed by Mass Hunter workstation software B4.00. The method was conducted according to Yoshioka et al. (2011). 1 μ L of sample was injected and separated through using an Obelisc N column (150 mm x 2.1 mm I.D, 5 μ m) distributed by SIELC Technologies (Interchim, Montluçon, France). The mobile phase was composed of acetonitrile/water (20/80, v/v) acidified with 0.1% formic acid with the flow rate of 0.2 mL.min⁻¹. The column was kept at 40°C in the column oven. After LC separation, the solution was introduced into the atmospheric pressure ionization source and ionized by electrospray in negative ion mode (ESI) leading to the formation of the [M - H]⁻ ions of the analytes. Working conditions were as follows: fragmentor 140 V, capillary 3000 V, skimmer 65 V. Nitrogen was used as the drying (350°C, 10 L.min⁻¹), nebulizing (30 psi) and sheath (350°C, 8 L.min⁻¹) gas. Scanning was performed from m/z 50 to 1000 amu with 10 038 transients per spectrum. Extracted Ion Current (EIC) chromatograms were used for glyphosate quantification. The retention time, mass of deprotonated molecules and EIC target molecular weight ranges of glyphosate is 7.455 min, 168.0111 amu and [167.8-168.2 amu], respectively. The quantification of glyphosate concentrations was based on linear regression (R²>0.999) obtained by injecting glyphosate standard solutions with the range of concentrations of 5-200 μ g.mL⁻¹. Instrumental QC was performed by regular analyses of solvent blanks and random injection of standards. Measured values were not deviating more than 15% from the theoretical values.

Due to the evaporation, the flow rates of the outlet were measured using a balance (KERN PCB 3500-2) through the change of the mass of the effluents with time. Thus, according to mass balance, the removal efficiencies of glyphosate, TOC and COD were calculated by:

$$X(\%) = \frac{Q_{inf}A_0 - Q_{eff}A}{Q_{inf}A_0} \times 100 \quad \text{Eq. 4-1}$$

where X is the removal efficiency of glyphosate, TOC or COD; Q_{inf} and Q_{eff} is the flow rate of the

influent and effluent, respectively; A_0 and A is the initial concentration and the concentration after the residence time of glyphosate, TOC and COD, respectively. Residence time (τ) was defined by the following equation:

$$\tau = \frac{V_m}{Q} \quad \text{Eq. 4-2}$$

where V_m is the total internal volume of the microchannel which can be calculated through the inner diameter and the length of steel-stainless pipe and Q is the flowrate of the fluids.

Furthermore, aminomethylphosphonic acid (AMPA) and sarcosine, the two possible primary byproducts which are generally found in glyphosate oxidation process through the cleavage of C-N and C-P bond (Chen et al., 2007a; Echavia et al., 2009; Manassero et al., 2010; Xing et al., 2018), respectively, were also measured in this study. The detection of sarcosine was conducted by UV-Vis spectrophotometry (photoLab® 6600 UV-VIS) through using a specific test kit (Biovision kit Sarcosine, K636-100) with the maximum absorption wavelength of 570 nm. AMPA was measured by LC/MS using the same procedure with glyphosate analysis which was described above. The quantification of AMPA concentrations was based on linear regression ($R^2 > 0.999$) obtained with the range of concentrations of 5-200 $\mu\text{g}\cdot\text{mL}^{-1}$. The retention time, mass of deprotonated molecules and EIC target molecular weight ranges of AMPA is 3.695 min, 110.0032 amu and [109.8-110.2 amu], respectively.

4.3 Results and discussion

4.3.1 Glyphosate degradation

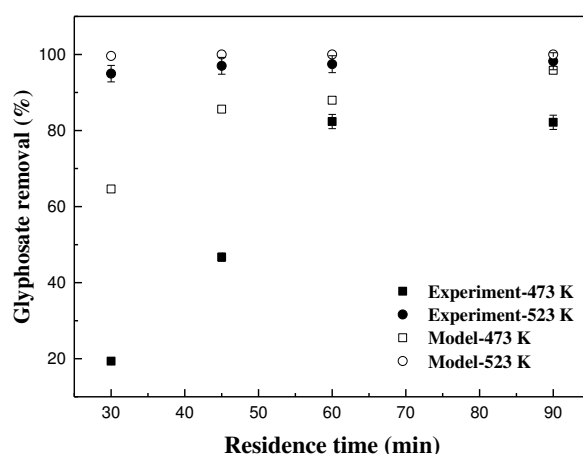


Fig. 4.2 Effect of residence time on glyphosate removal through comparison between experiments and modeling results at 473 and 523 K.

According to previous work of glyphosate degradation by WAO process using a batch reactor, the reaction temperature has a significant effect on the glyphosate removal. Thus, in this study, two reaction temperatures of 473 and 523 K were tested to know its effect on glyphosate degradation, which is shown in Fig. 4.2. At each residence time, the glyphosate removal efficiencies at 523 K are all obviously higher than that at 473 K, especially at low residence time. It is noting that almost complete glyphosate degradation (>94%) has been achieved at each residence time at 523 K, while for 473 K, the maximum glyphosate removal is 82.36%.

Residence time is another factor which determines the reaction time of the glyphosate solution with oxygen. Fig. 4.2 displays the effect of residence time on glyphosate removal at 473 K and 523 K. At 473 K, the glyphosate removal efficiency significantly increases from 19.38% to 82.36% with an increase in the residence time from 30 to 60 min. This is intuitive since an increase in residence time would result in more contact time for glyphosate to react with oxygen. This phenomena is consistent with other literatures reported on photocatalytic oxidation of organic compounds through using microfluidic devices (Lei et al., 2010; Charles et al., 2011; Gao et al., 2012; Eskandarloo et al., 2015). When the residence time is further increased to 90 min, the glyphosate removal efficiency is almost constant with that at 60 min, indicating that the glyphosate oxidation reaction has already achieved equilibrium after 60 min. However, at 523 K, the residence time slightly affects the glyphosate removal efficiency. The glyphosate removal slightly increases from 94.96% to 98.22% with the residence time ranging from 30 to 90 min. This is because the residence time of 30 min was sufficiently high to convert almost all glyphosate under mass transfer kinetic control. Scialdone et al. (2011) found the same trend of residence time on formic acid oxidation by microfluidic electrochemical reactors.

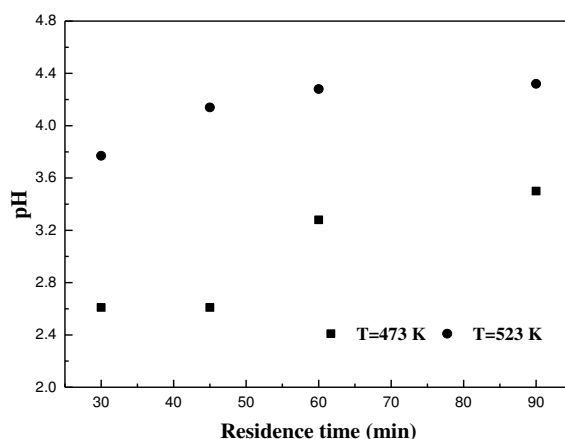


Fig. 4.3 Effect of residence time on pH values at 473 and 523 K.

The change of pH values before and after reaction plays an important role to confirm the degradation of glyphosate, which is shown in Fig. 4.3. After oxidation, the pH value of the solution

increase from 2.61 to 3.5 and from 3.77 to 4.32 with residence time range of 30–45 min at temperature of 473 and 523 K, respectively. It may be caused by the generation of alkaline substance, such as phosphate, during the degradation of glyphosate.

4.3.2 TOC and COD reduction

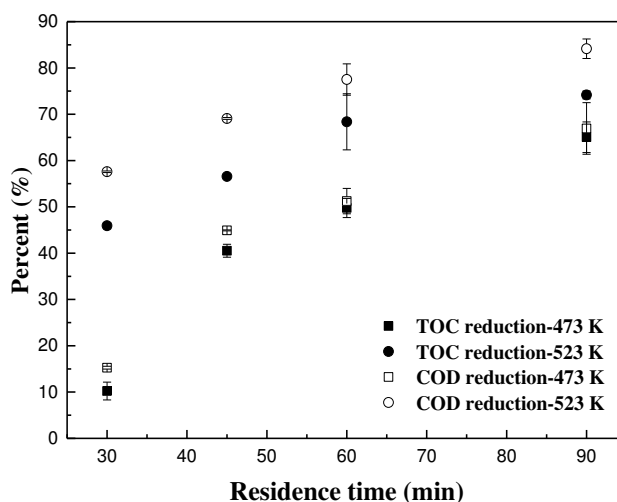


Fig. 4.4 Effect of residence time on TOC and COD reduction at 473 and 523 K.

The TOC and COD of the glyphosate solution was measured before and after oxidation in the microfluidic device at different residence time under 473 and 523 K and then the TOC and COD reductions were calculated using the Eq. 4-1. The results are shown in Fig. 4.4. It is found that at each residence time, the TOC and COD reductions at 523 K are significantly higher than that at 473 K, following the same trend with glyphosate removal. The maximum TOC and COD reduction is 65.04% and 66.93% at 473 K, respectively, 74.16% and 84.15% at 523 K, respectively. However, the TOC and COD reduction are all less than glyphosate removal at the same residence time and temperature, indicating that glyphosate is degraded into some organic intermediate compounds.

Furthermore, with the increase of residence time from 30 to 90 min, the TOC reduction is continuously increased, even when the glyphosate removal keeps constant, from 10.23% to 65.04% and from 45.92% to 74.16% for 473 and 523 K, respectively. The COD reduction follows the same trend, from 15.27% to 66.93% and from 57.58% to 84.15% at 473 and 523 K, respectively. This is due to the further oxidation of the organic intermediate compounds of glyphosate.

4.3.3 The formation of byproducts

In this study, two frequently detected primary byproducts of glyphosate, AMPA and sarcosine were measured. Sarcosine was not detected in the samples by UV-vis spectrophotometer. However, AMPA was detected in all samples after reaction by LC/MS with the m/z of 110.0032 amu, indicating

that glyphosate oxidation in the microfluidic device follows the mechanism of C-N bond cleavage of glyphosate. To further understand the relationship between glyphosate destruction and AMPA formation, AMPA yield and P mass balance are calculated by following equations:

$$AMPA \text{ yield } (\%) = \frac{n_{AMPA}}{n_{GLY}^0} \times 100 \quad \text{Eq. 4-3}$$

$$P \text{ mass balance } (\%) = \frac{n_{AMPA}}{n_{GLY}^0 - n_{GLY}^t} \times 100 \quad \text{Eq. 4-4}$$

where n_{AMPA} is the AMPA molar concentration at time t ; n_{GLY}^0 is the glyphosate initial molar concentration; n_{GLY}^t is the glyphosate molar concentration at time t .

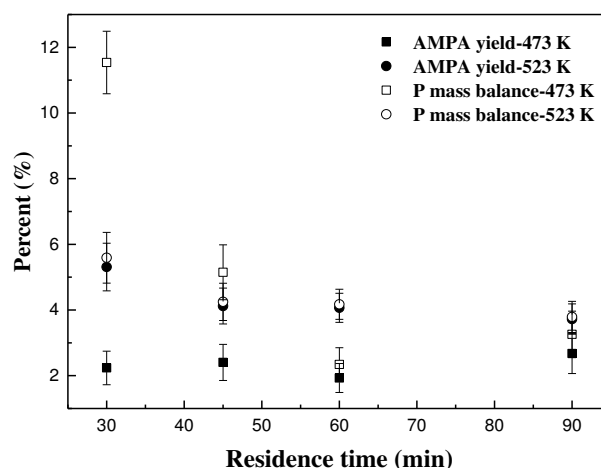


Fig. 4.5 AMPA yield and P mass balance under different residence time at 473 and 523 K.

The results of AMPA yield and P mass balance under different residence times at 473 K and 523 K are shown in Fig. 4.5. It shows that AMPA yield at 523 K is bigger than that at 473 K under the same residence time, due to the higher glyphosate destruction at 523 K. In addition, AMPA yield slightly increases with the increase of residence time at 473 K due to the increase of glyphosate destruction, while slightly decreases with an increase in residence time at 523 K, due to the continuously oxidation of AMPA. However, AMPA yield is small under all tested conditions. The low AMPA yield and high glyphosate removal indicates that most of AMPA is degraded into other byproducts. Furthermore, the P mass balance are all higher than AMPA yield, further confirming the oxidation of AMPA.

4.3.4 Modelling

In this study, the microfluidic reactor is first considered to be a perfect plug-flow reactor with the assumption of the absence of mass-transfer limitation (kinetic regime), i.e. the degradation rate only depends on the kinetics. Then the glyphosate outlet concentration can be expressed by first-

order model through using equation 4-5 with assuming that the reactor is at permanent regime and without considering dispersion:

$$C = C_0 e^{-k\tau} \quad \text{Eq. 4-5}$$

where C_0 is the initial glyphosate concentration, k is the kinetic constant. According to the previous kinetics studies of glyphosate oxidation in a batch reactor, the kinetic constants of 0.034 and 0.177 $\text{mM}\cdot\text{min}^{-1}$ at 473 and 523 K, respectively, have been obtained.

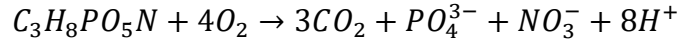
Therefore, glyphosate removal efficiency was calculated using the Eq. 4-1. Fig. 4.2 shows the calculated and experimental glyphosate removal as a function of the residence time. As expected, the glyphosate removal increases with the residence time which corresponds to a longer contact time in the microfluidic device, especially at 473 K. At 523 K, the model describes correctly the experimental data. The experimental and calculated glyphosate removal efficiencies are all approximately 100% for four tested residence times, indicating that the reaction equilibrium has been obtained before 30 min at 523 K and the mass transfer has not been a limitation for glyphosate oxidation. However, at 473 K, a significant disagreement between the model and experimental data, especially at short residence time. The experimental points are all lower than the correspondence calculated data. This phenomenon occurs due to the existence of mass transfer, which is needed to be further studied. It has reported that highly uniform bubbles can be generated in microfluidic device (Fu et al., 2011). According to our previous reported work (Feng et al., 2019), with the decrease of temperature, the bubble size increases, while gas holdup and interfacial area decreases, causing the decrease of mass transfer. This maybe explain the limitation of mass transfer at 473 K. Furthermore, the solubility of oxygen at 473 K is lower than that at 523 K, which may cause that oxygen become the limitation of mass transfer, resulting the inconsistency between the calculated and experimental data.

4.4 Conclusions

The microfluidic device used for WAO process could be a potential technology to continuously treat glyphosate-containing wastewater. The glyphosate degradation performance of the microreactor was increased with the increase of temperature and the residence time. Almost complete glyphosate degradation and 74.14% and 84.15% of TOC and COD reduction, respectively, have been achieved at 523 K with the residence time of 90 min. Thus, the microfluidic device exhibits a broad range of applications in the treatment of other organic pollutants by WAO process and can be expected for good performance of the practical application in wastewater treatment plants, which needs further studies.

In the previous chapter is presenting a model only based on kinetics evolution. This model does not represent very well the experimental evolutions. In order to provide a new model, it is necessary to take into account mass transfer limitations. A first modelling and first results are presented here.

In order to describe the mass-transfer limitation, a hydrodynamic model is considered to explain experimental data. The microfluidic reactor was modelled with j perfectly mixed reactors. Furthermore, these reactors were assumed to be in a steady state. The complete oxidation of glyphosate can be summarized as (Rubí-Juárez et al., 2016):



As there is a dynamic evolution due to mass transfer of oxygen from gas phase to liquid phase, and reaction of oxygen with glyphosate in the liquid phase, it is necessary, for each perfectly mixed reactor, to solve mass balances in transitory state, up to steady state values of concentrations. Therefore, the mass balance for glyphosate in liquid phase and oxygen in liquid and gas phase between two adjacent small reactors (reactor i and reactor $i + 1$) in the presence of mass-transfer limitation without considering axial dispersion and convection is given by following equations.

Mass balance on glyphosate in liquid phase.

$$Q_L C_{GLY}^i - k C_{GLY}^{i+1} C_{O_2,L}^{i+1} V_L = Q_L C_{GLY}^{i+1} + V_L \frac{dC_{GLY}^i}{dt} \quad \text{Eq. 4-6}$$

Mass balance on oxygen in liquid phase.

$$Q_L C_{O_2,L}^i - 4k C_{GLY}^{i+1} C_{O_2,L}^{i+1} V_L + k_L a V_G (C_{O_2}^* - C_{O_2,L}^{i+1}) = Q_L C_{O_2,L}^{i+1} + V_L \frac{dC_{O_2,L}^{i+1}}{dt} \quad \text{Eq. 4-7}$$

Mass balance on oxygen in gas phase.

$$Q_G C_{O_2,G}^i = Q_G C_{O_2,G}^{i+1} + k_L a V_G (C_{O_2}^* - C_{O_2,L}^{i+1}) + V_G \frac{dC_{O_2,G}^{i+1}}{dt} \quad \text{Eq. 4-8}$$

Thermodynamic equilibrium between gas and liquid phases.

$$C_{O_2}^* = k^* C_{O_2,G}^{i+1} \quad \text{Eq. 4-9}$$

$$k^* = \frac{55.6ZRT}{H} \quad \text{Eq. 4-10}$$

Volume between gas and liquid phases.

$$V_L = V_{total} \frac{Q_L}{Q_L + Q_G} \quad \text{Eq. 4-11}$$

$$V_{total} = \frac{1}{4} \pi r^2 \times L \quad \text{Eq. 4-12}$$

$$V_G = V_{total} - V_L \quad \text{Eq. 4-13}$$

where Q_L and Q_G are the flowrates of liquid and gas phase, respectively; V_{total} , V_L and V_G are the total volume of the reactor and the volumes of liquid and gas phase, respectively; L is the length of the microfluidic device; r is the inner diameter of microfluidic device; C_{GLY}^i and C_{GLY}^{i+1} are glyphosate concentrations in reactor i and reactor $i + 1$, respectively; t is the reaction time; $C_{O_2,L}^i$ and $C_{O_2,L}^{i+1}$ are oxygen concentrations in liquid phase in reactor i and reactor $i + 1$, respectively; $C_{O_2,G}^i$ and $C_{O_2,G}^{i+1}$ are oxygen concentrations in gas phase in reactor i and reactor $i + 1$, respectively; $C_{O_2}^*$ is oxygen saturation concentration in the liquid phase; Z is the oxygen compressibility factor; R is perfect gas constant; T is the temperature. H is Henry constant (calculated from the equation proposed by (Himmelblau, 1960)); $k_L a$ is volumetric mass transfer coefficient of oxygen in the liquid phase, which is assumed to equal to 0.6 min^{-1} (Joglekar et al., 1991).

Since the oxygen mass transfer limitation is considered in this model, the kinetic model is also needed to consider the effect of oxygen in order to obtain the correspondence kinetic constant (k). Thus, in the present study, k was modified to incorporate oxygen concentration in the liquid phase with oxygen order of 1. The kinetic constant was modified to 0.829 and $3.150 \text{ L.mol}^{-1}.\text{min}^{-1}$ at 473 K and 523 K , respectively. These above equations will be solved by Matlab R2019a with the function `ode45`, which implements a Runge-Kutta method with a variable time step for efficient computation, in order to obtain the simulated outlet concentration of glyphosate, oxygen concentration in liquid and gas phase, and the optimal number (j) of reactors. The model gives a number of reactors j varying from 50 to 200, depending on the length of the microfluidic device. However, the evaluation of the glyphosate degradation efficiency is not sufficiently accurate to be presented in this document. Analysis of the results shows that the evaluation of the $k_L a$ with the operating conditions needs more investigation to obtain a better modelling. This is an important perspective for this part.

As mentioned in the Chapter 1, it is necessary to study the glyphosate degradation by the individual WAO and biological process to evaluate the performance of the integrated WAO-biological process for glyphosate degradation. The performance of WAO process for glyphosate oxidation has been described in Chapter 3 and 4. Complete glyphosate removal could be both achieved by WAO process in the batch reactor or microfluidic reactor at 523 K, but not a total TOC reduction. Moreover, complete mineralization of glyphosate has not been obtained by the two reactors at all conditions, due to the generation of other intermediates. Thus, it is necessary to further study the following biological treatment. Biological treatment is an easy and eco-friendly process to treat glyphosate-containing wastewater. The mixed cultures, such as activated sludge, are likely able to degrade glyphosate, which would be more meaningful, informative and practical for industrial applications, compared to pure culture. In order to further enhance the degradation capacities of activated sludge, an acclimation process of the culture has been proposed. Thus, in the next chapter, the acclimation process of aerobic activated sludge to degrade glyphosate was studied and discussed. Furthermore, the microbial growth and substrate utilization kinetics during glyphosate biodegradation process were also studied in order to optimize the operational conditions to meet discharge requirements and for the accurate prediction of effluent quality from engineered treatment processes. Byproducts were identified in order to propose a biodegradation pathway of glyphosate in the case of an acclimated sludge.

Chapter 5 Acclimation of aerobic activated sludge to glyphosate biodegradation: experimental study and kinetics modelling

Abstract

The acclimation of activated sludge from a wastewater treatment plant for degradation of glyphosate and its biodegradation kinetics were studied in batch process. The parameters monitored included the concentration of glyphosate and total organic carbon (TOC), pH, dissolved oxygen (DO) and biomass concentration. The results showed that acclimation with glyphosate can increase the degradation activity of activated sludge and almost complete glyphosate removal was achieved by acclimated activated sludge. Conventional Monod model was able to accurately predict the experimental kinetics results of glyphosate biodegradation by acclimated activated sludge. Finally, a possible biodegradation pathway of glyphosate by acclimated activated sludge was proposed.

Keywords: Glyphosate; acclimation; biodegradation; kinetics; Monod model.

5.1 Introduction

Glyphosate (N-(phosphonomethyl)glycine), a synthetic phosphonate compound, is a broad-spectrum, post-emergent, and non-selective systemic herbicide used to eliminate grasses and herbaceous plants (Baylis, 2000; Manassero et al., 2010; Zhan et al., 2018). Glyphosate is one of the most widely used herbicides in the world against annual and perennial weeds in agriculture, urban areas, domestic gardens and silviculture (Aparicio et al., 2013b; Shushkova et al., 2016; Zhan et al., 2018). Glyphosate acts on plants by inhibiting the activity of enolpyruvyl shikimate-3-phosphate synthase, an enzyme for aromatic amino acid biosynthesis in shikimate pathway (Duke et al., 2012; Tazdaït et al., 2018). Massive use of this molecule has been reported to weaken plant defense system (Johal and Huber, 2009), disturb the metabolism (Cattani et al., 2017) and cause DNA or liver damage (Muneer and Boxall, 2008) both for terrestrial and aquatic animals (Cağlar and Kolankaya, 2008; Séralini et al., 2014). In 2015, the International Agency for Research on Cancer (IARC) of World Health Organization (WHO) classified glyphosate as “probably carcinogenic to humans” based on epidemiological, animal and in vitro studies. Thus, it is necessary to remove glyphosate from the Environment.

Glyphosate contaminates the aqueous environment from various sources such as industrial effluents, agricultural runoff and chemical spill (Baylis, 2000; Muneer and Boxall, 2008). Xing et al (2017) reported that glyphosate concentration in waste stream could achieve up to 2560 mg.L⁻¹. There are several processes used for the removal of glyphosate, e.g. biodegradation, photodegradation, chlorine, ozone, adsorption, membrane processes, advanced oxidation, flocculation and filtration

(Jönsson et al., 2013). Among these technologies, biological treatment is considered as an easy, eco-friendly and cost effective process (Nourouzi et al., 2012). Many microorganisms were reported to be able to utilize glyphosate as carbon, nitrogen or phosphorus source (Lerbs et al., 1990; Klimek et al., 2001; Obojska et al., 2002; Sviridov et al., 2012; Firdous et al., 2017). The two main degradation pathways in glyphosate-degrading microorganisms are conversions to aminomethylphosphonic acid (AMPA) through the cleavage of C-N bond, catalyzed by an oxidase, and to sarcosine through the direct cleavage of C-P bond, catalyzed by C-P lyase (Zhan et al., 2018). Single AMPA or sarcosine pathway or both pathways have been frequently found in glyphosate-degrading microorganisms using glyphosate as phosphorus source. Little information was reported for glyphosate as carbon or nitrogen source. However, during the growth and metabolism process of culture, the demand for carbon sources by microorganisms is much higher than that for nitrogen or phosphorus sources. Thus, using glyphosate as carbon source for microorganisms is a potential technology to increase removal efficiency at high glyphosate concentration.

Moreover, most research on the biodegradation of glyphosate focuses on pure microbial cultures, but a few studies are available on the application of mixed cultures, such as activated sludge. The mixed cultures are more likely able to completely degrade contaminants, compared to pure culture due to the various enzymes available in mixed culture, which would be more meaningful, informative, and practical (Nourouzi et al., 2012). Moreover, due to the high requirements of pure culture, mixed culture processes are more suitable for industrial applications. Thus, it is necessary to find mixed culture able to remove glyphosate from aqueous effluents.

The above-mentioned studies have focused on the biodegradability of glyphosate and the pathways of degradation. However, little attention has been paid to the acclimation process. Literature reported that the degradation capacities of activated sludge can be enhanced by the acclimation of the culture (Ye and Shen, 2004). Furthermore, most studies related to glyphosate biodegradation focus on the isolation and identification of the glyphosate-degrading microorganisms, the information on kinetics of glyphosate biodegradation remained poor. Only several literatures have been studied on Monod and Haldane model to describe glyphosate biodegradation kinetics. Monod expression has been reported by Nourouzi et al. (2012) to describe glyphosate consumption kinetics by mixed culture isolated from soil with a specific maximum growth rate of 0.18-0.87 h⁻¹. Haldane model has been used to describe the glyphosate inhibition to biomass growth with a low ratio of self-inhibition and half-saturation constants (<8) (Nourouzi et al., 2012; Tazdaït et al., 2018). It is important to predict the removal kinetics of glyphosate used as carbon source by culture in order to effectively control and enhance the treatment performance of biological treatment for glyphosate.

In aerobic activated sludge process, oxygen is an important substrate used for growth, maintenance and some metabolic routes (including bioproduct synthesis) of bacteria (Garcia-Ochoa et al., 2010). The oxygen uptake rate (OUR) is a decisive important physiological characteristic of culture growth, which can be used to evaluate the performance of aerobic activated sludge process (Garcia-Ochoa et al., 2010; Zou et al., 2009). OUR monitoring is crucial for the assessment of the viability of the microorganisms.

Therefore, the objective of this paper is to investigate the performance of acclimation process of activated sludge for glyphosate biodegradation and its biodegradation kinetics. These studies have important engineering implications for the treatment of wastewater containing glyphosate.

5.2 Materials and methods

5.2.1 Chemicals

Glyphosate (powder, purity>95%) was purchased from Leap Labchem Co., Limited, China. AMPA (powder, purity of 99%) was purchased from Sigma-Aldrich (Saint Quentin Fallavier, France). Ninhydrin (crystals) and sodium molybdate (powder) of analytical grade were obtained from Sigma-Aldrich (France). All other chemicals and solvents used were also obtained from Sigma-Aldrich. Aqueous stock solutions were prepared in polypropylene bottles, as well as standards and injection solutions.

5.2.2 Acclimation process of activated sludge

Table 5.1 Composition of medium used for acclimating activated sludge

Component	Concentration (mg.L ⁻¹)
pH	7±0.05
Glyphosate	100-1000
Glucose	0-480
(NH ₄) ₂ SO ₄	223
K ₂ HPO ₄	27
KH ₂ PO ₄	21
MgCl ₂ ·2H ₂ O	160
CaCl ₂	20
FeSO ₄ ·7H ₂ O	1
NaMoO ₄	2
MnCl ₂	1

Acclimation experiments were conducted using a 5-L fed-batch reactor. The raw activated sludge was collected from a wastewater treatment plant in Aix-en-Provence, France. 4.5 L of raw activated sludge was placed into a 5L-stirred reactor. The concentration of activated sludge was 5.35

$\text{g}\cdot\text{L}^{-1}$ MLSS (mixed liquor suspended solids) at the beginning of the acclimation process with synthetic glyphosate-based substrate (see Table 5.1). Every 24 h (72 h for the weekend), the bioreactor received a pulse feeding of synthetic substrate-glyphosate mixture. Every week, the medium was refreshed with increasing glyphosate concentration from 100 to 1000 $\text{mg}\cdot\text{L}^{-1}$ and decreasing glucose concentration from 480 to 0 $\text{mg}\cdot\text{L}^{-1}$. The TOC concentration of the daily added solution is kept constant (213 $\text{mg}\cdot\text{L}^{-1}$) whatever the carbon source (pure glyphosate, pure glucose or mix) during the whole acclimation process. An air pump with gas distributor was used to provide the aeration conditions to maintain dissolved oxygen (DO) concentration above 3 $\text{mg}\cdot\text{L}^{-1}$. The reactor was maintained at room temperature.

5.2.3 Experiments with acclimated and non-acclimated sludge

In order to validate the acclimated sludge degradation performance, experiments were performed simultaneously with acclimated and fresh sludge. 500 mL of synthetic wastewater with only glyphosate as carbon source were prepared with concentrations of 500 and 1000 $\text{mg}\cdot\text{L}^{-1}$ of glyphosate respectively in addition to the micronutrients specified in Table 5.1. These experiments were performed at room temperature in stirred and aerated reactors with the volume of 1 L. MLSS concentration was kept constant in acclimated and non-acclimated sludges. The hydraulic residence time was set to 24 h. The efficiency of glyphosate biodegradation was followed by the mean of 10 mL- samples collected regularly for glyphosate and TOC analyses.

5.2.4 Analytical methods

During the experimental processes, different parameters have been followed: MLSS, pH, Total Organic Carbon (TOC), Dissolved Oxygen (DO), Oxygen Uptake Rate (OUR) (APHA, 1998) and the concentration of glyphosate and its possible byproducts.

5.2.4.1 Effluent composition analysis

pH was determined by the mean of a pH-meter (HACH Sension+ PH3). TOC concentration was calculated from the difference between total carbon (TC) concentration and inorganic carbon concentration (IC) determined using a TOC-L SHIMADZU analyzer. The procedure for the measurement of MLSS is outlined in *Standard Method 2540 D* ("NEMI Method Summary - 2540 D," n.d.).

The concentration of glyphosate were firstly monitored by absorbance measurements using a spectrophotometer (photoLab® 6600 UV-VIS) during the preliminary acclimation process and compared experiments between acclimated and non-acclimated sludge. This method is based on the

reaction ability of glyphosate with ninhydrin and sodium molybdate to produce *Ruhemann's* purple dye with maximum absorption at 570 nm (Bhaskara and Nagaraja, 2006).

In order to investigate the glyphosate biodegradation kinetics by acclimated activated sludge, 500 mL of synthetic glyphosate wastewater with initial concentration of 200, 500, and 1000 mg.L⁻¹ were treated by acclimated activated sludge using the procedures described in section 5.2.3. The concentrations of glyphosate and its potential byproducts were measured regularly. In order to achieve higher accuracy, during kinetic experiments, the residual concentration of glyphosate and its by-product, AMPA, were analyzed by liquid chromatography/mass spectrometry technique (LC/MS). LC/MS analyses were conducted using an Agilent 1290 Infinity system coupled to an Agilent 6530 Q-TOF tandem mass spectrometer equipped with an Agilent jet stream (AJS) ion source. Mass Hunter workstation software B4.00 was used to perform instrument control, data analysis, and processing. The analysis method was performed according to Yoshioka et al. (2011). Briefly, 1 µL of sample was injected and separation was performed by using an Obelisc N column (150 mm x 2.1 mm I.D, 5µm) distributed by SIELC Technologies (Interchim, Montluçon, France). The mobile phase was composed of acetonitrile/water (20/80, v/v) acidified with 0.1% formic. The flow rate was 0.2 mL.min⁻¹. The column was kept at 40°C in the column oven. After LC separation, the solution was introduced into the atmospheric pressure ionization source and ionized by electrospray in negative ion mode (ESI) leading to the formation of the [M - H]⁻ ions of the analytes. Working conditions were as follows: fragmentor 140 V, capillary 3000 V, skimmer 65 V. Nitrogen was used as the drying (350°C, 10 L.min⁻¹), nebulizing (30 psi) and sheath (350°C, 8 L.min⁻¹) gas. Scanning was performed from m/z 50 to 1000 amu with 10 038 transients per spectrum. For quantification of the two targeted analytes, Extracted Ion Current (EIC) chromatograms were applied. Retention times, mass of deprotonated molecules and EIC target molecular weight ranges shown between brackets were as follows: AMPA (3.695 min, 110.0032 amu, [109.8-110.2 amu]) and glyphosate (7.455 min, 168.0111 amu, [167.8-168.2 amu]). The quantification of glyphosate and AMPA concentrations was based on linear regression (R²>0.999) obtained by injecting glyphosate or AMPA standard solutions in a range of concentrations of 5-200 µg.mL⁻¹. Instrumental QC was performed by regular analyses of solvent blanks and random injection of standards. Measured values were not deviating more than 15% from the theoretical values.

The other possible byproducts, sarcosine, formaldehyde, PO₄³⁻, NH₄⁺, and NO₃⁻ (Zhan et al., 2018), were also measured by UV-vis spectrophotometry (photoLab® 6600 UV-VIS). Sarcosine was detected by a specific test kit (Biovision kit Sarcosine, K636-100) with a maximum absorption at 570 nm. HCHO is measured by Spectroquant® test kit (1.14678.0001, Merck Chemicals) with a maximum

absorption at 565 nm. PO_4^{3-} was quantified through using Spectroquant[®] test kit (1.00798.0001, Merck Chemicals) with a maximum absorption at $\lambda=690$ nm. NH_4^+ was detected by UV-vis spectrophotometry through using Spectroquant[®] test kit (1.14752.0001, Merck Chemicals) with the maximum wavelength of 690 nm. NO_3^- was measured by UV-vis spectroscopy (Spectroquant[®] test kit 1.09713.0001, Merck Chemicals). The maximum of absorption is at $\lambda=340$ nm.

5.2.4.2 OUR measurements

OUR was measured during the biodegradation kinetic process with the mean of an open respirometer technique. The open respirometer consisted in a reactor with a 500 mL working volume. A sludge sample without glyphosate is introduced in the reactor at room temperature. The sludge was continuously stirred, and an air pump was used to keep aeration conditions in the reactor. The DO concentration was recorded as a function of time (t) using a DO probe (HACH, HQ 40d). In actual biodegradation processes endogenous OUR (OUR_{en}) and exogenous OUR (OUR_{ex}) should be taken into account (Mineta et al., 2011). The apparent oxygen mass transfer coefficient ($k_L a$) and the OUR_{en} were obtained using a dynamic method based on an unsteady-state procedure (Bandyopadhyay et al., 2009). By stopping the aeration, the DO concentration decreases due to the oxygen consumption by the micro-organisms; with restarting the aeration, the DO concentration increased to reach a steady-state value (Bandyopadhyay et al., 2009). $k_L a$ and OUR_{en} can be obtained through the monitoring of DO concentration evolution. OUR_{ex} can be calculated according to the DO mass balance by following equation (Contreras et al., 2008):

$$OUR_{ex} = k_L a(C_s - C) - OUR_{en} - dC/dt \quad \text{Eq. 5-1}$$

where C_s and C are the saturated and instantaneous DO concentrations (mg.L^{-1}), respectively.

OUR_{ex} is associated with glyphosate aerobic biodegradation and can be written as Eq. 5-2 (Mineta et al., 2011):

$$OUR_{ex} = \frac{1}{Y_{S/O}} \frac{dS}{dt} \quad \text{Eq. 5-2}$$

where S is glyphosate concentration (mg.L^{-1}), $Y_{S/O}$ is glyphosate yield on oxygen ($\text{mg-glyphosate} \cdot (\text{mg O}_2)^{-1}$)

5.3 Results and discussion

5.3.1 Bacteria activity validation during acclimation process

Biomass acclimation process to hardly biodegradable organic compounds is a critical step to induce microbial selection and physiological transformations of the metabolic pathways during the biodegradation process (Karahan et al., 2010). Biomass concentration has an important effect on biological treatment performance of activated sludge (Cordi, 2012).

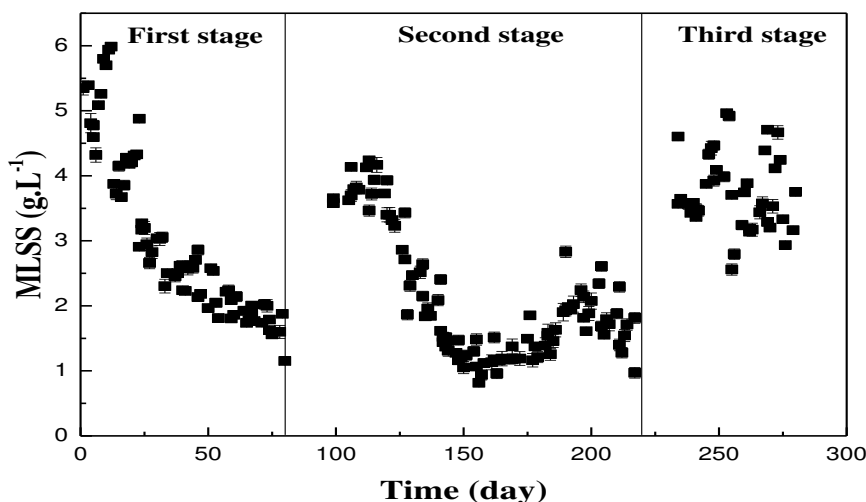


Fig. 5.1 MLSS concentration profile along the acclimation process

The acclimation process was divided into three stages. Each stage was conducted with increasing glyphosate concentration to 1000 mg.L^{-1} and decreasing glucose concentration to 0 mg.L^{-1} . Between each stage, in order to keep high bacteria concentration, glyphosate concentration was reduced to 100 mg.L^{-1} with increasing glucose concentration. The acclimation process lasted 280 days. The average concentration of MLSS during the acclimation process of an activated sludge sample is shown in Fig. 5.1. The decrease of concentration observed in most of first stage periods and in the early second stage period revealed a low sludge activity. This effect is due to the change of growth medium for the bacteria causing inhibition of bacterial metabolism. Therefore, the sludge activity decreased. Then, in the later period of the second stage, MLSS began to slowly rise because of the capability of the bacteria to adapt themselves to the new medium. The concentrations of MLSS in the third stage generally higher than that in the most period of the first and second stage, indicating that glyphosate became well utilized by the culture. In the third stage of the acclimation process, the increase and decrease of MLSS both existed. The increase is due to the utilization of glyphosate by the bacteria. The reason for the decrease could be the accumulation of byproducts from glyphosate which could

inhibit the bacterial metabolism such as AMPA (Blot et al., 2019). Thus, next, the performance of the third stage was mainly discussed.

pH is another crucial parameter that can affect growth rates and activities of the culture because of its influence on metabolic rate and ion transport system (Mayo and Noike, 1996). Therefore, the evolution of pH is an indicator of biochemical reactions. In this study, pH was not buffered but adjusted to 7 ± 0.5 each time nutrients were refreshed. Manogaran et al. (2018) reported that glyphosate-degrading bacteria prefer acidic condition, whereas most authors showed that these metabolisms were enhanced by neutral-alkaline pH (Singh and Shaner, 1998; Benslama and Boulahrouf, 2013). Fig. 5.2a shows the evolutions of pH values in the third stage of the acclimation process indicating that biochemical processes are involved. The changes of pH values during the acclimation process may be affected by microbial decomposition and the byproducts generated during glyphosate biodegradation.

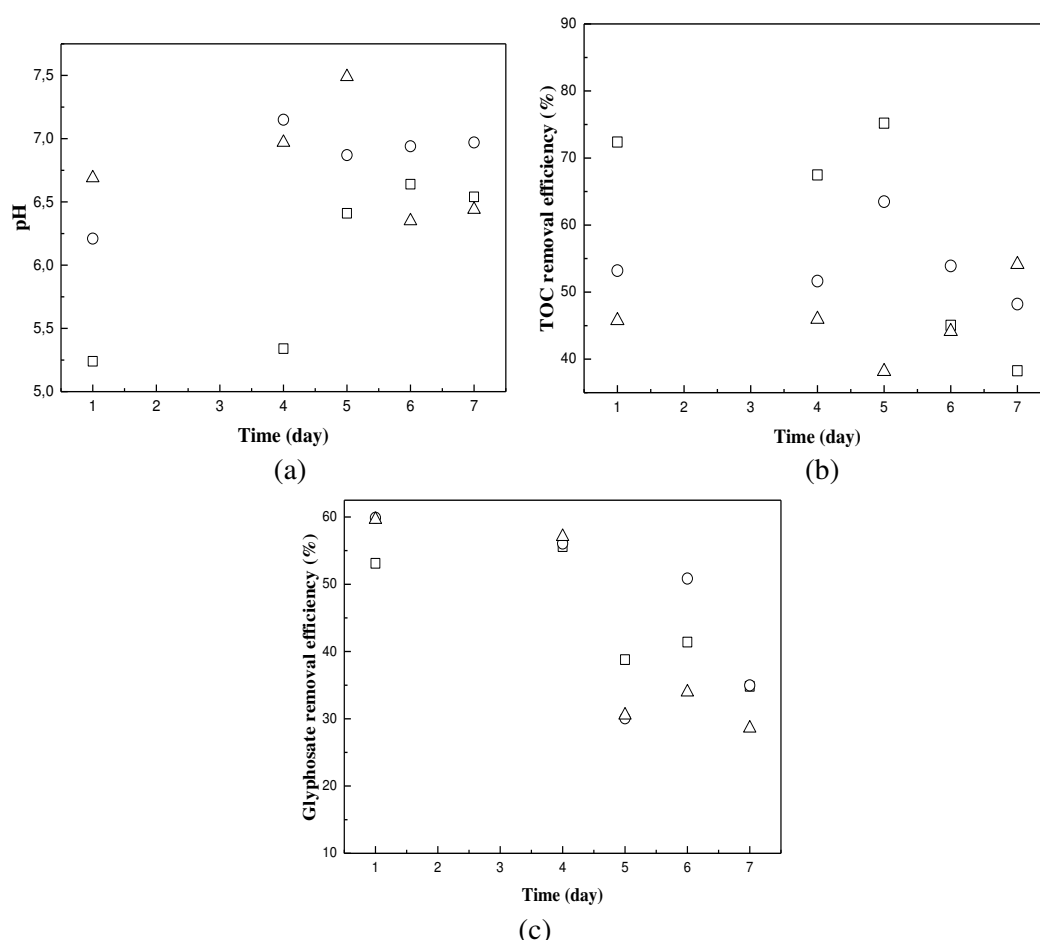


Fig. 5.2 pH values (a) and the removal efficiency of TOC (b) and glyphosate (c) with time in the third stage of the acclimation process: (1) \square 200 mg.L⁻¹ glyphosate + 426 mg.L⁻¹ glucose; (2) \circ 500 mg.L⁻¹ glyphosate + 266 mg.L⁻¹ glucose; (3) \triangle 1000 mg.L⁻¹ glyphosate

5.3.2 Removal efficiency of glyphosate and TOC during acclimation process

In parallel of measurements of bacterial activity, TOC and glyphosate removal were followed. The results obtained for a batch of 7 days showed a global decrease of the TOC and glyphosate in the third stage (Fig. 5.2b and Fig. 5.2c).

From Fig. 5.2b, it is observed that in the first week with initial glyphosate concentration of 200 mg.L⁻¹, the TOC removal efficiency ranged from 38.27% to 75.19%; in the second week with initial glyphosate concentration of 500 mg.L⁻¹, the TOC removal efficiency was in the range of 45.77%-63.49%; for the third week with initial glyphosate concentration of 1000 mg.L⁻¹, the TOC removal efficiency was 38.17%-54.13%.

Fig. 5.2c also shows that under different glyphosate concentration, the glyphosate removal efficiency generally decreased with time, maybe caused by the inhibition of the accumulation of byproducts from glyphosate. The glyphosate removal efficiencies at different initial glyphosate concentrations were 34.82%-55.59% for 200 mg.L⁻¹, 34.96%-59.88% for 500 mg.L⁻¹, and 28.60%-59.63% for 1000 mg.L⁻¹, respectively.

5.3.3 Validation of the acclimation performances compared to fresh activated sludge

Table 5.2 The change of MLSS and pH values in the acclimated activated sludge and non-acclimated activated sludge after 24 h at various glyphosate concentration

Treatment	Glyphosate concentration (mg.L ⁻¹)	Initial		After 24 h culture	
		MLSS (g.L ⁻¹)	pH	MLSS (g.L ⁻¹)	pH
Acclimated activated sludge	500	3±0.39	7±0.05	2.70	6.14
	1000	3±0.39	7±0.05	2.75	6.38
Non-acclimated activated sludge	500	3±0.1	7±0.05	1.21	5.9
	1000	3±0.1	7±0.05	1.59	6.03

In order to evaluate the degradation performance of the acclimation process, compared experiment of glyphosate biodegradation between acclimated activated sludge and non-acclimated sludge were conducted. Table 5.2 shows the change of MLSS and pH values in the acclimated and non-acclimated sludge after 24 h at two initial glyphosate concentrations of 500 and 1000 mg.L⁻¹. From the Table 5.2, it is shown that after 24 h, the MLSS for acclimated activated sludge at two initial glyphosate concentration is almost the same with the initial MLSS, indicating the stability of the bacterial activities in acclimated activated sludge. While for non-acclimated activated sludge, the MLSS significantly decreases to 1.21 and 1.59 g.L⁻¹ compared with initial MLSS of 3 g.L⁻¹ at initial glyphosate concentration of 500 and 1000 mg.L⁻¹, respectively. This indicates that glyphosate

inhibits the growth of biomass in the non-acclimated activated sludge. After 24 h, pH values both decrease for acclimated and non-acclimated activated sludge at two initial glyphosate concentrations. And the final pH values in acclimated activated sludge are bigger than that in non-acclimated activated sludge. The final pH values increase with the increase of glyphosate concentration. The pH decrease for non-acclimated activated sludge may be due to the bacteria decomposition caused by the inhibition effect of glyphosate to generate acids. The increase of pH for acclimated activated sludge with glyphosate concentration is possibly caused by the higher concentration of PO_4^{3-} generated under higher glyphosate concentration during glyphosate biodegradation.

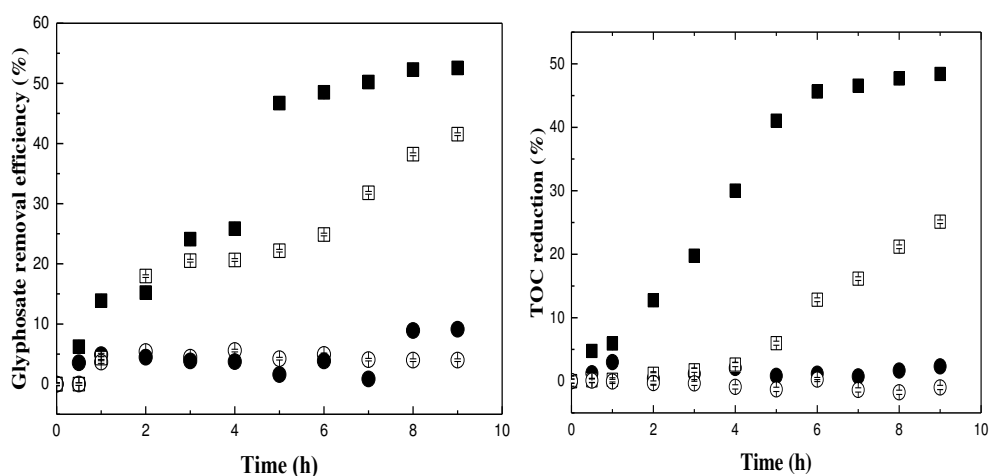


Fig. 5.3 The removal efficiency of glyphosate (left) and TOC (right) with time: (1) ■ acclimated activated sludge at 500 mg.L^{-1} glyphosate; (2) ● non-acclimated activated sludge at 500 mg.L^{-1} glyphosate; (3) □ acclimated activated sludge at 1000 mg.L^{-1} glyphosate; (4) ○ non-acclimated activated sludge at 1000 mg.L^{-1} glyphosate

Concentration profiles of glyphosate and TOC in the acclimated and non-acclimated activated sludge in 9 h are illustrated in Fig. 5.3. It shows that for acclimated activated sludge, glyphosate concentration first decreases fast, and then slowly decreases until to achieve the equilibrium. Namely, the glyphosate removal increases with time at the two initial glyphosate concentration, with the range of 0-52,56% for 500 mg.L^{-1} and 0-41,55% for 1000 mg.L^{-1} in 9 h. And the time for 500 mg.L^{-1} glyphosate to achieve the equilibrium is shorter than that for 1000 mg.L^{-1} glyphosate. For 500 mg.L^{-1} glyphosate, the equilibrium was achieved before 9 h, while not enough for 1000 mg.L^{-1} glyphosate. Thus, the glyphosate concentrations were measured after 24 h. The glyphosate removal efficiencies were 55.31% and 60.73% (Table 5.3) by acclimated activated sludge at 500 and 1000 mg.L^{-1} glyphosate, respectively.

While for non-acclimated activated sludge, glyphosate concentration almost keeps the same with the initial one, indicating no obvious glyphosate degradation by non-acclimated activated sludge. The

same trend is found for TOC reduction by acclimated and non-acclimated activated sludge (Fig. 5.4). The TOC removal efficiencies for acclimated activated sludge are 0-50.30% for 500 mg.L⁻¹ and 0-58.72% for 1000 mg.L⁻¹ after 24 h, which are both slower than glyphosate removal efficiencies, indicating the presence of some intermediates during the biodegradation process. For non-acclimated activated sludge, the TOC reduction is very low (less than 3%) and negative value appears at the initial glyphosate concentration of 1000 mg.L⁻¹. This is due to the inhibition of bacteria growth by the high concentration of glyphosate, resulting the death of bacteria. The significant difference in the glyphosate and TOC removal between acclimated and non-acclimated activated sludge gives an obvious indication that acclimation of heterotrophic biomass to the glyphosate is essential for the effective removal of glyphosate.

Table 5.3 Glyphosate removal efficiency by acclimated and non-acclimated sludge at two initial glyphosate after 24 h

Type	Initial glyphosate concentration (mg.L ⁻¹)	Glyphosate removal efficiency (%)	TOC reduction (%)
Acclimated activated sludge	500	55.31±0.44%	50.31±0.59%
	1000	60.73±0.20%	58.72±0.23%
Non-acclimated activated sludge	500	4.17±0.60%	2.33±0.90%
	1000	4.79±0.27%	-2.58±0.34%

5.3.4 Kinetics of glyphosate biodegradation

In order to study degradation kinetics of glyphosate by the acclimated activated sludge, the experiments of glyphosate biodegradation were conducted with concentrations of 200, 500 and 1000 mg.L⁻¹ using the same process with the section 5.2.3.

5.3.3.1 Glyphosate and TOC reduction

Fig. 5.4 shows the glyphosate and TOC reduction by acclimated activated sludge with time under three initial glyphosate concentrations of 200-1000 mg.L⁻¹. It can be seen from the figure that the acclimated activated sludge was able to transform glyphosate for all the concentrations tested. It should be noticed that it was possible to almost completely remove glyphosate for all concentrations tested after 3 h of culture. However, after 3 h, TOC reduction is 45.1, 42.4 and 43.42% for glyphosate concentration of 200, 500 and 1000 mg.L⁻¹, respectively and it increases to 52.6, 58.1 and 57.8% after 24 h. At the same reaction time, the TOC reduction is found to be smaller than glyphosate removal. This is attributed to the formation of intermediates, which remained in the solution and were not further metabolized, and not analyzed.

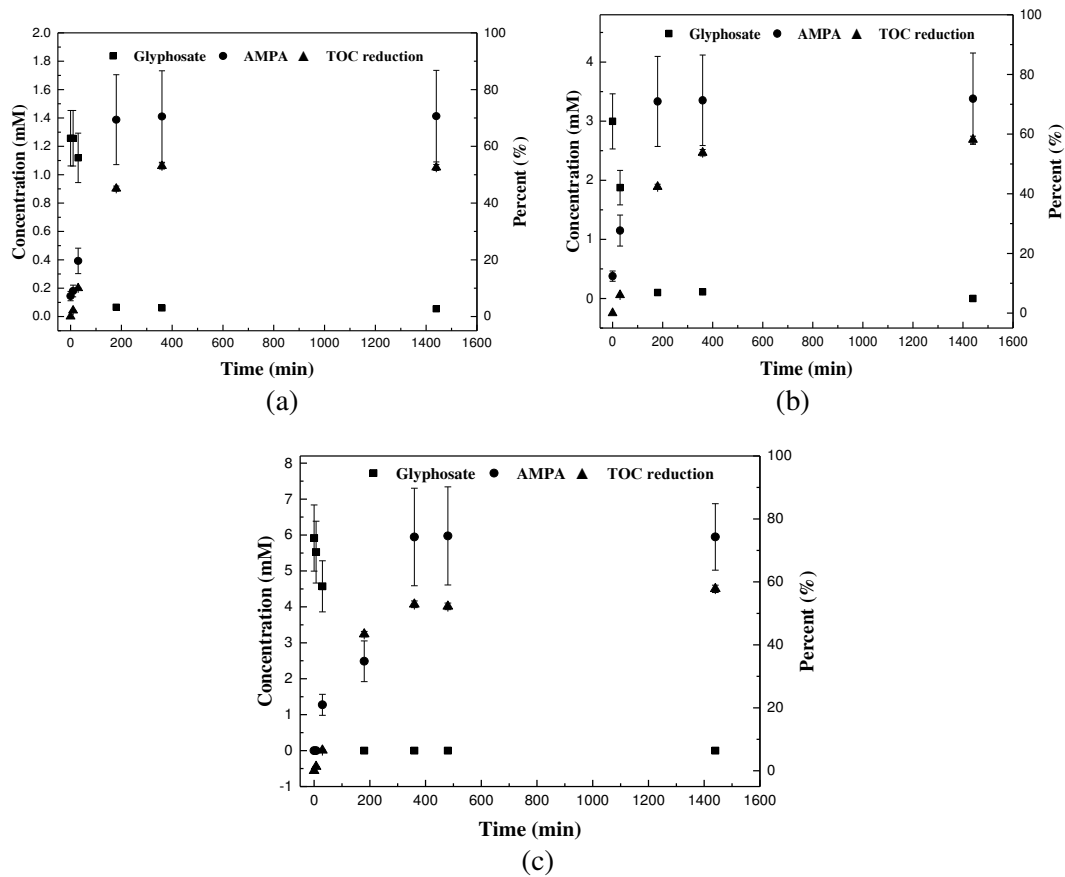


Fig. 5.4 Glyphosate and AMPA concentration and TOC reduction under three initial glyphosate concentration: (a) 200 mg.L⁻¹; (b) 500 mg.L⁻¹; (c) 1000 mg.L⁻¹.

5.3.3.2 Respirometer experiments

Bacterial activity was confirmed by DO measurements. The respirometer experiments were performed to evaluate the effects of the initial glyphosate concentration on the total OUR (OUR_T), which represented the sum of the exogenous OUR (OUR_{ex}) and endogenous OUR (OUR_{en}), calculated from Eq. 5-1. The results for respirometer experiments is shown in Table 5.4. It shows that the oxygen mass transfer coefficient obtained for the acclimation process was $0.14 \pm 0.03 \text{ min}^{-1}$, which is in the range of those found in the literature (Al-Ahmady, 2010; Mineta et al., 2011). Moreover, it depicts that the OUR_{en} of the acclimated activated sludge was $0.11 \pm 0.02 \text{ mgO}_2 \cdot \text{L}^{-1} \cdot \text{min}^{-1}$, which was defined as the oxygen consumption of microorganisms in the absence of substrate. Generally, OUR_{en} could increase with an increase in MLSS (Mineta et al., 2011). However, in this work, the initial concentration of MLSS was kept constant at different initial glyphosate concentration, thus making the same values for different initial glyphosate concentration. When glyphosate was added to activated sludge, the OUR_T values increased, which was higher than the initial value (OUR_{en}). And its values increased with the increase of initial glyphosate concentration, revealing the metabolism of

glyphosate by bacteria. The glyphosate yield on oxygen ($Y_{s/O}$) was significantly increased with the increase of glyphosate concentration from 200 to 500 mg.L⁻¹. This phenome could be explained by the half-saturation constant (K_s) which is discussed below.

Table 5.4 OUR in the kinetics process under different initial glyphosate concentration

Glyphosate concentration (mg.L ⁻¹)	OUR _{en} (mgO ₂ ·L ⁻¹ ·min ⁻¹)	k_{La} (min ⁻¹)	OUR _T (mg O ₂ ·g ⁻¹ ·min ⁻¹)	$Y_{s/O}$ (mg.mg ⁻¹ O ₂)
200			0.97±0.14	0.89
500	0.11±0.02	0.14±0.03	1.36±0.12	5.70
1000			1.51±0.20	5.48

5.3.3.3 Kinetic model

Growth kinetics of microorganisms in activated sludge process can be expressed by Monod model (Monod, 1949), which describes the growth of culture on the utilization of single substrates.

The Monod model can describe cell growth rate as follows:

$$dX/dt = \mu X \quad \text{Eq. 5-3}$$

Monod described the specific growth rate of bacteria depending on a specific maximum growth rate and a limiting substrate concentration:

$$\mu = \mu_{max} \frac{S}{K_s + S} \quad \text{Eq. 5-4}$$

The rate of glyphosate consumption by bacteria could be described by the Monod expression in a batch reactor (Eq. 5-4):

$$-\frac{dS}{dt} = \frac{\mu_{max} SX}{Y(K_s + S)} \quad \text{Eq. 5-5}$$

where X is the bacteria concentration (i.e. MLSS, g.L⁻¹); dX/dt is the bacteria growth rate (g.L⁻¹.h⁻¹); μ and μ_{max} is the specific bacteria growth rate and maximum specific bacteria growth rate (h⁻¹), respectively; S is the glyphosate concentration (mg.L⁻¹); dS/dt is the glyphosate utilization rate (mg.L⁻¹.h⁻¹); K_s is the half-saturation constant (defined as the substrate concentration at 1/2 the maximum specific bacteria growth rate, g.L⁻¹); Y is the bacteria cell yield (mg.mg⁻¹).

The Monod's system of differential equations is solved with the ode's Matlab solver through using the forth order Runge-Kutta method to obtain the time evolution of S and X . An optimization procedure through coupling the fsolve function of Matlab with the Levenberg-Marquardt optimization algorithm has been also implemented to obtaine the optimal parameters: Y , μ_{max} and K_s that lead to the best quadratic error between experimental and computed values for S .

Time evolution and comparison with the experimental data are presented on Fig. 5.5. It shows that Monod model can well fit the growth kinetic of glyphosate. The bacteria cell yield (Y) derived from the model was 0.69, which is in the range of values reported for other organic compounds biodegradation by activated sludge (Karahan et al., 2010; Vázquez-Rodríguez et al., 2006). The maximum growth rate (μ_{max}) on glyphosate was found as 0.34 h^{-1} for the acclimated activated sludge, which is in the middle range of those ($0.05\text{-}0.87 \text{ h}^{-1}$) found in the literature (Nourouzi et al., 2012; Tazdaït et al., 2018). However, it is lower than that for glucose (0.79 h^{-1}) (Schulze and Lipe, 1964). This difference can be explained by several factors, such as the difference of biodegradability between glyphosate and glucose, different microbial species selected during the acclimation process and different metabolism pathways. Moreover, during glyphosate biodegradation process, some metabolic intermediates generated, could be inhibitory substrates for microorganisms. The half-saturation constant (K_s) was 1600 mg.L^{-1} , which is higher than that of glyphosate biodegradation by mixed culture ($33\text{-}181 \text{ mg.L}^{-1}$) and non-acclimated activate sludge (340 mg.L^{-1}) reported by Nourouzi et al. (2012) and Tazdaït et al. (2018), respectively. Literature shows that the difference of kinetic parameters is caused by several factors, such as inoculum history (acclimation), changes in the predominating microbial species during the assays, and environmental factors (pH, temperature) (Contreras et al., 2008). Furthermore, during acclimation process, the conditions changes, such as substrate concentration, dilution rate, or substrate to microorganism ratio, which can modify the population metabolic state also affect kinetic parameters (Ben-Youssef and Vázquez-Rodríguez, 2011).

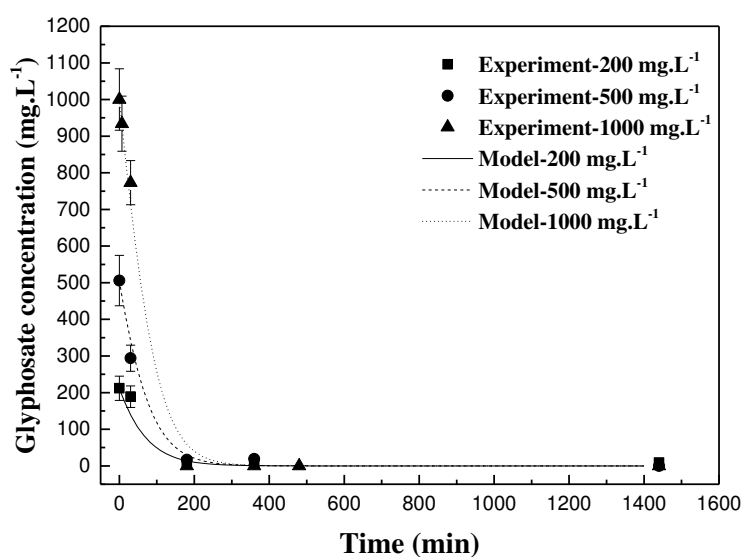


Fig. 5.5 Time evolution of glyphosate concentration using Monod model and comparison with experimental data

5.3.3.4 Proposed biodegradation pathway

Two pathways have been always proposed for glyphosate biodegradation: (1) the conversion of glyphosate to AMPA and glyoxylate through the C-N cleavage by the presence of glyphosate oxidoreductase; (2) the formation of sarcosine through the C-P cleavage catalyzed by C-P lyase (Liu et al., 1991; Sviridov et al., 2015; Zhao et al., 2015). In order to elucidate the glyphosate pathway in the acclimated activate sludge in this study, the possible degradation products of glyphosate were analyzed. Sarcosine was not detected in the samples, indicating the absence of the sarcosine pathway. However, AMPA was detected by LC-MS analysis with the m/z of 110.0032 amu and the concentrations of AMPA were shown in Fig. 5.4. It presents that the AMPA concentration increases with time under three glyphosate concentration tested. It can be noticed that for each mole of glyphosate that decomposed, approximately one mole of AMPA generated, indicating the only AMPA pathway existing in the glyphosate biodegradation. The results is consistent with the previous results from literature(Obojska et al., 2002; Hadi et al., 2013).

Table 5.5 The concentration of possible byproducts of glyphosate before and after 24 h treatment

Glyphosate concentration (mg.L ⁻¹)	Before treatment (mM)				After 24 h treatment (mM)			
	HCHO	PO ₄ ³⁻	NH ₄ ⁺	NO ₃ ⁻	HCHO	PO ₄ ³⁻	NH ₄ ⁺	NO ₃ ⁻
200					0.038	0.19	-	0.24
500	0.007	0.16	2.79	0.04	0.045	0.20	-	0.32
1000					0.091	0.24	-	0.52

Furthermore, other possible byproducts of glyphosate before and after 24 h treatment were measured by UV-Vis spectrophotometry and shown in Table 5.5. It is interesting to note that PO₄³⁻ slightly increased after 24 h treatment, even that glyphosate was completely degraded into AMPA, indicating that PO₄³⁻ is not directly converted from glyphosate, similar to previous studies (Annett et al., 2014; Kryuchkova et al., 2014). It is most probably that AMPA is transformed into PO₄³⁻ by C-P lyase (Pipke et al., 1987; Ermakova et al., 2017). The further possible metabolite, formaldehyde (HCHO), was also detected with increasing concentration from 0.038 to 0.091 mM with glyphosate concentration ranging from 200 to 1000 mg.L⁻¹ after biological treatment (Table 5.5), respectively. The amount of formaldehyde generated is approximately equivalent to the amount of PO₄³⁻ formed, possibly indicating the existence of phosphonate pathway which has been proposed in the literature (Lee et al., 1992; Sviridov et al., 2012): (1) the transamination of AMPA to phosphonoformaldehyde catalyzed by a aminotransferase; (2) the formation of formaldehyde and PO₄³⁻ from C-P bond cleavage of phosphonoformaldehyde. However, the phosphonate pathway of glyphosate biodegradation is still a hypothesis as none of its enzymes have been isolated nor characterized

(Sviridov et al., 2012). Although there is no direct evidence yet to confirm this pathway, the existence of such pathway of glyphosate mineralization is the most convenient explanation of the results presented in this study.

NH_4^+ , a possible final mineralization product of AMPA, is not detected after biological treatment (Table 5.5), possibly due to be used as nitrogen source of the synthesis of bacterial cell substances or nitrogen-containing metabolites. However, the concentration of NO_3^- is found to increase with the increase of glyphosate concentration after 24 h treatment. This is possibly due to the nitrification of microorganisms to generate NO_3^- .

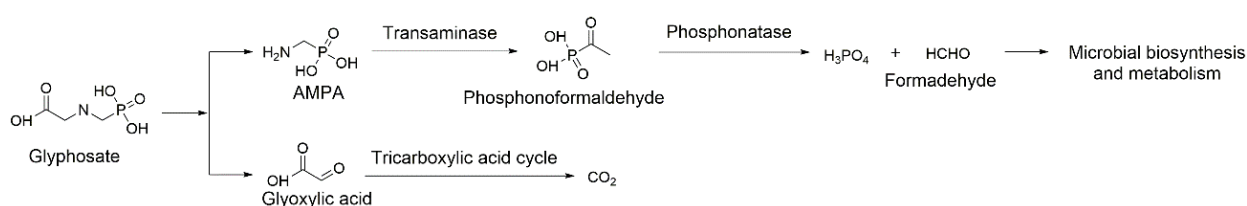


Fig. 5.6 Proposed biodegradation pathway of glyphosate

According to the above evaluation of byproducts of glyphosate, a possible biodegradation pathway was proposed in Fig. 5.6. First, the acclimated activated sludge is able to utilize glyphosate as the sole carbon source with stoichiometric formation of AMPA and glyoxylic acid through the cleavage of C-N bond by the presence of glyphosate oxidoreductase. Glyoxylic acid may be incorporated in tricarboxylic acid cycle (Jacob, 1988; Sviridov et al., 2012). AMPA was further metabolized to phosphonoformaldehyde through the transamination catalyzed by an aminotransferase and then transfer to formaldehyde and PO_4^{3-} from C-P bond cleavage of phosphonoformaldehyde. The resulting formaldehyde can enter the carbon metabolic pathways of cellular growth (Tazdaït et al., 2018).

5.4 Conclusion

The results obtained in this study suggested that an acclimated process promote the biodegradation of glyphosate by activated sludge through using glyphosate as sole carbon source. Complete glyphosate removal has been obtained by acclimated activated sludge. The conventional Monod model was used to describe adequately both biomass growth and glyphosate degradation profiles at various glyphosate initial concentrations. With the help of these results, a biodegradation pathway of glyphosate by acclimated activated sludge was proposed. This study has important engineering implications for the biological treatment of real glyphosate-containing wastewater.

The treatment of glyphosate-containing wastewater by individually WAO or biological process has been discussed in the previous chapters. Through the Chapter 3 and 4, it is known that complete glyphosate removal efficiency could be achieved by WAO process, while many intermediates are generated requiring further treatment. Chapter 5 indicates that the acclimation process promoted the glyphosate biodegradation by activated sludge through using glyphosate as sole carbon source and a complete glyphosate removal was achieved. Thus, in the next chapter, the performance of the combined process for glyphosate degradation is discussed. The glyphosate-containing wastewater after WAO pre-treatment (as discussed in the Chapter 3) was further treated by the acclimated activated sludge, as described in the Chapter 5. Concerning this purpose, removal efficiencies of glyphosate, total organic carbon (TOC) and chemical oxygen demand (COD) and the formation of byproducts during WAO and biological steps were analyzed in order to evaluate the feasibility of the coupled process for glyphosate-containing wastewater treatment.

***Chapter 6 The removal of glyphosate from wastewater by a compact
process combining wet air oxidation and biological treatment***

Abstract

This work investigated the treatment of a synthetic wastewater containing glyphosate through an integrated wet air oxidation (WAO)-biological treatment process. Aqueous solutions of 1 g.L⁻¹ of glyphosate were first treated by WAO process at temperature in the range of 423-523 K (P = 15 MPa and reaction time of 30 min). Then the oxidized effluents were treated by acclimated and non-acclimated activated sludge in a batch reactor with a residence time of 24 h. Several parameters were evaluated, such as pH, mixed liquor suspended solid (MLSS), and glyphosate, TOC and COD removal rates. Complete glyphosate degradation and 59.43% and 56.72% of TOC and COD reduction, were achieved respectively by the integrated process. Identification and quantification of by-products were also studied. Finally, a possible degradation pathway of glyphosate by the integrated WAO-biological process was proposed.

Keywords: Glyphosate; wet air oxidation; kinetics; biological treatment; combined processes

6.1 Introduction

The pesticide industry is one of the major industries in chemicals. Among different pesticides, organophosphorus pesticides are widely used in the world due to its high efficiency and broad spectrum. Synthetic organophosphorus pesticides are extensively used as insecticides, fungicides and herbicides in agriculture and domestic use (Richins et al., 1997). The increasing use of organophosphorus pesticides can cause potential adverse environmental and human health effects (Srivastava et al., 2009). A variety of different physical, chemical and biological technologies have been reported to treat organophosphorus pesticides present in wastewater (Richins et al., 1997; Chen and Cao, 2005; Chen et al., 2007; Srivastava et al., 2009). There is no doubt that biological treatments can be continuously used as a baseline treatment process for most organic compounds, which is always considered as a friendly and low cost wastewater treatment technology (Mantzavinos et al., 1999). However, some refractory and complex effluents cannot be well treated by biological processes, due to the the presence of inhibitory, toxic or resistant compounds to biological metabolism (Suarez-Ojeda et al., 2007). Wastewater discharged from the organophosphorus pesticide-manufacturing factory is characteristic of high value of Chemical Oxygen Demand (COD), strong toxicity, poor biodegradability and complicated constituents (Li and Yang, 2008). Thus, it is necessary to develop new technologies to easily degrade such substances. Recently, coupling advanced oxidation processes (AOPs) and biological processes has been reported as a promising

treatment technology for these compounds (Mantzavinos and Kalogerakis, 2005; Minière et al., 2017) considering both environmental and economic advantages.

AOPs is a potential technology to oxidize a wide range of organic compounds into carbon dioxide or less toxic oxidation intermediates, using highly and non-specific reactive hydroxyl radicals (Mantzavinos and Kalogerakis, 2005; Azabou et al., 2010). AOPs include UV irradiation, photocatalysis, ozonation, Fenton oxidation, electrochemical oxidation, wet air oxidation as well as various combination (Divyapriya et al., 2016). AOPs was reported to be efficient to degrade different types of pesticides as well as different inhibitory organic pollutants (Lafi and Al-Qodah, 2006). However, the operational cost of AOPs is relatively high compared to biological processes This could be explained by the formation of intermediates which tend to be difficult for complete chemical degradation and consume energy and chemical reagents (Oller et al., 2011). Moreover, the pollutants concentration after AOPs treatment seldomly achieves a safe discharge standard for the treated wastewater into the Environment (Lin and Chuang, 1994; Lafi and Al-Qodah, 2006). Thus, these effluents are needed to be further treated by a biological process in order to overtake the previous drawbacks. The main idea of coupling processes is to treat toxic and/or non-biodegradable effluent by an AOP during a short time to generate intermediates which are fully biodegradable, then achieving the treatment by a biological step for the complete degradation of organic compounds (Azabou et al., 2010). Among the various AOPs, wet air oxidation (WAO) is a very interesting technology for the treatment of organic compounds from wastewater, due to its fast reaction rate and high efficiency (Chakchouk et al., 1994; Lin and Chuang, 1994; Kaçar et al., 2003; Suarez-Ojeda et al., 2005). It consists in oxidizing organic compounds into CO₂ or less toxic oxidation intermediates at elevated temperature (398-573 K) and pressure (0.5-20 MPa), using oxygen (generally from air) as oxidant (Debellefontaine and Foussard, 2000; Lefèvre et al., 2011a, 2011b; Lefevre et al., 2012). In the past decades, WAO process has been frequently used by researchers as a pretreatment step before a biological step (Lin and Chuang, 1994; Patterson et al., 2002; Kaçar et al., 2003; Minière et al., 2017). Literatures survey on WAO and biological combined processes shows high removal efficiency for different organic compounds or various wastewaters, such as polyethylene glycol (Mantzavinos et al., 1997), substituted phenols (Suarez-Ojeda et al., 2007), linear alkylbenzene sulfonates (Patterson et al., 2002), deltamethrin (Lafi and Al-Qodah, 2006). However, no information in the literature regarding the applications of combined WAO with biological treatment to eliminate organophosphorus pesticides have been reported.

Therefore, the purpose of this study is to apply an integrated WAO-biological process to treat organophosphorus pesticides effluents. Glyphosate (N-(phosphonomethyl)glycine) is selected as the

typical organophosphorus pesticides for this study. Glyphosate is a broad-spectrum, nonselective and post-emergence organophosphorus herbicide, used to eradicate weeds, especially annual broadleaf weeds and grasses (Waiman et al., 2012; Junges et al., 2013). Due to its extensive use, glyphosate has been reported to contaminate the Environment from various sources, such as industrial effluents, agricultural runoff and chemical spill (Botta et al., 2009). Thus, in this study, a combined WAO-biological process was used to treat wastewater containing glyphosate. The removal performance of the subsequent biological process for the effluents treated by WAO process were compared between the acclimated and non-acclimated activated sludge. Moreover, the pathways for glyphosate degradation by the combined WAO-biological process were proposed. This study provides a potential technology for the treatment of wastewaters containing organophosphorus pesticides.

6.2 Materials and methods

6.2.1 Materials

High purity (>95%) glyphosate was purchased from Leap Labchem Co., Limited, China. Aminomethylphosphonic acid (AMPA), sarcosine and other chemicals were obtained from Sigma-Aldrich (Saint Quentin Fallavier, France). The synthetic air used as oxidant had a purity of 99.999% (Air Liquid, France). Glyphosate stock concentrations were taken as 1 g.L⁻¹.

6.2.2 Experimental set-up for WAO process

WAO experiments were conducted in a 202 mL stainless steel batch reactor (Top Industrie, France). Fig. 6.1 shows the schematic diagram of the WAO batch reactor. The autoclave is equipped with a stirrer (rushton propeller) and can reach the maximum temperature and pressure of 350°C and 30 MPa, respectively. The temperature is regulated by a cooling jacket and an electric heating collar.

A glyphosate solution of 1000 mg.L⁻¹ was prepared. 120 mL of glyphosate solutions was injected into the reactor and then the reactor was isolated. The operating conditions were chosen from previous kinetics experiments of glyphosate oxidation by WAO process conducted in Chapter 3. Pressure was set at 15 MPa and temperature at 423, 473 and 523 K, respectively, with a reaction time of 30 min, and an air factor (ratio between the oxygen injected into the batch reactor and the stoichiometry oxygen quantity) of 1.7. The reactor was first pressurized at an initial pressure with nitrogen. This first pressure was calculated from the Soave-Redlich-Kwong equation of state (Lefèvre et al., 2011b), in order to reach required final pressure and temperature in the batch reactor. The initial nitrogen pressure was 7.78, 6 and 2.15 MPa with respect to the temperature of 423, 473 and 523 K, respectively. When the set temperature was achieved, the air was injected into the reactor at a calculated and the

reaction began ($t=0$). The agitation speed was set at 1000 rpm in order to overcome the limitations of mass transfer (Lefèvre et al., 2011a). Finally, after 30 min, the reactor was purged, and sample was collected. The sample was stored at 4°C (to limit further oxidation reactions) for further biological treatment. This procedure was done 2 times in order to recover 240 mL of pre-oxidized sample. This volume is necessary for further biological operation.

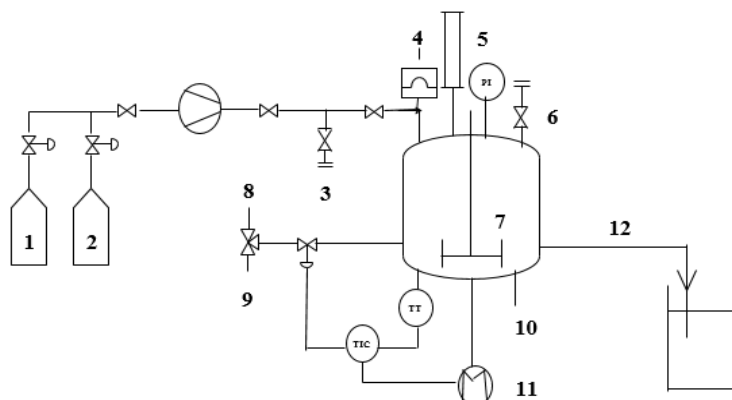


Fig. 6.1 Schematic diagram of WAO setup using the batch reactor. 1 – air bottle; 2 – nitrogen bottle; 3 – gas purge; 4 – bursting disk; 5 – liquid injection; 6 – gas purge; 7 – stir; 8 – cooling water inlet; 9 – compressed air; 10 – cooling water outlet; 11 – heater; 12 – liquid sampling

6.2.3 Experimental set-up for biological treatment process

To enhance glyphosate biodegradation, an acclimation process was performed in a 5 L fed-batch reactor. The reactor was inoculated with 4.5 L of raw activated sludge, collected from a wastewater treatment plant (Aix-en-Provence, France) at a concentration of 5.35 g.L⁻¹(MLSS). The activated sludge was mixed with synthetic substrate-glyphosate mixture. The basic composition of medium was: (NH₄)₂SO₄ 223 mg L⁻¹, K₂HPO₄ 27 mg L⁻¹, KH₂PO₄ 21 mg L⁻¹, MgCl₂·2H₂O 160 mg L⁻¹, CaCl₂ 20 mg L⁻¹, FeSO₄·7H₂O 1 mg L⁻¹, NaMoO₄ 2 mg L⁻¹ and MnCl₂ 1 mg L⁻¹. The pH was adjusted to 7.0 ±0.05 by using NaOH (1 mol.L⁻¹) and HCl (1 mol.L⁻¹) solutions. Every 24 h (72 h for the weekend), a pulse feeding of synthetic substrate-glyphosate mixture was injected into the reactor. Every week, the medium was totally refreshed through increasing glyphosate concentration up to 1000 mg·L⁻¹ and decreasing glucose concentration to 0 mg·L⁻¹. An air pump with gas distributor was applied to maintain dissolved oxygen concentration (DO) above 3 mg·L⁻¹. A stirring device was used to retain MLSS in suspension and distribute oxygen. The sludge was incubated at room temperature. The acclimation process lasted 280 days as described in Chapter 5.2.2. Chapter 5 showed that after the acclimation process, complete glyphosate removal has been obtained.

The biological experiments for the effluents treated by the WAO process were conducted in a 500 mL batch reactor at ambient temperature in aerobic conditions. 200 mL of the effluent coming

from the WAO process was mixed with other nutrients as above, but without glucose. A certain mass of acclimated and non-acclimated activated sludge were collected with the same concentration of MLSS of 3 g.L⁻¹. Two oxygen pumps and stirring devices were used to support aerobic conditions and completely mix the effluent and activated sludge. The hydraulic residence time (HRT) was 24 h. The operating conditions for glyphosate degradation are summarized in Table 6.1. 10 mL of samples were collected regularly for glyphosate and TOC concentration measurements. After 24 h, MLSS, pH and the concentration of by-products were measured.

Table 6.1 Operation conditions for glyphosate degradation by the compact process

Initial glyphosate concentration (mg.L ⁻¹)	WAO conditions			Biological treatment
	T (K)	P (MPa)	Reaction time (min)	HRT (h)
1000	423	15	30	24
1000	473	15	30	24
1000	523	15	30	24

6.2.4 Analytical procedures

pH values were performed using a pH meter (HACH Sension+ PH3). The procedure for the measurement of MLSS is outlined in *Standard Method 2540 D* (“NEMI Method Summary - 2540 D,” n.d.). TOC concentration was calculated from the difference between total carbon (TC) concentration and inorganic carbon (IC) concentration measured by a TOC-L analyzer (SHIMADZU). COD concentration was conducted by COD Cell Test C4/25 (1.14541.0001, Merck Chemicals) using UV-vis spectrophotometry at the wavelength of 605 nm.

For WAO process, glyphosate and its possible by-product, AMPA, were measured by liquid chromatography/mass spectrometry technique (LC/MS), an Agilent 1290 Infinity system coupled to an Agilent 6530 Q-TOF tandem mass spectrometer equipped with an Agilent jet stream (AJS) ion source. Mass Hunter workstation software B4.00 was used to perform instrument control, data analysis and processing. The analysis method was performed according to Yoshioka et al. (2011). An Obelisc N column (150 mm x 2.1 mm I.D, 5µm) was used for sample separation, purchased by SIELC Technologies (Interchim, Montluçon, France). The column was kept at 40°C. 1 µL of sample was injected for separation. The mobile phase was composed of acetonitrile/water (20/80, v/v) acidified with 0.1% formic acid and the flow rate was 0.2 mL.min⁻¹. After LC separation, the solution was introduced into the atmospheric pressure ionization source and ionized by electrospray in negative ion mode (ESI) leading to the formation of the [M - H]⁻ ions of the analytes. Working conditions were as follows: fragmentor 140 V, capillary 3000 V, skimmer 65 V and nitrogen used as the drying (350°C,

10 L.min⁻¹), nebulizing (30 pis) and sheath (350°C, 8 L.min⁻¹) gas. Scanning was performed from m/z 50 to 1000 amu with 10 038 transients per spectrum. The quantification of glyphosate and AMPA concentrations through using Extracted Ion Current (EIC) chromatograms was based on linear regression ($R^2 > 0.999$) obtained by injecting glyphosate or AMPA standard solutions with the range of concentrations of 5-200 µg.mL⁻¹. Retention times, mass of deprotonated molecules and EIC target molecular weight ranges shown between brackets were as follows: AMPA (3.695 min, 110.0032 amu, [109.8-110.2 amu]) and glyphosate (7.455 min, 168.0111 amu, [167.8-168.2 amu]). For biological process, the concentrations of glyphosate were monitored by UV-Vis spectrophotometer (photoLab® 6600 UV-VIS) according to Bhaskara and Nagaraja, (2006) with maximum absorption at 570 nm. Through comparing the results from other studies between LC/MS and UV analysis for glyphosate concentration at same condition, a linear relationship was obtained. Thus, the glyphosate concentration after biological can be corrected by the equation $y = 1.48x - 339.96$ ($R^2 = 0.980$) using UV results (x: glyphosate concentration measured by UV; Y: corrected glyphosate concentration).

In this work, the efficiency of each component in the integrated treatment was calculated by the following equations:

$$A_1 = \frac{c_0 - c_1}{c_0} \times 100 \quad \text{Eq. 6-1}$$

$$A_2 = \frac{c_1 - c_2}{c_1} \times 100 \quad \text{Eq. 6-2}$$

$$A_3 = \frac{c_0 - c_2}{c_0} \times 100 \quad \text{Eq. 6-3}$$

where A_1 , A_2 and A_3 represent the removal efficiency of glyphosate (X), TOC (Y) and COD (Z) after WAO pre-treatment, biological treatment and the combined process (total removal efficiency) respectively. C_0 , C_1 , and C_2 are the initial concentration, the concentration after WAO pretreatment and the concentration after biological treatment of glyphosate, TOC and COD respectively.

The following possible by-products of glyphosate degradation by the WAO-biological process combination were also measured: sarcosine, NH_4^+ , NO_3^- , PO_4^{3-} , and formaldehyde (HCHO). The detection of sarcosine was conducted by a specific test kit (Biovision kit Sarcosine, K636-100) with the maximum absorption wavelength of 570 nm. NH_4^+ was determined by UV-vis spectrophotometry using Spectroquant® test kit (1.14752.0001, Merck Chemicals) with the maximum wavelength of 690 nm. NO_3^- was measured by UV-vis spectroscopy (Spectroquant® test kit 1.09713.0001, Merck Chemicals). The absorption maximum is at $\lambda = 340$ nm. PO_4^{3-} was quantified by UV-vis spectroscopy through using Spectroquant® test kit (1.00798.0001, Merck Chemicals) with the absorption maximum

at $\lambda=690$ nm. Formadehyde is measured by UV-vis spectrophotometry by Spectroquant[®] test kit (1.14678.0001, Merck Chemicals). The maximum absorption wavelength is 565 nm.

6.3 Results and discussion

6.3.1 WAO pretreatment

The effect of temperature on the glyphosate degradation by WAO process as pretreatment under a constant pressure of 15 MPa with a residence time of 30 min has been studied in terms of glyphosate (X_I), TOC (Y_I) and COD (Z_I) removal efficiency and the results are shown in Table 6.2. It is obvious from Table 6.2 that glyphosate, TOC and COD reduction all increased with WAO temperature, with the range of 18.61-100%, 8.17-46.24% and 9.06-44.38%, respectively. As expected, the glyphosate decomposition appears to be faster than the corresponding TOC and COD reduction under the same operation conditions. For instance, after 30 min of WAO oxidation at 523 K, complete glyphosate removal was achieved while there was more than 50% TOC and COD existing in aqueous phase. This is because in addition to carbon dioxide and water as final by-products of glyphosate oxidation, decomposition of glyphosate also generates other small molecule organic intermediates, which would be partially oxidized to carbon dioxide and water. The undecomposed small molecule intermediates contribute to the bulk of TOC and COD in the treated effluent. The same trend was also reported on WAO process for other organic contaminates, such as substituted phenols (Lin and Chuang, 1994b; Suárez-Ojeda et al., 2008), alkylbenzene sulfonates (Patterson et al., 2002), and polyethylene glycols (Mantzavinos et al., 1996). Suárez-Ojeda et al. (2008) pointed out that the higher difference between the removal efficiency of organic compounds and TOC or COD reduction, the higher amount of partially oxidized intermediates generates in the effluent and the lower mineralization. This can be also confirmed by the change of pH during the oxidation of glyphosate at three temperatures. The pH values increased 0.07-1.23 unit compared to the initial pH of 2.51 within 30 min of oxidation at temperatures from 423 to 523 K, in consistent with Xing et al. (2018). This implies that alkaline substance was formed during the glyphosate oxidation, such as PO_4^{3-} and their concentration increased with WAO temperature.

As mentioned above, the aim of WAO pretreatment is to eliminate glyphosate present in the wastewater to give more biodegradable compounds which would be degraded in the following biological treatment.

6.3.2 Biological process

As mentioned above, the WAO process as pretreatment is conducted mainly to eliminate glyphosate and to combine this step with a biological step through using the treated effluent as a substrate to the biomass in the bioreactor. In the biological process, the effluent from WAO process (with nutrients presented in the Section 5.2.2) was used as the substrate for activated sludge non acclimated or previously acclimated to glyphosate. The pH of the effluent was adjusted to 7 ± 0.05 before biological treatment. The biological experiments were conducted in a 500 mL stirred-batch reactor with a residence time of 24 h.

Table 6.2 shows the glyphosate (X_2), TOC (Y_2) and COD (Z_2) removal after 24 h in biological process after WAO pretreatment for acclimated and non-acclimated activated sludge and the biomass concentration represented by MLSS and pH value after 24 h culture is shown in Table 6.3.

For non-acclimated sludge, glyphosate, TOC and COD removal were all very low, after WAO pretreatment, indicating that glyphosate cannot be well used by non-acclimated sludge. The negative values of TOC and COD removal for the effluent after WAO treatment under the temperature of 423 K in non-acclimated sludge comes most likely from cell lysis and excretion of soluble microbial products due to the death of microbial cell (Patterson et al., 2002). The decrease of MLSS (Table 6.3) for non-acclimated sludge is further confirming that glyphosate inhibits the growth of biomass and the inhibition effect enhances with the increase of glyphosate concentration in the effluent after WAO pretreatment. After WAO pretreatment, TOC and COD reduction were further found after biological treatment, respectively, even no glyphosate removal achieved at 523 K. Therefore, it indicates that some organic intermediate produced at high WAO temperature could be utilized by the non-acclimated sludge. Table 6.3 also shows that the pH in the non-acclimated activated sludge ranged from initial value of 7 to 6.81, 7.11 and 7.39 with the WAO temperature conditions of 423, 473 and 523 K, respectively. The decrease of pH at 423 K may be due to the decomposition of microorganisms caused by the inhibition effect of glyphosate which could generate acids. While the increase of pH at 473 and 523 K is possibly caused by the degradation of intermediates generated in WAO process which produces alkaline substances. The specific mechanism is needed to be further studied.

Table 6.2 Glyphosate, TOC and COD removal efficiency for each treatment and the combine process

WAO			Biological treatment				Total			
T (K)	Glyphosate removal (X_1 , %)	TOC removal (Y_1 , %)	COD removal (Z_1 , %)	Sludge	Glyphosate removal (X_2 , %)	TOC removal (Y_2 , %)	COD removal (Z_2 , %)	Glyphosate removal (X_3 , %)	TOC removal (Y_3 , %)	COD removal (Z_3 , %)
423	18.61	8.17	9.06	Acclimated activated sludge	51.26	30.21	28.35	60.33	35.92	34.84
473	75.95	31.03	35.00		17.57	34.72	30.77	80.18	54.98	55.00
523	100.00	46.24	44.38		-	24.52	22.19	100	59.43	56.72
423	18.61	8.17	9.06	Non-acclimated activated sludge	0.69	-6.19	-3.61	19.17	2.49	5.78
473	75.95	31.03	35.00		15.09	11.50	4.33	79.58	38.97	37.81
523	100.00	46.24	44.38		-	11.35	7.58	100	52.35	48.59

Table 6.3 The change of MLSS and pH values for glyphosate degradation in the biological treatment after WAO pretreatment

WAO conditions			Biological treatment				
T (K)	P (MPa)	Reaction time (min)	Sludge	initial		After 24 h culture	
				MLSS (g.L ⁻¹)	pH	MLSS (g.L ⁻¹)	pH
423	15	30	Acclimated activated sludge	3±0.39	7±0.05	2.65±0.12	7.77
473	15	30		3±0.39	7±0.05	3.28±0.24	7.14
523	15	30		3±0.39	7±0.05	3.10±0.14	7.28
423	15	30	Non-acclimated activated sludge	3±0.1	7±0.05	1.60±0.03	6.81
473	15	30		3±0.1	7±0.05	1.92±0.07	7.11
523	15	30		3±0.1	7±0.05	1.89±0.15	7.39

For acclimated sludge, glyphosate, TOC and COD reduction were all much higher than that for non-acclimated sludge and in the range of 0-51.26%, 24.52-34.72% and 22.19-28.35%, respectively. This indicates that the acclimation process leads to increase the ability of the sludge to degrade glyphosate. The glyphosate removal in biological process decreased with WAO temperature. This is because more glyphosate was removed by WAO pre-treatment at high temperature, with little additional glyphosate reduction by the aerobic biodegradation treatment. Table 6.2 shows that higher removal efficiency of glyphosate, TOC and COD removal was obtained by acclimated sludge than that by WAO pretreatment at 423 K, indicating the enhancement of the biodegradability of WAO effluents. Furthermore, higher TOC and COD removal than glyphosate removal are obtained by acclimated sludge after WAO pretreatment at 473 and 523 K, indicating that the intermediates generated after WAO pre-treatment could be further utilized by acclimated sludge. This also reveals that the biodegradability of glyphosate solution treated by WAO process improves, similar to previous literature results on other molecules (Patterson et al., 2002; Kaçar et al., 2003; Suárez-Ojeda et al., 2008).

Generally, since WAO treatment is considered to be more costly than biological treatment, most of the TOC removal should take place in the biodegradation process, i.e. $Y_2 > Y_1$ (Patterson et al., 2002). $Y_2 > Y_1$ was found the WAO temperature of 423 and 473 K for acclimated sludge, in consistent with the description above, while $Y_2 < Y_1$ obtained at 523 K. There are less organics compound to degrade and glyphosate is oxidized into increasingly smaller molecules at higher WAO temperature which are inert to be metabolized by microorganisms. Patterson et al. (2002) found a similar trend for the degradation of linear alkylbenzene sulfonates by an integrated WAO-biological treatment process.

Moreover, Table 6.3 depicts that the MLSS of acclimated sludge after 24 h culture was almost the same with the initial MLSS of 3 ± 0.39 , indicating that the biomass concentration almost kept constant during the biological treatment. This reveals that the effluents from WAO pretreatment do not cause an inhibition effect for the growth of acclimated activated sludge. The pH for acclimated activate sludge after 24 h at different WAO process were all higher than the initial pH of 7, which may be caused by glyphosate or its intermediates generated in WAO pretreatment.

6.3.3 Combination of WAO and biological process

As shown in Table 6.2, the glyphosate, TOC and COD destruction achieved by the combined process was all larger than that of single WAO or biological treatment. The maximum total glyphosate, TOC and COD reduction was 100%, 59.43% and 56.72%, respectively, for acclimated sludge, higher than non-acclimated asludge. This implies that pretreatment by glyphosate improves the following biological treatment, resulting in the increase of the degradation and mineralization of glyphosate. This may be attributed to the factor that some intermediates of glyphosate generate during WAO process, which can be degraded by the following biological treatment. The total glyphosate, TOC and COD removal all increased with the increase of the WAO temperature. The total glyphosate removal was mainly attributed to the WAO pretreatment. The total TOC and COD reduction at 423 and 473 K was mainly owing to the biological treatment, while for 523 K attributed to the WAO process which has explained above.

Complete glyphosate removal has been achieved by the compact process, which is meet the China standard (GB21523-2008) of glyphosate release ($1.0 \text{ mg}\cdot\text{L}^{-1}$) in environment, However, the resulting COD and TOC values exceeded the limits for effluent discharge of 80 and 40 $\text{mg}\cdot\text{L}^{-1}$ (GB21523-2008), respectively. It needs further study to increase the performance of this compact process through further decreasing COD and TOC concentration in order to meet the limitation of the release of glyphosate effluent. For example, it is possible to optimize several elements, such as HRT, type of reactor and its hydrodynamic behavior, temperature for biological process and pressure for WAO process.

6.3.4 Identification and quantification of by-products

Previous studied reported that the possible by-products of glyphosate oxidation are AMPA, glyoxylate, sarcosine, glycine, NH_4^+ , NO_3^- , PO_4^{3-} , and formaldehyde (Barrett and McBride, 2005; Chen et al., 2007a; Echavia et al., 2009; Manassero et al., 2010; Xing et al., 2018). In this study, the identification of by-products was conducted by LC/MS analyses and UV-vis spectrophotometry. The

analyses of glyphosate solutions before and after WAO and biological treatment were measured according to the same procedure described in previous section. Sarcosine was both not detected in samples after WAO or biological treatment. The comparison of the two mass spectra obvious shows a significant decrease of glyphosate characteristic peak ($m/z=168.0111$) and an obvious increase of the characteristic peak of AMPA ($m/z=110.0032$), which is similar to Ndjeri et al. (2013). The concentration of AMPA after WAO process was quantified by LC-MS (Section 6.2.4) and the results is shown in Table 6.4, as well as its yield (= molar concentration of AMPA generated/initial glyphosate molar concentration $\times 100$). Table 4 shows that AMPA concentration and yield increase with the temperature from 423 K and 473 K with respect to the increase of glyphosate destruction, while decrease with the temperature further increased to 523 K, indicating that AMPA is the primary products of glyphosate and can be further oxidized at high temperature. This has been confirmed in the kinetic experiments of glyphosate oxidation by WAO process in Chapter 3.

Table 6.4 The concentration and yield of AMPA after WAO pretreatment.

T (K)	Effluent after WAO	
	Concentration (mg.L ⁻¹)	Yield (%)
423	35.37	5.39
473	364.00	55.42
523	73.43	11.18

The UV-vis spectrometry measurements described in the experimental section indicates the generation of NH_4^+ , NO_3^- , PO_4^{3-} , and formaldehyde. The results are shown in Table 6.5. It can be seen that NH_4^+ only existed at 523 K in the effluent after WAO treatment with the concentration of 9.2 mg.L⁻¹. NH_4^+ is generally as the final mineralization product of AMPA (Aquino Neto and de Andrade, 2009). The low concentration of NH_4^+ indicates the presence of other intermediates during the conversion from AMPA to NH_4^+ during WAO process. According to previous literatures (Annett et al., 2014; Fu et al., 2017) and the previous work of Chapter 3, methylamine (CH_3NH_2) could be an possible intermediate during the degradation of AMPA to NH_4^+ . Thus, the presence of methylamine is also expected in our results. NH_4^+ both disappeared in acclimated and non-acclimated activated sludge, possibly used as nitrogen source for the synthesis of bacterial cell substances or nitrogen-containing metabolites. The concentration of NO_3^- after WAO pretreatment almost kept the same with the initial influent, indicating that NO_3^- is not generated during WAO process. However, its concentration increased after biological treatment in acclimated and non-acclimated sludge. Generally, NH_4^+ is the mineralization product containing nitrogen in the glyphosate biodegradation

(Annett et al., 2014; Kryuchkova et al., 2014; Fu et al., 2017). Thus, this increase is most likely due to the nitrification of microorganisms, resulting in NH_4^+ conversion into NO_3^- .

Moreover, the concentration of PO_4^{3-} in the effluent increased fast with the increase of WAO temperature. PO_4^{3-} is often considered as one of the final oxidation products of glyphosate (Echavia et al., 2009; Xing et al., 2018). Therefore, the mineralization efficiency of glyphosate by WAO pretreatment increased, which is consistent with the results of TOC and COD. Furthermore, according to our previous work on the kinetics of glyphosate by WAO process, PO_4^{3-} has been confirmed to be transferred from AMPA, not directly from glyphosate. After the biological treatment, for non-acclimated activated sludge, PO_4^{3-} concentration is slightly reduced (except at 423 K). This reduction may be attributed to PO_4^{3-} used as P source for microorganism. While for acclimated activated sludge, PO_4^{3-} concentration always increased. This is because during glyphosate biodegradation, PO_4^{3-} is produced, as it is also found in previous studies (Annett et al., 2014; Kryuchkova et al., 2014; Fu et al., 2017; Zhan et al., 2018).

During WAO pretreatment, the concentration of HCHO increased significantly from the initial concentration of 0.12 mg.L^{-1} to 5.9 and 54.25 mg.L^{-1} when the temperature increased from 423 to 473 K, respectively. With temperature further increased up to 523 K, HCHO concentration decreased, indicating the further oxidation of HCHO at higher temperature. After the treatment by acclimated and non-acclimated sludge, the HCHO concentration always reduced below 2 mg.L^{-1} , indicating that HCHO had been utilized by microorganisms as C source. This can be explained by our previous study on the kinetics of glyphosate biodegradation by acclimated activated sludge. The previous work indicated that glyphosate can be utilized by acclimated sludge to generate stoichiometric quantity of AMPA and glyoxylic acid through the cleavage of C-N bond by the presence of glyphosate oxidoreductase. Then AMPA was metabolized to phosphonoformaldehyde through transamination catalyzed by an aminotransferase and then transferred to formaldehyde and PO_4^{3-} from C-P bond cleavage of phosphonoformaldehyde. The resulting formaldehyde can enter the carbon metabolic pathways of cellular growth.

Table 6.5 The concentration of byproducts of glyphosate after the treatment of the combined process.

T (K)	Sludge	Influent				Effluent after WAO				Effluent after biological treatment			
		NH ₄ ⁺ (mg.L ⁻¹)	NO ₃ ⁻ (mg.L ⁻¹)	PO ₄ ³⁻ (mg.L ⁻¹)	HCHO (mg.L ⁻¹)	NH ₄ ⁺ (mg.L ⁻¹)	NO ₃ ⁻ (mg.L ⁻¹)	PO ₄ ³⁻ (mg.L ⁻¹)	HCHO (mg.L ⁻¹)	NH ₄ ⁺ (mg.L ⁻¹)	NO ₃ ⁻ (mg.L ⁻¹)	PO ₄ ³⁻ (mg.L ⁻¹)	HCHO (mg.L ⁻¹)
423	Acclimated activated sludge	0	2.5	0.5	0.12	0	2.7	5.9	3.15	0	30.9	19.6	0.82
473		0	2.5	0.5	0.12	0	2.5	41.1	42.25	0	42.2	50.4	1.54
523		0	2.5	0.5	0.12	9.2	2.6	99.8	35.45	0	18.2	113.4	0.33
423	Non-acclimated activated sludge	0	2.5	0.5	0.12	0	2.7	5.9	3.15	0	9.4	28.8	0.3
473		0	2.5	0.5	0.12	0	2.5	41.1	42.25	0	9	39.2	0.67
523		0	2.5	0.5	0.12	9.2	2.6	99.8	35.45	0	7.9	76.8	0.39

6.3.5 The degradation pathway of glyphosate

Through the above analysis of the identification and quantification of by-products of glyphosate treated by the combined system, a possible degradation pathway of glyphosate is proposed as shown in Fig. 6.2. Glyphosate could both convert to AMPA and glyoxylic acid through the cleavage of C-N bond promoted by OH attack and catalyzed by glyphosate oxidoreductase in the WAO and biological processes. In WAO process, AMPA was oxidized through the C-P bond cleavage to methylamine, HCHO and PO_4^{3-} . Methylamine could be oxidized into NH_4^+ and HCHO. However, in the biological process, AMPA was first metabolized to phosphonoformaldehyde through the transamination catalyzed by an aminotransferase and then transferred to formaldehyde and PO_4^{3-} through the C-P bond cleavage. During WAO process, little HCHO can be oxidized to HCOOH or further into CO_2 and H_2O (Xing et al., 2018). Most of HCHO was metabolized by microorganisms during biological process.

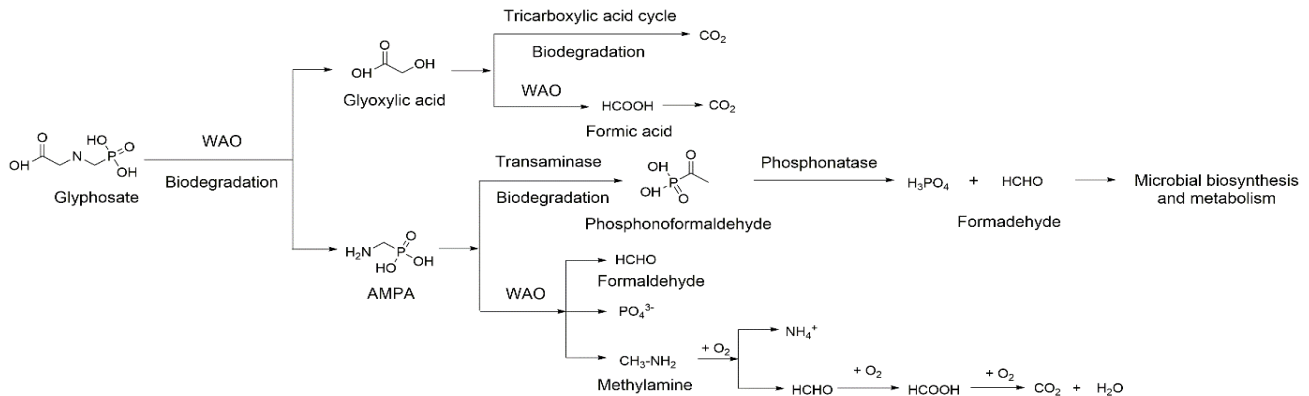


Fig. 6.2 A proposed degradation pathway of glyphosate by the integrated WAO-biological treatment

6.4 Conclusions

This work demonstrated that WAO process coupled with a biological treatment was a feasible technology for glyphosate-containing wastewater. An acclimation process to activated sludge is needed to increase glyphosate biodegradation. The maximum glyphosate, TOC and COD removal of 100, 59.43 and 56.72% was achieved for WAO conditions of 523 K coupled with a 24 h residence time of acclimation activated sludge treatment. For the optimization of the integrated process, knowledge of the main reaction intermediates was studied, and a possible degradation pathway was proposed. This could provide a systematic approach to design an efficient integrated treatment process for the real glyphosate wastewater.

Chapter 7 Conclusion and Perspectives

7.1 Conclusion

This thesis concerns the treatment of wastewater containing glyphosate, a typical emerging contaminant, by an integrated WAO-biological process. This work is divided into six main stages. The main conclusions could be summarized as follows:

(1) The bibliographic work showed that glyphosate has been frequently detected in the Environment and could cause adverse effects, which is necessary to remove it from environment. The integrated WAO-biological treatment may be a very promising method to effectively treat glyphosate-containing wastewater. Moreover, the utilization of microfluidic device for WAO process may be a potential method to reduce mass transfer limitation, thereby further increasing the performance for WAO process.

(2) The bubble characteristics were significantly influenced by superficial gas velocity and the type of the liquid phase, while not considerably affected by superficial liquid velocity, temperature, pressure and the type of gas phase. Two correlations for bubble mean diameter and gas holdup were proposed, which could be used for the prediction of the mass transfer for WAO process and recommended to scale-up WAO system.

(3) Complete glyphosate removal and 54% of TOC reduction were obtained at 523 K after 60 min by WAO process in a batch reactor. Glyphosate oxidation reactions obey a first-order kinetics with respect to glyphosate concentration. The activation energy is 68.44 kJ.mol⁻¹. Moreover, a possible degradation pathway of glyphosate via WAO was proposed.

(4) The performance of glyphosate degradation performance in microfluidic device increases with the increase of temperature and of residence time. Almost complete glyphosate degradation, 74.14% and 84.15% of TOC and COD reduction, respectively, have been obtained at 523 K with a residence time of 90 min.

(5) The acclimated process promotes the glyphosate biodegradation by activated sludge. The acclimated activated sludge could utilize glyphosate as sole carbon source. Complete glyphosate removal and 57.8% TOC reduction has been achieved by acclimated sludge with an initial glyphosate concentration of 1000 mg.L⁻¹. A possible biodegradation of glyphosate was also proposed.

(6) The integrated WAO-biological treatment is a feasible technology for the treatment of glyphosate-containing wastewater. Complete glyphosate removal, 59,43 and 56,72% of TOC and COD reduction, respectively, were obtained by the combined process at 523 K of WAO process with a reaction time of 30 min and with a residence time of 24 h for acclimated activated sludge. A possible degradation pathway of glyphosate by the combined process was proposed.

7.2 Perspectives

The present work contributes to the advances in the fundamental knowledge of the treatment of glyphosate-containing wastewater by the integrated WAO-biological process. Although extensive experiments have been performed on each stage and the combined process, there are still many tasks in this field which are needed to be further studied. Moreover, the present study only represents a first attempt at the application of microfluidic device for WAO process. There is still much work which can and should be carried out. Thus, in the near future, in order to continue this study of the combined process and microfluidic device, we recommend as follows:

(1) Regarding the approach of the coupling process for glyphosate degradation, several elements can be improved from the experimental point. Thus, it will be interesting to integrate more parameters in the study of WAO process, such as pressure, pH and glyphosate initial concentration. Likewise, it is possible to optimize certain parameters of the activated-sludge system before the coupling, such as organic load, pH, temperature and the type of reactor (stirred reactor, packed-bed reactor, etc). Finally, a more clearly identification of the compositions of intermediate effluent at each stage should be tested.

(2) The kinetic model of WAO process can be improved with taking the kinetics of the oxidation of main intermediates into account.

(3) This combined process shows good potential for the treatment of the pure glyphosate synthetic wastewater. However, the composition of actual glyphosate wastewater is more complicated. For example, glyphosate production wastewater contains some organic compounds, such as iminodiacetic acid salt, chloroacetic acid, triacetic acid amine, etc., with high COD concentration and poor biodegradability. Thus, it is necessary to study the performance of this method for the real glyphosate wastewater in order to determine if it can be used in practice.

(4) The microfluidic device showed interesting results for glyphosate degradation. However more experiments should be conducted to investigate the influences of the size, section and length of microchannel, operating parameters, etc. on the oxidation. Moreover, more oxidation of other emerging contaminants in microchannel reactor should be investigated in order to enrich the microreaction technology.

(5) Process simulation is a useful method to verify the possibility of the combined process for practical application. Therefore, it is interesting to use computer software, such as ProSimPlus, to numerically study glyphosate oxidation via the integrated WAO-biological method aiming to confirm the possibility of the scale-up of this method.

References

- Acosta-Cortés, A.G., Martínez-Ledezma, C., López-Chuken, U.J., Kaushik, G., Nimesh, S., Villarreal-Chiu, J.F., 2019. Polyphosphate recovery by a native *Bacillus cereus* strain as a direct effect of glyphosate uptake. *ISME J.* <https://doi.org/10.1038/s41396-019-0366-3>
- Acquavella, J.F., Alexander, B.H., Mandel, J.S., Gustin, C., Baker, B., Chapman, P., Bleeke, M., 2004. Glyphosate biomonitoring for farmers and their families: results from the Farm Family Exposure Study. *Environ. Health Perspect.* 112, 321–326.
- Akita, K., Yoshida, F., 1974. Bubble size, interfacial area, and liquid-phase mass transfer coefficient in bubble columns. *Ind. Eng. Chem. Process Des. Dev.* 13, 84–91.
- Akita, K., Yoshida, F., 1973. Gas Holdup and Volumetric Mass Transfer Coefficient in Bubble Columns. Effects of Liquid Properties. *Ind. Eng. Chem. Process Des. Dev.* 12, 76–80. <https://doi.org/10.1021/i260045a015>
- Al Momani, F., Gonzalez, O., Sans, C., Esplugas, S., 2004. Combining photo-Fenton process with biological sequencing batch reactor for 2,4-dichlorophenol degradation. *Water Sci. Technol.* 49, 293–298. <https://doi.org/10.2166/wst.2004.0288>
- Al-Ahmady, K.K., 2010. Mathematical Model for Calculating Oxygen Mass Transfer Coefficient in Diffused Air Systems.
- Amat, Ana.M., Arques, A., Beneyto, H., García, A., Miranda, M.A., Seguí, S., 2003. Ozonisation coupled with biological degradation for treatment of phenolic pollutants: a mechanistically based study. *Chemosphere* 53, 79–86. [https://doi.org/10.1016/S0045-6535\(03\)00450-8](https://doi.org/10.1016/S0045-6535(03)00450-8)
- Amatore, C., Klymenko, O.V., Oleinick, A.I., Svir, I., 2009. Electrochemical Determination of Flow Velocity Profile in a Microfluidic Channel from Steady-State Currents: Numerical Approach and Optimization of Electrode Layout. *Anal. Chem.* 81, 7667–7676. <https://doi.org/10.1021/ac9010827>
- Amatore, C., Klymenko, O.V., Svir, I., 2006. In situ and Online Monitoring of Hydrodynamic Flow Profiles in Microfluidic Channels Based upon Microelectrochemistry: Optimization of Electrode Locations. *ChemPhysChem* 7, 482–487. <https://doi.org/10.1002/cphc.200500400>
- Annett, R., Habibi, H.R., Hontela, A., 2014. Impact of glyphosate and glyphosate-based herbicides on the freshwater environment. *J. Appl. Toxicol. JAT* 34, 458–479. <https://doi.org/10.1002/jat.2997>
- Aparicio, V.C., De Gerónimo, E., Marino, D., Primost, J., Carriquiriborde, P., Costa, J.L., 2013a. Environmental fate of glyphosate and aminomethylphosphonic acid in surface waters and soil of agricultural basins. *Chemosphere* 93, 1866–1873. <https://doi.org/10.1016/j.chemosphere.2013.06.041>
- Aparicio, V.C., De Gerónimo, E., Marino, D., Primost, J., Carriquiriborde, P., Costa, J.L., 2013b. Environmental fate of glyphosate and aminomethylphosphonic acid in surface waters and soil of agricultural basins. *Chemosphere* 93, 1866–1873. <https://doi.org/10.1016/j.chemosphere.2013.06.041>
- APHA, 1998. *Standard Methods for the Examination of Water and Wastewater*, 20th edn. ed. American Public Health Association, Washington, D.C.
- Aquino Neto, S., de Andrade, A.R., 2009. Electrooxidation of glyphosate herbicide at different DSA® compositions: pH, concentration and supporting electrolyte effect. *Electrochimica Acta* 54, 2039–2045. <https://doi.org/10.1016/j.electacta.2008.07.019>
- Aquino Neto, S., De Andrade, A.R., 2009. Electrochemical degradation of glyphosate formulations at DSA® anodes in chloride medium: an AOX formation study. *J. Appl. Electrochem.* 39, 1863. <https://doi.org/10.1007/s10800-009-9890-6>
- Aramyan, S.M., 2017. Advances in Fenton and Fenton Based Oxidation Processes for Industrial Effluent Contaminants Control-A Review. *Int. J. Environ. Sci. Nat. Resour.* 2, 1–18. <https://doi.org/10.19080/IJESNR.2017.02.555594>
- Arslan-Alaton, I., Eremektar, G., Germirli-Babuna, F., Insel, G., Selcuk, H., Ozerkan, B., Teksoy, S., 2005. Advanced Oxidation of Commercial Textile Biocides in Aqueous Solution: Effects on Acute Toxicity and Biomass Inhibition. *Water Sci. Technol.* 52, 309–316. <https://doi.org/10.2166/wst.2005.0707>
- Assalin, M.R., Moraes, S.G.D., Queiroz, S.C.N., Ferracini, V.L., Duran, N., 2009. Studies on degradation of glyphosate by several oxidative chemical processes: Ozonation, photolysis and heterogeneous photocatalysis. *J. Environ. Sci. Health Part B* 45, 89–94. <https://doi.org/10.1080/03601230903404598>
- Azabou, S., Najjar, W., Bouaziz, M., Ghorbel, A., Sayadi, S., 2010. A compact process for the treatment of olive mill wastewater by combining wet hydrogen peroxide catalytic oxidation and biological techniques. *J. Hazard. Mater.* 183, 62–69. <https://doi.org/10.1016/j.jhazmat.2010.06.104>

- Badawy, M.I., Gohary, F.El., Ghaly, M.Y., Ali, M.E.M., 2009. Enhancement of olive mill wastewater biodegradation by homogeneous and heterogeneous photocatalytic oxidation. *J. Hazard. Mater.* 169, 673–679. <https://doi.org/10.1016/j.jhazmat.2009.04.038>
- Baillod, C.R., Faith, B.M., Masi, O., 1982. Fate of specific pollutants during wet oxidation and ozonation. Where do the pollutants wind up in oxidational purification processes? Here is a well documented experimental study. *Environ. Prog.* 1, 217–227. <https://doi.org/10.1002/ep.670010316>
- Balci, B., Oturan, M.A., Oturan, N., Sirés, I., 2009. Decontamination of Aqueous Glyphosate, (Aminomethyl)phosphonic Acid, and Glufosinate Solutions by Electro-Fenton-like Process with Mn²⁺ as the Catalyst. *J. Agric. Food Chem.* 57, 4888–4894. <https://doi.org/10.1021/jf900876x>
- Ballesteros Martín, M.M., Sánchez Pérez, J.A., Casas López, J.L., Oller, I., Malato Rodríguez, S., 2009. Degradation of a four-pesticide mixture by combined photo-Fenton and biological oxidation. *Water Res.* 43, 653–660. <https://doi.org/10.1016/j.watres.2008.11.020>
- Balthazor, T.M., Hallas, L.E., 1986. Glyphosate-Degrading Microorganisms from Industrial Activated Sludge. *Appl. Environ. Microbiol.* 51, 432–434.
- Bandyopadhyay, B., Humphrey, A.E., Taguchi, H., Rao, I. by G., 2009. Dynamic measurement of the volumetric oxygen transfer coefficient in fermentation systems. *Biotechnol. Bioeng.* 104, 841–853. <https://doi.org/10.1002/bit.22566>
- Barbeau, C., Deschênes, L., Karamanev, D., Comeau, Y., Samson, R., 1997. Bioremediation of pentachlorophenol-contaminated soil by bioaugmentation using activated soil. *Appl. Microbiol. Biotechnol.* 48, 745–752.
- Barge, A.S., Vaidya, P.D., 2018. Wet air oxidation of cresylic spent caustic – A model compound study over graphene oxide (GO) and ruthenium/GO catalysts. *J. Environ. Manage.* 212, 479–489. <https://doi.org/10.1016/j.jenvman.2018.01.066>
- Barrett, K.A., McBride, M.B., 2005. Oxidative Degradation of Glyphosate and Aminomethylphosphonate by Manganese Oxide. *Environ. Sci. Technol.* 39, 9223–9228. <https://doi.org/10.1021/es051342d>
- Battaglin, W.A., Kolpin, D.W., Scribner, E.A., Kuivila, K.M., Sandstrom, M.W., 2005. Glyphosate, Other Herbicides, and Transformation Products in Midwestern Streams, 20021. *JAWRA J. Am. Water Resour. Assoc.* 41, 323–332. <https://doi.org/10.1111/j.1752-1688.2005.tb03738.x>
- Battaglin, W.A., Meyer, M.T., Kuivila, K.M., Dietze, J.E., 2014. Glyphosate and Its Degradation Product AMPA Occur Frequently and Widely in U.S. Soils, Surface Water, Groundwater, and Precipitation. *JAWRA J. Am. Water Resour. Assoc.* 50, 275–290. <https://doi.org/10.1111/jawr.12159>
- Battaglin, W.A., Rice, K.C., Focazio, M.J., Salmons, S., Barry, R.X., 2009. The occurrence of glyphosate, atrazine, and other pesticides in vernal pools and adjacent streams in Washington, DC, Maryland, Iowa, and Wyoming, 2005–2006. *Environ. Monit. Assess.* 155, 281–307. <https://doi.org/10.1007/s10661-008-0435-y>
- Baylis, A.D., 2000. Why glyphosate is a global herbicide: strengths, weaknesses and prospects. *Pest Manag. Sci.* 56, 299–308. [https://doi.org/10.1002/\(SICI\)1526-4998\(200004\)56:4<299::AID-PS144>3.0.CO;2-K](https://doi.org/10.1002/(SICI)1526-4998(200004)56:4<299::AID-PS144>3.0.CO;2-K)
- Baz-Rodríguez, S.A., Botello-Alvarez, J.E., Estrada-Baltazar, A., Vilchiz-Bravo, L.E., Padilla-Medina, J.A., Miranda-López, R., 2014. Effect of electrolytes in aqueous solutions on oxygen transfer in gas–liquid bubble columns. *Chem. Eng. Res. Des.* 92, 2352–2360. <https://doi.org/10.1016/j.cherd.2014.02.023>
- Behkish, A., Lemoine, R., Sehabiague, L., Oukaci, R., Morsi, B.I., 2007a. Gas holdup and bubble size behavior in a large-scale slurry bubble column reactor operating with an organic liquid under elevated pressures and temperatures. *Chem. Eng. J.* 128, 69–84. <https://doi.org/10.1016/j.cej.2006.10.016>
- Behkish, A., Lemoine, R., Sehabiague, L., Oukaci, R., Morsi, B.I., 2007b. Gas holdup and bubble size behavior in a large-scale slurry bubble column reactor operating with an organic liquid under elevated pressures and temperatures. *Chem. Eng. J.* 128, 69–84. <https://doi.org/10.1016/j.cej.2006.10.016>
- Benachour, N., Séralini, G.-E., 2009. Glyphosate Formulations Induce Apoptosis and Necrosis in Human Umbilical, Embryonic, and Placental Cells. *Chem. Res. Toxicol.* 22, 97–105. <https://doi.org/10.1021/tx800218n>
- Benbrook, C.M., 2016. Trends in glyphosate herbicide use in the United States and globally. *Environ. Sci. Eur.* 28, 3. <https://doi.org/10.1186/s12302-016-0070-0>
- Benslama, O., Boulahrouf, A., 2013. Isolation and characterization of glyphosate-degrading bacteria from different soils of Algeria. *Afr. J. Microbiol. Res.* 7, 5587–5595. <https://doi.org/10.5897/AJMR2013.6080>

- Ben-Youssef, C., Vázquez-Rodríguez, G.A., 2011. Model-based design of different fedbatch strategies for phenol degradation in acclimatized activated sludge cultures. *Bioresour. Technol.* 102, 3740–3747. <https://doi.org/10.1016/j.biortech.2010.11.122>
- Besagni, G., Gallazzini, L., Inzoli, F., 2018. Effect of gas sparger design on bubble column hydrodynamics using pure and binary liquid phases. *Chem. Eng. Sci.* 176, 116–126. <https://doi.org/10.1016/j.ces.2017.10.036>
- Bhargava, S.K., Tardio, J., Prasad, J., Föger, K., Akolekar, D.B., Grocott, S.C., 2006. Wet Oxidation and Catalytic Wet Oxidation. *Ind. Eng. Chem. Res.* 45, 1221–1258. <https://doi.org/10.1021/ie051059n>
- Bhaskara, B.L., Nagaraja, P., 2006. Direct Sensitive Spectrophotometric Determination of Glyphosate by Using Ninhydrin as a Chromogenic Reagent in Formulations and Environmental Water Samples. *Helv. Chim. Acta* 89, 2686–2693. <https://doi.org/10.1002/hlca.200690240>
- Bijan, L., Mohseni, M., 2008. Novel Membrane Pretreatment to Increase the Efficiency of Ozonation-BioOxidation. *Environ. Eng. Sci.* 25, 229–238. <https://doi.org/10.1089/ees.2006.0264>
- Birch, H., Mikkelsen, P.S., Jensen, J.K., Lützhøft, H.-C.H., 2011. Micropollutants in stormwater runoff and combined sewer overflow in the Copenhagen area, Denmark. *Water Sci. Technol.* 64, 485–493. <https://doi.org/10.2166/wst.2011.687>
- Birchmeier, M.J., Hill, C.G., Houtman, C.J., Atalla, R.H., Weinstock, I.A., 2000. Enhanced Wet Air Oxidation: Synergistic Rate Acceleration upon Effluent Recirculation. *Ind. Eng. Chem. Res.* 39, 55–64. <https://doi.org/10.1021/ie990149n>
- Blot, N., Veillat, L., Rouzé, R., Delatte, H., 2019. Glyphosate, but not its metabolite AMPA, alters the honeybee gut microbiota. *PLoS ONE* 14. <https://doi.org/10.1371/journal.pone.0215466>
- Bokare, A.D., Choi, W., 2014. Review of iron-free Fenton-like systems for activating H₂O₂ in advanced oxidation processes. *J. Hazard. Mater.* 275, 121–135. <https://doi.org/10.1016/j.jhazmat.2014.04.054>
- Bolong, N., Ismail, A.F., Salim, M.R., Matsuura, T., 2009. A review of the effects of emerging contaminants in wastewater and options for their removal. *Desalination* 239, 229–246. <https://doi.org/10.1016/j.desal.2008.03.020>
- Borggaard, O.K., Gimsing, A.L., 2008. Fate of glyphosate in soil and the possibility of leaching to ground and surface waters: a review. *Pest Manag. Sci.* 64, 441–456.
- Botta, F., Lavison, G., Couturier, G., Alliot, F., Moreau-Guigon, E., Fauchon, N., Guery, B., Chevreuil, M., Blanchoud, H., 2009. Transfer of glyphosate and its degradate AMPA to surface waters through urban sewerage systems. *Chemosphere* 77, 133–139. <https://doi.org/10.1016/j.chemosphere.2009.05.008>
- Bujacz, B., Wiczorek, P., Krzysko-Lupicka, T., Golab, Z., Lejczak, B., Kavfarski, P., 1995. Organophosphonate Utilization by the Wild-Type Strain of *Penicillium notatum*. *Appl. Environ. Microbiol.* 61, 2905–2910.
- Cağlar, S., Kolankaya, D., 2008. The effect of sub-acute and sub-chronic exposure of rats to the glyphosate-based herbicide Roundup. *Environ. Toxicol. Pharmacol.* 25, 57–62. <https://doi.org/10.1016/j.etap.2007.08.011>
- Cassigneul, A., Benoit, P., Bergheaud, V., Dumeny, V., Etiévant, V., Goubard, Y., Maylin, A., Justes, E., Alletto, L., 2016. Fate of glyphosate and degradates in cover crop residues and underlying soil: A laboratory study. *Sci. Total Environ.* 545–546, 582–590. <https://doi.org/10.1016/j.scitotenv.2015.12.052>
- Castro, J.V., Peralba, M.C.R., Ayub, M.A.Z., 2007. Biodegradation of the herbicide glyphosate by filamentous fungi in platform shaker and batch bioreactor. *J. Environ. Sci. Health Part B* 42, 883–886. <https://doi.org/10.1080/03601230701623290>
- Cattani, D., Cesconetto, P.A., Tavares, M.K., Parisotto, E.B., De Oliveira, P.A., Rieg, C.E.H., Leite, M.C., Prediger, R.D.S., Wendt, N.C., Razzera, G., Filho, D.W., Zamoner, A., 2017. Developmental exposure to glyphosate-based herbicide and depressive-like behavior in adult offspring: Implication of glutamate excitotoxicity and oxidative stress. *Toxicology* 387, 67–80. <https://doi.org/10.1016/j.tox.2017.06.001>
- Celius, T., Haugen, T.B., Grotmol, T., Walther, B.T., 1999. A sensitive zogenetic assay for rapid in vitro assessment of estrogenic potency of xenobiotics and mycotoxins. *Environ. Health Perspect.* 107, 63–68.
- Chakchouk, M., Hamdi, M., Foussard, J.N., Debellefontaine, H., 1994. Complete treatment of olive mill wastewaters by a wet air oxidation process coupled with a biological step. *Environ. Technol.* 15, 323–332. <https://doi.org/10.1080/09593339409385435>
- Chang, C.J., Li, S.-S., Ko, C.-M., 1995. Catalytic wet oxidations of phenol- and p-chlorophenol-contaminated waters. *J. Chem. Technol. Biotechnol.* 64, 245–252. <https://doi.org/10.1002/jctb.280640306>

- Chang, F., Simcik, M.F., Capel, P.D., 2011. Occurrence and fate of the herbicide glyphosate and its degradate aminomethylphosphonic acid in the atmosphere. *Environ. Toxicol. Chem.* 30, 548–555. <https://doi.org/10.1002/etc.431>
- Chaumat, H., Billet-Duquenne, A.M., Augier, F., Mathieu, C., Delmas, H., 2005. Mass transfer in bubble column for industrial conditions—effects of organic medium, gas and liquid flow rates and column design. *Chem. Eng. Sci.*, 7th International Conference on Gas-Liquid and Gas-Liquid-Solid Reactor Engineering 60, 5930–5936. <https://doi.org/10.1016/j.ces.2005.04.026>
- Chen, C.-Y., Wu, P.-S., Chung, Y.-C., 2009. Coupled biological and photo-Fenton pretreatment system for the removal of di-(2-ethylhexyl) phthalate (DEHP) from water. *Bioresour. Technol.* 100, 4531–4534. <https://doi.org/10.1016/j.biortech.2009.04.020>
- Chen, F., Zhou, C., Li, G., Peng, F., 2016. Thermodynamics and kinetics of glyphosate adsorption on resin D301. *Arab. J. Chem.* 9, S1665–S1669. <https://doi.org/10.1016/j.arabjc.2012.04.014>
- Chen, G., Lei, L., Yue, P.-L., 1999. Wet Oxidation of High-Concentration Reactive Dyes. *Ind. Eng. Chem. Res.* 38, 1837–1843. <https://doi.org/10.1021/ie980617d>
- Chen, S., Cao, G., 2005. Photocatalytic degradation of organophosphorus pesticides using floating photocatalyst TiO₂-SiO₂/beads by sunlight. *Sol. Energy* 79, 1–9. <https://doi.org/10.1016/j.solener.2004.10.006>
- Chen, S., Liu, Y., 2007. Study on the photocatalytic degradation of glyphosate by TiO₂ photocatalyst. *Chemosphere* 67, 1010–1017. <https://doi.org/10.1016/j.chemosphere.2006.10.054>
- Chen, S., Sun, D., Chung, J.-S., 2007. Treatment of pesticide wastewater by moving-bed biofilm reactor combined with Fenton-coagulation pretreatment. *J. Hazard. Mater.* 144, 577–584. <https://doi.org/10.1016/j.jhazmat.2006.10.075>
- Chen, Y., Wu, F., Lin, Y., Deng, N., Bazhin, N., Glebov, E., 2007a. Photodegradation of glyphosate in the ferrioxalate system. *J. Hazard. Mater.* 148, 360–365. <https://doi.org/10.1016/j.jhazmat.2007.02.044>
- Chen, Y., Wu, F., Zhang, X., Deng, N., Bazhin, N., Glebov, E., 2007b. Fe(III)-pyruvate and Fe(III)-citrate induced photodegradation of glyphosate in aqueous solutions. *J. Coord. Chem.* 60, 2431–2439. <https://doi.org/10.1080/00958970701272102>
- Chilekar, V.P., 2007. Hydrodynamics and mass transfer in slurry bubble columns: Scale and pressure effects. Citeseer.
- Chilekar, V.P., van der Schaaf, J., Kuster, B.F.M., Tinge, J.T., Schouten, J.C., 2010. Influence of elevated pressure and particle lyophobicity on hydrodynamics and gas–liquid mass transfer in slurry bubble columns. *AIChE J.* 56, 584–596. <https://doi.org/10.1002/aic.11987>
- Chong, M.N., Jin, B., Chow, C.W.K., Saint, C., 2010. Recent developments in photocatalytic water treatment technology: A review. *Water Res.* 44, 2997–3027. <https://doi.org/10.1016/j.watres.2010.02.039>
- Clark, K.N., 1990. The effect of high pressure and temperature on phase distributions in a bubble column. *Chem. Eng. Sci.* 45, 2301–2307.
- Colborn, T., 1995. Pesticides--how research has succeeded and failed to translate science into policy: endocrinological effects on wildlife. *Environ. Health Perspect.* 103, 81–85.
- Contreras, E.M., Albertario, M.E., Bertola, N.C., Zaritzky, N.E., 2008. Modelling phenol biodegradation by activated sludges evaluated through respirometric techniques. *J. Hazard. Mater.* 158, 366–374. <https://doi.org/10.1016/j.jhazmat.2008.01.082>
- Corbel, S., Becheikh, N., Roques-Carmes, T., Zahraa, O., 2014. Mass transfer measurements and modeling in a microchannel photocatalytic reactor. *Chem. Eng. Res. Des.*, ECCE9 – 9th European Congress of Chemical Engineering 92, 657–662. <https://doi.org/10.1016/j.cherd.2013.10.011>
- Cordi, L., 2012. Identification of Microbiota for Activated Sludge Acclimated By Paper Mill Effluent Kraft E1 Bioremediation. *J. Bioremediation Biodegrad.* 03. <https://doi.org/10.4172/2155-6199.1000169>
- Coupe, R.H., Kalkhoff, S.J., Capel, P.D., Gregoire, C., 2012. Fate and transport of glyphosate and aminomethylphosphonic acid in surface waters of agricultural basins. *Pest Manag. Sci.* 68, 16–30. <https://doi.org/10.1002/ps.2212>
- da Silva, A.S., Fernandes, F.C.B., Tognolli, J.O., Pezza, L., Pezza, H.R., 2011. A simple and green analytical method for determination of glyphosate in commercial formulations and water by diffuse reflectance spectroscopy. *Spectrochim. Acta. A. Mol. Biomol. Spectrosc.* 79, 1881–1885. <https://doi.org/10.1016/j.saa.2011.05.081>
- Das, S., Srivastava, V.C., 2016. Microfluidic-based photocatalytic microreactor for environmental application: a review of fabrication substrates and techniques, and operating parameters. *Photochem. Photobiol. Sci.* 15, 714–730. <https://doi.org/10.1039/C5PP00469A>

- Daughton, C.G., Ternes, T.A., 1999. Pharmaceuticals and personal care products in the environment: agents of subtle change? *Environ. Health Perspect.* 107, 907–938.
- Day, D.C., Hudgins, R.R., Silveston, P.L., 1973. Oxidation of propionic acid solutions. *Can. J. Chem. Eng.* 51, 733–740. <https://doi.org/10.1002/cjce.5450510618>
- Debellefontaine, H., Chakchouk, M., Foussard, J.N., Tissot, D., Striolo, P., 1996. Treatment of organic aqueous wastes: Wet air oxidation and wet peroxide oxidation®. *Environ. Pollut.* 92, 155–164. [https://doi.org/10.1016/0269-7491\(95\)00100-X](https://doi.org/10.1016/0269-7491(95)00100-X)
- Debellefontaine, H., Foussard, J.N., 2000. Wet air oxidation for the treatment of industrial wastes. Chemical aspects, reactor design and industrial applications in Europe. *Waste Manag.* 20, 15–25. [https://doi.org/10.1016/S0956-053X\(99\)00306-2](https://doi.org/10.1016/S0956-053X(99)00306-2)
- Deckwer, W.-D., Louisi, Y., Zaidi, A., Ralek, M., 1980. Hydrodynamic Properties of the Fischer-Tropsch Slurry Process. *Ind. Eng. Chem. Process Des. Dev.* 19, 699–708. <https://doi.org/10.1021/i260076a032>
- Demirel, M., Kayan, B., 2012. Application of response surface methodology and central composite design for the optimization of textile dye degradation by wet air oxidation. *Int. J. Ind. Chem.* 3, 24. <https://doi.org/10.1186/2228-5547-3-24>
- Deng, Z., Wang, T., Zhang, N., Wang, Z., 2010. Gas holdup, bubble behavior and mass transfer in a 5m high internal-loop airlift reactor with non-Newtonian fluid. *Chem. Eng. J.* 160, 729–737. <https://doi.org/10.1016/j.cej.2010.03.078>
- Devlin, H.R., Harris, I.J., 1984. Mechanism of the oxidation of aqueous phenol with dissolved oxygen. *Ind. Eng. Chem. Fundam.* 23, 387–392. <https://doi.org/10.1021/i100016a002>
- Dick, R.E., Quinn, J.P., 1995. Control of glyphosate uptake and metabolism in *Pseudomonas* sp. 4ASW. *FEMS Microbiol. Lett.* 134, 177–182.
- Divyapriya, G., Nambi, I.M., Senthilnathan, J., 2016. Nanocatalysts in Fenton Based Advanced Oxidation Process for Water and Wastewater Treatment. *J. Bionanoscience* 10, 356–368. <https://doi.org/info:doi/10.1166/jbns.2016.1387>
- Dodds, E.C., Lawson, W., 1938. Molecular structure in relation to oestrogenic activity. Compounds without a phenanthrene nucleus. *Proc R Soc Lond B* 125, 222–232. <https://doi.org/10.1098/rspb.1938.0023>
- Duke, S.O., Lydon, J., Koskinen, W.C., Moorman, T.B., Chaney, R.L., Hammerschmidt, R., 2012. Glyphosate Effects on Plant Mineral Nutrition, Crop Rhizosphere Microbiota, and Plant Disease in Glyphosate-Resistant Crops. *J. Agric. Food Chem.* 60, 10375–10397. <https://doi.org/10.1021/jf302436u>
- Duke, S.O., Powles, S.B., 2008. Glyphosate: a once-in-a-century herbicide. *Pest Manag. Sci.* 64, 319–325. <https://doi.org/10.1002/ps.1518>
- Echavia, G.R.M., Matzusawa, F., Negishi, N., 2009. Photocatalytic degradation of organophosphate and phosphonoglycine pesticides using TiO₂ immobilized on silica gel. *Chemosphere* 76, 595–600. <https://doi.org/10.1016/j.chemosphere.2009.04.055>
- El-Gohary, F.A., Badawy, M.I., El-Khateeb, M.A., El-Kalliny, A.S., 2009. Integrated treatment of olive mill wastewater (OMW) by the combination of Fenton's reaction and anaerobic treatment. *J. Hazard. Mater.* 162, 1536–1541. <https://doi.org/10.1016/j.jhazmat.2008.06.098>
- Emerging substances | NORMAN [WWW Document], n.d. URL <https://www.norman-network.net/?q=node/19> (accessed 9.5.18).
- ENDS, 1999. Industry Glimpses New Challenges as Endocrine Science Advances (No. ENDS Report 290).
- Ermakova, I.T., Kiseleva, N.I., Shushkova, T., Zharikov, M., Zharikov, G.A., Leontievsky, A.A., 2010. Bioremediation of glyphosate-contaminated soils. *Appl. Microbiol. Biotechnol.* 88, 585–594. <https://doi.org/10.1007/s00253-010-2775-0>
- Ermakova, I.T., Shushkova, T.V., Sviridov, A.V., Zelenkova, N.F., Vinokurova, N.G., Baskunov, B.P., Leontievsky, A.A., 2017. Organophosphonates utilization by soil strains of *Ochrobactrum anthropi* and *Achromobacter* sp. *Arch. Microbiol.* 199, 665–675. <https://doi.org/10.1007/s00203-017-1343-8>
- Eskandarloo, H., Badiei, A., Behnajady, M.A., Ziarani, G.M., 2015. UV-LEDs assisted preparation of silver deposited TiO₂ catalyst bed inside microchannels as a high efficiency microphotoreactor for cleaning polluted water. *Chem. Eng. J.* 270, 158–167. <https://doi.org/10.1016/j.cej.2015.01.117>
- Fan, J., Yang, G., Zhao, H., Shi, G., Geng, Y., Hou, T., Tao, K., 2012. Isolation, identification and characterization of a glyphosate-degrading bacterium, *Bacillus cereus* CB4, from soil. *J. Gen. Appl. Microbiol.* 58, 263–271.
- Farinos, R.M., Ruotolo, L.A.M., 2017. Comparison of the electrooxidation performance of three-dimensional RVC/PbO₂ and boron-doped diamond electrodes. *Electrochimica Acta* 224, 32–39. <https://doi.org/10.1016/j.electacta.2016.12.025>

- Feng, D., Ferrasse, J.-H., Soric, A., Boutin, O., 2019. Bubble characterization and gas–liquid interfacial area in two phase gas–liquid system in bubble column at low Reynolds number and high temperature and pressure. *Chem. Eng. Res. Des.* 144, 95–106. <https://doi.org/10.1016/j.cherd.2019.02.001>
- Firdous, S., Iqbal, S., Anwar, S., 2017. Optimization and Modeling of Glyphosate Biodegradation by a Novel *Comamonas odontotermitis* P2 Through Response Surface Methodology. *Pedosphere*. [https://doi.org/10.1016/S1002-0160\(17\)60381-3](https://doi.org/10.1016/S1002-0160(17)60381-3)
- Firdous, S., Iqbal, S., Anwar, S., Jabeen, H., 2018. Identification and analysis of 5-enolpyruvylshikimate-3-phosphate synthase (EPSPS) gene from glyphosate-resistant *Ochrobactrum intermedium* Sq20. *Pest Manag. Sci.* 74, 1184–1196. <https://doi.org/10.1002/ps.4624>
- Foussard Jean-Noël, Debellefontaine Hubert, Besombes-Vailhé Jean, 1989. Efficient Elimination of Organic Liquid Wastes: Wet Air Oxidation. *J. Environ. Eng.* 115, 367–385. [https://doi.org/10.1061/\(ASCE\)0733-9372\(1989\)115:2\(367\)](https://doi.org/10.1061/(ASCE)0733-9372(1989)115:2(367))
- Fransolet, E., Crine, M., Marchot, P., Toye, D., 2005. Analysis of gas holdup in bubble columns with non-Newtonian fluid using electrical resistance tomography and dynamic gas disengagement technique. *Chem. Eng. Sci.*, 7th International Conference on Gas-Liquid and Gas-Liquid-Solid Reactor Engineering 60, 6118–6123. <https://doi.org/10.1016/j.ces.2005.03.046>
- Fu, G., Chen, Y., Li, R., Yuan, X., Liu, C., Li, B., Wan, Y., 2017. Pathway and rate-limiting step of glyphosate degradation by *Aspergillus oryzae* A-F02. *Prep. Biochem. Biotechnol.* 47, 782–788. <https://doi.org/10.1080/10826068.2017.1342260>
- Fu, T., Ma, Y., Funfschilling, D., Li, H.Z., 2011. Bubble formation in non-Newtonian fluids in a microfluidic T-junction. *Chem. Eng. Process. Process Intensif.* 50, 438–442. <https://doi.org/10.1016/j.cep.2011.03.002>
- García-Molina, V., Kallas, J., Esplugas, S., 2007. Wet oxidation of 4-chlorophenol: Kinetic study. *Chem. Eng. J.* 126, 59–65. <https://doi.org/10.1016/j.cej.2006.05.022>
- Garcia-Ochoa, F., Gomez, E., Santos, V.E., Merchuk, J.C., 2010. Oxygen uptake rate in microbial processes: An overview. *Biochem. Eng. J.* 49, 289–307. <https://doi.org/10.1016/j.bej.2010.01.011>
- Gavrilescu, M., Demnerová, K., Aamand, J., Agathos, S.N., Fava, F.H., 2015. Emerging pollutants in the environment: present and future challenges in biomonitoring, ecological risks and bioremediation. *New Biotechnol.* 32, 147–156. <https://doi.org/10.1016/j.nbt.2014.01.001>
- Geissen, V., Mol, H., Klumpp, E., Umlauf, G., Nadal, M., van der Ploeg, M., van de Zee, S.E.A.T.M., Ritsema, C.J., 2015. Emerging pollutants in the environment: A challenge for water resource management. *Int. Soil Water Conserv. Res.* 3, 57–65. <https://doi.org/10.1016/j.iswcr.2015.03.002>
- Giesy, J.P., Dobson, S., Solomon, K.R., 2000. Ecotoxicological Risk Assessment for Roundup® Herbicide, in: Ware, G.W. (Ed.), *Reviews of Environmental Contamination and Toxicology: Continuation of Residue Reviews, Reviews of Environmental Contamination and Toxicology*. Springer New York, New York, NY, pp. 35–120. https://doi.org/10.1007/978-1-4612-1156-3_2
- Gill, J.P.K., Sethi, N., Mohan, A., 2017. Analysis of the glyphosate herbicide in water, soil and food using derivatising agents. *Environ. Chem. Lett.* 15, 85–100. <https://doi.org/10.1007/s10311-016-0585-z>
- Gillezeau, C., van Gerwen, M., Shaffer, R.M., Rana, I., Zhang, L., Sheppard, L., Taioli, E., 2019. The evidence of human exposure to glyphosate: a review. *Environ. Health* 18, 2. <https://doi.org/10.1186/s12940-018-0435-5>
- Goi, D., Di Giorgio, G., Cimarosti, I., Lesa, B., Rossi, G., Dolcetti, G., 2009. Treatment of Landfill Leachate by H₂O₂ Promoted Wet Air Oxidation: COD-AOX Reduction, Biodegradability Enhancement and Comparison with a Fenton-type Oxidation. *Chem. Biochem. Eng. Q.* 23, 343–349.
- Gomes, M.P., Le Manac’h, S.G., Maccario, S., Labrecque, M., Lucotte, M., Juneau, P., 2016. Differential effects of glyphosate and aminomethylphosphonic acid (AMPA) on photosynthesis and chlorophyll metabolism in willow plants. *Pestic. Biochem. Physiol.* 130, 65–70. <https://doi.org/10.1016/j.pestbp.2015.11.010>
- Gorges, R., Meyer, S., Kreisel, G., 2004. Photocatalysis in microreactors. *J. Photochem. Photobiol. Chem.* 167, 95–99. <https://doi.org/10.1016/j.jphotochem.2004.04.004>
- Grover, G.S., Rode, C.V., Chaudhari, R.V., 1986. Effect of temperature on flow regimes and gas hold-up in a bubble column. *Can. J. Chem. Eng.* 64, 501–504. <https://doi.org/10.1002/cjce.5450640321>
- Guilherme, S., Gaivão, I., Santos, M.A., Pacheco, M., 2010. European eel (*Anguilla anguilla*) genotoxic and pro-oxidant responses following short-term exposure to Roundup--a glyphosate-based herbicide. *Mutagenesis* 25, 523–530. <https://doi.org/10.1093/mutage/geq038>

- Hadi, F., Mousavi, A., Noghabi, K.A., Tabar, H.G., Salmanian, A.H., 2013. New bacterial strain of the genus *Ochrobactrum* with glyphosate-degrading activity. *J. Environ. Sci. Health Part B* 48, 208–213. <https://doi.org/10.1080/03601234.2013.730319>
- HALLAS, L.E., ADAMS, W.J., 1992. Glyphosate Degradation by Immobilized Bacteria: Field Studies with Industrial Wastewater Effluent. *APPL Env. MICROBIOL* 58, 5.
- Han, Z., Li, J., He, W., Li, S., Li, Z., Chu, J., Chen, Y., 2013. A microfluidic device with integrated ZnO nanowires for photodegradation studies of methylene blue under different conditions. *Microelectron. Eng.* 111, 199–203. <https://doi.org/10.1016/j.mee.2013.03.154>
- Hao, O.J., Phull, K.K., Chen, J.M., 1994. Wet oxidation of TNT red water and bacterial toxicity of treated waste. *Water Res.* 28, 283–290. [https://doi.org/10.1016/0043-1354\(94\)90265-8](https://doi.org/10.1016/0043-1354(94)90265-8)
- Hao, O.J., Phull, K.K., Davis, A.P., Chen, J.M., Maloney, S.W., 1993. Wet Air Oxidation of Trinitrotoluene Manufacturing Red Water. *Water Environ. Res.* 65, 213–220.
- Harris, M.T., Jolley, R.L., Oswald, G.E., Rose, J.C., 1983. Wet oxidation of phenol and naphthalene (as a surrogate PAH) in aqueous and sludge solution: application to coal-conversion wastewater and sludge treatment. [In autoclaves: 130 to 250/sup 0/C; 6 to 11 MPa oxygen; in water solution] (No. ORNL/TM-8576). Oak Ridge National Lab., TN (USA).
- Hashemi, S., Macchi, A., Servio, P., 2009. Gas–liquid mass transfer in a slurry bubble column operated at gas hydrate forming conditions. *Chem. Eng. Sci.* 64, 3709–3716. <https://doi.org/10.1016/j.ces.2009.05.023>
- Hecht Kristin, Bey Oliver, Etmüller Jürgen, Graefen Patrick, Friehmelt Rainer, Nilles Michael, 2015. Effect of Gas Density on Gas Holdup in Bubble Columns. *Chem. Ing. Tech.* 87, 762–772. <https://doi.org/10.1002/cite.201500010>
- Heitkamp, M.A., Adams, W.J., Hallas, L.E., 1992. Glyphosate degradation by immobilized bacteria: laboratory studies showing feasibility for glyphosate removal from waste water. *Can. J. Microbiol.* 38, 921–928. <https://doi.org/10.1139/m92-149>
- Helander, M., Saloniemi, I., Saikkonen, K., 2012. Glyphosate in northern ecosystems. *Trends Plant Sci.* 17, 569–574. <https://doi.org/10.1016/j.tplants.2012.05.008>
- Helling, R.K., Strobel, M.K., Torres, R.J., 1981. Kinetics of wet oxidation of biological sludges from coal-conversion wastewater treatment (No. ORNL/MIT-332). Oak Ridge National Lab., TN (USA); Massachusetts Inst. of Tech., Oak Ridge, TN (USA). School of Chemical Engineering Practice.
- Herath, I., Kumarathilaka, P., Al-Wabel, M.I., Abduljabbar, A., Ahmad, M., Usman, A.R.A., Vithanage, M., 2016. Mechanistic modeling of glyphosate interaction with rice husk derived engineered biochar. *Microporous Mesoporous Mater.* 225, 280–288. <https://doi.org/10.1016/j.micromeso.2016.01.017>
- Himmelblau, D.M., 1960. Solubilities of Inert Gases in Water. 0° C. to Near the Critical Point of Water. *J. Chem. Eng. Data* 5, 10–15. <https://doi.org/10.1021/je60005a003>
- Hu, S.-T., Yu, Y.-H., 1994. Preozonation of Chlorophenolic Wastewater for Subsequent Biological Treatment. *Ozone Sci. Eng.* 16, 13–28. <https://doi.org/10.1080/01919519408552377>
- Hu, X., Lei, L., Chen, G., Yue, P.L., 2001. On the degradability of printing and dyeing wastewater by wet air oxidation. *Water Res.* 35, 2078–2080. [https://doi.org/10.1016/S0043-1354\(00\)00481-4](https://doi.org/10.1016/S0043-1354(00)00481-4)
- Hu, Y.S., Zhao, Y.Q., Sorohan, B., 2011. Removal of glyphosate from aqueous environment by adsorption using water industrial residual. *Desalination* 271, 150–156. <https://doi.org/10.1016/j.desal.2010.12.014>
- Huber, D.M., Cheng, M.W., Winsor, B.A., 2005. Association of severe *Corynespora* root rot of soybean with glyphosate-killed giant ragweed. *Phytopathology* 95, S45.
- Humphries, Dave., Humphries, D., Anderson, A.-M., Byrtus, G., Council, A.R., Alberta, 2005. Glyphosate residues in Alberta's atmospheric deposition, soils and surface waters /. Alberta Environment, [Edmonton] :
- Huston, P.L., Pignatello, J.J., 1999. Degradation of selected pesticide active ingredients and commercial formulations in water by the photo-assisted Fenton reaction. *Water Res.* 33, 1238–1246. [https://doi.org/10.1016/S0043-1354\(98\)00330-3](https://doi.org/10.1016/S0043-1354(98)00330-3)
- IEH, 1995. Environmental oestrogens: consequences to human health and wildlife, UK. ed. Institute for Environemnt and Health.
- Imamura, S., 1999. Catalytic and Noncatalytic Wet Oxidation. *Ind. Eng. Chem. Res.* 38, 1743–1753. <https://doi.org/10.1021/ie9805761>
- Inga, J.R., Morsi, B.I., 1999. Effect of Operating Variables on the Gas Holdup in a Large-Scale Slurry Bubble Column Reactor Operating with an Organic Liquid Mixture. *Ind. Eng. Chem. Res.* 38, 928–937. <https://doi.org/10.1021/ie980384q>

- Jacob, G.S., 1988. Metabolism of Glyphosate in *Pseudomonas* sp. Strain LBr. *Appl. Environ. Microbiol.* 54, 2953–2958.
- Jacobson, J.L., Jacobson, S.W., 1997. Evidence for PCBs as neurodevelopmental toxicants in humans. *Neurotoxicology* 18, 415–424.
- Jayamohan, H., Smith, Y.R., Gale, B.K., Mohanty, S.K., Misra, M., 2016. Photocatalytic microfluidic reactors utilizing titania nanotubes on titanium mesh for degradation of organic and biological contaminants. *J. Environ. Chem. Eng.* 4, 657–663. <https://doi.org/10.1016/j.jece.2015.12.018>
- Jayamohan, H., Smith, Y.R., Hansen, L.C., Mohanty, S.K., Gale, B.K., Misra, M., 2015. Anodized titania nanotube array microfluidic device for photocatalytic application: Experiment and simulation. *Appl. Catal. B Environ.* 174–175, 167–175. <https://doi.org/10.1016/j.apcatb.2015.02.041>
- Jia, D.M., Li, C.H., Li, A.M., 2017. Effective removal of glyphosate from water by resin-supported double valent nano-sized hydroxyl iron oxide. *RSC Adv.* 7, 24430–24437. <https://doi.org/10.1039/C7RA03418K>
- Jin, H., Liu, D., Yang, S., He, G., Guo, Z., Tong, Z., 2004. Experimental Study of Oxygen Mass Transfer Coefficient in Bubble Column with High Temperature and High Pressure. *Chem. Eng. Technol.* 27, 1267–1272. <https://doi.org/10.1002/ceat.200402111>
- Jin, H., Yang, S., He, G., Liu, D., Tong, Z., Zhu, J., 2014. Gas–Liquid Mass Transfer Characteristics in a Gas–Liquid–Solid Bubble Column under Elevated Pressure and Temperature. *Chin. J. Chem. Eng.* 22, 955–961. <https://doi.org/10.1016/j.cjche.2014.06.019>
- Jobling, S., Reynolds, T., White, R., Parker, M.G., Sumpter, J.P., 1995. A variety of environmentally persistent chemicals, including some phthalate plasticizers, are weakly estrogenic. *Environ. Health Perspect.* 103, 582–587.
- Joglekar, H.S., Samant, S.D., Joshi, J.B., 1991. Kinetics of wet air oxidation of phenol and substituted phenols. *Water Res.* 25, 135–145. [https://doi.org/10.1016/0043-1354\(91\)90022-I](https://doi.org/10.1016/0043-1354(91)90022-I)
- Johal, G.S., Huber, D.M., 2009. Glyphosate effects on diseases of plants. *Eur. J. Agron., Glyphosate Interactions with Physiology, Nutrition, and Diseases of Plants: Threat to Agricultural Sustainability?* 31, 144–152. <https://doi.org/10.1016/j.eja.2009.04.004>
- Jones, B.M., Sakaji, R.H., Daughton, C.G., 1985. Effects of ozonation and ultraviolet irradiation on biodegradability of oil shale wastewater organic solutes. *Water Res.* 19, 1421–1428. [https://doi.org/10.1016/0043-1354\(85\)90309-4](https://doi.org/10.1016/0043-1354(85)90309-4)
- Jönsson, J., Camm, R., Hall, T., 2013. Removal and degradation of glyphosate in water treatment: a review. *J. Water Supply Res. Technol.-Aqua* 62, 395–408. <https://doi.org/10.2166/aqua.2013.080>
- Junges, C.M., Vidal, E.E., Attademo, A.M., Mariani, M.L., Cardell, L., Negro, A.C., Cassano, A., Peltzer, P.M., Lajmanovich, R.C., Zalazar, C.S., 2013. Effectiveness evaluation of glyphosate oxidation employing the H₂O₂/UVC process: Toxicity assays with *Vibrio fischeri* and *Rhinella arenarum* tadpoles. *J. Environ. Sci. Health Part B* 48, 163–170. <https://doi.org/10.1080/03601234.2013.730011>
- Kaçar, Y., Alpay, E., Ceylan, V.K., 2003. Pretreatment of Afyon alcaolide factory's wastewater by wet air oxidation (WAO). *Water Res.* 37, 1170–1176. [https://doi.org/10.1016/S0043-1354\(02\)00448-7](https://doi.org/10.1016/S0043-1354(02)00448-7)
- Kanaris, A.G., Pavlidis, T.I., Chatzidafni, A.P., Mouza, A.A., 2018. On the design of bubble columns equipped with a fine pore sparger: Effect of gas properties. *Gas* 2, 2.
- Kang, J., Zhan, W., Li, D., Wang, X., Song, J., Liu, D., 2011. Integrated catalytic wet air oxidation and biological treatment of wastewater from Vitamin B6 production. *Phys. Chem. Earth Parts ABC, Science, Technology and Policy for Water Pollution Control at the Watershed Scale: Current issues and future challenges* 36, 455–458. <https://doi.org/10.1016/j.pce.2010.03.043>
- Karahan, Ö., Olmez-Hanci, T., Arslan-Alaton, I., Orhon, D., 2010. Modelling biodegradation of nonylphenol ethoxylate in acclimated and non-acclimated microbial cultures. *Bioresour. Technol.* 101, 8058–8066. <https://doi.org/10.1016/j.biortech.2010.05.081>
- Kastánek, F., Zahradník, J., Kratochvíl, J., Cermák, J., 1993. *Chemical reactors for gas-liquid systems*. Ellis Horwood: New York.
- Kataoka, H., Ryu, S., Sakiyama, N., Makita, M., 1996. Simple and rapid determination of the herbicides glyphosate and glufosinate in river water, soil and carrot samples by gas chromatography with flame photometric detection. *J. Chromatogr. A* 726, 253–258. [https://doi.org/10.1016/0021-9673\(95\)01071-8](https://doi.org/10.1016/0021-9673(95)01071-8)
- Kawase, Y., Umeno, S., Kumagai, T., 1992. The prediction of gas hold-up in bubble column reactors: Newtonian and non-newtonian fluids. *Chem. Eng. J.* 50, 1–7. [https://doi.org/10.1016/0300-9467\(92\)80001-Q](https://doi.org/10.1016/0300-9467(92)80001-Q)

- Kazakis, N.A., Mouza, A.A., Paras, S.V., 2008. Experimental study of bubble formation at metal porous spargers: Effect of liquid properties and sparger characteristics on the initial bubble size distribution - ScienceDirect. *Chem. Eng. J.* 137, 265–281.
- Kim, K.-H., Ihm, S.-K., 2011. Heterogeneous catalytic wet air oxidation of refractory organic pollutants in industrial wastewaters: A review. *J. Hazard. Mater.* 186, 16–34. <https://doi.org/10.1016/j.jhazmat.2010.11.011>
- KIRSCHNER, E.M., 1997. BOOMER'S QUEST FOR AGELESSNESS. *Chem. Eng. News Arch.* 75, 19–25. <https://doi.org/10.1021/cen-v075n009.p019>
- Kishore, G.M., Jacob, G.S., 1987. Degradation of Glyphosate by *Pseudomonas* sp. PG2982 via a Sarcosine Intermediate. *J. Biol. Chem.* 262, 12164–12168.
- Klimek, M., Lejczak, B., Kafarski, P., Forlani, G., 2001. Metabolism of the phosphonate herbicide glyphosate by a non-nitrate-utilizing strain of *Penicillium chrysogenum*. *Pest Manag. Sci.* 57, 815–821. <https://doi.org/10.1002/ps.366>
- Kolaczowski, S.T., Beltran, F.J., McLurgh, D.B., Rivas, F.J., 1997. Wet Air Oxidation of Phenol: Factors that May Influence Global Kinetics. *Process Saf. Environ. Prot.* 75, 257–265. <https://doi.org/10.1205/095758297529138>
- Kolaczowski, S.T., Plucinski, P., Beltran, F.J., Rivas, F.J., McLurgh, D.B., 1999. Wet air oxidation: a review of process technologies and aspects in reactor design. *Chem. Eng. J.* 73, 143–160. [https://doi.org/10.1016/S1385-8947\(99\)00022-4](https://doi.org/10.1016/S1385-8947(99)00022-4)
- Kotsou, M., Kyriacou, A., Lasaridi, K., Pilidis, G., 2004. Integrated aerobic biological treatment and chemical oxidation with Fenton's reagent for the processing of green table olive wastewater. *Process Biochem.* 39, 1653–1660. [https://doi.org/10.1016/S0032-9592\(03\)00308-X](https://doi.org/10.1016/S0032-9592(03)00308-X)
- Krishnan, A.V., Stathis, P., Permuth, S.F., Tokes, L., Feldman, D., 1993. Bisphenol-A: an estrogenic substance is released from polycarbonate flasks during autoclaving. *Endocrinology* 132, 2279–2286. <https://doi.org/10.1210/endo.132.6.8504731>
- Kryuchkova, Y.V., Burygin, G.L., Gogoleva, N.E., Gogolev, Y.V., Chernyshova, M.P., Makarov, O.E., Fedorov, E.E., Turkovskaya, O.V., 2014. Isolation and characterization of a glyphosate-degrading rhizosphere strain, *Enterobacter cloacae* K7. *Microbiol. Res.* 169, 99–105. <https://doi.org/10.1016/j.micres.2013.03.002>
- Krzyśko-Lupicka, T., Strof, W., Kubś, K., Skorupa, M., Wieczorek, P., Lejczak, B., Kafarski, P., 1997. The ability of soil-borne fungi to degrade organophosphonate carbon-to-phosphorus bonds. *Appl. Microbiol. Biotechnol.* 48, 549–552. <https://doi.org/10.1007/s002530051095>
- Kukurina, O., Elemesova, Z., Syskina, A., 2014. Mineralization of Organophosphorous Pesticides by Electro-generated Oxidants. *Procedia Chem.*, XV International Scientific Conference “Chemistry and Chemical Engineering in XXI century” dedicated to Professor L.P. Kulyov 10, 209–216. <https://doi.org/10.1016/j.proche.2014.10.036>
- Kumar, S., Munshi, P., Khanna, A., 2012. High Pressure Experiments and Simulations in Cocurrent Bubble Columns. *Procedia Eng.*, CHISA 2012 42, 842–853. <https://doi.org/10.1016/j.proeng.2012.07.477>
- Kwiatkowska, M., Huras, B., Bukowska, B., 2014. The effect of metabolites and impurities of glyphosate on human erythrocytes (in vitro). *Pestic. Biochem. Physiol.* 109, 34–43. <https://doi.org/10.1016/j.pestbp.2014.01.003>
- Kwiatkowska, M., Reszka, E., Woźniak, K., Jabłońska, E., Michałowicz, J., Bukowska, B., 2017. DNA damage and methylation induced by glyphosate in human peripheral blood mononuclear cells (in vitro study). *Food Chem. Toxicol. Int. J. Publ. Br. Ind. Biol. Res. Assoc.* 105, 93–98. <https://doi.org/10.1016/j.fct.2017.03.051>
- Lafi, W.K., Al-Qodah, Z., 2006. Combined advanced oxidation and biological treatment processes for the removal of pesticides from aqueous solutions. *J. Hazard. Mater.* 137, 489–497. <https://doi.org/10.1016/j.jhazmat.2006.02.027>
- Lafi, W.K., Shannak, B., Al-Shannag, M., Al-Anber, Z., Al-Hasan, M., 2009. Treatment of olive mill wastewater by combined advanced oxidation and biodegradation. *Sep. Purif. Technol.* 70, 141–146. <https://doi.org/10.1016/j.seppur.2009.09.008>
- Laitinen, P., Rämö, S., Siimes, K., 2007. Glyphosate translocation from plants to soil – does this constitute a significant proportion of residues in soil? *Plant Soil* 300, 51–60. <https://doi.org/10.1007/s11104-007-9387-1>
- Lan, H., He, W., Wang, A., Liu, R., Liu, H., Qu, J., Huang, C.P., 2016. An activated carbon fiber cathode for the degradation of glyphosate in aqueous solutions by the Electro-Fenton mode: Optimal operational

- conditions and the deposition of iron on cathode on electrode reusability. *Water Res.* 105, 575–582. <https://doi.org/10.1016/j.watres.2016.09.036>
- Lan, H., Jiao, Z., Zhao, X., He, W., Wang, A., Liu, H., Liu, R., Qu, J., 2013. Removal of glyphosate from water by electrochemically assisted MnO₂ oxidation process. *Sep. Purif. Technol.* 117, 30–34. <https://doi.org/10.1016/j.seppur.2013.04.012>
- Lapworth, D.J., Baran, N., Stuart, M.E., Ward, R.S., 2012. Emerging organic contaminants in groundwater: A review of sources, fate and occurrence. *Environ. Pollut.* 163, 287–303. <https://doi.org/10.1016/j.envpol.2011.12.034>
- Lapworth, D.J., Gooddy, D.C., 2006. Source and persistence of pesticides in a semi-confined chalk aquifer of southeast England. *Environ. Pollut.* 144, 1031–1044. <https://doi.org/10.1016/j.envpol.2005.12.055>
- Lau, R., Peng, W., Velazquez-Vargas, L.G., Yang, G.Q., Fan, L.-S., 2004. Gas–Liquid Mass Transfer in High-Pressure Bubble Columns. *Ind. Eng. Chem. Res.* 43, 1302–1311. <https://doi.org/10.1021/ie030416w>
- Lee, C.-Y., Chang, C.-L., Wang, Y.-N., Fu, L.-M., 2011. Microfluidic Mixing: A Review. *Int. J. Mol. Sci.* 12, 3263–3287. <https://doi.org/10.3390/ijms12053263>
- Lee, K.S., Metcalf, W.W., Wanner, B.L., 1992. Evidence for two phosphonate degradative pathways in *Enterobacter aerogenes*. *J. Bacteriol.* 174, 2501–2510. <https://doi.org/10.1128/jb.174.8.2501-2510.1992>
- Lee, S.H., Carberry, J.B., 1992. Biodegradation of PCP Enhanced by Chemical Oxidation Pretreatment. *Water Environ. Res.* 64, 682–690.
- Lefèvre, S., Boutin, O., Ferrasse, J.-H., Malleret, L., Faucherand, R., Viand, A., 2011a. Thermodynamic and kinetic study of phenol degradation by a non-catalytic wet air oxidation process. *Chemosphere* 84, 1208–1215. <https://doi.org/10.1016/j.chemosphere.2011.05.049>
- Lefèvre, S., Ferrasse, J.-H., Boutin, O., Sergent, M., Faucherand, R., Viand, A., 2011b. Process optimisation using the combination of simulation and experimental design approach: Application to wet air oxidation. *Chem. Eng. Res. Des.* 89, 1045–1055. <https://doi.org/10.1016/j.cherd.2010.12.009>
- Lefevre, S., Ferrasse, J.-H., Faucherand, R., Viand, A., Boutin, O., 2012. Energetic optimization of wet air oxidation process using experimental design coupled with process simulation. *Energy*, 23rd International Conference on Efficiency, Cost, Optimization, Simulation and Environmental Impact of Energy Systems, ECOS 2010 41, 175–183. <https://doi.org/10.1016/j.energy.2011.09.043>
- Lehr, F., Millies, M., Mewes, D., 2002. Bubble-Size distributions and flow fields in bubble columns. *AIChE J.* 48, 2426–2443.
- Lei, L., Dai, Q., Zhou, M., Zhang, X., 2007. Decolorization of cationic red X-GRL by wet air oxidation: Performance optimization and degradation mechanism. *Chemosphere* 68, 1135–1142. <https://doi.org/10.1016/j.chemosphere.2007.01.075>
- Lei, L., Hu, X., Chen, G., Porter, J.F., Yue, P.L., 2000. Wet Air Oxidation of Desizing Wastewater from the Textile Industry. *Ind. Eng. Chem. Res.* 39, 2896–2901. <https://doi.org/10.1021/ie990607s>
- Lei, L., Wang, N., Zhang, X.M., Tai, Q., Tsai, D.P., Chan, H.L.W., 2010. Optofluidic planar reactors for photocatalytic water treatment using solar energy. *Biomicrofluidics* 4, 043004. <https://doi.org/10.1063/1.3491471>
- Lei, M., Zhang, L., Lei, J., Zong, L., Li, J., Wu, Z., Wang, Z., 2015. Overview of Emerging Contaminants and Associated Human Health Effects [WWW Document]. *BioMed Res. Int.* <https://doi.org/10.1155/2015/404796>
- Leonard, C., Ferrasse, J.-H., Boutin, O., Lefevre, S., Viand, A., 2015. Bubble column reactors for high pressures and high temperatures operation. *Chem. Eng. Res. Des.* 100, 391–421. <https://doi.org/10.1016/j.cherd.2015.05.013>
- Leonard, C., Ferrasse, J.-H., Lefevre, S., Viand, A., Boutin, O., 2019. Gas hold up in bubble column at high pressure and high temperature. *Chem. Eng. Sci.* 200, 186–202. <https://doi.org/10.1016/j.ces.2019.01.055>
- Lerbs, W., Stock, M., Parthier, B., 1990. Physiological aspects of glyphosate degradation in *Alcaligenes spec.* strain GL. *Arch. Microbiol.* 153, 146–150. <https://doi.org/10.1007/BF00247812>
- Levec, J., Pintar, A., 2007. Catalytic wet-air oxidation processes: A review. *Catal. Today, Advanced Catalytic Oxidation Processes* 124, 172–184. <https://doi.org/10.1016/j.cattod.2007.03.035>
- Li, F., Wang, Y., Yang, Q., Evans, D.G., Forano, C., Duan, X., 2005. Study on adsorption of glyphosate (N-phosphonomethyl glycine) pesticide on MgAl-layered double hydroxides in aqueous solution. *J. Hazard. Mater.* 125, 89–95. <https://doi.org/10.1016/j.jhazmat.2005.04.037>
- Li, L., Chen, P., Gloyna, E.F., 1991. Generalized kinetic model for wet oxidation of organic compounds. *AIChE J.* 37, 1687–1697. <https://doi.org/10.1002/aic.690371112>

- Li, R., Yang, C., 2008. Progress of Treatment Technologies for Organic Phosphorous Pesticide Wastewater. *Environ. Sci. Manag.* 33, 84–87.
- Li, X., Jaworski, A.J., Mao, X., 2018. Bubble size and bubble rise velocity estimation by means of electrical capacitance tomography within gas-solids fluidized beds. *Measurement* 117, 226–240. <https://doi.org/10.1016/j.measurement.2017.12.017>
- Liao, H., Tan, B., Ke, M., Li, Z., Lu, J., 2009. Pretreatment of GLyphosate Wastewater with Fenton Reagent. *Technol. Dev. Chem. Ind.* 38.
- Licklider, Larry., Kuhr, W.G., 1994. Optimization of Online Peptide Mapping by Capillary Zone Electrophoresis. *Anal. Chem.* 66, 4400–4407. <https://doi.org/10.1021/ac00096a003>
- Lin, L., Zhang, X.J., Xiao, G.Q., Xiong, X., 2012. Photocatalytic Degradation Glyphosate with Cerium and Nitrogen Co-Doped TiO₂ under Visible Irradiation. *Adv. Mater. Res.* 430–432, 1048–1051. <https://doi.org/10.4028/www.scientific.net/AMR.430-432.1048>
- Lin, S.H., Chuang, T.S., 1994a. Combined treatment of phenolic wastewater by wet air oxidation and activated sludge. *Toxicol. Environ. Chem.* 44, 243–258. <https://doi.org/10.1080/02772249409358063>
- Lin, S.H., Chuang, T.S., 1994b. Wet air oxidation and activated sludge treatment of phenolic wastewater. *J. Environ. Sci. Health Part Environ. Sci. Eng. Toxicol.* 29, 547–564. <https://doi.org/10.1080/10934529409376054>
- Lin, S.H., Ho, S.J., 1997. Treatment of high-strength industrial wastewater by wet air oxidation—A case study. *Waste Manag.* 17, 71–78. [https://doi.org/10.1016/S0956-053X\(97\)00039-1](https://doi.org/10.1016/S0956-053X(97)00039-1)
- Lin, S.H., Ho, S.J., Wu, C.L., 1996. Kinetic and Performance Characteristics of Wet Air Oxidation of High-Concentration Wastewater. *Ind. Eng. Chem. Res.* 35, 307–314. <https://doi.org/10.1021/ie950251u>
- Lin, T.-J., Tsuchiya, K., Fan, L.-S., 1998. Bubble flow characteristics in bubble columns at elevated pressure and temperature. *AIChE J.* 44, 545–560.
- Liu, C.M., McLean, P.A., Sookdeo, C.C., Cannon, F.C., 1991. Degradation of the Herbicide Glyphosate by Members of the Family Rhizobiaceae. *APPL Env. MICROBIOL* 57, 1799–1804.
- Liu, Z., Zhu, M., Yu, P., Xu, Y., Zhao, X., 2013. Pretreatment of membrane separation of glyphosate mother liquor using a precipitation method. *Desalination* 313, 140–144. <https://doi.org/10.1016/j.desal.2012.12.011>
- Liu, Z.Y., Xie, M., Ni, F., Xu, Y.H., 2012. Nanofiltration process of glyphosate simulated wastewater. *Water Sci. Technol.* 65, 816–822. <https://doi.org/10.2166/wst.2012.808>
- López, A., Coll, A., Lescano, M., Zalazar, C., 2018. Advanced oxidation of commercial herbicides mixture: experimental design and phytotoxicity evaluation. *Environ. Sci. Pollut. Res.* 25, 21393–21402. <https://doi.org/10.1007/s11356-017-9041-2>
- López, J.B., Portela, J.M., Nebot, E.S., Martínez, E. de la O., 1999. Wet air oxidation of oily wastes generated aboard ships: kinetic modeling. *J. Hazard. Mater.* 67, 61–73. [https://doi.org/10.1016/S0304-3894\(99\)00013-8](https://doi.org/10.1016/S0304-3894(99)00013-8)
- Lu, Z.Y., Li, Y.P., Mu, J.H., JIAO, H.C., Cui, H.H., Lu, H.W., Shen, Z., 2007. Treatment of TNT Red Water by Wet Oxidation. *Chin. J. Explos. Propellants* 30, 48–51.
- Luan, M., Jing, G., Piao, Y., Liu, D., Jin, L., 2017. Treatment of refractory organic pollutants in industrial wastewater by wet air oxidation. *Arab. J. Chem.* 10, S769–S776. <https://doi.org/10.1016/j.arabjc.2012.12.003>
- Luck, F., 1999. Wet air oxidation: past, present and future. *Catal. Today* 53, 81–91. [https://doi.org/10.1016/S0920-5861\(99\)00112-1](https://doi.org/10.1016/S0920-5861(99)00112-1)
- Luo, X., Lee, D.J., Lau, R., Yang, G., Fan, L.-S., 1999. Maximum stable bubble size and gas holdup in high-pressure slurry bubble columns. *AIChE J.* 45, 665–680.
- Maalej, S., Benadda, B., Otterbein, M., 2003. Interfacial area and volumetric mass transfer coefficient in a bubble reactor at elevated pressures. *Chem. Eng. Sci.* 58, 2365–2376. [https://doi.org/10.1016/S0009-2509\(03\)00085-X](https://doi.org/10.1016/S0009-2509(03)00085-X)
- Maceiras, R., Álvarez, E., Cancela, M.A., 2010. Experimental interfacial area measurements in a bubble column. *Chem. Eng. J.* 163, 331–336. <https://doi.org/10.1016/j.cej.2010.08.011>
- Mahler, B.J., Van Metre, P.C., Burley, T.E., Loftin, K.A., Meyer, M.T., Nowell, L.H., 2017. Similarities and differences in occurrence and temporal fluctuations in glyphosate and atrazine in small Midwestern streams (USA) during the 2013 growing season. *Sci. Total Environ.* 579, 149–158. <https://doi.org/10.1016/j.scitotenv.2016.10.236>
- Majumder, S.K., Kundu, G., Mukherjee, D., 2006. Bubble size distribution and gas–liquid interfacial area in a modified downflow bubble column. *Chem. Eng. J.* 122, 1–10. <https://doi.org/10.1016/j.cej.2006.04.007>

- Malato, S., Blanco, J., Cáceres, J., Fernández-Alba, A.R., Agüera, A., Rodríguez, A., 2002. Photocatalytic treatment of water-soluble pesticides by photo-Fenton and TiO₂ using solar energy. *Catal. Today* 76, 209–220. [https://doi.org/10.1016/S0920-5861\(02\)00220-1](https://doi.org/10.1016/S0920-5861(02)00220-1)
- Manassero, A., Passalia, C., Negro, A.C., Cassano, A.E., Zalazar, C.S., 2010. Glyphosate degradation in water employing the H₂O₂/UVC process. *Water Res.* 44, 3875–3882. <https://doi.org/10.1016/j.watres.2010.05.004>
- Manogaran, M., Shukor, M.Y., Yasid, N.A., Johari, W.L.W., Ahmad, S.A., 2017. Isolation and characterisation of glyphosate-degrading bacteria isolated from local soils in Malaysia. *Rendiconti Lincei* 28, 471–479. <https://doi.org/10.1007/s12210-017-0620-4>
- Mantzavinos, D., Kalogerakis, N., 2005. Treatment of olive mill effluents. *Environ. Int.* 31, 289–295. <https://doi.org/10.1016/j.envint.2004.10.005>
- Mantzavinos, D., Lauer, E., Hellenbrand, R., Livingston, A.G., Metcalfe, I.S., 1997. Wet oxidation as a pretreatment method for wastewaters contaminated by bioresistant organics. *Water Sci. Technol., Pretreatment of Industrial Wastewaters II* 36, 109–116. [https://doi.org/10.1016/S0273-1223\(97\)00376-4](https://doi.org/10.1016/S0273-1223(97)00376-4)
- Mantzavinos, D., Livingston, A.G., Hellenbrand, R., Metcalfe, I.S., 1996. Wet air oxidation of polyethylene glycols; mechanisms, intermediates and implications for integrated chemical-biological wastewater treatment. *Chem. Eng. Sci.* 51, 4219–4235. [https://doi.org/10.1016/0009-2509\(96\)00272-2](https://doi.org/10.1016/0009-2509(96)00272-2)
- Mantzavinos, D., Sahibzada, M., Livingston, A.G., Metcalfe, I.S., Hellgardt, K., 1999. Wastewater treatment: wet air oxidation as a precursor to biological treatment. *Catal. Today* 53, 93–106. [https://doi.org/10.1016/S0920-5861\(99\)00105-4](https://doi.org/10.1016/S0920-5861(99)00105-4)
- Maqueda, C., Undabeytia, T., Villaverde, J., Morillo, E., 2017. Behaviour of glyphosate in a reservoir and the surrounding agricultural soils. *Sci. Total Environ.* 593–594, 787–795. <https://doi.org/10.1016/j.scitotenv.2017.03.202>
- Marco, A., Esplugas, S., Saum, G., 1997. How and why combine chemical and biological processes for wastewater treatment. *Water Sci. Technol., Oxidation Technologies for Water and Wastewater Treatment* 35, 321–327. [https://doi.org/10.1016/S0273-1223\(97\)00041-3](https://doi.org/10.1016/S0273-1223(97)00041-3)
- Mayakaduwa, S.S., Kumarathilaka, P., Herath, I., Ahmad, M., Al-Wabel, M., Ok, Y.S., Usman, A., Abduljabbar, A., Vithanage, M., 2016. Equilibrium and kinetic mechanisms of woody biochar on aqueous glyphosate removal. *Chemosphere* 144, 2516–2521. <https://doi.org/10.1016/j.chemosphere.2015.07.080>
- Mayo, A.W., Noike, T., 1996. Effects of temperature and pH on the growth of heterotrophic bacteria in waste stabilization ponds. *Water Res.* 30, 447–455. [https://doi.org/10.1016/0043-1354\(95\)00150-6](https://doi.org/10.1016/0043-1354(95)00150-6)
- McAuliffe, K.S., Hallas, L.E., Kulpa, C.F., 1990. Glyphosate degradation by *Agrobacterium radiobacter* isolated from activated sludge. *J. Ind. Microbiol.* 6, 219–221. <https://doi.org/10.1007/BF01577700>
- McKinney, J.D., Waller, C.L., 1994. Polychlorinated biphenyls as hormonally active structural analogues. *Environ. Health Perspect.* 102, 290–297.
- McMurry, L.M., Oethinger, M., Levy, S.B., 1998. Triclosan targets lipid synthesis. *Nature* 394, 531–532.
- McQueen, H., Callan, A.C., Hinwood, A.L., 2012. Estimating maternal and prenatal exposure to glyphosate in the community setting. *Int. J. Hyg. Environ. Health* 215, 570–576. <https://doi.org/10.1016/j.ijheh.2011.12.002>
- Menéndez-Helman, R.J., Ferreyroa, G.V., dos Santos Afonso, M., Salibián, A., 2012. Glyphosate as an acetylcholinesterase inhibitor in *Cnesterodon decemmaculatus*. *Bull. Environ. Contam. Toxicol.* 88, 6–9. <https://doi.org/10.1007/s00128-011-0423-8>
- Meng, Z., Zhang, X., Qin, J., 2013. A high efficiency microfluidic-based photocatalytic microreactor using electrospun nanofibrous TiO₂ as a photocatalyst. *Nanoscale* 5, 4687–4690. <https://doi.org/10.1039/C3NR00775H>
- Merchant, K.P., 1992. *Studies in Heterogeneous Reactions* (PhD thesis). Department of Chemical Technology, University of Bombay, India.
- Mercurio, P., Flores, F., Mueller, J.F., Carter, S., Negri, A.P., 2014. Glyphosate persistence in seawater. *Mar. Pollut. Bull.* 85, 385–390. <https://doi.org/10.1016/j.marpolbul.2014.01.021>
- Mesnager, R., Defarge, N., Spiroux de Vendômois, J., Séralini, G.E., 2015. Potential toxic effects of glyphosate and its commercial formulations below regulatory limits. *Food Chem. Toxicol.* 84, 133–153. <https://doi.org/10.1016/j.fct.2015.08.012>
- Mineta, R., Salehi, Z., Yoshikawa, H., Kawase, Y., 2011. Oxygen transfer during aerobic biodegradation of pollutants in a dense activated sludge slurry bubble column: Actual volumetric oxygen transfer

- coefficient and oxygen uptake rate in p-nitrophenol degradation by acclimated waste activated sludge. *Biochem. Eng. J.* 53, 266–274. <https://doi.org/10.1016/j.bej.2010.11.006>
- Minière, M., Boutin, O., Soric, A., 2018. Evaluation of degradation and kinetics parameters of acid orange 7 through wet air oxidation process. *Can. J. Chem. Eng.* 96, 2450–2454.
- Minière, M., Boutin, O., Soric, A., 2017. Experimental coupling and modelling of wet air oxidation and packed-bed biofilm reactor as an enhanced phenol removal technology. *Environ. Sci. Pollut. Res. Int.* 24, 7693–7704. <https://doi.org/10.1007/s11356-017-8435-5>
- Mishra, V.S., Mahajani, V.V., Joshi, J.B., 1995. Wet Air Oxidation. *Ind. Eng. Chem. Res.* 34, 2–48. <https://doi.org/10.1021/ie00040a001>
- Misra, V.S., Joshi, J.B., Mahajani, V.V., 1993. Kinetics of p-Cresol Destruction Via Wet Air Oxidation. *INDIAN Chem. Eng.* 35, 211.
- Mohagheghian, S., Elbing, B.R., 2018. Characterization of Bubble Size Distributions within a Bubble Column. *Fluids* 3, 13. <https://doi.org/10.3390/fluids3010013>
- Moneke, A.N., Okpala, G.N., Anyanwu, C.U., 2010. Biodegradation of glyphosate herbicide in vitro using bacterial isolates from four rice fields. *Afr. J. Biotechnol.* 9, 4067–4074.
- Monod, J., 1949. The growth of bacterial cultures. *Annu. Rev. Microbiol.* 3, 371–394. <https://doi.org/10.1146/annurev.mi.03.100149.002103>
- Moreira, F.C., Boaventura, R.A.R., Brillas, E., Vilar, V.J.P., 2017. Electrochemical advanced oxidation processes: A review on their application to synthetic and real wastewaters. *Appl. Catal. B Environ.* 202, 217–261. <https://doi.org/10.1016/j.apcatb.2016.08.037>
- Mörtl, M., Németh, G., Juracsek, J., Darvas, B., Kamp, L., Rubio, F., Székács, A., 2013. Determination of glyphosate residues in Hungarian water samples by immunoassay. *Microchem. J.*, XIV Hungarian - Italian Symposium on Spectrochemistry: Analytical Techniques and Preservation of Natural Resources, Sumeg (Hungary), October 5-7, 2011 107, 143–151. <https://doi.org/10.1016/j.microc.2012.05.021>
- Mota, A.L.N., Albuquerque, L.F., Beltrame, L.T.C., Chiavone-Filho, O., Jr, A.M., Nascimento, C.A.O., 2008. ADVANCED OXIDATION PROCESSES AND THEIR APPLICATION IN THE PETROLEUM INDUSTRY: A REVIEW. *Braz. J. Pet. GAS* 2, 21.
- Mouza, A.A., Dalakoglou, G.K., Paras, S.V., 2005. Effect of liquid properties on the performance of bubble column reactors with fine pore spargers. *Chem. Eng. Sci.* 60, 1465–1475. <https://doi.org/10.1016/j.ces.2004.10.013>
- Muneer, M., Boxall, C., 2008. Photocatalyzed Degradation of a Pesticide Derivative Glyphosate in Aqueous Suspensions of Titanium Dioxide. *Int. J. Photoenergy.* <https://doi.org/10.1155/2008/197346>
- Nadarajah, N., Van Hamme, J., Pannu, J., Singh, A., Ward, O., 2002. Enhanced transformation of polycyclic aromatic hydrocarbons using a combined Fenton's reagent, microbial treatment and surfactants. *Appl. Microbiol. Biotechnol.* 59, 540–544. <https://doi.org/10.1007/s00253-002-1073-x>
- Ndjeri, M., Pensel, A., Peulon, S., Haldys, V., Desmazières, B., Chaussé, A., 2013. Degradation of glyphosate and AMPA (amino methylphosphonic acid) solutions by thin films of birnessite electrodeposited: A new design of material for remediation processes? *Colloids Surf. Physicochem. Eng. Asp.* 435, 154–169. <https://doi.org/10.1016/j.colsurfa.2013.01.022>
- NEMI Method Summary - 2540 D [WWW Document], n.d. URL https://www.nemi.gov/methods/method_summary/9819/ (accessed 6.6.19).
- Nourouzi, M.M., Chuah, T.G., Choong, T.S.Y., 2010. Adsorption of glyphosate onto activated carbon derived from waste newspaper. *Desalination Water Treat.* 24, 321–326. <https://doi.org/10.5004/dwt.2010.1461>
- Nourouzi, M.M., Chuah, G.T., Choong, T.S.Y., Rabier, F., 2012. Modeling biodegradation and kinetics of glyphosate by artificial neural network. *J. Environ. Sci. Health Part B* 47, 455–465.
- Obojska, A., Lejczak, B., Kubrak, M., 1999. Degradation of phosphonates by streptomycete isolates. *Appl. Microbiol. Biotechnol.* 51, 872–876. <https://doi.org/10.1007/s002530051476>
- Obojska, A., Ternan, N.G., Lejczak, B., Kafarski, P., McMullan, G., 2002. Organophosphonate Utilization by the Thermophile *Geobacillus caldxylosilyticus* T20. *Appl. Environ. Microbiol.* 68, 2081–2084. <https://doi.org/10.1128/AEM.68.4.2081-2084.2002>
- Ojha, A., Al-Dahhan, M., 2018. Local gas holdup and bubble dynamics investigation during microalgae culturing in a split airlift photobioreactor. *Chem. Eng. Sci.* 175, 185–198. <https://doi.org/10.1016/j.ces.2017.08.026>
- Okada, E., Costa, J.L., Bedmar, F., 2016. Adsorption and mobility of glyphosate in different soils under no-till and conventional tillage. *Geoderma* 263, 78–85. <https://doi.org/10.1016/j.geoderma.2015.09.009>

- Okumura, T., Nishikawa, Y., 1996. Gas chromatography—mass spectrometry determination of triclosans in water, sediment and fish samples via methylation with diazomethane - ScienceDirect. *Anal. Chim. Acta* 325, 175–184. [https://doi.org/10.1016/0003-2670\(96\)00027-X](https://doi.org/10.1016/0003-2670(96)00027-X)
- Oliveira, G.C., Mocellini, S.K., Castilho, M., Terezo, A.J., Possavatz, J., Magalhães, M.R.L., Dores, E.F.G.C., 2012. Biosensor based on atemoya peroxidase immobilised on modified nanoclay for glyphosate biomonitoring. *Talanta* 98, 130–136. <https://doi.org/10.1016/j.talanta.2012.06.059>
- Oller, I., Malato, S., Sánchez-Pérez, J.A., 2011. Combination of Advanced Oxidation Processes and biological treatments for wastewater decontamination—A review. *Sci. Total Environ.* 409, 4141–4166. <https://doi.org/10.1016/j.scitotenv.2010.08.061>
- Otal, E., Mantzavinos, D., Delgado, M.V., Hellenbrand, R., Lebrato, J., Metcalfe, I.S., Livingston, A.G., 1997. Integrated Wet Air Oxidation and Biological Treatment of Polyethylene Glycol-Containing Wastewaters. *J. Chem. Technol. Biotechnol.* 70, 147–156. [https://doi.org/10.1002/\(SICI\)1097-4660\(199710\)70:2<147::AID-JCTB747>3.0.CO;2-3](https://doi.org/10.1002/(SICI)1097-4660(199710)70:2<147::AID-JCTB747>3.0.CO;2-3)
- Oyevaar, M.H., Bos, R., Westerterp, K.R., 1991. Interfacial areas and gas hold-ups in gas—liquid contactors at elevated pressures from 0.1 to 8.0 MPa. *Chem. Eng. Sci.* 46, 1217–1231. [https://doi.org/10.1016/0009-2509\(91\)85050-8](https://doi.org/10.1016/0009-2509(91)85050-8)
- Paddon, C.A., Atobe, M., Fuchigami, T., He, P., Watts, P., Haswell, S.J., Pritchard, G.J., Bull, S.D., Marken, F., 2006. Towards paired and coupled electrode reactions for clean organic microreactor electrosyntheses. *J. Appl. Electrochem.* 36, 617–634. <https://doi.org/10.1007/s10800-006-9122-2>
- Pariante, M.I., Martínez, F., Melero, J.A., Botas, J.Á., Velegraki, T., Xekoukoulotakis, N.P., Mantzavinos, D., 2008. Heterogeneous photo-Fenton oxidation of benzoic acid in water: Effect of operating conditions, reaction by-products and coupling with biological treatment. *Appl. Catal. B Environ.* 85, 24–32. <https://doi.org/10.1016/j.apcatb.2008.06.019>
- Park, S.-J., Yoon, T.-I., Bae, J.-H., Seo, H.-J., Park, H.-J., 2001. Biological treatment of wastewater containing dimethyl sulphoxide from the semi-conductor industry. *Process Biochem.* 36, 579–589. [https://doi.org/10.1016/S0032-9592\(00\)00252-1](https://doi.org/10.1016/S0032-9592(00)00252-1)
- Patterson, D.A., Metcalfe, I.S., Xiong, F., Livingston, A.G., 2002. Biodegradability of linear alkylbenzene sulfonates subjected to wet air oxidation. *J. Chem. Technol. Biotechnol.* 77, 1039–1049. <https://doi.org/10.1002/jctb.676>
- Paudel, P., Negusse, A., Jaisi, D.P., 2015. Birnessite-Catalyzed Degradation of Glyphosate: A Mechanistic Study Aided by Kinetics Batch Studies and NMR Spectroscopy. *Soil Sci. Soc. Am. J.* 79, 815–825. <https://doi.org/10.2136/sssaj2014.10.0394>
- Paz-y-Miño, C., Sánchez, M.E., Arévalo, M., Muñoz, M.J., Witte, T., De-la-Carrera, G.O., Leone, P.E., 2007. Evaluation of DNA damage in an Ecuadorian population exposed to glyphosate. *Genet. Mol. Biol.* 30, 456–460. <https://doi.org/10.1590/S1415-47572007000300026>
- Peñalosa-Vazquez, A., Mena, G.L., Herrera-Estrella, L., Bailey, A.M., 1995. Cloning and Sequencing of the Genes Involved in Glyphosate Utilization by *Pseudomonas pseudomallei*. *APPL Env. MICROBIOL* 61, 6.
- Pérez, J.F., Llanos, J., Sáez, C., López, C., Cañizares, P., Rodrigo, M.A., 2017. A microfluidic flow-through electrochemical reactor for wastewater treatment: A proof-of-concept. *Electrochem. Commun.* 82, 85–88. <https://doi.org/10.1016/j.elecom.2017.07.026>
- Pipke, R., Amrhein, N., 1988. Degradation of the Phosphonate Herbicide Glyphosate by *Arthrobacter atrocyaneus* ATCC 13752. *APPL Env. MICROBIOL* 54, 1293–1296.
- Pipke, R., Amrhein, N., Jacob, G.S., Schaefer, J., Kishore, G.M., 1987. Metabolism of glyphosate in an *Arthrobacter* sp. GLP-1. *Eur. J. Biochem.* 165, 267–273. <https://doi.org/10.1111/j.1432-1033.1987.tb11437.x>
- Pjontek, D., Parisien, V., Macchi, A., 2014. Bubble characteristics measured using a monofibre optical probe in a bubble column and freeboard region under high gas holdup conditions. *Chem. Eng. Sci.* 111, 153–169. <https://doi.org/10.1016/j.ces.2014.02.024>
- Pohorecki, R., Moniuk, W., Zdrójkowski, A., 1999. Hydrodynamics of a bubble column under elevated pressure. *Chem. Eng. Sci.* 54, 5187–5193.
- Pohorecki, R., Moniuk, W., Zdrójkowski, A., Bielski, P., 2001. Hydrodynamics of a pilot plant bubble column under elevated temperature and pressure. *Chem. Eng. Sci.*, 16th International Conference on Chemical Reactor Engineering 56, 1167–1174. [https://doi.org/10.1016/S0009-2509\(00\)00336-5](https://doi.org/10.1016/S0009-2509(00)00336-5)
- Poiger, T., Buerge, I.J., Bächli, A., Müller, M.D., Balmer, M.E., 2017. Occurrence of the herbicide glyphosate and its metabolite AMPA in surface waters in Switzerland determined with on-line solid phase

- extraction LC-MS/MS. *Environ. Sci. Pollut. Res. Int.* 24, 1588–1596. <https://doi.org/10.1007/s11356-016-7835-2>
- Postle, J.K., Rheineck, B.D., Allen, P.E., Baldock, J.O., Cook, C.J., Zogbaum, R., Vandenberg, J.P., 2004. Chloroacetanilide Herbicide Metabolites in Wisconsin Groundwater: 2001 Survey Results. *Environ. Sci. Technol.* 38, 5339–5343. <https://doi.org/10.1021/es040399h>
- Poynton, H.C., Vulpe, C.D., 2009. Ecotoxicogenomics: Emerging Technologies for Emerging Contaminants I. *JAWRA J. Am. Water Resour. Assoc.* 45, 83–96. <https://doi.org/10.1111/j.1752-1688.2008.00291.x>
- Pruden, B.B., Le, H., 1976. Wet air oxidation of soluble components in waste water. *Can. J. Chem. Eng.* 54, 319–325. <https://doi.org/10.1002/cjce.5450540413>
- Raffainer, I.I., Rudolf von Rohr, P., 2001. Promoted Wet Oxidation of the Azo Dye Orange II under Mild Conditions. *Ind. Eng. Chem. Res.* 40, 1083–1089. <https://doi.org/10.1021/ie000629a>
- Rafin, C., Veignie, E., Fayeulle, A., Surpateanu, G., 2009. Benzo[a]pyrene degradation using simultaneously combined chemical oxidation, biotreatment with *Fusarium solani* and cyclodextrins. *Bioresour. Technol.* 100, 3157–3160. <https://doi.org/10.1016/j.biortech.2009.01.012>
- Ramezani, M., Mostoufi, N., Mehrnia, M.R., 2012. Improved Modeling of Bubble Column Reactors by Considering the Bubble Size Distribution. *Ind. Eng. Chem. Res.* 51, 5705–5714. <https://doi.org/10.1021/ie202914s>
- Ramos, B., Ookawara, S., Matsushita, Y., Yoshikawa, S., 2014. Photocatalytic Decolorization of Methylene Blue in a Glass Channel Microreactor. *J. Chem. Eng. Jpn.* 47, 788–791. <https://doi.org/10.1252/jcej.14we040>
- Rendon-von Osten, J., Dzul-Caamal, R., 2017. Glyphosate Residues in Groundwater, Drinking Water and Urine of Subsistence Farmers from Intensive Agriculture Localities: A Survey in Hopelchén, Campeche, Mexico. *Int. J. Environ. Res. Public Health* 14. <https://doi.org/10.3390/ijerph14060595>
- Rice, R.G., 1996. Applications of ozone for industrial wastewater treatment — A review. *Ozone Sci. Eng.* 18, 477–515. <https://doi.org/10.1080/01919512.1997.10382859>
- Richard, S., Moslemi, S., Sipahutar, H., Benachour, N., Seralini, G.-E., 2005. Differential Effects of Glyphosate and Roundup on Human Placental Cells and Aromatase. *Environ. Health Perspect.* 113, 716–720. <https://doi.org/10.1289/ehp.7728>
- Richins, R.D., Kaneva, I., Mulchandani, A., Chen, W., 1997. Biodegradation of organophosphorus pesticides by surface-expressed organophosphorus hydrolase. *Nat. Biotechnol.* 15, 984–987. <https://doi.org/10.1038/nbt1097-984>
- Rissouli, L., Benicha, M., Chafik, T., Chabbi, M., 2017. Decontamination of water polluted with pesticide using biopolymers: Adsorption of glyphosate by chitin and chitosan. *J. Mater. Environ. Sci.* 8, 4544–4549. <https://doi.org/10.26872/jmes.2017.8.12.479>
- Rivas, F.J., Kolaczowski, S.T., Beltran, F.J., McLurgh, D.B., 1998. Development of a model for the wet air oxidation of phenol based on a free radical mechanism - ScienceDirect. *Chem. Eng. Sci.* 53, 2575–2586.
- Robert, R., Barbati, S., Ricq, N., Ambrosio, M., 2002. Intermediates in wet oxidation of cellulose: identification of hydroxyl radical and characterization of hydrogen peroxide. *Water Res.* 36, 4821–4829.
- Rosenbom, A.E., 2010. The Danish Pesticide Leaching Assessment Programme.
- Routledge, E.J., Sheahan, D., Desbrow, C., Brighty, G.C., Waldock, M., Sumpter, J.P., 1998. Identification of Estrogenic Chemicals in STW Effluent. 2. In Vivo Responses in Trout and Roach. *Environ. Sci. Technol.* 32, 1559–1565. <https://doi.org/10.1021/es970796a>
- Rubalcaba, A., Suárez-Ojeda, M.E., Stüber, F., Fortuny, A., Bengoa, C., Metcalfe, I., Font, J., Carrera, J., Fabregat, A., 2007. Phenol wastewater remediation: advanced oxidation processes coupled to a biological treatment. *Water Sci. Technol.* 55, 221–227. <https://doi.org/10.2166/wst.2007.412>
- Rubí-Juárez, H., Cotillas, S., Sáez, C., Cañizares, P., Barrera-Díaz, C., Rodrigo, M.A., 2016. Removal of herbicide glyphosate by conductive-diamond electrochemical oxidation. *Appl. Catal. B Environ.* 188, 305–312. <https://doi.org/10.1016/j.apcatb.2016.02.006>
- Saitúa, H., Giannini, F., Padilla, A.P., 2012. Drinking water obtaining by nanofiltration from waters contaminated with glyphosate formulations: Process evaluation by means of toxicity tests and studies on operating parameters. *J. Hazard. Mater.* 227–228, 204–210. <https://doi.org/10.1016/j.jhazmat.2012.05.035>
- Salman, J.M., Abid, F.M., Muhammed, A.A., 2012. Batch Study for Pesticide Glyphosate Adsorption onto Palm Oil Fronds Activated Carbon. *Asian J. Chem.* 24, 5646–5648.

- Sanchís, J., Kantiani, L., Llorca, M., Rubio, F., Ginebreda, A., Fraile, J., Garrido, T., Farré, M., 2012. Determination of glyphosate in groundwater samples using an ultrasensitive immunoassay and confirmation by on-line solid-phase extraction followed by liquid chromatography coupled to tandem mass spectrometry. *Anal. Bioanal. Chem.* 402, 2335–2345. <https://doi.org/10.1007/s00216-011-5541-y>
- Sandel, S., Weber, S.K., Trapp, O., 2012. Oxidations with bonded salen-catalysts in microcapillaries. *Chem. Eng. Sci., Mathematics in Chemical Kinetics and Engineering International Workshop 2011* 83, 171–179. <https://doi.org/10.1016/j.ces.2011.10.034>
- Sandrini, J.Z., Rola, R.C., Lopes, F.M., Buffon, H.F., Freitas, M.M., Martins, C. de M.G., da Rosa, C.E., 2013. Effects of glyphosate on cholinesterase activity of the mussel *Perna perna* and the fish *Danio rerio* and *Jenynsia multidentata*: in vitro studies. *Aquat. Toxicol. Amst. Neth.* 130–131, 171–173. <https://doi.org/10.1016/j.aquatox.2013.01.006>
- Sandy, E.H., Blake, R.E., Chang, S.J., Jun, Y., Yu, C., 2013. Oxygen isotope signature of UV degradation of glyphosate and phosphonoacetate: Tracing sources and cycling of phosphonates. *J. Hazard. Mater.* 260, 947–954. <https://doi.org/10.1016/j.jhazmat.2013.06.057>
- Sarkar, S., Das, R., 2017. PVP capped silver nanocubes assisted removal of glyphosate from water—A photoluminescence study. *J. Hazard. Mater.* 339, 54–62. <https://doi.org/10.1016/j.jhazmat.2017.06.014>
- Sauvé, S., Desrosiers, M., 2014. A review of what is an emerging contaminant. *Chem. Cent. J.* 8, 15. <https://doi.org/10.1186/1752-153X-8-15>
- Schäfer, R., Merten, C., Eigenberger, G., 2002. Bubble size distributions in a bubble column reactor under industrial conditions. *Exp. Therm. Fluid Sci.* 26, 595–604.
- Schoonenberg Kegel, F., Rietman, B.M., Verliefde, A.R.D., 2010. Reverse osmosis followed by activated carbon filtration for efficient removal of organic micropollutants from river bank filtrate. *Water Sci. Technol.* 61, 2603–2610. <https://doi.org/10.2166/wst.2010.166>
- Schulze, K.L., Lipe, R.S., 1964. Relationship between substrate concentration, growth rate, and respiration rate of *Escherichia coli* in continuous culture. *Arch. Für Mikrobiol.* 48, 1–20. <https://doi.org/10.1007/BF00406595>
- Scialdone, O., Galia, A., Guarisco, C., La Mantia, S., 2012. Abatement of 1,1,2,2-tetrachloroethane in water by reduction at silver cathode and oxidation at boron doped diamond anode in micro reactors. *Chem. Eng. J.* 189–190, 229–236. <https://doi.org/10.1016/j.cej.2012.02.062>
- Scialdone, O., Galia, A., Sabatino, S., 2013. Electro-generation of H₂O₂ and abatement of organic pollutant in water by an electro-Fenton process in a microfluidic reactor. *Electrochem. Commun.* 26, 45–47. <https://doi.org/10.1016/j.elecom.2012.10.006>
- Scialdone, O., Guarisco, C., Galia, A., 2011. Oxidation of organics in water in microfluidic electrochemical reactors: Theoretical model and experiments. *Electrochimica Acta* 58, 463–473. <https://doi.org/10.1016/j.electacta.2011.09.073>
- Scialdone, O., Guarisco, C., Galia, A., Filardo, G., Silvestri, G., Amatore, C., Sella, C., Thouin, L., 2010. Anodic abatement of organic pollutants in water in micro reactors. *J. Electroanal. Chem.* 638, 293–296. <https://doi.org/10.1016/j.jelechem.2009.10.031>
- Scott, J.P., Ollis, D.F., 1997. Integration of Chemical and Biological Oxidation Processes for Water Treatment: II. Recent Illustrations and Experiences. *J. Adv. Oxid. Technol.* 2, 374–381. <https://doi.org/10.1515/jaots-1997-0304>
- Scott, J.P., Ollis, D.F., 1995. Integration of chemical and biological oxidation processes for water treatment: Review and recommendations. *Environ. Prog.* 14, 88–103. <https://doi.org/10.1002/ep.670140212>
- Sehabiague, L., Lemoine, R., Behkish, A., Heintz, Y.J., Morsi, B.I., 2005. Hydrodynamic and Mass Transfer Parameters in a Slurry Bubble Column Reactor Operating under Fischer-Tropsch Conditions. Presented at the Conference Proceedings of AIChE Annual Meeting, Cincinnati, USA, p. 9918.
- Selvapandiyan, A., Bhatnagar, R.K., 1994. Isolation of a glyphosate-metabolising *Pseudomonas*: detection, partial purification and localisation of carbon-phosphorus lyase. *Appl Microbiol Biotechnol* 40, 876–882.
- Séralini, G.-E., Clair, E., Mesnage, R., Gress, S., Defarge, N., Malatesta, M., Hennequin, D., de Vendôme, J.S., 2014. Republished study: long-term toxicity of a Roundup herbicide and a Roundup-tolerant genetically modified maize. *Environ. Sci. Eur.* 26, 14. <https://doi.org/10.1186/s12302-014-0014-5>
- Shah, Y.T., Kelkar, B.G., Godbole, S.P., Deckwer, W.-D., 1982. Design parameters estimations for bubble column reactors. *AIChE J.* 28, 353–379. <https://doi.org/10.1002/aic.690280302>

- Shahrouz Mohagheghian, Brian Elbing, 2018. Characterization of Bubble Size Distributions within a Bubble Column. *Fluids* 3, 13. <https://doi.org/10.3390/fluids3010013>
- Shannon, M.A., Bohn, P.W., Elimelech, M., Georgiadis, J.G., Mariñas, B.J., Mayes, A.M., 2008. Science and technology for water purification in the coming decades. *Nature* 452, 301–310. <https://doi.org/10.1038/nature06599>
- Sharifi, Y., Pourbabaei, A.A., Javadi, A., Abdolmohammadi, M.H., Saffari, M., Morovvati, A., 2015. Biodegradation of glyphosate herbicide by *Salinicoccus* spp isolated from Qom Hoze-soltan lake, Iran. *Environ. Health Eng. Manag. J.* 2, 31–36.
- Shen, C., Wang, Y.J., Xu, J.H., Luo, G.S., 2015. Glass capillaries with TiO₂ supported on inner wall as microchannel reactors. *Chem. Eng. J.* 277, 48–55. <https://doi.org/10.1016/j.cej.2015.04.013>
- Shende, R.V., Levec, J., 2000. Subcritical Aqueous-Phase Oxidation Kinetics of Acrylic, Maleic, Fumaric, and Muconic Acids. *Ind. Eng. Chem. Res.* 39, 40–47. <https://doi.org/10.1021/ie990385y>
- Shende, R.V., Levec, J., 1999. Kinetics of Wet Oxidation of Propionic and 3-Hydroxypropionic Acids. *Ind. Eng. Chem. Res.* 38, 2557–2563. <https://doi.org/10.1021/ie9900061>
- Shende, R.V., Mahajani, V.V., 1997. Kinetics of Wet Oxidation of Formic Acid and Acetic Acid. *Ind. Eng. Chem. Res.* 36, 4809–4814. <https://doi.org/10.1021/ie970048u>
- Shende, R.V., Mahajani, V.V., 1994. Kinetics of Wet Air Oxidation of Glyoxalic Acid and Oxalic Acid. *Ind. Eng. Chem. Res.* 33, 3125–3130. <https://doi.org/10.1021/ie00036a030>
- Shushkova, T.V., Vinokurova, N.G., Baskunov, B.P., Zelenkova, N.F., Sviridov, A.V., Ermakova, I.T., Leontievsky, A.A., 2016. Glyphosate acetylation as a specific trait of *Achromobacter* sp. Kg 16 physiology. *Appl. Microbiol. Biotechnol.* 100, 847–855. <https://doi.org/10.1007/s00253-015-7084-1>
- Sidoli, P., Baran, N., Angulo-Jaramillo, R., 2016. Glyphosate and AMPA adsorption in soils: laboratory experiments and pedotransfer rules. *Environ. Sci. Pollut. Res. Int.* 23, 5733–5742. <https://doi.org/10.1007/s11356-015-5796-5>
- Singh, B.K., Shaner, D.L., 1998. Rapid Determination of Glyphosate Injury to Plants and Identification of Glyphosate-Resistant Plants. *Weed Technol.* 12, 527–530. <https://doi.org/10.1017/S0890037X00044250>
- Sirés, I., Brillas, E., Oturan, M.A., Rodrigo, M.A., Panizza, M., 2014. Electrochemical advanced oxidation processes: today and tomorrow. A review. *Environ. Sci. Pollut. Res.* 21, 8336–8367. <https://doi.org/10.1007/s11356-014-2783-1>
- Skark, C., Zullei-seibert, N., Schöttler, U., Schlett, C., 1998. The Occurrence of Glyphosate in Surface Water. *Int. J. Environ. Anal. Chem.* 70, 93–104. <https://doi.org/10.1080/03067319808032607>
- Song, J., Li, X.-M., Figoli, A., Huang, H., Pan, C., He, T., Jiang, B., 2013. Composite hollow fiber nanofiltration membranes for recovery of glyphosate from saline wastewater. *Water Res.* 47, 2065–2074. <https://doi.org/10.1016/j.watres.2013.01.032>
- Songa, E.A., Somerset, V.S., Waryo, T., Baker, P.G.L., Iwuoha, E.I., 2009. Amperometric nanobiosensor for quantitative determination of glyphosate and glufosinate residues in corn samples. *Pure Appl. Chem.* 81, 123–139. <https://doi.org/10.1351/PAC-CON-08-01-15>
- Souza, D.R. de, Trovó, A.G., Filho, A., R, N., Silva, M.A.A., Machado, A.E.H., 2013. Degradation of the commercial herbicide glyphosate by photo-fenton process: evaluation of kinetic parameters and toxicity. *J. Braz. Chem. Soc.* 24, 1451–1460. <https://doi.org/10.5935/0103-5053.20130185>
- Speth, T.F., 1993. Glyphosate Removal from Drinking Water. *J. Environ. Eng.* 119, 1139–1157. [https://doi.org/10.1061/\(ASCE\)0733-9372\(1993\)119:6\(1139\)](https://doi.org/10.1061/(ASCE)0733-9372(1993)119:6(1139))
- Srivastava, B., Jhelum, V., Basu, D.D., Patanjali, P.K., 2009. Adsorbents for pesticide uptake from contaminated water: A review. *J. Sci. Ind. Res.* 68, 839–850.
- Stegeman, D., Knop, P.A., Wijnands, A.J.G., Westerterp*, K.R., 1996. Interfacial Area and Gas Holdup in a Bubble Column Reactor at Elevated Pressures - Industrial & Engineering Chemistry Research (ACS Publications). *Ind. Eng. Chem. Res.* 35, 3842–3847.
- Stockinger, Hermann., Heinzle, Elmar., Kut, O.M., 1995. Removal of Chloro and Nitro Aromatic Wastewater Pollutants by Ozonation and Biotreatment. *Environ. Sci. Technol.* 29, 2016–2022. <https://doi.org/10.1021/es00008a021>
- Stöffler, B., Luft, G., 1999. Influence of the Radical Scavenger t-Butanol on the Wet Air Oxidation of p-Toluenesulfonic Acid. *Chem. Eng. Technol.* 22, 409–412. [https://doi.org/10.1002/\(SICI\)1521-4125\(199905\)22:5<409::AID-CEAT409>3.0.CO;2-D](https://doi.org/10.1002/(SICI)1521-4125(199905)22:5<409::AID-CEAT409>3.0.CO;2-D)
- Sturges, H.A., 1926. The Choice of a Class Interval. *J. Am. Stat. Assoc.* 21, 65–66. <https://doi.org/10.1080/01621459.1926.10502161>

- Suárez-Ojeda, M.E., Carrera, J., Metcalfe, I.S., Font, J., 2008. Wet air oxidation (WAO) as a precursor to biological treatment of substituted phenols: Refractory nature of the WAO intermediates. *Chem. Eng. J.* 144, 205–212. <https://doi.org/10.1016/j.cej.2008.01.022>
- Suarez-Ojeda, M.E., Guisasola, A., Baeza, J.A., Fabregat, A., Stüber, F., Fortuny, A., Font, J., Carrera, J., 2007. Integrated catalytic wet air oxidation and aerobic biological treatment in a municipal WWTP of a high-strength o-cresol wastewater. *Chemosphere* 66, 2096–2105. <https://doi.org/10.1016/j.chemosphere.2006.09.035>
- Suárez-Ojeda, M.E., Kim, J., Carrera, J., Metcalfe, I.S., Font, J., 2007. Catalytic and non-catalytic wet air oxidation of sodium dodecylbenzene sulfonate: Kinetics and biodegradability enhancement. *J. Hazard. Mater.*, " Selected papers of the proceedings of the 5th European Meeting on Chemical Industry and Environment, EMChIE 2006 " held in Vienna, Austria, 3-5 May 2006 144, 655–662. <https://doi.org/10.1016/j.jhazmat.2007.01.091>
- Suarez-Ojeda, M.E., Stüber, F., Fortuny, A., Fabregat, A., Carrera, J., Font, J., 2005. Catalytic wet air oxidation of substituted phenols using activated carbon as catalyst. *Appl. Catal. B Environ.* 58, 105–114. <https://doi.org/10.1016/j.apcatb.2004.11.017>
- Suryawanshi, P.L., Gumfekar, S.P., Bhanvase, B.A., Sonawane, S.H., Pimplapure, M.S., 2018. A review on microreactors: Reactor fabrication, design, and cutting-edge applications. *Chem. Eng. Sci.* 189, 431–448. <https://doi.org/10.1016/j.ces.2018.03.026>
- Sviridov, A.V., Shushkova, T.V., Ermakova, I.T., Ivanova, E.V., Epiktetov, D.O., Leontievsky, A.A., 2015. Microbial degradation of glyphosate herbicides (Review). *Appl. Biochem. Microbiol.* 51, 188–195. <https://doi.org/10.1134/S0003683815020209>
- Sviridov, A.V., Shushkova, T.V., Ermakova, I.T., Ivanova, E.V., Leontievsky, A.A., 2014. Glyphosate: Safety Risks, Biodegradation, and Bioremediation, in: Cao, G., Orrù, R. (Eds.), *Current Environmental Issues and Challenges*. Springer Netherlands, Dordrecht, pp. 183–195. https://doi.org/10.1007/978-94-017-8777-2_11
- Sviridov, A.V., Shushkova, T.V., Zelenkova, N.F., Vinokurova, N.G., Morgunov, I.G., Ermakova, I.T., Leontievsky, A.A., 2012. Distribution of glyphosate and methylphosphonate catabolism systems in soil bacteria *Ochrobactrum anthropi* and *Achromobacter* sp. *Appl. Microbiol. Biotechnol.* 93, 787–796. <https://doi.org/10.1007/s00253-011-3485-y>
- Tang, C., Heindel, T.J., 2006. Estimating gas holdup via pressure difference measurements in a cocurrent bubble column. *Int. J. Multiph. Flow* 32, 850–863. <https://doi.org/10.1016/j.ijmultiphaseflow.2006.02.008>
- Tang, W., Zeng, X., Li, Y., Ni, Y., Zhao, J., Gu, G., 2000. The Study on the Wet Air Oxidation of Highly Concentrated Emulsified Wastewater and Its Kinetics, in: *Sustainable Energy and Environmental Technologies*. WORLD SCIENTIFIC, pp. 336–340. https://doi.org/10.1142/9789812791924_0061
- Tardio, J., Bhargava, S., Eyer, S., Sumich, M., Akolekar, D.B., 2004. Interactions between Specific Organic Compounds during Catalytic Wet Oxidation of Bayer Liquor. *Ind. Eng. Chem. Res.* 43, 847–851. <https://doi.org/10.1021/ie030539g>
- Tazdaït, D., Salah, R., Grib, H., Abdi, N., Mameri, N., 2018. Kinetic study on biodegradation of glyphosate with unacclimated activated sludge. *Int. J. Environ. Health Res.* 28, 448–459. <https://doi.org/10.1080/09603123.2018.1487043>
- Thermophysical properties of fluid systems [WWW Document], n.d. URL <http://webbook.nist.gov/chemistry/fluid/> (accessed 3.1.18).
- Therning, P., Rasmuson, A., 2001. Liquid dispersion, gas holdup and frictional pressure drop in a packed bubble column at elevated pressures. *Chem. Eng. J.* 81, 331–335. [https://doi.org/10.1016/S1385-8947\(00\)00222-9](https://doi.org/10.1016/S1385-8947(00)00222-9)
- Thompson, M., Klymenko, O.V., Compton, R.G., 2005. Modelling homogeneous kinetics in the double channel electrode. *Journal Electroanal. Chem.* 576, 333–338.
- Thomsen, A.B., 1998. DEGRADATION OF QUINOLINE BY WET OXIDATION— KINETIC ASPECTS AND REACTION MECHANISMS. *Water Res.* 32, 136–146. [https://doi.org/10.1016/S0043-1354\(97\)00200-5](https://doi.org/10.1016/S0043-1354(97)00200-5)
- Toor, R., Mohseni, M., 2007. UV-H₂O₂ based AOP and its integration with biological activated carbon treatment for DBP reduction in drinking water. *Chemosphere* 66, 2087–2095. <https://doi.org/10.1016/j.chemosphere.2006.09.043>
- Torres, R.A., Sarria, V., Torres, W., Peringer, P., Pulgarin, C., 2003. Electrochemical treatment of industrial wastewater containing 5-amino-6-methyl-2-benzimidazolone: toward an electrochemical–biological coupling. *Water Res.* 37, 3118–3124. [https://doi.org/10.1016/S0043-1354\(03\)00179-9](https://doi.org/10.1016/S0043-1354(03)00179-9)

- Tran, N., Drogui, P., Doan, T.L., Le, T.S., Nguyen, H.C., 2017. Electrochemical degradation and mineralization of glyphosate herbicide. *Environ. Technol.* 38, 2939–2948. <https://doi.org/10.1080/09593330.2017.1284268>
- Trgovcich, B., Kirsch, E.J., Grady, C.P.L., 1983. Characteristics of Activated Sludge Effluents before and after Breakpoint Chlorination. *J. Water Pollut. Control Fed.* 55, 966–976.
- Tu, S.-T., Yu, X., Luan, W., Löwe, H., 2010. Development of micro chemical, biological and thermal systems in China: A review. *Chem. Eng. J.* 163, 165–179. <https://doi.org/10.1016/j.cej.2010.07.021>
- Urseanu, M.I., Guit, R.P.M., Stankiewicz, A., van Kranenburg, G., Lommen, J.H.G.M., 2003. Influence of operating pressure on the gas hold-up in bubble columns for high viscous media. *Chem. Eng. Sci.*, 17th International Symposium of Chemical Reaction Engineering (IS CRE 17) 58, 697–704. [https://doi.org/10.1016/S0009-2509\(02\)00597-3](https://doi.org/10.1016/S0009-2509(02)00597-3)
- Vaidya, P.D., Mahajani, V.V., 2002. Insight into sub-critical wet oxidation of phenol. *Adv. Environ. Res.* 6, 429–439. [https://doi.org/10.1016/S1093-0191\(01\)00071-5](https://doi.org/10.1016/S1093-0191(01)00071-5)
- Van Bruggen, A.H.C., He, M.M., Shin, K., Mai, V., Jeong, K.C., Finckh, M.R., Morris, J.G., 2018. Environmental and health effects of the herbicide glyphosate. *Sci. Total Environ.* 616–617, 255–268. <https://doi.org/10.1016/j.scitotenv.2017.10.309>
- Vázquez-Rodríguez, G., Youssef, C.B., Waissman-Vilanova, J., 2006. Two-step modeling of the biodegradation of phenol by an acclimated activated sludge. *Chem. Eng. J.* 117, 245–252. <https://doi.org/10.1016/j.cej.2005.11.015>
- Veiga, F., Zapata, J.M., Fernandez Marcos, M.L., Alvarez, E., 2001. Dynamics of glyphosate and aminomethylphosphonic acid in a forest soil in Galicia, north-west Spain. *Sci. Total Environ.* 271, 135–144. [https://doi.org/10.1016/S0048-9697\(00\)00839-1](https://doi.org/10.1016/S0048-9697(00)00839-1)
- Verenich, S., Laari, A., Kallas, J., 2000. Wet oxidation of concentrated waste water of paper mills for water cycle closing. *Waste Manag.* 20, 287–293. [https://doi.org/10.1016/S0956-053X\(99\)00308-6](https://doi.org/10.1016/S0956-053X(99)00308-6)
- Vicente, J., Rosal, R., Díaz, M., 2002. Noncatalytic Oxidation of Phenol in Aqueous Solutions. *Ind. Eng. Chem. Res.* 41, 46–51. <https://doi.org/10.1021/ie010130w>
- Vidal, E., Negro, A., Cassano, A., Zalazar, C., 2015. Simplified reaction kinetics, models and experiments for glyphosate degradation in water by the UV/H₂O₂ process. *Photochem. Photobiol. Sci.* 14, 366–377. <https://doi.org/10.1039/C4PP00248B>
- Villa, M.V., Sánchez-Martín, M.J., Sánchez-Camazano, M., 1999. Hydrotalcites and organo-hydrotalcites as sorbents for removing pesticides from water. *J. Environ. Sci. Health Part B* 34, 509–525. <https://doi.org/10.1080/03601239909373211>
- Villamar-Ayala, C.A., Carrera-Cevallos, J.V., Vasquez-Medrano, R., Espinoza-Montero, P.J., 2019. Fate, ecotoxicological characteristics, and treatment processes applied to water polluted with glyphosate: A critical review. *Crit. Rev. Environ. Sci. Technol.* 49, 1476–1514. <https://doi.org/10.1080/10643389.2019.1579627>
- Villeneuve, A., Larroude, S., Humbert, J.F., 2011. Herbicide Contamination of Freshwater Ecosystems: Impact on Microbial Communities. *Pestic. - Formul. Eff. Fate* 285–312. <https://doi.org/10.5772/13515>
- Wackett, L.P., Shames, S.L., Venditti, C.P., Walsh, C.T., 1987. Bacterial carbon-phosphorus lyase: products, rates, and regulation of phosphonic and phosphinic acid metabolism. *J. Bacteriol.* 169, 710–717.
- Waiman, C.V., Avena, M.J., Garrido, M., Fernández Band, B., Zanini, G.P., 2012. A simple and rapid spectrophotometric method to quantify the herbicide glyphosate in aqueous media. Application to adsorption isotherms on soils and goethite. *Geoderma* 170, 154–158. <https://doi.org/10.1016/j.geoderma.2011.11.027>
- Wang, M., Zhang, G., Qiu, G., Cai, D., Wu, Z., 2016. Degradation of herbicide (glyphosate) using sunlight-sensitive MnO₂/C catalyst immediately fabricated by high energy electron beam. *Chem. Eng. J.* 306, 693–703. <https://doi.org/10.1016/j.cej.2016.07.063>
- Wang, S., Seiwert, B., Kästner, M., Miltner, A., Schäffer, A., Reemtsma, T., Yang, Q., Nowak, K.M., 2016. (Bio)degradation of glyphosate in water-sediment microcosms – A stable isotope co-labeling approach. *Water Res.* 99, 91–100. <https://doi.org/10.1016/j.watres.2016.04.041>
- Wang, X.-J., Song, Y., Mai, J.-S., 2008. Combined Fenton oxidation and aerobic biological processes for treating a surfactant wastewater containing abundant sulfate. *J. Hazard. Mater.* 160, 344–348. <https://doi.org/10.1016/j.jhazmat.2008.02.117>
- Wang, Y.-T., 1992. Effect of Chemical Oxidation on Anaerobic Biodegradation of Model Phenolic Compounds. *Water Environ. Res.* 64, 268–273.

- Wigfield, Y.Y., Lanouette, M., 1990. Simplified liquid chromatographic determination of glyphosate and metabolite residues in environmental water using post-column fluorogenic labelling. *Anal. Chim. Acta* 233, 311–314. [https://doi.org/10.1016/S0003-2670\(00\)83495-9](https://doi.org/10.1016/S0003-2670(00)83495-9)
- Wilhelmi, A.R., Knopp, P.V., 1979. WET AIR OXIDATION - AN ALTERNATIVE TO INCINERATION. *Chem. Eng. Prog.* 75, 46–52.
- Wilkinson, P.M., Haringa, H., Van Dierendonck, L.L., 1994. Mass transfer and bubble size in a bubble column under pressure. *Chem. Eng. Sci.* 49, 1417–1427. [https://doi.org/10.1016/0009-2509\(93\)E0022-5](https://doi.org/10.1016/0009-2509(93)E0022-5)
- Wilkinson, P.M., Spek, A.P., Dierendonck, V., L, L., 1992. Design parameters estimation for scale-up of high-pressure bubble columns. *AIChE J.* 38, 544–554. <https://doi.org/10.1002/aic.690380408>
- Wilkinson, P.M., Spek, A.P., van Dierendonck, L.L., 1991. Design parameters estimation for scale-up of high-pressure bubble columns. *AIChE J.* 38, 544–554. <https://doi.org/10.1002/aic.690380408>
- Willms, R.S., Balinsky, A.M., Reible, D.D., Wetzel, D.M., Harrison, D.P., 1987. Aqueous-phase oxidation: the intrinsic kinetics of single organic compounds. *Ind. Eng. Chem. Res.* 26, 148–154. <https://doi.org/10.1021/ie00061a028>
- Witte, W., 1998. Medical Consequences of Antibiotic Use in Agriculture. *Science* 279, 996–997. <https://doi.org/10.1126/science.279.5353.996>
- Wu, Q., Hu, X., Yue, P.L., Zhao, X.S., Lu, G.Q., 2001. Copper/MCM-41 as catalyst for the wet oxidation of phenol. *Appl. Catal. B Environ.* 32, 151–156. [https://doi.org/10.1016/S0926-3373\(01\)00131-X](https://doi.org/10.1016/S0926-3373(01)00131-X)
- Wu, X.H., Fu, G.M., Wan, Y., Guo, D., Chen, Y.H., Luo, Y.F., Wu, X.F., 2010. Isolation and identification of glyphosate-degraded strain *Aspergillus oryzae* sp. A-F02 and its degradation characteristics. *Plant Dis. Pests* 1, 54–57.
- Xie, M., Liu, Z., Xu, Y., 2010. Removal of glyphosate in neutralization liquor from the glycine-dimethylphosphit process by nanofiltration. *J. Hazard. Mater.* 181, 975–980. <https://doi.org/10.1016/j.jhazmat.2010.05.109>
- Xing, B., Chen, H., Zhang, X., 2018a. Efficient degradation of organic phosphorus in glyphosate wastewater by catalytic wet oxidation using modified activated carbon as a catalyst. *Environ. Technol.* 39, 749–758. <https://doi.org/10.1080/09593330.2017.1310935>
- Xing, B., Chen, H., Zhang, X., 2018b. Efficient degradation of organic phosphorus in glyphosate wastewater by catalytic wet oxidation using modified activated carbon as a catalyst. *Environ. Technol.* 39, 749–758. <https://doi.org/10.1080/09593330.2017.1310935>
- Xing, B., Chen, H., Zhang, X., 2017. Removal of organic phosphorus and formaldehyde in glyphosate wastewater by CWO and the lime-catalyzed formose reaction. *Water Sci. Technol.* 75, 1390–1398. <https://doi.org/10.2166/wst.2017.006>
- Xue, W., Zhang, G., Xu, X., Yang, X., Liu, C., Xu, Y., 2011. Preparation of titania nanotubes doped with cerium and their photocatalytic activity for glyphosate. *Chem. Eng. J.* 167, 397–402. <https://doi.org/10.1016/j.cej.2011.01.007>
- Yamada, Y., Mizutani, M., Nakamura, T., Yano, K., 2010. Mesoporous Microcapsules with Decorated Inner Surface: Fabrication and Photocatalytic Activity. *Chem. Mater.* 22, 1695–1703. <https://doi.org/10.1021/cm9031072>
- Yan, M., Wang, D., Ma, X., Ni, J., Zhang, H., 2010. THMs precursor removal by an integrated process of ozonation and biological granular activated carbon for typical Northern China water. *Sep. Purif. Technol.* 72, 263–268. <https://doi.org/10.1016/j.seppur.2010.02.015>
- Yang, W., Wang, J., Jin, Y., 2001. Mass Transfer Characteristics of Syngas Components in Slurry System at Industrial Conditions. *Chem. Eng. Technol.* 24, 651–657. [https://doi.org/10.1002/1521-4125\(200106\)24:6<651::AID-CEAT651>3.0.CO;2-X](https://doi.org/10.1002/1521-4125(200106)24:6<651::AID-CEAT651>3.0.CO;2-X)
- Yang, Y., Deng, Q., Yan, W., Jing, C., Zhang, Y., 2018. Comparative study of glyphosate removal on goethite and magnetite: Adsorption and photo-degradation. *Chem. Eng. J.* 352, 581–589. <https://doi.org/10.1016/j.cej.2018.07.058>
- Yao, X., Zhang, Y., Du, L., Liu, J., Yao, J., 2015. Review of the applications of microreactors. *Renew. Sustain. Energy Rev.* 47, 519–539. <https://doi.org/10.1016/j.rser.2015.03.078>
- Ye, F., Shen, D., 2004. Acclimation of anaerobic sludge degrading chlorophenols and the biodegradation kinetics during acclimation period. *Chemosphere* 54, 1573–1580. <https://doi.org/10.1016/j.chemosphere.2003.08.019>
- Yi, S.J., Park, J.M., Chang, S.-C., Kim, K.C., 2014. Design and validation of a uniform flow microreactor. *J. Mech. Sci. Technol.* 28, 157–166. <https://doi.org/10.1007/s12206-013-0954-5>

- Yongrui, P., Zheng, Z., Bao, M., Li, Y., Zhou, Y., Sang, G., 2015. Treatment of partially hydrolyzed polyacrylamide wastewater by combined Fenton oxidation and anaerobic biological processes. *Chem. Eng. J.* 273, 1–6. <https://doi.org/10.1016/j.cej.2015.01.034>
- Yoon, T.-H., Hong, L.-Y., Kim, D.-P., 2011. Photocatalytic reaction using novel inorganic polymer derived packed bed microreactor with modified TiO₂ microbeads. *Chem. Eng. J., Special Issue - IMRET 11: 11th International Conference on Microreaction Technology* 167, 666–670. <https://doi.org/10.1016/j.cej.2010.08.090>
- Yoshioka, N., Asano, M., Kuse, A., Mitsuhashi, T., Nagasaki, Y., Ueno, Y., 2011. Rapid determination of glyphosate, glufosinate, bialaphos, and their major metabolites in serum by liquid chromatography–tandem mass spectrometry using hydrophilic interaction chromatography. *J. Chromatogr. A* 1218, 3675–3680. <https://doi.org/10.1016/j.chroma.2011.04.021>
- Yu, X.M., Yu, T., Yin, G.H., Dong, Q.L., An, M., Wang, H.R., Ai, C.X., 2015. Glyphosate biodegradation and potential soil bioremediation by *Bacillus subtilis* strain Bs-15. *Genet. Mol. Res.* 14, 14717–14730. <https://doi.org/10.4238/2015.November.18.37>
- Zeng, X.P., Tang, W.W., Zhao, J.F., Gu, G.W., 2004. Study on wet air oxidation of strength recalcitrant organic wastewater. *Acta Sci. Circumstantiae* 24, 945–949.
- Zhan, H., Feng, Y., Fan, X., Chen, S., 2018. Recent advances in glyphosate biodegradation. *Appl. Microbiol. Biotechnol.* 102, 5033–5043. <https://doi.org/10.1007/s00253-018-9035-0>
- Zhang, H.Y., Lu, X.M., Liu, Z.Y., Xu, Y.H., 2007. Treatment of degradation-resistant pesticide wastewater with high salinity by wet air oxidation. *Chem. Ind. Eng. Prog.* 26, 417–425.
- Zhang, M.D., Wei, Y.F., Zhao, K., Mei, R.W., Huang, M., 2011. Glyphosate Degradation with Industrial Wastewater Effluent by Combined Adsorption Treatment and Advanced Oxidation Processes. *Adv. Mater. Res.* 233–235, 369–372. <https://doi.org/10.4028/www.scientific.net/AMR.233-235.369>
- Zhang, M.H., Dong, H., Zhao, L., Wang, D.X., Meng, D., 2019. A review on Fenton process for organic wastewater treatment based on optimization perspective. *Sci. Total Environ.* 670, 110–121. <https://doi.org/10.1016/j.scitotenv.2019.03.180>
- Zhang, P., Sun, H., Yu, L., Sun, T., 2013. Adsorption and catalytic hydrolysis of carbaryl and atrazine on pig manure-derived biochars: Impact of structural properties of biochars. *J. Hazard. Mater.* 244–245, 217–224. <https://doi.org/10.1016/j.jhazmat.2012.11.046>
- Zhang, Q., Zhang, Qinghong, Wang, H., Li, Y., 2013. A high efficiency microreactor with Pt/ZnO nanorod arrays on the inner wall for photodegradation of phenol. *J. Hazard. Mater.* 254–255, 318–324. <https://doi.org/10.1016/j.jhazmat.2013.04.012>
- Zhao, H., Tao, K., Zhu, J., Liu, S., Gao, H., Zhou, X., 2015. Bioremediation potential of glyphosate-degrading *Pseudomonas* spp. strains isolated from contaminated soil. *J. Gen. Appl. Microbiol.* 61, 165–170. <https://doi.org/10.2323/jgam.61.165>
- Zhou, C.R., Li, G.P., Jiang, D.G., 2014. Study on behavior of alkalescent fiber FFA-1 adsorbing glyphosate from production wastewater of glyphosate. *Fluid Phase Equilibria* 362, 69–73. <https://doi.org/10.1016/j.fluid.2013.09.002>
- Zhou, J., Li, J., An, R., Yuan, H., Yu, F., 2012. Study on a New Synthesis Approach of Glyphosate. *J. Agric. Food Chem.* 60, 6279–6285. <https://doi.org/10.1021/jf301025p>
- Zhou, M., He, J., 2007. Degradation of azo dye by three clean advanced oxidation processes: Wet oxidation, electrochemical oxidation and wet electrochemical oxidation—A comparative study. *Electrochimica Acta, POLYMER ELECTROLYTES Selection of papers from The 10th International Symposium (ISPE-10)15-19 October 2006, Foz do Iguaçu-PR, Brazil* 53, 1902–1910. <https://doi.org/10.1016/j.electacta.2007.08.056>
- Zimmermann, F.J., 1954. Waste disposal. US2665249A.
- Zou, X., Hang, H., Chu, J., Zhuang, Y., Zhang, S., 2009. Oxygen uptake rate optimization with nitrogen regulation for erythromycin production and scale-up from 50 L to 372 m³ scale. *Bioresour. Technol.* 100, 1406–1412. <https://doi.org/10.1016/j.biortech.2008.09.017>

Annexe

Treatment technologies and degradation pathways of glyphosate: A critical review

This review has been submitted to “Water Research” by 18 July, 2019.

Abstract

Glyphosate, a most widely used post-emergence broad-spectrum herbicide, could accumulate and transfer in the environment and cause adverse effects to plants, animals, microorganisms, and humans. Glyphosate has been frequently found in the surface water, groundwater and industrial effluents. This review considers the occurrence and fate of glyphosate in the environment as well as its treatment technologies from urban and industrial wastewaters, with associated degradation pathways. Current research into removal focuses on physical, biological and advanced oxidation processes (AOPs). Advantages and disadvantages of these technologies are discussed, which will require continual research effort to improve their performance. Furthermore, more research is needed to scale up the laboratory studies to an industrial scale and to know the precise degradation pathways of glyphosate by different treatment methods.

Keywords: Glyphosate; fate; treatment technology; wastewater; degradation pathways

1 Introduction

Wastewater treatment (WWT) is a severe worldwide problem. Liquid aqueous wastes, from the domestic or industrial origin, are becoming more and more complex for their treatment, due to the presence of many molecules difficult to remove, especially the case of emerging contaminants. They are defined as natural or synthetic chemicals which are not commonly found in the environment but are known or suspected to ecological or human health effects (Geissen et al., 2015). Emerging contaminants include many types of molecules such as pesticides and herbicides, pharmaceuticals, personal care products, plasticizers, fragrances, flame retardants, hormones, nanoparticles, water treatment by-products, surfactants, and so on (Sauvé and Desrosiers, 2014). Among these emerging contaminants, glyphosate has attracted more and more attention from researchers.

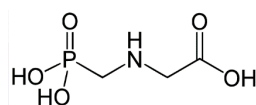


Fig. 1 The structure of glyphosate

Glyphosate (N-(phosphonomethyl)glycine, $C_3H_8NO_5P$, Fig. 1, Table 1) is a post-emergence, nonselective broad-spectrum herbicide, used in agriculture to control many annual and perennial weeds (Waiman et al., 2012). Glyphosate is the herbicide most extensively used in agricultural, forestry and urban setting in the world, due to its high ability to control weeds and its low toxicity (da Silva et al., 2011; Zhang et al., 2011). Glyphosate is a biosynthesis inhibitor of essential aromatic amino acids, resulting in various metabolic disorders, which include the deregulation of the shikimate pathway and the suspension of protein synthesis, leading to general metabolic disruption and the plant death (Oliveira et al., 2012). Glyphosate interrupts aromatic amino acid biosynthesis in plants through inhibiting the enzymes 5-enolpyruvylshikimate-3-phosphate synthase or 3-deoxy-D-arabino-heptulosonate-7-phosphate synthase, which is a precursor for aromatic amino acids, ultimately hormones, vitamins and other important metabolites for plants (Kataoka et al., 1996). The mechanism of inhibition effect which has been reported is that the binding site for glyphosate overlaps closely with the binding site of shikimate 3-phosphate (Helander et al., 2012).

Table 1 Chemical and physical properties of glyphosate (Mackay et al., 2006)

Properties	Values	Units
Molecular weight	169.07	$g.mol^{-1}$
Physical state	White solid	-
Odor	Odorless	-
Density	1.704	$g.cm^{-3}$
pKa	0.78 (first proton phosphonate group) 2.29 (proton of the carboxyl group) 5.96 (second phosphonate proton) 10.98 (proton of the amino group)	-
Melting point	184.5	$^{\circ}C$
Boiling point	187	$^{\circ}C$
Solubility (20 $^{\circ}C$)	1.01	$g\ glyphosate/100\ mL\ H_2O$

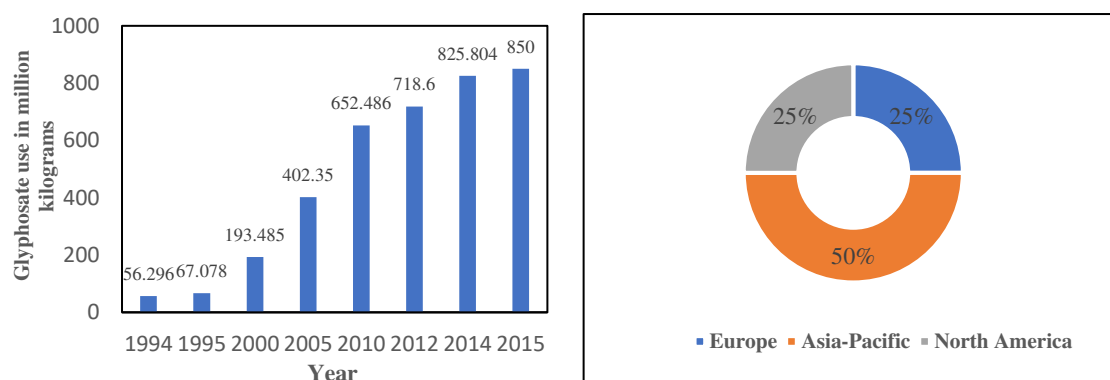


Fig. 2 Glyphosate use worldwide from 1994 to 2015 (in million kilograms) and its application by regions in 2014 (from: “Glyphosate Market Share, Size - Industry Trends Report 2024,” n.d., “Glyphosate use worldwide 1994-2014 | Statistic,” n.d.; “Glyphosate Market Analysis, Size, Share and Forecasts - 2022 | MarketsandMarkets,” n.d.)

Glyphosate is available in various chemical forms, such as ammonium salt, diammonium salt, isopropylamine salt, dimethylammonium salt, and potassium salt (Benbrook, 2016; Gillezeau et al., 2019). Glyphosate mixed with other chemicals known as “inert ingredients” constitutes glyphosate-based herbicides (Benbrook, 2016; Gillezeau et al., 2019). Fig. 2 shows the glyphosate use worldwide from 1994 to 2015 and its application by regions in 2014 (available from: “Glyphosate Market Share, Size - Industry Trends Report 2024,” n.d., “Glyphosate use worldwide 1994-2014 | Statistic,” n.d.; “Glyphosate Market Analysis, Size, Share and Forecasts - 2022 | MarketsandMarkets,” n.d.). Generally, glyphosate-based herbicides are used in the preparation of soils for sowing and in crop areas with its sprayed applications from 6.7 to 8.9 kg.ha⁻¹ and from 0.53 to 1.0 kg.ha⁻¹, respectively (Giesy et al., 2000; Benbrook, 2016; Villamar-Ayala et al., 2019). These herbicides are also used to control annual perennial species (agriculture), invasive vegetation (forestry), and aquatic algae (aquaculture) during the post-harvest activities with the applications up to 0.84 kg.ha⁻¹ of its acid equivalent (active ingredient) (Giesy et al., 2000; Duke and Powles, 2008; Villamar-Ayala et al., 2019).

Due to the intensive use and accumulation of glyphosate in the environment, some harmful effects of glyphosate have been reported for plant, animal and human health. Glyphosate weakened plant system, decreased photosynthesis and caused cell damage (Huber et al., 2005; Gomes et al., 2016; Van Bruggen et al., 2018). Authors reported that glyphosate suppressed the acetylcholinesterase activity, disturbed the metabolism and may cause DNA or liver damage both for terrestrial and aquatic animals (Menéndez-Helman et al., 2012; Sandrini et al., 2013; Kwiatkowska et al., 2014, 2017; Mesnage et al., 2015; Cattani et al., 2017). Although humans are not a direct target for glyphosate, they could contact glyphosate due to occupational exposure by agricultural practices (Acquavella et al., 2004; Paz-y-Miño et al., 2007) or through the food chain (Wigfield and Lanouette, 1990; McQueen et al., 2012). Glyphosate has been reported to cause cell and DNA damage and endocrine disruption to humans (Richard et al., 2005; Paz-y-Miño et al., 2007; Benachour and Séralini, 2009; Mesnage et al., 2015). In 2015, the International Agency for Research on Cancer (IARC) classified glyphosate as “probably carcinogenic to humans”, while authors disagree on this conclusion which require further research (Andreotti et al., 2018). Numerous studies and reviews have been reported on the adverse effects of glyphosate and glyphosate-based formulations on plants, animals and human (Tsui and Chu, 2003; Vendrell et al., 2009; Vera et al., 2010; Kier and Kirkland, 2013; Tarazona et al., 2017). Acute toxicity tests show that the 96-hour LD₅₀ of glyphosate ranged from 2.3 to 150 mg.L⁻¹ for different fish species (Armiliato et al., 2014; Sandun et al., 2015; Rodrigues et al., 2017; Vajargah et al., 2018).

Furthermore, due to the extensive use of glyphosate, glyphosate has been frequently detected in the aqueous environment (Humphries et al., 2005; Battaglin et al., 2009; Villeneuve et al., 2011; Aparicio et al., 2013; Mahler et al., 2017; Poiger et al., 2017). Saunders and Pezeshki (2015) reviewed the occurrence of glyphosate in runoff waters and in the root-zone.

Several review papers have been published with regard to the treatment technologies for glyphosate (Jönsson et al., 2013; Sviridov et al., 2015; Villamar-Ayala et al., 2019). Jönsson et al. (2013) and Villamar-Ayala et al. (2019) both reviewed the treatment of glyphosate through using physical treatment processes, biological treatment and advanced oxidation processes (AOPs) and briefly compared their advantages and disadvantages. Sviridov et al. (2015) focused on metabolic pathways of glyphosate in microorganisms. However, almost no attempt has been made to provide a comprehensive summary of degradation pathways of glyphosate by different processes such as biological treatment and AOPs.

Thus, this review will consider the occurrence, behavior, and fate of glyphosate in aqueous environment and provide a comparative assessment of current treatment methods used to remove glyphosate. Some development will focus on the improvement of these techniques and novel removal attempts to treat glyphosate in wastewater treatment. In addition, this article also provides an assessment of degradation pathways of glyphosate by biological treatment or different AOPs based on reaction mechanisms.

2 Occurrence, behavior, and fate of glyphosate in environment

Glyphosate-containing herbicides may contaminate the environment after application. First, through air spraying, glyphosate can directly enter atmosphere environment, with its concentration in air up to 0.48 g.L^{-1} (Helander et al., 2012; Villamar-Ayala et al., 2019). Then, through wind or rain, glyphosate reaches the target organisms by foliar contact or the soil (Villamar-Ayala et al., 2019). In the target plant, glyphosate is first absorbed by foliage and then translocated to the shoots and roots via the phloem (Helander et al., 2012). Without degradation in the plant, large root systems of some weeds transport glyphosate into deep soil layers (Laitinen et al., 2007; Helander et al., 2012). A part of glyphosate which enters the soil through rain, wind or transportation by root of the plant may stay at the soil surface. Glyphosate can be adsorbed to organic matter and clay of soils, resulting in its accumulation in soils over time (Cassigneul et al., 2016; Okada et al., 2016; Sidoli et al., 2016; Van Bruggen et al., 2018). As glyphosate possesses three polar functional groups (amino, carboxyl and phosphonate groups), it can be strongly adsorbed by soil minerals (Borggaard and Gimsing, 2008). Glyphosate mobility in the soil depends on the adsorption and desorption processes which related to soil characteristics and other environmental conditions (Helander et al., 2012; Villamar-Ayala et al.,

2019). Microbial degradation is the most important transformation process to determine the persistence of glyphosate in the soil (Aparicio et al., 2013). Glyphosate can be degraded to aminomethylphosphonic acid (AMPA) or sarcosine as primary metabolite under aerobic and anaerobic conditions by the microflora in the soil/sediment (Ermakova et al., 2010; Aparicio et al., 2013). The AMPA pathway is the main microbial process, whereas the sarcosine pathway is only found in pure microbial culture (Vereecken, 2005; Villamar-Ayala et al., 2019). Glyphosate has been reported to have a soil half-life between 2 and 215 days (Battaglin et al., 2014; Maqueda et al., 2017). Due to the runoff, such as rain and erosion, glyphosate and AMPA can be transferred into surface water (Wang et al., 2016; Maqueda et al., 2017; Rendon-von Osten and Dzul-Caamal, 2017).

Table 2 Glyphosate occurrence and concentration in surface or groundwater samples in several countries in North America, South America, and Europe (Van Bruggen et al., 2018)

Country	Date	Glyphosate occurrence and concentrations	Refer.
Canada	2002	22% of samples positive, up to 6.07 $\mu\text{g.L}^{-1}$	(Humphries et al., 2005)
US (Midwest)	2002	36% of stream samples positive, up to 8.7 $\mu\text{g.L}^{-1}$	(Battaglin et al., 2005)
US (Midwest)	2013	44% of steam samples positive, up to 27.8 $\mu\text{g.L}^{-1}$	(Mahler et al., 2017)
US (Washington, Maryland, Iowa, Wyoming)	2005-2006	All streams positive, up to 328 $\mu\text{g.L}^{-1}$	(Battaglin et al., 2009)
US (Iowa, Indiana, Mississippi)	2004-2008	Most rivers positive, up to 430 $\mu\text{g.L}^{-1}$ after a storm	(Coupe et al., 2012)
Mexico	2015	All groundwater samples positive, up to 1.42 $\mu\text{g.L}^{-1}$	(Rendon-von Osten and Dzul-Caamal, 2017)
Argentina	2012	35% of surface water samples positive, 0.1-7.6 $\mu\text{g.L}^{-1}$	(Aparicio et al., 2013)
Germany	1998	Few positive samples in two tributaries to the Ruhr river, up to 0.59 $\mu\text{g.L}^{-1}$	(Skark et al., 1998)
Switzerland	2016	Most stream water samples, up to 2.1 $\mu\text{g.L}^{-1}$	(Poiger et al., 2017)
Spain	2007-2010	41% positive groundwater samples, up to 2.5 $\mu\text{g.L}^{-1}$	(Sanchís et al., 2012)
Hungary	2010-2011	Most river and groundwater samples positive, up to 0.001 $\mu\text{g.L}^{-1}$	(Mörrtl et al., 2013)
Denmark	1999-2009	25% of surface water samples positive, up to 31 $\mu\text{g.L}^{-1}$, 4% of groundwater samples positive, up to 0.67 $\mu\text{g.L}^{-1}$	(Rosenbom, 2010)
France	2003-2004	91% of stream samples positive, up to 165 $\mu\text{g.L}^{-1}$	(Villeneuve et al., 2011)

Glyphosate is highly water soluble and can be mobile in aqueous environment (Veiga et al., 2001). The mobility of AMPA is found 1.6 to 4.0 times higher than glyphosate (Coupe et al., 2012; Villamar-Ayala et al., 2019). Thus, glyphosate and AMPA have been frequently detected in surface or groundwater (Table 2). Table 2 shows that glyphosate has been detected in river water and stream water with the concentration range of 2-430 $\mu\text{g.L}^{-1}$ in the USA, which is at higher levels than in Europe. In areas of the USA, genetically modified glyphosate-resistant crops are grown, thus glyphosate and AMPA occur widely in soil, surface, and groundwater (Battaglin et al., 2014). However, in Europe, growing genetically modified crops is not allowed yet, which makes glyphosate

to be detected in various water sources at lower levels (Van Bruggen et al., 2018). It is also reported that glyphosate can be detected in air and rain during the crop growing season and in water from spring snowmelt (Battaglin et al., 2009, 2014; Chang et al., 2011). Ultimately, glyphosate enters to the seawater with high persistence (Mercurio et al., 2014; Van Bruggen et al., 2018).

Moreover, Birch et al. (2011) reported that glyphosate and AMPA were found in samples of sewage and storm water overflows with the concentration of 0.043-1.3 $\mu\text{g.L}^{-1}$ and 0.06-1.3 $\mu\text{g.L}^{-1}$, respectively. Rendon-von Osten and Dzul-Caamal (2017) found that even in the bottled drinking water, glyphosate concentration could achieve up to 0.79 $\mu\text{g.L}^{-1}$ which exceeded the acceptable limits for human consumption in the European Union (0.1 $\mu\text{g.L}^{-1}$) (“Emerging substances | NORMAN,” n.d.). Currently, glyphosate has been in the list of the U.S. national primary drinking water contaminants with a maximum contaminant level goal of 0.7 mg.L^{-1} (Songa et al., 2009).

Table 3 Glyphosate concentration in industrial wastewater

Refer.	Sampling point	Glyphosate concentration
(Heitkamp et al., 1992)	Glyphosate production wastewater	500-2000 mg.L^{-1}
(Manassero et al., 2010)	Rinsing herbicide containers	50.7-76.05 mg.L^{-1}
(Zhang et al., 2011)	Zhejiang Wynca Chemical Industry Group Co., Ltd. (China)	258 mg.L^{-1}
(Zhou et al., 2014)	Xinan Chemical Plant (Zhejiang, Chian)	1% wt
(Xing et al., 2017)	Jiangsu Good Harvest-Weien agrochemical Ind. Co. Ltd.; Jiema Chemical Ind. Co. Ltd.; Guangan Ind. Co. Ltd. (China)	213-2560 mg.L^{-1}

Glyphosate contaminants the environment from various sources: agricultural runoff, chemical spill as well as industrial effluents (Baylis, 2000; Romero et al., 2011; Guo et al., 2018). Three major industrial synthesis methods were used for glyphosate production: hydrocyanic acid (HCN), diethanolamine (DEA) and glycine process. All of these processes have a large amount of industrial wastewater and other environmental pollutions (Zhou et al., 2012). To obtain 1 ton of glyphosate, about 5-6 tons of crystallized mother liquid is generated with ~ 1% glyphosate, 1-4% formaldehyde (CH_2O) and other byproducts (Xing et al., 2018). Most of glyphosate is recovered from the mother liquor through nanofiltration (Song et al., 2013), while 200-3000 mg.L^{-1} glyphosate remains in the nanofiltration permeate wastewater in China (Xing et al., 2018). It has also reported that the glyphosate concentration in industrial effluents could achieve up to 2,560 mg.L^{-1} (Table 3). Therefore, it is necessary to develop some processes able to degrade glyphosate during the wastewater treatment, in urban and industrial systems.

3 Treatment technologies for glyphosate-containing wastewater

Conventional methods, such as adsorption, filtration, and biological treatment have been applied to treat glyphosate-containing wastewater. Moreover, advanced oxidation processes (AOPs), such as photolysis oxidation, Fenton oxidation, electrochemical oxidation, and ozonation oxidation, have been proposed as an alternative treatment technology for glyphosate-containing wastewater (Villamar-Ayala et al., 2019). All these treatment technologies are described in detail below.

3.1 Adsorption

Table 4 Removal of glyphosate from wastewater by adsorption

Refer.	Adsorbent	Glyphosate concentration (mg.L ⁻¹)	Marks
(Villa et al., 1999)	Hydrotalcites and organo-hydrotalcites	5-25	Adsorption capacity: 1-4 µg.g ⁻¹
(Li et al., 2005)	MgAl-layered double hydroxides	169	Maximum adsorption capacity: 184 mg.L ⁻¹
(Nourouzi et al., 2010)	Activated carbon	5-100	Maximum adsorption capacity: 48.4 mg.g ⁻¹
(Hu et al., 2011)	Dewatered alum sludge (DAS) and liquid alum sludge (LAS)	50-100 for DAS; 200-500 for LAS	Removal efficiency: 65.4%-91.6% For DAS; 64.7%-97.4% for LAS Maximum adsorption capacity: 85.9 mg.g ⁻¹ for DAS; 113.6 mg.g ⁻¹ for LAS
(Salman et al., 2012)	Palm oil fronds activated carbon	25-250	Maximum adsorption capacity: 104.2 mg.g ⁻¹
(Chen et al., 2016)	Resin D301	1% mass fraction	Maximum adsorption capacity: 400-833.33 mg.g ⁻¹
(Herath et al., 2016)	Rice husk derived engineered biochar	0-100	Maximum removal: 82.0%; maximum adsorption capacity: 123.03 mg.g ⁻¹
(Mayakaduwa et al., 2016)	Woody biochar	20	Maximum adsorption capacity: 44 mg.g ⁻¹
(Jia et al., 2017)	Resin-supported double valent nano-sized hydroxyl iron oxide	400	Maximum adsorption capacity: 401.12 mg.g ⁻¹
(Rissouli et al., 2017)	Chitin and chitosan	1-30	Maximum adsorption capacity: 14.04 mg.g ⁻¹ for chitin and 35.08 mg.g ⁻¹ for chitosan
(Sarkar and Das, 2017)	PVP capped silver nanocubes	100	No data for glyphosate removal efficiency

Currently, adsorption is widely used in large-scale biochemical and purification for wastewater treatment due to simple design, non-toxic and low-cost adsorbents and high efficiency (Mayakaduwa et al., 2016). Several materials have been used as adsorbents for glyphosate adsorptive removal, such as activated carbon, biochar, water industrial residues, clay substances, resin, biopolymers, polyvinylpyrrolidone (PVP) capped silver nanocubes, etc. Table 4 shows that activated carbon, biochar or resin used as adsorbents could achieve higher removal efficiency and higher maximum adsorption capacity of glyphosate. Recently, biochar, an eco-friendly material, has drawn more attention because of its low cost and highly aromatic and porous structure, which contributes to high removal efficiency of biochar (Zhang et al., 2013). However, with this process, disposal of the residue after adsorption remains a problem which needs further research (Mayakaduwa et al., 2016).

3.2 Filtration

Bank filtration process can achieve up to 95% and 87% of glyphosate and AMPA removal efficiency, respectively (Jönsson et al., 2013). Xie et al. (2010) reported that a high glyphosate removal of 95.5% was obtained by nanofiltration using a Desal-5 DK membrane from neutralization liquor produced by the glycine-dimethylphosphite process. Schoonenberg Kegel et al. (2010) obtained a glyphosate removal efficiency higher than 99% by a technology equipped with reverse osmosis and subsequently activated carbon filtration. Saitúa et al. (2012) observed that more than 85% of glyphosate could be removed by nanofiltration for the initial glyphosate concentration up to 250 mg.L⁻¹, depending on pressure and pH value. Liu et al. (2012) reported that nanofiltration separation of glyphosate from wastewater using a GE Osmonic DK membrane could achieve a high glyphosate removal efficiency. Thus, although glyphosate-containing wastewater can be effectively treated by filtration, it is likely highly dependent on physicochemical conditions. Large scale production of water by these methods is expensive, which is unable to commonly used in practice and unlikely to be adopted for the treatment of organic compounds (Jönsson et al., 2013).

3.3 Biological treatment

Biodegradation of organic compounds is known as an effective and eco-friendly method to remove organic pollutants from the aqueous environment (Zhan et al., 2018). Various micro-organisms, including bacteria and fungi, have been reported to use glyphosate as a sole source of carbon, nitrogen, and phosphorus. Table 5 shows that the microorganisms responsible for glyphosate biodegradation are mainly bacteria, only little fungi strains have been reported to degrade glyphosate. Among these microorganisms, most species utilize glyphosate as sole phosphorus source. Some exceptions use glyphosate as nitrogen or carbon source.

To assess the glyphosate-degradation performance of microorganisms, it is necessary to optimize the culture conditions, including culture temperature, initial pH, glyphosate concentration, inoculation biomass and incubation time (Zhan et al., 2018). The culture conditions most used for glyphosate-degrading microorganism are a temperature of 25-37°C, pH of 6-7.5 and aerobic medium. Only Obojska et al. (2002) observed a thermophilic bacteria, *Geobacillus caldxylosilyticus* T20, which could achieve more than 65% of glyphosate removal at 60°C with initial glyphosate concentration of 169 mg.L⁻¹. Kryuchkova et al. (2014) found a facultative anaerobic strain, *Enterobacter cloacae* K7, which could utilize glyphosate as sole phosphorus source and obtain 40% degradation with glyphosate initial concentration of 845 mg.L⁻¹.

Table 5 Glyphosate-degrading microorganisms reported in the literature

Microorganism	Source	Source type for glyphosate used	Culture conditions	Type of degradation pathway	Comments	References
Bacteria						
<i>Acetobacter</i> sp.	Glyphosate-contaminated rice field	Carbon or phosphorus source	30°C; aerobic	Not shown	Bacteria could tolerate up to 250 mg.ml ⁻¹ glyphosate	(Moneke et al., 2010)
<i>Achromobacter</i> sp. Kg 16	Glyphosate-contaminated soil	Sole phosphorus source	28-30°C; pH: 6.0-7.5; aerobic	Acetylgyphosate pathway	A new pathway of glyphosate utilization: acetylation	(Shushkova et al., 2016)
<i>Achromobacter</i> sp. LW9	Activated sludge from glyphosate process waste stream	Sole carbon source	28°C; pH: 7; aerobic	AMPA pathway	100% glyphosate (0.1%, w/v) transformation to AMPA	(McAuliffe et al., 1990)
<i>Achromobacter</i> sp. MPK 7A	Glyphosate-contaminated soil	Sole phosphorus source	28-30°C; pH: 7; aerobic	Sarcosine pathway	About 60% glyphosate (500 mg.L ⁻¹) removal	(Ermakova et al., 2017)
<i>Achromobacter</i> sp. MPS 12A	Alkylphosphonates-contaminated soil	Sole phosphorus source	28°C; pH: 6.5-7.5; aerobic	Sarcosine pathway	Glyphosate consumption: 124 µmol g ⁻¹ biomass	(Sviridov et al., 2012)
<i>Agrobacterium radiobacter</i>	Sludge from waste treatment plant	Sole phosphorus source	30°C; pH:7; aerobic	Sarcosine pathway	No data for glyphosate removal efficiency	(Wackett et al., 1987)
<i>Alcaligenes</i> sp. GL	Non-axenic cultures of the cyanobacterium <i>Anacystis nidulans</i>	Sole phosphorus source	28°C; pH:7.5; aerobic	Sarcosine pathway	50-80% glyphosate (5 mM) removal	(Lerbs et al., 1990)
<i>Arthrobacter atrocyaneus</i> ATCC 13752	Collection of microorganisms and cell cultures, Germany	Sole phosphorus source	Room temperature; pH: 7.2; aerobic	AMPA pathway	Capable of degrading glyphosate without previous culture selection	(Pipke and Amrhein, 1988)
<i>Arthrobacter</i> sp. GLP-1	Mixture culture with <i>Klebsiella pneumoniae</i>	Sole phosphorus source	Room temperature; pH: 7; aerobic	Sarcosine pathway	Capable of degrading glyphosate without previous culture selection	(Pipke et al., 1987)
<i>Bacillus cereus</i> CB4	Glyphosate-contaminated soil	Sole phosphorus source	35°C; pH: 6; aerobic	Both AMPA and sarcosine pathway	94.47% degradation (6 g.L ⁻¹) in 5 days	(Fan et al., 2012)
<i>Bacillus cereus</i> 6 P	Glyphosate-exposed orange plantation site	Sole phosphorus source	28°C; pH: 7; aerobic	Not shown	37.7% glyphosate (1 mM) removal	(Acosta-Cortés et al., 2019)
<i>Bacillus subtilis</i> Bs-15	Rhizospheric soil of a pepper plant	Carbon and phosphorus source	35°C; pH: 8; aerobic	Not shown	65% glyphosate removal	(Yu et al., 2015)
<i>Burkholderia vietnamiensis</i> AO5-12 and <i>Burkholderia</i> sp. AO5-13	Glyphosate contaminated sites in Malaysia	Sole phosphorus source	30°C; pH: 6; aerobic	Not shown	91% and 74% glyphosate (50 mg.L ⁻¹) degradation for AQ5-12 and AQ5-13, respectively	(Manogaran et al., 2017)

<i>Comamonas odontotermitis</i> P2	Glyphosate-contaminated soil in Australia	Carbon and phosphorus source	29.9°C; pH: 7.4; aerobic	Not shown	Complete degradation (1.5 g.L ⁻¹) within 104 h	(Firdous et al., 2017)
<i>Enterobacter cloacae</i> K7	Rhizoplane of various plants in Russia	Sole phosphorus source	30-37°C; pH: 6.8-7; Facultative anaerobe	Sarcosine pathway	40% glyphosate (5 mM) degradation	(Kryuchkova et al., 2014)
<i>Flavobacterium</i> sp. GD1	Monsanto activated sludge	Sole phosphorus source	25°C; pH: 6.8-7; aerobic	AMPA pathway	Complete degradation of glyphosate (0.02%)	(Balthazor and Hallas, 1986)
<i>Geobacillus caldoxylosilyticus</i> T20	Central heating system water	Sole phosphorus source	60°C; pH: 7; aerobic	AMPA pathway	>65% glyphosate (1 mM) removal	(Obojska et al., 2002)
<i>Ochrobacterium anthropic</i> GPK3	Glyphosate-contaminated soil	Sole phosphorus source	28°C; pH: 6.5-7.5; aerobic	Both AMPA and sarcosine pathway	Glyphosate consumption: 283.8 μmol g ⁻¹ biomass	(Sviridov et al., 2012)
<i>Ochrobactrum intermedium</i> Sq20	Glyphosate-contaminated soil	Sole carbon source	Room temperature; pH 7; aerobic	Sarcosine pathway	Complete degradation (500 mg.L ⁻¹) within 4 days	(Firdous et al., 2018)
<i>Ochrobactrum</i> sp. GDOS	Soil	Sole phosphorus source	30°C; pH: 7; aerobic	AMPA pathway	Complete degradation (3 mM) within 60 h	(Hadi et al., 2013)
<i>P.fluorescens</i>	Glyphosate-contaminated rice field	Carbon or phosphorus source	30°C; aerobic	Not shown	Bacteria could tolerate up to 250 mg/ml glyphosate	(Moneke et al., 2010)
<i>Pseudomonas pseudomallei</i> 22	Soil	Sole phosphorus source	28°C; aerobic	AMPA pathway (putative)	50% glyphosate (170 mg.L ⁻¹) degradation in 40 h	(Peñaloza-Vazquez et al., 1995)
<i>Pseudomonas</i> sp. 4ASW	Glyphosate-contaminated soil	Sole phosphorus source	29°C; pH: 7.2; aerobic	Sarcosine pathway	100% glyphosate (0.25 mM) removal	(Dick and Quinn, 1995)
<i>Pseudomonas</i> sp. GLC11	Mutant of <i>Pseudomonas</i> sp. PAO1 on selective medium	Sole phosphorus source	37°C; pH: 7; aerobic	Sarcosine pathway	Capable of tolerating up to 125 mM glyphosate	(Selvapandiyan and Bhatnagar, 1994)
<i>Pseudomonas</i> sp. LBr	A glyphosate process waste stream	Sole phosphorus source	Room temperature; pH: 7; aerobic	Both AMPA and sarcosine pathway	Capable of eliminating 20 mM glyphosate from growth medium	(Jacob, 1988)
<i>Pseudomonas</i> sp. PG2982	<i>Pseudomonas aeruginosa</i> -ATCC 9027	Sole phosphorus source	Room temperature; aerobic	Sarcosine pathway	No data for glyphosate removal efficiency	(Kishore and Jacob, 1987)
<i>Pseudomonas</i> spp. strains GA07, GA09 and GC04	Glyphosate-contaminated soil in China	Sole carbon source	33°C; pH: 7; aerobic	Both AMPA and sarcosine pathways	Glyphosate (500 mg.L ⁻¹) removal: 53.6%-80.8%	(Zhao et al., 2015)
<i>Rhizobiaeae meliloti</i> 1021	Spontaneous mutation of a wild-type strain	Sole phosphorus source	28-32°C; pH: 7; aerobic	Sarcosine pathway	50% glyphosate (0.5 mM) removal	(Liu et al., 1991)
<i>Salinicoccus</i> spp.	Qom Hoze-Soltan Lake in Iran	Sole carbon source	Salt concentration: 5%-10%; 30°C; pH: 6.5-8.2; aerobic	Not shown	The native halophilic isolates could biodegrade glyphosate	(Sharifi et al., 2015)
<i>Streptomyces</i> sp. StC	Activated sludge from a municipal sewage treatment plant	Sole phosphorus, nitrogen or nitrogen	28°C; pH: 7.2; aerobic	Sarcosine pathway	60% degradation (10 mM) within 10 days	(Obojska et al., 1999)

		and phosphorus source	Fungi					
<i>Aspergillus niger</i>	Soil	Sole phosphorus source	28°C; pH: 6; aerobic	AMPA pathway	No data for removal efficiency	(Krzyśko-Lupicka et al., 1997)		
<i>Aspergillus oryzae</i> sp. A-F02	Sludge in an aeration tank of a glyphosate manufacture	Sole carbon source	30°C; pH: 7.5; aerobic	Not shown	86.82% degradation (1000 mg.L ⁻¹) within 7 days	(Wu et al., 2010)		
<i>Fusarium oxysporum</i>	Sugar cane	Sole phosphorus source	30°C; pH: 6; aerobic	Not shown	41% glyphosate (50 mg.L ⁻¹) removal	(Castro et al., 2007)		
<i>Penicillium chrysogenum</i>	Soil	Sole nitrogen source	Dark at 28 (±1) °C; pH:7.0; aerobic	AMPA pathway (putatively)	40% degradation (5 mM) after 15 days	(Klimek et al., 2001)		
<i>Penicillium notanum</i>	Spontaneous growth on hydroxyfluorenyl-9-phosphate	Sole phosphorus source	28°C; pH: 7.2; aerobic	AMPA pathway	Capable to degrade glyphosate at sublethal doses (<0.5 mM)	(Bujacz et al., 1995)		
<i>Scopulariopsis sp.</i>	Soil	Sole phosphorus source	28°C; pH: 6; aerobic	AMPA pathway	No data for removal efficiency	(Krzyśko-Lupicka et al., 1997)		
<i>Trichoderma harzianum</i>	Soil	Sole phosphorus source	28°C; pH: 6; aerobic	AMPA pathway	No data for removal efficiency	(Krzyśko-Lupicka et al., 1997)		

Table 6 Summary of glyphosate biodegradation kinetics reported in the literature

Reference	Strain	Concentration range (mg.L ⁻¹)	Monod model		Haldane model			First-order model	
			μ_m (h ⁻¹)	K_s (mg.L ⁻¹)	μ_m (h ⁻¹)	K_s (mg.L ⁻¹)	K_i / K_s (mg.L ⁻¹)	k (h ⁻¹)	$t_{1/2}$ (h)
(Nourouzi et al., 2012)	Mixed culture isolated from soil	100-800	0.18-0.87	33-181	0.05-0.7	-	1.1-8	-	-
(Zhao et al., 2015)	<i>Pseudomonas</i> spp. GA07, GA09 and GC04	500	-	-	-	-	-	0.0018-0.0039	178.3-385.7
(Firdous et al., 2018)	<i>Ochrobactrum intermedium</i> Sq20	500	-	-	-	-	-	0.0464	14.9
(Tazdaït et al., 2018)	Unacclimated activated sludge	100-5000	-	-	0.06	340	1.21	-	-
(Acosta-Cortés et al., 2019)	<i>Bacillus cereus</i> 6 P	169	-	-	-	-	-	0.003	279

Two major degradation pathways exist in glyphosate-degrading microorganisms (Fig. 3). One pathway is glyphosate converted to stoichiometric quantities of AMPA and glyoxylate through the cleavage of C-N bond by the enzyme glyphosate oxidoreductase (Zhan et al., 2018). Glyoxylate usually enters the tricarboxylic acid cycle as a convenient energy substrate for most glyphosate-degrading bacteria (Sviridov et al., 2015). Three pathways exist for AMPA: (i) AMPA releases to the environment (Jacob, 1988; Lerbs et al., 1990); (ii) AMPA is further metabolized to methylamine and phosphate, catalyzed by C-P lyase (Pipke et al., 1987; Jacob, 1988; Pipke and Amrhein, 1988); (iii) AMPA is first metabolized to phosphonoformaldehyde by transaminase and then transformed to phosphate and formaldehyde for further metabolism by phosphonate (Sviridov et al., 2014).

The second degradation pathway is glyphosate metabolized to phosphate and sarcosine through the direct cleavage of the C-P bond, catalyzed by C-P lyase (Firdous et al., 2017). Sarcosine can be used as growth nutrient (carbon and nitrogen source) for microorganism and is further metabolized to glycine and formaldehyde by sarcosine-oxidase (Borggaard and Gimsing, 2008). Glycine is further metabolized by microorganism and formaldehyde enters the tetrahydrofolate-directed pathway of single-carbon transfers to generate CO_2 and NH_4^+ (Borggaard and Gimsing, 2008). Some reports indicate that AMPA and sarcosine pathways simultaneously exist in some bacteria, such as *Bacillus cereus* CB4, *Ochrobacterium anthropic* GPK3, and *Pseudomonas* sp. LBr (Jacob, 1988; Fan et al., 2012; Sviridov et al., 2012). The AMPA pathway is not generally subjected to P_i (inorganic phosphorus) concentration, however, glyphosate conversion to sarcosine strongly depends on the concentrations of exogenous and endogenous P_i , which rarely occurs in natural environments (Sviridov et al., 2015) due to C-P lyase activity generally induced under phosphate starvation condition (Borggaard and Gimsing, 2008; Sviridov et al., 2015).

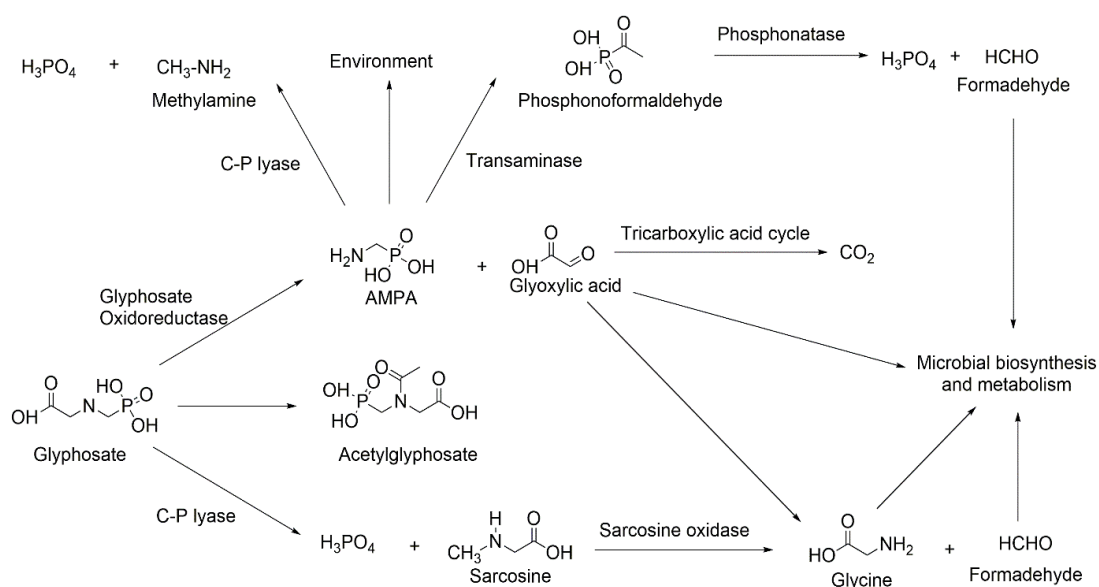


Fig. 3 Biodegradation pathways of glyphosate in microorganisms (Zhan et al., 2018).

At least, another degradation pathway was observed in *Achromobacter* sp. Kg16 which utilized glyphosate as sole phosphorus source, resulting in production of acetylglyphosate (Shushkova et al., 2016). However, *Achromobacter* sp. Kg16 is not able to further utilize acetylglyphosate as a phosphorus source, causing its poor growth. Although the glyphosate biodegradation has been extensively studied, the precise degradation mechanism and pathways are until not known.

Most studies reported have focused on the glyphosate biodegradation by pure culture of bacteria. Little research on glyphosate biodegradation was carried on mixed culture. Hallas and Adams (1992) reported glyphosate removal from wastewater effluent discharged from an activated sludge process in lab columns and found that more than 90% of glyphosate degradation was achieved for an initial concentration of 50 mg.L⁻¹. Nourouzi et al. (2010) reported that 99.5% of glyphosate (300 mg.L⁻¹) was converted to AMPA and 2% of AMPA was degraded to further metabolites by mixed bacteria isolated from oil palm plantation soil. The mixed cultures are more likely able to completely degrade contaminants, compared to pure culture due to the various enzymes available in mixed culture (Barbeau et al., 1997; Nourouzi et al., 2012). Moreover, due to the high requirements of pure culture, mixed culture processes are more suitable for industrial applications.

In order to provide practical information for bioremediation processes of the pollutants, it is necessary to study the microbial degradation kinetics (Nourouzi et al., 2012). Monod model is widely used for biodegradation kinetics in case of pure cultures, limited substrate and non-inhibitory biomass growth (Tanyolaç and Beyenal, 1998; de Lucas et al., 2005; Singh et al., 2008; Nourouzi et al., 2012). Due to the substrate inhibition to biomass growth at high substrate concentrations, Monod model has been further developed to include substrate inhibition, such as Haldane model (Singh et al., 2008; Nourouzi et al., 2012; Tazdaït et al., 2018). Moreover, a first-order model is also used to evaluate biodegradation process in order to obtain degradation rate constant (k) and half-life ($t_{1/2}$). Table 6 summarizes glyphosate biodegradation kinetics which has reported in the literature. Almost no information is reported on yield coefficient for glyphosate-degrading bacteria, which needs to be further study. The half-life of glyphosate in *Pseudomonas* spp. GA07, GA09 and GC04 (Zhao et al., 2015) and *Bacillus cereus* 6 P (Acosta-Cortés et al., 2019) is varied from 178.3 to 279 h, which is much higher than the half-life of 14.9 h in *Ochrobactrum intermedium* Sq20 (Firdous et al., 2017). Although the biodegradation of glyphosate has been extensively studied, the information on glyphosate biodegradation kinetics, especially on the inhibitory effect, is still rarely studied. The inhibitory effect of herbicide on its own biodegradation is necessary to investigate since the assessment of substrate inhibition to enzymatic reactions is becoming increasingly crucial in the treatment of general toxic compounds, particularly for pesticides degradation (Hao et al., 2002; Tazdaït et al., 2018).

Nevertheless, biological treatment is a promising method to treat glyphosate-containing wastewater, most research is conducted at a lab scale and focused on the isolation and identification of strains. The information to apply this technology to treat glyphosate-containing wastewater at an industrial scale is still rare.

3.4 Advanced oxidation processes (AOPs)

AOPs are promising technologies, which have been widely used for the treatment of toxic, recalcitrant organic compounds in water (Divyapriya et al., 2016), including photolysis, ozonation, Fenton, electro-oxidation, wet air oxidation (WAO) and supercritical water oxidation. The mechanism in AOPs system is to oxidize organic contaminants to CO₂, H₂O and inorganic ions due to the generation of hydroxyl radical ($\cdot\text{OH}$), hydrogen peroxide (H₂O₂), and superoxide (O₂ \cdot^-) in the system (Malato et al., 2002; Manassero et al., 2010). The hydroxyl radical ($\cdot\text{OH}$) is a non-selective, strong oxidant (2.8 V oxidation potential), which can act very fast on a wide range of organic compounds (Mota et al., 2008; Divyapriya et al., 2016). Compared to conventional treatment, AOPs can non-selectively mineralize pollutants without sludge production.

AOPs could be an alternative technology to effectively treat glyphosate at a short time compared to physical (adsorption and filtration) and biological treatment. Recently, single or combined AOPs have been reported to treat glyphosate-containing wastewater, such as photolysis oxidation, Fenton oxidation, electrochemical oxidation, ozonation oxidation, and combined oxidation process. Table 7 summarizes some AOPs process used for glyphosate treatment.

Table 7 shows that photolysis-based oxidation can lead to high glyphosate removal efficiency up to 99.8% at low concentration (less than 50 mg.L⁻¹) and the use of photocatalyst improve the photodegradation of glyphosate. TiO₂ is the common used heterogeneous photocatalyst for glyphosate photocatalytic degradation because of its stability, non-toxic and low cost (Echavia et al., 2009). In order to improve the photocatalytic activity of TiO₂, several attempts have been reported, such as non-metal doping (Echavia et al., 2009), metal doping (Xue et al., 2011) and metal and non-metal codoping (Lin et al., 2012). Although complete glyphosate removal has achieved (Echavia et al., 2009), while, the mineralization efficiency is not high (less than 74%). Meanwhile, the preparation processes for modified TiO₂ are generally complicated, resulting in an increase of the cost. In order to decrease the cost, the combination of hydrogen processes and UV radiation (H₂O₂/UV) has been reported to treat glyphosate with higher concentration (up to 91.26 mg.L⁻¹) compared to photocatalytic degradation, which is a simple and convenient process (Manassero et al., 2010; Junges et al., 2013; Vidal et al., 2015; López et al., 2018). H₂O₂/UV process induced a good degradation of glyphosate (>70%), but it requires a long treatment time (more than 5 h). Meanwhile, due to the high

cost of electricity associated with using energy-consuming UV lamps (Echavia et al., 2009), the disposal of catalysts and difficulties to control the conditions (Zhan et al., 2018) hamper the development of these photolysis-based processes at large scale application (Tran et al., 2017).

Fenton based oxidation (Table 7) has been reported to be a successful technology for glyphosate treatment, which has the advantages of simple operation, no mass transfer limitation and easy implementation as a stand-alone or hybrid system and easy integration in existing water treatment processes (Chen et al., 2007; Bokare and Choi, 2014). 95.7% and 62.9% removal of total phosphate and chemical oxygen demand (COD), respectively, have been achieved by conventional Fenton process (Liao et al., 2009). However, several drawbacks exist in conventional Fenton process: the continuous loss of oxidants and iron ions, the formation of solid sludge and the high costs and risks associated with handling, transportation, and storage of reagents (Zhang et al., 2019). In order to overcome these shortcomings, Fenton process is improved to form various optimized Fenton processes for glyphosate treatment, i.e. electro-Fenton (Balci et al., 2009; Lan et al., 2016) and Photo-Fenton processes (Huston and Pignatello, 1999; Souza et al., 2013). Electro-Fenton process overcomes the limitations of the accumulation of iron sludge and the high costs and risks related to the handling, transportation, and storage of reagents. Photo-Fenton process can reduce iron sludge production (Zhang et al., 2019). Electro-Fenton and photo-Fenton processes have both reported to achieve complete glyphosate removal and good mineralization at low concentration (Balci et al., 2009; Souza et al., 2013). However, electro-Fenton consumes extensive anode (Aramyan, 2017; Zhang et al., 2019). Photo-Fenton process faces several challenges, such as short working life span, high energy consumption and economic costs (Aramyan, 2017; Zhang et al., 2019). Moreover, Fenton based process needs an acidic reaction condition (usual pH at 2-4). This consumes a lot of acid along with high cost due to extra electrical energy (UV lamp). Thus, Fenton-based processes are generally used in a synthetic and low concentration glyphosate wastewater rather than real wastewater from the glyphosate production (Huston and Pignatello, 1999; Balci et al., 2009; Liao et al., 2009; Souza et al., 2013).

Table 7 Some AOPs process reported to be used for glyphosate treatment

Refer.	Type	Conditions	Glyphosate concentration (mg.L ⁻¹)	Remarks
(Chen et al., 2007)	Photodegradation	T: 22°C; pH: 3.5-6; illumination time: 3 h; the presence of Fe ³⁺ and C ₂ O ₄ ²⁻	5.0	Maximum degradation efficiency: 63.2%
(Chen and Liu, 2007)	Photocatalytic degradation	Catalyst: TiO ₂ ; T: 30°C; pH: 2-12; illumination time: 0.5-3.5 h	0.042	Maximum degradation efficiency: 92.0%
(Assalin et al., 2009)	Photocatalytic degradation	Catalyst: TiO ₂ ; illumination time: 30 min	42.3	TOC removal: 92%
(Echavia et al., 2009)	Photocatalytic degradation	Catalyst: TiO ₂ immobilized on silica gel; T: 22°C; illumination time: 2 h	16.9	Glyphosate conversion: 100%; TOC conversion: 74%
(Xue et al., 2011)	Photocatalytic degradation	Catalyst: Ce-TiO ₂ nanotubes; pH: 7; illumination time: 1 h	22.8	Glyphosate degradation: 76%
(Lin et al., 2012)	Photocatalytic degradation	Catalyst: Cerium and nitrogen Co-Doped TiO ₂ ; illumination time: 100 min	50	Glyphosate removal: 99.8%
(Yang et al., 2018)	Photocatalytic degradation	Catalyst: Goethite or magnetite; T: 20°C; pH: 3-9; illumination time: 2 h	10	Maximum glyphosate removal: 92.0% for goethite and 99.3% for magnetite
(Manassero et al., 2010)	H ₂ O ₂ /UV	T: 25°C; pH: 3.5-10; illumination time: 5 h	27.04-91.26	Maximum glyphosate conversion: 70%; TOC conversion: 29%
(Junges et al., 2013)	H ₂ O ₂ /UV	T: 20°C; pH: 5.2; illumination time: 2-6 h	50	Maximum glyphosate conversions: 90%; TOC conversion: 70%
(Vidal et al., 2015)	H ₂ O ₂ /UV	T: 25°C; pH: 5.2; reaction time: 12 h	30.4-72.7	Glyphosate removal: 80%; TOC conversion: 70%
(López et al., 2018)	H ₂ O ₂ /UV	T: 25°C; pH: 3-10; reaction time: 8 h	30.0	TOC removal: 71%
(Liao et al., 2009)	Fenton	T: 90°C; pH: 3-4; reaction time: 2 h; n(H ₂ O ₂)/n(Fe ²⁺)=4:1	-	TP removal: 95.7%; COD removal: 62.9%
(Zhang et al., 2011)	Adsorption-Fenton	Adsorbent: nano-tungsten/D201resin; pH: 2-4	258	Maximum glyphosate degradation: 60.5%
(Balci et al., 2009)	Electro-Fenton	Mn ²⁺ as catalyst; T: 23±2°C; pH: 3; anode: Pt cylindrical mesh; cathode: carbon felt; electrolyte: 0.05 M Na ₂ SO ₄ ; current: 100 mA	16.9	Complete glyphosate removal at 3 h; 82% TOC reduction in 5 h
(Lan et al., 2016)	Electro-Fenton	room temperature; pH 3-6; anode: RuO ₂ /Ti mesh; cathode: activated carbon fiber; electrolyte: 0.1 M Na ₂ SO ₄ ; current: 0.12-0.36 A	16.9-253.5	85% glyphosate removal after 2 h; 72% COD removal in 6 h
(Huston and Pignatello, 1999)	Photo-Fenton	T: 25°C; pH: 2.8; reaction time: 2 h; H ₂ O ₂ : 0.01 M; Fe ³⁺ : 5.0×10 ⁻⁵ M; UV irradiation: 300-400 nm	0.034	TOC removal: 35.0%
(Souza et al., 2013)	Photo-Fenton	T: 40±2°C; pH 2.8±0.2; reaction time: 2 h; H ₂ O ₂ : 10.3 M; Fe ²⁺ /Fe ³⁺ : 0.27 M; oxalate: 1.3 M; UV irradiation: 320-400 nm	100	Complete glyphosate removal; TOC removal: 74.4%

(Aquino Neto and de Andrade, 2009)	Electrochemical oxidation	Anode: RuO ₂ and IrO ₂ DSA [®] ; T: 25±1°C; pH: 3; current density: 50 mA cm ⁻² ; reaction time: 4 h; electrolyte: NaCl	1000	91% COD removal
(Lan et al., 2013)	Electrochemical oxidation	Anode: RuO ₂ and IrO ₂ DSA [®] ; room temperature; pH: 5.0; current density: 10 mA.cm ⁻² ; MnO ₂ dosage: 0.25 mM; reaction time: 2 h; electrolyte: Na ₂ SO ₄	16.9	40% and 80% glyphosate removal for electrochemical and electro-MnO ₂ process
(Kukurina et al., 2014)	Electrochemical oxidation	Anode: PbO ₂ ; room temperature; current density: 0.12 A.cm ⁻² ; reaction time: 4 h; electrolyte: H ₂ SO ₄	16.9	Completely glyphosate mineralization
(Rubí-Juárez et al., 2016)	Electrochemical oxidation	Anode: Born doped diamond (BBD); room temperature; natural pH; current density: 10-100 mA.cm ⁻² ; electrolyte: Na ₂ CO ₃ , Na ₂ SO ₄ , NaCl	100	Complete glyphosate mineralization in NaCl media
(Farinos and Ruotolo, 2017)	Electrochemical oxidation	Anode: PbO ₂ and BBD; T: 30°C; current density: 30 mA.cm ⁻² ; reaction time: 8 h	150.0	95% TOC removal
(Tran et al., 2017)	Electrochemical oxidation	Anode: Ti/PbO ₂ ; pH: 3-10; current intensity: 4.55-90.9 mA.cm ⁻² ; reaction time: 360 min; electrolyte: Na ₂ SO ₄	4.3-33.8	95.5% glyphosate removal
(Speth, 1993)	O ₃	Gas flowrate: 0.62 L.min ⁻¹ ; O ₃ : 1.0-2.9 mg.L ⁻¹	0.8-1	Complete glyphosate degradation
(Assalin et al., 2009)	O ₃	O ₃ : 14 mg.L ⁻¹ ; pH: 6.5 and 10; reaction time: 30 min	42.275	97.5% TOC reduction
(Jönsson et al., 2013)	O ₃ /H ₂ O ₂	T: 15°C; O ₃ : 0.5 and 1.0 mg.L ⁻¹ ; H ₂ O ₂ : 0.5 and 1.0 mg.L ⁻¹	0.00259-0.00365	>99% glyphosate and >85% AMPA removal

Electrochemical oxidation is one of the cleanest technologies to effectively degrade glyphosate compared to other AOPs (Villamar-Ayala et al., 2019), with high energy efficiency and easy operations (Sirés et al., 2014). And electrochemical oxidation has been reported to treat effluents with wider glyphosate concentration ranging from 16.9 to 1000 mg.L⁻¹, compared to other AOPs. Complete glyphosate mineralization has been achieved by electrochemical oxidation at glyphosate concentration less than 100 mg.L⁻¹ (Kukurina et al., 2014; Rubí-Juárez et al., 2016). Even when the initial glyphosate concentration up to 1000 mg.L⁻¹, high mineralization (91%) was also obtained by Aquino Neto and De Andrade (2009), on PuO₂ and IrO₂ dimensionally stable anode (DSA[®]). PbO₂, boron doped diamond (BDD) and Ti/PbO₂ has been also used as anode for electrochemical oxidation of glyphosate (Kukurina et al., 2014; Rubí-Juárez et al., 2016; Farinos and Ruotolo, 2017; Tran et al., 2017). Electrochemical degradation could be affected by several parameters: pH, glyphosate initial concentration, supporting electrolyte nature and concentration, electronic composition, electrolysis and current density (Aquino Neto and de Andrade, 2009; Aquino Neto and De Andrade, 2009; Moreira et al., 2017). However, some drawbacks exist during electrochemical oxidation process: the high costs related to the electrical supply, the addition of electrolytes required due to the low conductance of wastewaters and the loss of activity and the short lifetime of electrode by fouling due to the deposition of organic compounds on the surface of electrode (Sirés et al., 2014). More research should be studied to overcome these disadvantages.

Compared to other AOPs, ozonation oxidation can effectively treat glyphosate-containing wastewater at a shortest time under low concentration. Complete glyphosate degradation and 97.5% mineralization have been obtained by Speth (1993) and Assalin et al. (2009), respectively. Both high removal efficiencies of glyphosate (>99%) and AMPA (85%) were achieved with simultaneous use of O₃ and H₂O₂ under a short reaction time (Jönsson et al., 2013). However, it is generally applied to treat glyphosate-containing wastewater at low concentration rather than real glyphosate industrial wastewater. Furthermore, there are several drawbacks for ozonation which hinders its application into practice: (1) ozone is unstable under normal conditions; (2) due to its low solubility in water, special mixing techniques are needed; (3) ozone water treatment is much expensive due to the high service and maintenance; (4) high toxicity and chemical hazards; (5) harmful disinfection by-products maybe generate (Rice, 1996).

In addition, Barrett and McBride (2005) obtained 71% and 47% of glyphosate and AMPA removal efficiency by Manganese oxidation, respectively. Zhang et al. (2011) combined adsorption treatment and Fenton oxidation using the nano-metal/resin complexes as the adsorbent to treat the industrial wastewater containing glyphosate. They found that the maximum degradation rate of glyphosate (258 mg.L⁻¹) was enhanced up to 60.5%. Xing et al. (2018) reported that 100% glyphosate

removal and over 93% organic phosphorus removal for real glyphosate wastewater (containing 200-3000 mg.L⁻¹ glyphosate) was achieved by catalytic wet oxidation using modified activated carbon as a catalyst in a co-current upflow fixed bed reactor, which could be a potential method for glyphosate-containing wastewater treatment.

As can be noticed, although glyphosate-containing wastewater has been reported to be effectively treated by these above technologies which are mostly conducted at lab scale, detailed studies of the treatment of industrial wastewater polluted by glyphosate are necessary in order to scale-up to an industrial scale.

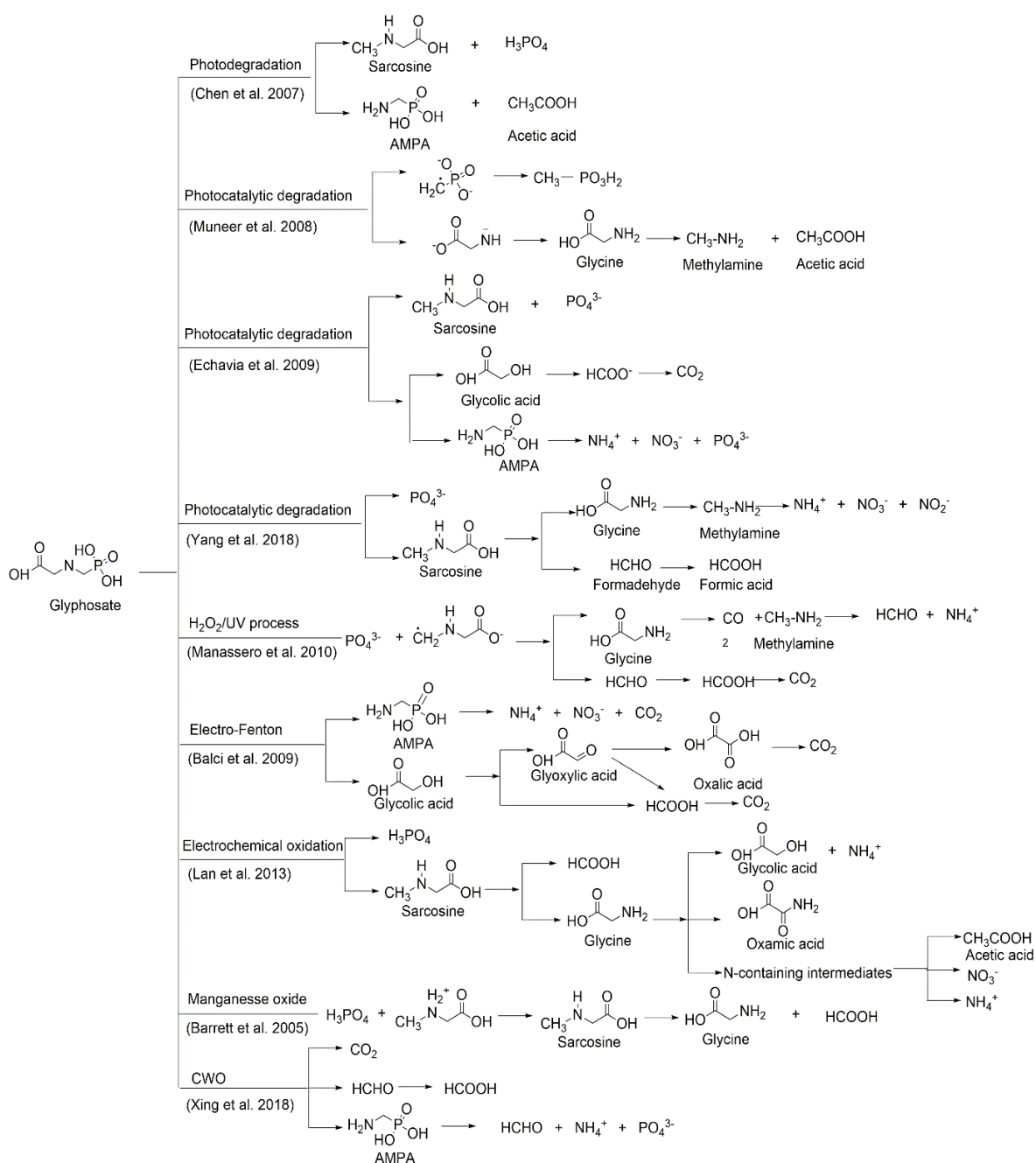


Fig. 4 The possible oxidation pathway of glyphosate under different processes.

Meanwhile, Fig. 4 summarizes the possible oxidation pathway of glyphosate under different AOPs reported in the literature. It shows that glyphosate oxidation process generally follows two mechanisms related to the cleavage of C-P and C-N bonds attributed to hydroxyl radicals. In the first case, glyphosate is attacked by hydroxyl radicals to yield sarcosine and PO_4^{3-} and to generate AMPA and glycolic acid in the second case. The two mechanisms can exist alone or together during glyphosate oxidation process. The glyphosate photo-degradation are often related to the both AMPA and sarcosine pathways, however, only sarcosine pathway during glyphosate photo-degradation is presented by Yang et al. (2018) on goethite and magnetite. This is because the formation of Fe-O-P bond in the presence of iron oxide would change the electron density distribution around the phosphorus center of glyphosate, and potentially induce the C-P bond more assailable to reactive oxygen species generated in goethite and magnetite suspension under UV irradiation (Yang et al., 2018). Besides, a few studies have proved the direct generation of glycine at high pH without the generation of sarcosine in TiO_2/UV process (Muneer and Boxall, 2008; Manassero et al., 2010). The mechanism for this phenomenon is still unclear and further research is needed. The single sarcosine pathway is also been reported in the electrochemical and Manganese oxidation of glyphosate (Barrett and McBride, 2005; Lan et al., 2013), whereas, the single AMPA pathway is found in electro-Fenton and CWO process of glyphosate (Balci et al., 2009; Xing et al., 2018). Sarcosine could be further oxidized to glycine, formaldehyde or formic acid. Glycine could be transferred to methylamine, formaldehyde, and NH_4^+ . AMPA may be further converted to formaldehyde, NH_4^+ , NO_3^- and PO_4^{3-} through the cleavage of C-P bond. Other small molecules organic compounds may also exist in the glyphosate oxidation processes, such as acetic acid and glycolic acid. Even though the possible oxidation pathways of glyphosate have been abundantly reported, the precise mechanisms are still unknown which is needed further studies.

4 Conclusions

Glyphosate, a most extensively used herbicide in the world, could accumulate and transfer in the environment, resulting in its frequent detection in surface water, groundwater, and industrial effluents. It causes several adverse effects to plants, animals, and microorganisms, and further endangers humans due to occupational exposure by agricultural practices or through the food chain. Plenty of treatment technologies have been used to effectively remove glyphosate from wastewater. AOPs is an alternative method to treat glyphosate-containing wastewater compared to physical and biological treatment. However, some problems exist for different types of treatment technologies: post-treatment needed for physical treatment, various removal efficiency and long residence time for biological treatment and high cost and incomplete mineralization for AOPs. Further work in this area is essential to develop a more effective, safe and affordable technology to degrade glyphosate.

Moreover, it is necessary to scale-up the laboratory studies for these treatment processes to an industrial scale and know the precise degradation pathways of glyphosate by different treatment methods.

Acknowledgements

This work was supported by the Chinese Scholarship Council (File No. 201604490033).

References

- Acosta-Cortés, A.G., Martínez-Ledezma, C., López-Chuken, U.J., Kaushik, G., Nimesh, S., Villarreal-Chiu, J.F., 2019. Polyphosphate recovery by a native *Bacillus cereus* strain as a direct effect of glyphosate uptake. *ISME J.* <https://doi.org/10.1038/s41396-019-0366-3>
- Acquavella, J.F., Alexander, B.H., Mandel, J.S., Gustin, C., Baker, B., Chapman, P., Bleeke, M., 2004. Glyphosate biomonitoring for farmers and their families: results from the Farm Family Exposure Study. *Environ. Health Perspect.* 112, 321–326.
- Andreotti, G., Koutros, S., Hofmann, J.N., Sandler, D.P., Lubin, J.H., Lynch, C.F., Lerro, C.C., Roos, D., J, A., Parks, C.G., Alavanja, M.C., Silverman, D.T., Freeman, B., E, L., 2018. Glyphosate Use and Cancer Incidence in the Agricultural Health Study. *JNCI J. Natl. Cancer Inst.* 110. <https://doi.org/10.1093/jnci/djx233>
- Aparicio, V.C., De Gerónimo, E., Marino, D., Primost, J., Carriquiriborde, P., Costa, J.L., 2013. Environmental fate of glyphosate and aminomethylphosphonic acid in surface waters and soil of agricultural basins. *Chemosphere* 93, 1866–1873. <https://doi.org/10.1016/j.chemosphere.2013.06.041>
- Aquino Neto, S., De Andrade, A.R., 2009. Electrochemical degradation of glyphosate formulations at DSA® anodes in chloride medium: an AOX formation study. *J. Appl. Electrochem.* 39, 1863. <https://doi.org/10.1007/s10800-009-9890-6>
- Aquino Neto, S., de Andrade, A.R., 2009. Electrooxidation of glyphosate herbicide at different DSA® compositions: pH, concentration and supporting electrolyte effect. *Electrochimica Acta* 54, 2039–2045. <https://doi.org/10.1016/j.electacta.2008.07.019>
- Aramyan, S.M., 2017. Advances in Fenton and Fenton Based Oxidation Processes for Industrial Effluent Contaminants Control-A Review. *Int. J. Environ. Sci. Nat. Resour.* 2, 1–18. <https://doi.org/10.19080/IJESNR.2017.02.555594>
- Armiliato, N., Ammar, D., Nezzi, L., Straliotto, M., Muller, Y.M.R., Nazari, E.M., 2014. Changes in Ultrastructure and Expression of Steroidogenic Factor-1 in Ovaries of Zebrafish *Danio rerio* Exposed to Glyphosate. *J. Toxicol. Environ. Health A* 77, 405–414. <https://doi.org/10.1080/15287394.2014.880393>
- Assalin, M.R., Moraes, S.G.D., Queiroz, S.C.N., Ferracini, V.L., Duran, N., 2009. Studies on degradation of glyphosate by several oxidative chemical processes: Ozonation, photolysis and heterogeneous photocatalysis. *J. Environ. Sci. Health Part B* 45, 89–94. <https://doi.org/10.1080/03601230903404598>
- Balci, B., Oturan, M.A., Oturan, N., Sirés, I., 2009. Decontamination of Aqueous Glyphosate, (Aminomethyl)phosphonic Acid, and Glufosinate Solutions by Electro-Fenton-like Process with Mn²⁺ as the Catalyst. *J. Agric. Food Chem.* 57, 4888–4894. <https://doi.org/10.1021/jf900876x>
- Balthazor, T.M., Hallas, L.E., 1986. Glyphosate-Degrading Microorganisms from Industrial Activated Sludge. *Appl. Environ. Microbiol.* 51, 432–434.
- Barbeau, C., Deschênes, L., Karamanev, D., Comeau, Y., Samson, R., 1997. Bioremediation of pentachlorophenol-contaminated soil by bioaugmentation using activated soil. *Appl. Microbiol. Biotechnol.* 48, 745–752.
- Barrett, K.A., McBride, M.B., 2005. Oxidative Degradation of Glyphosate and Aminomethylphosphonate by Manganese Oxide. *Environ. Sci. Technol.* 39, 9223–9228. <https://doi.org/10.1021/es051342d>
- Battaglin, W.A., Kolpin, D.W., Scribner, E.A., Kuivila, K.M., Sandstrom, M.W., 2005. Glyphosate, Other Herbicides, and Transformation Products in Midwestern Streams, 20021. *JAWRA J. Am. Water Resour. Assoc.* 41, 323–332. <https://doi.org/10.1111/j.1752-1688.2005.tb03738.x>
- Battaglin, W.A., Meyer, M.T., Kuivila, K.M., Dietze, J.E., 2014. Glyphosate and Its Degradation Product AMPA Occur Frequently and Widely in U.S. Soils, Surface Water, Groundwater, and Precipitation. *JAWRA J. Am. Water Resour. Assoc.* 50, 275–290. <https://doi.org/10.1111/jawr.12159>

- Battaglin, W.A., Rice, K.C., Focazio, M.J., Salmons, S., Barry, R.X., 2009. The occurrence of glyphosate, atrazine, and other pesticides in vernal pools and adjacent streams in Washington, DC, Maryland, Iowa, and Wyoming, 2005-2006. *Environ. Monit. Assess.* 155, 281–307. <https://doi.org/10.1007/s10661-008-0435-y>
- Baylis, A.D., 2000. Why glyphosate is a global herbicide: strengths, weaknesses and prospects. *Pest Manag. Sci.* 56, 299–308. [https://doi.org/10.1002/\(SICI\)1526-4998\(200004\)56:4<299::AID-PS144>3.0.CO;2-K](https://doi.org/10.1002/(SICI)1526-4998(200004)56:4<299::AID-PS144>3.0.CO;2-K)
- Benachour, N., Séralini, G.-E., 2009. Glyphosate Formulations Induce Apoptosis and Necrosis in Human Umbilical, Embryonic, and Placental Cells. *Chem. Res. Toxicol.* 22, 97–105. <https://doi.org/10.1021/tx800218n>
- Benbrook, C.M., 2016. Trends in glyphosate herbicide use in the United States and globally. *Environ. Sci. Eur.* 28, 3. <https://doi.org/10.1186/s12302-016-0070-0>
- Birch, H., Mikkelsen, P.S., Jensen, J.K., Lützhøft, H.-C.H., 2011. Micropollutants in stormwater runoff and combined sewer overflow in the Copenhagen area, Denmark. *Water Sci. Technol.* 64, 485–493. <https://doi.org/10.2166/wst.2011.687>
- Bokare, A.D., Choi, W., 2014. Review of iron-free Fenton-like systems for activating H₂O₂ in advanced oxidation processes. *J. Hazard. Mater.* 275, 121–135. <https://doi.org/10.1016/j.jhazmat.2014.04.054>
- Borggaard, O.K., Gimsing, A.L., 2008. Fate of glyphosate in soil and the possibility of leaching to ground and surface waters: a review. *Pest Manag. Sci.* 64, 441–456.
- Bujacz, B., Wiczorek, P., Krzysko-Lupicka, T., Golab, Z., Lejczak, B., Kavfarski, P., 1995. Organophosphonate Utilization by the Wild-Type Strain of *Penicillium notatum*. *Appl Env. Microbiol* 61, 2905–2910.
- Cassigneul, A., Benoit, P., Bergheaud, V., Dumeny, V., Etiévant, V., Goubard, Y., Maylin, A., Justes, E., Alletto, L., 2016. Fate of glyphosate and degradates in cover crop residues and underlying soil: A laboratory study. *Sci. Total Environ.* 545–546, 582–590. <https://doi.org/10.1016/j.scitotenv.2015.12.052>
- Castro, J.V., Peralba, M.C.R., Ayub, M.A.Z., 2007. Biodegradation of the herbicide glyphosate by filamentous fungi in platform shaker and batch bioreactor. *J. Environ. Sci. Health Part B* 42, 883–886. <https://doi.org/10.1080/03601230701623290>
- Cattani, D., Cesconetto, P.A., Tavares, M.K., Parisotto, E.B., De Oliveira, P.A., Rieg, C.E.H., Leite, M.C., Prediger, R.D.S., Wendt, N.C., Razzera, G., Filho, D.W., Zamoner, A., 2017. Developmental exposure to glyphosate-based herbicide and depressive-like behavior in adult offspring: Implication of glutamate excitotoxicity and oxidative stress. *Toxicology* 387, 67–80. <https://doi.org/10.1016/j.tox.2017.06.001>
- Chang, F., Simcik, M.F., Capel, P.D., 2011. Occurrence and fate of the herbicide glyphosate and its degradate aminomethylphosphonic acid in the atmosphere. *Environ. Toxicol. Chem.* 30, 548–555. <https://doi.org/10.1002/etc.431>
- Chen, F., Zhou, C., Li, G., Peng, F., 2016. Thermodynamics and kinetics of glyphosate adsorption on resin D301. *Arab. J. Chem.* 9, S1665–S1669. <https://doi.org/10.1016/j.arabjc.2012.04.014>
- Chen, S., Liu, Y., 2007. Study on the photocatalytic degradation of glyphosate by TiO₂ photocatalyst. *Chemosphere* 67, 1010–1017. <https://doi.org/10.1016/j.chemosphere.2006.10.054>
- Chen, S., Sun, D., Chung, J.-S., 2007. Treatment of pesticide wastewater by moving-bed biofilm reactor combined with Fenton-coagulation pretreatment. *J. Hazard. Mater.* 144, 577–584. <https://doi.org/10.1016/j.jhazmat.2006.10.075>
- Chen, Y., Wu, F., Lin, Y., Deng, N., Bazhin, N., Glebov, E., 2007. Photodegradation of glyphosate in the ferrioxalate system. *J. Hazard. Mater.* 148, 360–365. <https://doi.org/10.1016/j.jhazmat.2007.02.044>
- Coupe, R.H., Kalkhoff, S.J., Capel, P.D., Gregoire, C., 2012. Fate and transport of glyphosate and aminomethylphosphonic acid in surface waters of agricultural basins. *Pest Manag. Sci.* 68, 16–30. <https://doi.org/10.1002/ps.2212>
- da Silva, A.S., Fernandes, F.C.B., Tognolli, J.O., Pezza, L., Pezza, H.R., 2011. A simple and green analytical method for determination of glyphosate in commercial formulations and water by diffuse reflectance spectroscopy. *Spectrochim. Acta. A. Mol. Biomol. Spectrosc.* 79, 1881–1885. <https://doi.org/10.1016/j.saa.2011.05.081>
- de Lucas, A., Rodríguez, L., Villaseñor, J., Fernández, F.J., 2005. Biodegradation kinetics of stored wastewater substrates by a mixed microbial culture. *Biochem. Eng. J., Engineering Bioreaction Systems: A Spanish Perspective* 26, 191–197. <https://doi.org/10.1016/j.bej.2005.04.015>

- Dick, R.E., Quinn, J.P., 1995. Control of glyphosate uptake and metabolism in *Pseudomonas* sp. 4ASW. *FEMS Microbiol. Lett.* 134, 177–182.
- Divyapriya, G., Nambi, I.M., Senthilnathan, J., 2016. Nanocatalysts in Fenton Based Advanced Oxidation Process for Water and Wastewater Treatment. *J. Bionanoscience* 10, 356–368. <https://doi.org/info:doi/10.1166/jbns.2016.1387>
- Duke, S.O., Powles, S.B., 2008. Glyphosate: a once-in-a-century herbicide. *Pest Manag. Sci.* 64, 319–325. <https://doi.org/10.1002/ps.1518>
- Echavia, G.R.M., Matzusawa, F., Negishi, N., 2009. Photocatalytic degradation of organophosphate and phosphonoglycine pesticides using TiO₂ immobilized on silica gel. *Chemosphere* 76, 595–600. <https://doi.org/10.1016/j.chemosphere.2009.04.055>
- Emerging substances | NORMAN [WWW Document], n.d. URL <https://www.norman-network.net/?q=node/19> (accessed 9.5.18).
- Ermakova, I.T., Kiseleva, N.I., Shushkova, T., Zharikov, M., Zharikov, G.A., Leontievsky, A.A., 2010. Bioremediation of glyphosate-contaminated soils. *Appl. Microbiol. Biotechnol.* 88, 585–594. <https://doi.org/10.1007/s00253-010-2775-0>
- Ermakova, I.T., Shushkova, T.V., Sviridov, A.V., Zelenkova, N.F., Vinokurova, N.G., Baskunov, B.P., Leontievsky, A.A., 2017. Organophosphonates utilization by soil strains of *Ochrobactrum anthropi* and *Achromobacter* sp. *Arch. Microbiol.* 199, 665–675. <https://doi.org/10.1007/s00203-017-1343-8>
- Fan, J., Yang, G., Zhao, H., Shi, G., Geng, Y., Hou, T., Tao, K., 2012. Isolation, identification and characterization of a glyphosate-degrading bacterium, *Bacillus cereus* CB4, from soil. *J. Gen. Appl. Microbiol.* 58, 263–271.
- Farinos, R.M., Ruotolo, L.A.M., 2017. Comparison of the electrooxidation performance of three-dimensional RVC/PbO₂ and boron-doped diamond electrodes. *Electrochimica Acta* 224, 32–39. <https://doi.org/10.1016/j.electacta.2016.12.025>
- Firdous, S., Iqbal, S., Anwar, S., 2017. Optimization and Modeling of Glyphosate Biodegradation by a Novel *Comamonas odontotermitis* P2 Through Response Surface Methodology. *Pedosphere*. [https://doi.org/10.1016/S1002-0160\(17\)60381-3](https://doi.org/10.1016/S1002-0160(17)60381-3)
- Firdous, S., Iqbal, S., Anwar, S., Jabeen, H., 2018. Identification and analysis of 5-enolpyruvylshikimate-3-phosphate synthase (EPSPS) gene from glyphosate-resistant *Ochrobactrum intermedium* Sq20. *Pest Manag. Sci.* 74, 1184–1196. <https://doi.org/10.1002/ps.4624>
- Geissen, V., Mol, H., Klumpp, E., Umlauf, G., Nadal, M., van der Ploeg, M., van de Zee, S.E.A.T.M., Ritsema, C.J., 2015. Emerging pollutants in the environment: A challenge for water resource management. *Int. Soil Water Conserv. Res.* 3, 57–65. <https://doi.org/10.1016/j.iswcr.2015.03.002>
- Giesy, J.P., Dobson, S., Solomon, K.R., 2000. Ecotoxicological Risk Assessment for Roundup® Herbicide, in: Ware, G.W. (Ed.), *Reviews of Environmental Contamination and Toxicology: Continuation of Residue Reviews, Reviews of Environmental Contamination and Toxicology*. Springer New York, New York, NY, pp. 35–120. https://doi.org/10.1007/978-1-4612-1156-3_2
- Gillezeau, C., van Gerwen, M., Shaffer, R.M., Rana, I., Zhang, L., Sheppard, L., Taioli, E., 2019. The evidence of human exposure to glyphosate: a review. *Environ. Health* 18, 2. <https://doi.org/10.1186/s12940-018-0435-5>
- Glyphosate Market Share, Size - Industry Trends Report 2024 [WWW Document], n.d. URL <https://www.gminsights.com/industry-analysis/glyphosate-market> (accessed 9.5.18).
- Glyphosate use worldwide 1994-2014 | Statistic [WWW Document], n.d. . Statista. URL <https://www.statista.com/statistics/567250/glyphosate-use-worldwide/> (accessed 9.5.18).
- Gomes, M.P., Le Manac’h, S.G., Maccario, S., Labrecque, M., Lucotte, M., Juneau, P., 2016. Differential effects of glyphosate and aminomethylphosphonic acid (AMPA) on photosynthesis and chlorophyll metabolism in willow plants. *Pestic. Biochem. Physiol.* 130, 65–70. <https://doi.org/10.1016/j.pestbp.2015.11.010>
- Guo, L., Cao, Y., Jin, K., Han, L., Li, G., Liu, J., Ma, S., 2018. Adsorption Characteristics of Glyphosate on Cross-Linked Amino-Starch. *J. Chem. Eng. Data* 63, 422–428. <https://doi.org/10.1021/acs.jced.7b00842>
- Hadi, F., Mousavi, A., Noghabi, K.A., Tabar, H.G., Salmanian, A.H., 2013. New bacterial strain of the genus *Ochrobactrum* with glyphosate-degrading activity. *J. Environ. Sci. Health Part B* 48, 208–213. <https://doi.org/10.1080/03601234.2013.730319>
- HALLAS, L.E., ADAMS, W.J., 1992. Glyphosate Degradation by Immobilized Bacteria: Field Studies with Industrial Wastewater Effluent. *APPL Env. MICROBIOL* 58, 5.

- Hao, O.J., Kim, M.H., Seagren, E.A., Kim, H., 2002. Kinetics of phenol and chlorophenol utilization by *Acinetobacter* species. *Chemosphere* 46, 797–807. [https://doi.org/10.1016/S0045-6535\(01\)00182-5](https://doi.org/10.1016/S0045-6535(01)00182-5)
- Heitkamp, M.A., Adams, W.J., Hallas, L.E., 1992. Glyphosate degradation by immobilized bacteria: laboratory studies showing feasibility for glyphosate removal from waste water. *Can. J. Microbiol.* 38, 921–928. <https://doi.org/10.1139/m92-149>
- Helander, M., Saloniemi, I., Saikkonen, K., 2012. Glyphosate in northern ecosystems. *Trends Plant Sci.* 17, 569–574. <https://doi.org/10.1016/j.tplants.2012.05.008>
- Herath, I., Kumarathilaka, P., Al-Wabel, M.I., Abduljabbar, A., Ahmad, M., Usman, A.R.A., Vithanage, M., 2016. Mechanistic modeling of glyphosate interaction with rice husk derived engineered biochar. *Microporous Mesoporous Mater.* 225, 280–288. <https://doi.org/10.1016/j.micromeso.2016.01.017>
- Hu, Y.S., Zhao, Y.Q., Sorohan, B., 2011. Removal of glyphosate from aqueous environment by adsorption using water industrial residual. *Desalination* 271, 150–156. <https://doi.org/10.1016/j.desal.2010.12.014>
- Huber, D.M., Cheng, M.W., Winsor, B.A., 2005. Association of severe *Corynespora* root rot of soybean with glyphosate-killed giant ragweed. *Phytopathology* 95, S45.
- Humphries, Dave., Humphries, D., Anderson, A.-M., Byrtus, G., Council, A.R., Alberta, 2005. Glyphosate residues in Alberta's atmospheric deposition, soils and surface waters /. Alberta Environment, [Edmonton] :
- Huston, P.L., Pignatello, J.J., 1999. Degradation of selected pesticide active ingredients and commercial formulations in water by the photo-assisted Fenton reaction. *Water Res.* 33, 1238–1246. [https://doi.org/10.1016/S0043-1354\(98\)00330-3](https://doi.org/10.1016/S0043-1354(98)00330-3)
- Jacob, G.S., 1988. Metabolism of Glyphosate in *Pseudomonas* sp. Strain LBr. *Appl Env. Microbiol* 54, 2953–2958.
- Jia, D.M., Li, C.H., Li, A.M., 2017. Effective removal of glyphosate from water by resin-supported double valent nano-sized hydroxyl iron oxide. *RSC Adv.* 7, 24430–24437. <https://doi.org/10.1039/C7RA03418K>
- Jönsson, J., Camm, R., Hall, T., 2013. Removal and degradation of glyphosate in water treatment: a review. *J. Water Supply Res. Technol.-Aqua* 62, 395–408. <https://doi.org/10.2166/aqua.2013.080>
- Junges, C.M., Vidal, E.E., Attademo, A.M., Mariani, M.L., Cardell, L., Negro, A.C., Cassano, A., Peltzer, P.M., Lajmanovich, R.C., Zalazar, C.S., 2013. Effectiveness evaluation of glyphosate oxidation employing the H₂O₂/UVC process: Toxicity assays with *Vibrio fischeri* and *Rhinella arenarum* tadpoles. *J. Environ. Sci. Health Part B* 48, 163–170. <https://doi.org/10.1080/03601234.2013.730011>
- Kataoka, H., Ryu, S., Sakiyama, N., Makita, M., 1996. Simple and rapid determination of the herbicides glyphosate and glufosinate in river water, soil and carrot samples by gas chromatography with flame photometric detection. *J. Chromatogr. A* 726, 253–258. [https://doi.org/10.1016/0021-9673\(95\)01071-8](https://doi.org/10.1016/0021-9673(95)01071-8)
- Kier, L.D., Kirkland, D.J., 2013. Review of genotoxicity studies of glyphosate and glyphosate-based formulations. *Crit. Rev. Toxicol.* 43, 283–315. <https://doi.org/10.3109/10408444.2013.770820>
- Kishore, G.M., Jacob, G.S., 1987. Degradation of Glyphosate by *Pseudomonas* sp. PG2982 via a Sarcosine Intermediate. *J. Biol. Chem.* 262, 12164–12168.
- Klimek, M., Lejczak, B., Kafarski, P., Forlani, G., 2001. Metabolism of the phosphonate herbicide glyphosate by a non-nitrate-utilizing strain of *Penicillium chrysogenum*. *Pest Manag. Sci.* 57, 815–821. <https://doi.org/10.1002/ps.366>
- Kryuchkova, Y.V., Burygin, G.L., Gogoleva, N.E., Gogolev, Y.V., Chernyshova, M.P., Makarov, O.E., Fedorov, E.E., Turkovskaya, O.V., 2014. Isolation and characterization of a glyphosate-degrading rhizosphere strain, *Enterobacter cloacae* K7. *Microbiol. Res.* 169, 99–105. <https://doi.org/10.1016/j.micres.2013.03.002>
- Krzyśko-Lupicka, T., Strof, W., Kubś, K., Skorupa, M., Wieczorek, P., Lejczak, B., Kafarski, P., 1997. The ability of soil-borne fungi to degrade organophosphonate carbon-to-phosphorus bonds. *Appl. Microbiol. Biotechnol.* 48, 549–552. <https://doi.org/10.1007/s002530051095>
- Kukurina, O., Elemesova, Z., Syskina, A., 2014. Mineralization of Organophosphorous Pesticides by Electro-generated Oxidants. *Procedia Chem.*, XV International Scientific Conference “Chemistry and Chemical Engineering in XXI century” dedicated to Professor L.P. Kulyov 10, 209–216. <https://doi.org/10.1016/j.proche.2014.10.036>
- Kwiatkowska, M., Huras, B., Bukowska, B., 2014. The effect of metabolites and impurities of glyphosate on human erythrocytes (in vitro). *Pestic. Biochem. Physiol.* 109, 34–43. <https://doi.org/10.1016/j.pestbp.2014.01.003>

- Kwiatkowska, M., Reszka, E., Woźniak, K., Jabłońska, E., Michałowicz, J., Bukowska, B., 2017. DNA damage and methylation induced by glyphosate in human peripheral blood mononuclear cells (in vitro study). *Food Chem. Toxicol. Int. J. Publ. Br. Ind. Biol. Res. Assoc.* 105, 93–98. <https://doi.org/10.1016/j.fct.2017.03.051>
- Laitinen, P., Rämö, S., Siimes, K., 2007. Glyphosate translocation from plants to soil – does this constitute a significant proportion of residues in soil? *Plant Soil* 300, 51–60. <https://doi.org/10.1007/s11104-007-9387-1>
- Lan, H., He, W., Wang, A., Liu, R., Liu, H., Qu, J., Huang, C.P., 2016. An activated carbon fiber cathode for the degradation of glyphosate in aqueous solutions by the Electro-Fenton mode: Optimal operational conditions and the deposition of iron on cathode on electrode reusability. *Water Res.* 105, 575–582. <https://doi.org/10.1016/j.watres.2016.09.036>
- Lan, H., Jiao, Z., Zhao, X., He, W., Wang, A., Liu, H., Liu, R., Qu, J., 2013. Removal of glyphosate from water by electrochemically assisted MnO₂ oxidation process. *Sep. Purif. Technol.* 117, 30–34. <https://doi.org/10.1016/j.seppur.2013.04.012>
- Lerbs, W., Stock, M., Parthier, B., 1990. Physiological aspects of glyphosate degradation in *Alcaligenes* spec. strain GL. *Arch. Microbiol.* 153, 146–150. <https://doi.org/10.1007/BF00247812>
- Li, F., Wang, Y., Yang, Q., Evans, D.G., Forano, C., Duan, X., 2005. Study on adsorption of glyphosate (N-phosphonomethyl glycine) pesticide on MgAl-layered double hydroxides in aqueous solution. *J. Hazard. Mater.* 125, 89–95. <https://doi.org/10.1016/j.jhazmat.2005.04.037>
- Liao, H., Tan, B., Ke, M., Li, Z., Lu, J., 2009. Pretreatment of GLyphosate Wastewater with Fenton Reagent. *Technol. Dev. Chem. Ind.* 38.
- Lin, L., Zhang, X.J., Xiao, G.Q., Xiong, X., 2012. Photocatalytic Degradation Glyphosate with Cerium and Nitrogen Co-Doped TiO₂ under Visible Irradiation. *Adv. Mater. Res.* 430–432, 1048–1051. <https://doi.org/10.4028/www.scientific.net/AMR.430-432.1048>
- Liu, C.M., McLean, P.A., Sookdeo, C.C., Cannon, F.C., 1991. Degradation of the Herbicide Glyphosate by Members of the Family Rhizobiaceae. *APPL Env. MICROBIOL* 57, 1799–1804.
- Liu, Z.Y., Xie, M., Ni, F., Xu, Y.H., 2012. Nanofiltration process of glyphosate simulated wastewater. *Water Sci. Technol.* 65, 816–822. <https://doi.org/10.2166/wst.2012.808>
- López, A., Coll, A., Lescano, M., Zalazar, C., 2018. Advanced oxidation of commercial herbicides mixture: experimental design and phytotoxicity evaluation. *Environ. Sci. Pollut. Res.* 25, 21393–21402. <https://doi.org/10.1007/s11356-017-9041-2>
- Mackay, D., Shiu, W.Y., Ma, K.C., Lee, S.C., 2006. Handbook of Physical-Chemical Properties and Environmental Fate for Organic Chemicals (pp.4161). CRC Press, Boca Raton, FL.
- Mahler, B.J., Van Metre, P.C., Burley, T.E., Loftin, K.A., Meyer, M.T., Nowell, L.H., 2017. Similarities and differences in occurrence and temporal fluctuations in glyphosate and atrazine in small Midwestern streams (USA) during the 2013 growing season. *Sci. Total Environ.* 579, 149–158. <https://doi.org/10.1016/j.scitotenv.2016.10.236>
- Malato, S., Blanco, J., Cáceres, J., Fernández-Alba, A.R., Agüera, A., Rodríguez, A., 2002. Photocatalytic treatment of water-soluble pesticides by photo-Fenton and TiO₂ using solar energy. *Catal. Today* 76, 209–220. [https://doi.org/10.1016/S0920-5861\(02\)00220-1](https://doi.org/10.1016/S0920-5861(02)00220-1)
- Manassero, A., Passalia, C., Negro, A.C., Cassano, A.E., Zalazar, C.S., 2010. Glyphosate degradation in water employing the H₂O₂/UVC process. *Water Res.* 44, 3875–3882. <https://doi.org/10.1016/j.watres.2010.05.004>
- Manogaran, M., Shukor, M.Y., Yasid, N.A., Johari, W.L.W., Ahmad, S.A., 2017. Isolation and characterisation of glyphosate-degrading bacteria isolated from local soils in Malaysia. *Rendiconti Lincei* 28, 471–479. <https://doi.org/10.1007/s12210-017-0620-4>
- Maqueda, C., Undabeytia, T., Villaverde, J., Morillo, E., 2017. Behaviour of glyphosate in a reservoir and the surrounding agricultural soils. *Sci. Total Environ.* 593–594, 787–795. <https://doi.org/10.1016/j.scitotenv.2017.03.202>
- Mayakaduwa, S.S., Kumarathilaka, P., Herath, I., Ahmad, M., Al-Wabel, M., Ok, Y.S., Usman, A., Abduljabbar, A., Vithanage, M., 2016. Equilibrium and kinetic mechanisms of woody biochar on aqueous glyphosate removal. *Chemosphere* 144, 2516–2521. <https://doi.org/10.1016/j.chemosphere.2015.07.080>
- McAuliffe, K.S., Hallas, L.E., Kulpa, C.F., 1990. Glyphosate degradation by *Agrobacterium radiobacter* isolated from activated sludge. *J. Ind. Microbiol.* 6, 219–221. <https://doi.org/10.1007/BF01577700>

- McQueen, H., Callan, A.C., Hinwood, A.L., 2012. Estimating maternal and prenatal exposure to glyphosate in the community setting. *Int. J. Hyg. Environ. Health* 215, 570–576. <https://doi.org/10.1016/j.ijheh.2011.12.002>
- Menéndez-Helman, R.J., Ferreyroa, G.V., dos Santos Afonso, M., Salibián, A., 2012. Glyphosate as an acetylcholinesterase inhibitor in *Cnesterodon decemmaculatus*. *Bull. Environ. Contam. Toxicol.* 88, 6–9. <https://doi.org/10.1007/s00128-011-0423-8>
- Mercurio, P., Flores, F., Mueller, J.F., Carter, S., Negri, A.P., 2014. Glyphosate persistence in seawater. *Mar. Pollut. Bull.* 85, 385–390. <https://doi.org/10.1016/j.marpolbul.2014.01.021>
- Mesnage, R., Defarge, N., Spiroux de Vendômois, J., Séralini, G.E., 2015. Potential toxic effects of glyphosate and its commercial formulations below regulatory limits. *Food Chem. Toxicol.* 84, 133–153. <https://doi.org/10.1016/j.fct.2015.08.012>
- Moneke, A.N., Okpala, G.N., Anyanwu, C.U., 2010. Biodegradation of glyphosate herbicide in vitro using bacterial isolates from four rice fields. *Afr. J. Biotechnol.* 9, 4067–4074.
- Moreira, F.C., Boaventura, R.A.R., Brillas, E., Vilar, V.J.P., 2017. Electrochemical advanced oxidation processes: A review on their application to synthetic and real wastewaters. *Appl. Catal. B Environ.* 202, 217–261. <https://doi.org/10.1016/j.apcatb.2016.08.037>
- Mörtl, M., Németh, G., Juracek, J., Darvas, B., Kamp, L., Rubio, F., Székács, A., 2013. Determination of glyphosate residues in Hungarian water samples by immunoassay. *Microchem. J., XIV Hungarian - Italian Symposium on Spectrochemistry: Analytical Techniques and Preservation of Natural Resources, Sumeg (Hungary), October 5-7, 2011* 107, 143–151. <https://doi.org/10.1016/j.microc.2012.05.021>
- Mota, A.L.N., Albuquerque, L.F., Beltrame, L.T.C., Chiavone-Filho, O., Jr, A.M., Nascimento, C.A.O., 2008. ADVANCED OXIDATION PROCESSES AND THEIR APPLICATION IN THE PETROLEUM INDUSTRY: A REVIEW. *Braz. J. Pet. GAS* 2, 21.
- Muneer, M., Boxall, C., 2008. Photocatalyzed Degradation of a Pesticide Derivative Glyphosate in Aqueous Suspensions of Titanium Dioxide. *Int. J. Photoenergy.* <https://doi.org/10.1155/2008/197346>
- Nourouzi, M.M., Chuah, T.G., Choong, T.S.Y., 2010. Adsorption of glyphosate onto activated carbon derived from waste newspaper. *Desalination Water Treat.* 24, 321–326. <https://doi.org/10.5004/dwt.2010.1461>
- Nourouzi, M.M., Chuah, G.T., Choong, T.S.Y., Rabier, F., 2012. Modeling biodegradation and kinetics of glyphosate by artificial neural network: *Journal of Environmental Science and Health, Part B: Vol 47, No 5. J. Environ. Sci. Health Part B* 47, 455–465.
- Obojska, A., Lejczak, B., Kubrak, M., 1999. Degradation of phosphonates by streptomycete isolates. *Appl. Microbiol. Biotechnol.* 51, 872–876. <https://doi.org/10.1007/s002530051476>
- Obojska, A., Ternan, N.G., Lejczak, B., Kafarski, P., McMullan, G., 2002. Organophosphonate Utilization by the Thermophile *Geobacillus caldoxylosilyticus* T20. *Appl. Environ. Microbiol.* 68, 2081–2084. <https://doi.org/10.1128/AEM.68.4.2081-2084.2002>
- Okada, E., Costa, J.L., Bedmar, F., 2016. Adsorption and mobility of glyphosate in different soils under no-till and conventional tillage. *Geoderma* 263, 78–85. <https://doi.org/10.1016/j.geoderma.2015.09.009>
- Oliveira, G.C., Mocellini, S.K., Castilho, M., Terezo, A.J., Possavatz, J., Magalhães, M.R.L., Dores, E.F.G.C., 2012. Biosensor based on atemoya peroxidase immobilised on modified nanoclay for glyphosate biomonitoring. *Talanta* 98, 130–136. <https://doi.org/10.1016/j.talanta.2012.06.059>
- Paz-y-Miño, C., Sánchez, M.E., Arévalo, M., Muñoz, M.J., Witte, T., De-la-Carrera, G.O., Leone, P.E., 2007. Evaluation of DNA damage in an Ecuadorian population exposed to glyphosate. *Genet. Mol. Biol.* 30, 456–460. <https://doi.org/10.1590/S1415-47572007000300026>
- Peñaloza-Vazquez, A., Mena, G.L., Herrera-Estrella, L., Bailey, A.M., 1995. Cloning and Sequencing of the Genes Involved in Glyphosate Utilization by *Pseudomonas pseudomallei*. *APPL ENV. MICROBIOL* 61, 6.
- Pipke, R., Amrhein, N., 1988. Degradation of the Phosphonate Herbicide Glyphosate by *Arthrobacter atrocyaneus* ATCC 13752. *APPL ENV. MICROBIOL* 54, 1293–1296.
- Pipke, R., Amrhein, N., Jacob, G.S., Schaefer, J., Kishore, G.M., 1987. Metabolism of glyphosate in an *Arthrobacter* sp. GLP-1. *Eur. J. Biochem.* 165, 267–273. <https://doi.org/10.1111/j.1432-1033.1987.tb11437.x>
- Poiger, T., Buerge, I.J., Bächli, A., Müller, M.D., Balmer, M.E., 2017. Occurrence of the herbicide glyphosate and its metabolite AMPA in surface waters in Switzerland determined with on-line solid phase extraction LC-MS/MS. *Environ. Sci. Pollut. Res. Int.* 24, 1588–1596. <https://doi.org/10.1007/s11356-016-7835-2>

- Rendon-von Osten, J., Dzul-Caamal, R., 2017. Glyphosate Residues in Groundwater, Drinking Water and Urine of Subsistence Farmers from Intensive Agriculture Localities: A Survey in Hopelchén, Campeche, Mexico. *Int. J. Environ. Res. Public Health* 14. <https://doi.org/10.3390/ijerph14060595>
- Rice, R.G., 1996. Applications of ozone for industrial wastewater treatment — A review. *Ozone Sci. Eng.* 18, 477–515. <https://doi.org/10.1080/01919512.1997.10382859>
- Richard, S., Moslemi, S., Sipahutar, H., Benachour, N., Seralini, G.-E., 2005. Differential Effects of Glyphosate and Roundup on Human Placental Cells and Aromatase. *Environ. Health Perspect.* 113, 716–720. <https://doi.org/10.1289/ehp.7728>
- Rissouli, L., Benicha, M., Chafik, T., Chabbi, M., 2017. Decontamination of water polluted with pesticide using biopolymers: Adsorption of glyphosate by chitin and chitosan. *J. Mater. Environ. Sci.* 8, 4544–4549. <https://doi.org/10.26872/jmes.2017.8.12.479>
- Rodrigues, L. de B., Oliveira, R. de, Abe, F.R., Brito, L.B., Moura, D.S., Valadares, M.C., Grisolia, C.K., Oliveira, D.P. de, Oliveira, G.A.R. de, 2017. Ecotoxicological assessment of glyphosate-based herbicides: Effects on different organisms. *Environ. Toxicol. Chem.* 36, 1755–1763. <https://doi.org/10.1002/etc.3580>
- Romero, D.M., Ríos de Molina, M.C., Juárez, Á.B., 2011. Oxidative stress induced by a commercial glyphosate formulation in a tolerant strain of *Chlorella kessleri*. *Ecotoxicol. Environ. Saf.* 74, 741–747. <https://doi.org/10.1016/j.ecoenv.2010.10.034>
- Rosenbom, A.E., 2010. The Danish Pesticide Leaching Assessment Programme.
- Rubí-Juárez, H., Cotillas, S., Sáez, C., Cañizares, P., Barrera-Díaz, C., Rodrigo, M.A., 2016. Removal of herbicide glyphosate by conductive-diamond electrochemical oxidation. *Appl. Catal. B Environ.* 188, 305–312. <https://doi.org/10.1016/j.apcatb.2016.02.006>
- Saitúa, H., Giannini, F., Padilla, A.P., 2012. Drinking water obtaining by nanofiltration from waters contaminated with glyphosate formulations: Process evaluation by means of toxicity tests and studies on operating parameters. *J. Hazard. Mater.* 227–228, 204–210. <https://doi.org/10.1016/j.jhazmat.2012.05.035>
- Salman, J.M., Abid, F.M., Muhammed, A.A., 2012. Batch Study for Pesticide Glyphosate Adsorption onto Palm Oil Fronds Activated Carbon. *Asian J. Chem.* 24, 5646–5648.
- Sanchís, J., Kantiani, L., Llorca, M., Rubio, F., Ginebreda, A., Fraile, J., Garrido, T., Farré, M., 2012. Determination of glyphosate in groundwater samples using an ultrasensitive immunoassay and confirmation by on-line solid-phase extraction followed by liquid chromatography coupled to tandem mass spectrometry. *Anal. Bioanal. Chem.* 402, 2335–2345. <https://doi.org/10.1007/s00216-011-5541-y>
- Sandrini, J.Z., Rola, R.C., Lopes, F.M., Buffon, H.F., Freitas, M.M., Martins, C. de M.G., da Rosa, C.E., 2013. Effects of glyphosate on cholinesterase activity of the mussel *Perna perna* and the fish *Danio rerio* and *Jenynsia multidentata*: in vitro studies. *Aquat. Toxicol. Amst. Neth.* 130–131, 171–173. <https://doi.org/10.1016/j.aquatox.2013.01.006>
- Sandun, K.V., Bandara, N., Amarasinghe, U., 2015. Effect of glyphosate-based herbicide, Roundup™ on territory deference of male *Oreochromis mossambicus* (Osteichthyes, Cichlidae) associated with mating behaviour. *Sri Lanka J. Aquat. Sci.* 20. <https://doi.org/10.4038/sljas.v20i1.7451>
- Sarkar, S., Das, R., 2017. PVP capped silver nanocubes assisted removal of glyphosate from water—A photoluminescence study. *J. Hazard. Mater.* 339, 54–62. <https://doi.org/10.1016/j.jhazmat.2017.06.014>
- Saunders, L.E., Pezeshki, R., 2015. Glyphosate in Runoff Waters and in the Root-Zone: A Review. *Toxics* 3, 462–480. <https://doi.org/10.3390/toxics3040462>
- Sauvé, S., Desrosiers, M., 2014. A review of what is an emerging contaminant. *Chem. Cent. J.* 8, 15. <https://doi.org/10.1186/1752-153X-8-15>
- Schoonenberg Kegel, F., Rietman, B.M., Verliefde, A.R.D., 2010. Reverse osmosis followed by activated carbon filtration for efficient removal of organic micropollutants from river bank filtrate. *Water Sci. Technol.* 61, 2603–2610. <https://doi.org/10.2166/wst.2010.166>
- Selvapandiyan, A., Bhatnagar, R.K., 1994. Isolation of a glyphosate-metabolising *Pseudomonas*: detection, partial purification and localisation of carbon-phosphorus lyase. *Appl Microbiol Biotechnol* 40, 876–882.
- Sharifi, Y., Pourbabaei, A.A., Javadi, A., Abdolmohammadi, M.H., Saffari, M., Morovvati, A., 2015. Biodegradation of glyphosate herbicide by *Salinicoccus* spp isolated from Qom Hoze-soltan lake, Iran. *Environ. Health Eng. Manag. J.* 2, 31–36.

- Shushkova, T.V., Vinokurova, N.G., Baskunov, B.P., Zelenkova, N.F., Sviridov, A.V., Ermakova, I.T., Leontievsky, A.A., 2016. Glyphosate acetylation as a specific trait of *Achromobacter* sp. Kg 16 physiology. *Appl. Microbiol. Biotechnol.* 100, 847–855. <https://doi.org/10.1007/s00253-015-7084-1>
- Sidoli, P., Baran, N., Angulo-Jaramillo, R., 2016. Glyphosate and AMPA adsorption in soils: laboratory experiments and pedotransfer rules. *Environ. Sci. Pollut. Res. Int.* 23, 5733–5742. <https://doi.org/10.1007/s11356-015-5796-5>
- Singh, R.K., Kumar, Shashi, Kumar, Surendra, Kumar, A., 2008. Biodegradation kinetic studies for the removal of p-cresol from wastewater using *Gliomastix indicus* MTCC 3869. *Biochem. Eng. J.* 40, 293–303. <https://doi.org/10.1016/j.bej.2007.12.015>
- Sirés, I., Brillas, E., Oturan, M.A., Rodrigo, M.A., Panizza, M., 2014. Electrochemical advanced oxidation processes: today and tomorrow. A review. *Environ. Sci. Pollut. Res.* 21, 8336–8367. <https://doi.org/10.1007/s11356-014-2783-1>
- Skark, C., Zullei-seibert, N., Schöttler, U., Schlett, C., 1998. The Occurrence of Glyphosate in Surface Water. *Int. J. Environ. Anal. Chem.* 70, 93–104. <https://doi.org/10.1080/03067319808032607>
- Song, J., Li, X.-M., Figoli, A., Huang, H., Pan, C., He, T., Jiang, B., 2013. Composite hollow fiber nanofiltration membranes for recovery of glyphosate from saline wastewater. *Water Res.* 47, 2065–2074. <https://doi.org/10.1016/j.watres.2013.01.032>
- Songa, E.A., Somerset, V.S., Waryo, T., Baker, P.G.L., Iwuoha, E.I., 2009. Amperometric nanobiosensor for quantitative determination of glyphosate and glufosinate residues in corn samples. *Pure Appl. Chem.* 81, 123–139. <https://doi.org/10.1351/PAC-CON-08-01-15>
- Souza, D.R. de, Trovó, A.G., Filho, A., R, N., Silva, M.A.A., Machado, A.E.H., 2013. Degradation of the commercial herbicide glyphosate by photo-fenton process: evaluation of kinetic parameters and toxicity. *J. Braz. Chem. Soc.* 24, 1451–1460. <https://doi.org/10.5935/0103-5053.20130185>
- Speth, T.F., 1993. Glyphosate Removal from Drinking Water. *J. Environ. Eng.* 119, 1139–1157. [https://doi.org/10.1061/\(ASCE\)0733-9372\(1993\)119:6\(1139\)](https://doi.org/10.1061/(ASCE)0733-9372(1993)119:6(1139))
- Sviridov, A.V., Shushkova, T.V., Ermakova, I.T., Ivanova, E.V., Epiktetov, D.O., Leontievsky, A.A., 2015. Microbial degradation of glyphosate herbicides (Review). *Appl. Biochem. Microbiol.* 51, 188–195. <https://doi.org/10.1134/S0003683815020209>
- Sviridov, A.V., Shushkova, T.V., Ermakova, I.T., Ivanova, E.V., Leontievsky, A.A., 2014. Glyphosate: Safety Risks, Biodegradation, and Bioremediation, in: Cao, G., Orrù, R. (Eds.), *Current Environmental Issues and Challenges*. Springer Netherlands, Dordrecht, pp. 183–195. https://doi.org/10.1007/978-94-017-8777-2_11
- Sviridov, A.V., Shushkova, T.V., Zelenkova, N.F., Vinokurova, N.G., Morgunov, I.G., Ermakova, I.T., Leontievsky, A.A., 2012. Distribution of glyphosate and methylphosphonate catabolism systems in soil bacteria *Ochrobactrum anthropi* and *Achromobacter* sp. *Appl. Microbiol. Biotechnol.* 93, 787–796. <https://doi.org/10.1007/s00253-011-3485-y>
- Tanyolaç, A., Beyenal, H., 1998. Prediction of substrate consumption rate, average biofilm density and active thickness for a thin spherical biofilm at pseudo-steady state. *Biochem. Eng. J.* 2, 207–216. [https://doi.org/10.1016/S1369-703X\(98\)00035-7](https://doi.org/10.1016/S1369-703X(98)00035-7)
- Tarazona, J.V., Court-Marques, D., Tiramani, M., Reich, H., Pfeil, R., Istace, F., Crivellente, F., 2017. Glyphosate toxicity and carcinogenicity: a review of the scientific basis of the European Union assessment and its differences with IARC. *Arch. Toxicol.* 91, 2723–2743. <https://doi.org/10.1007/s00204-017-1962-5>
- Tazdaït, D., Salah, R., Grib, H., Abdi, N., Mameri, N., 2018. Kinetic study on biodegradation of glyphosate with unacclimated activated sludge. *Int. J. Environ. Health Res.* 28, 448–459. <https://doi.org/10.1080/09603123.2018.1487043>
- Tran, N., Drogui, P., Doan, T.L., Le, T.S., Nguyen, H.C., 2017. Electrochemical degradation and mineralization of glyphosate herbicide. *Environ. Technol.* 38, 2939–2948. <https://doi.org/10.1080/09593330.2017.1284268>
- Tsui, M.T.K., Chu, L.M., 2003. Aquatic toxicity of glyphosate-based formulations: comparison between different organisms and the effects of environmental factors. *Chemosphere* 52, 1189–1197. [https://doi.org/10.1016/S0045-6535\(03\)00306-0](https://doi.org/10.1016/S0045-6535(03)00306-0)
- Vajargah, M.F., Yalsuyi, A.M., Sattari, M., Hedayati, A., 2018. Acute toxicity effect of glyphosate on survival rate of common carp, *Cyprinus carpio*. *Environ. Health Eng. Manag. J.* 5, 61–66.
- Van Bruggen, A.H.C., He, M.M., Shin, K., Mai, V., Jeong, K.C., Finckh, M.R., Morris, J.G., 2018. Environmental and health effects of the herbicide glyphosate. *Sci. Total Environ.* 616–617, 255–268. <https://doi.org/10.1016/j.scitotenv.2017.10.309>

- Veiga, F., Zapata, J.M., Fernandez Marcos, M.L., Alvarez, E., 2001. Dynamics of glyphosate and aminomethylphosphonic acid in a forest soil in Galicia, north-west Spain. *Sci. Total Environ.* 271, 135–144. [https://doi.org/10.1016/S0048-9697\(00\)00839-1](https://doi.org/10.1016/S0048-9697(00)00839-1)
- Vendrell, E., Gómez de Barreda Ferraz, D., Sabater, C., Carrasco, J.M., 2009. Effect of Glyphosate on Growth of Four Freshwater Species of Phytoplankton: A Microplate Bioassay. *Bull. Environ. Contam. Toxicol.* 82, 538–542. <https://doi.org/10.1007/s00128-009-9674-z>
- Vera, M.S., Lagomarsino, L., Sylvester, M., Pérez, G.L., Rodríguez, P., Mugni, H., Sinistro, R., Ferraro, M., Bonetto, C., Zagarese, H., Pizarro, H., 2010. New evidences of Roundup® (glyphosate formulation) impact on the periphyton community and the water quality of freshwater ecosystems. *Ecotoxicology* 19, 710–721. <https://doi.org/10.1007/s10646-009-0446-7>
- Vereecken, H., 2005. Mobility and leaching of glyphosate: a review. *Pest Manag. Sci.* 61, 1139–1151. <https://doi.org/10.1002/ps.1122>
- Vidal, E., Negro, A., Cassano, A., Zalazar, C., 2015. Simplified reaction kinetics, models and experiments for glyphosate degradation in water by the UV/H₂O₂ process. *Photochem. Photobiol. Sci.* 14, 366–377. <https://doi.org/10.1039/C4PP00248B>
- Villa, M.V., Sánchez-Martín, M.J., Sánchez-Camazano, M., 1999. Hydrotalcites and organo-hydrotalcites as sorbents for removing pesticides from water. *J. Environ. Sci. Health Part B* 34, 509–525. <https://doi.org/10.1080/03601239909373211>
- Villamar-Ayala, C.A., Carrera-Cevallos, J.V., Vasquez-Medrano, R., Espinoza-Montero, P.J., 2019. Fate, ecotoxicological characteristics, and treatment processes applied to water polluted with glyphosate: A critical review. *Crit. Rev. Environ. Sci. Technol.* 49, 1476–1514. <https://doi.org/10.1080/10643389.2019.1579627>
- Villeneuve, A., Larroude, S., Humbert, J.F., 2011. Herbicide Contamination of Freshwater Ecosystems: Impact on Microbial Communities. *Pestic. - Formul. Eff. Fate* 285–312. <https://doi.org/10.5772/13515>
- Wackett, L.P., Shames, S.L., Venditti, C.P., Walsh, C.T., 1987. Bacterial carbon-phosphorus lyase: products, rates, and regulation of phosphonic and phosphinic acid metabolism. *J. Bacteriol.* 169, 710–717.
- Waiman, C.V., Avena, M.J., Garrido, M., Fernández Band, B., Zanini, G.P., 2012. A simple and rapid spectrophotometric method to quantify the herbicide glyphosate in aqueous media. Application to adsorption isotherms on soils and goethite. *Geoderma* 170, 154–158. <https://doi.org/10.1016/j.geoderma.2011.11.027>
- Wang, S., Seiwert, B., Kästner, M., Miltner, A., Schäffer, A., Reemtsma, T., Yang, Q., Nowak, K.M., 2016. (Bio)degradation of glyphosate in water-sediment microcosms – A stable isotope co-labeling approach. *Water Res.* 99, 91–100. <https://doi.org/10.1016/j.watres.2016.04.041>
- Wigfield, Y.Y., Lanouette, M., 1990. Simplified liquid chromatographic determination of glyphosate and metabolite residues in environmental water using post-column fluorogenic labelling. *Anal. Chim. Acta* 233, 311–314. [https://doi.org/10.1016/S0003-2670\(00\)83495-9](https://doi.org/10.1016/S0003-2670(00)83495-9)
- Wu, X.H., Fu, G.M., Wan, Y., Guo, D., Chen, Y.H., Luo, Y.F., Wu, X.F., 2010. Isolation and identification of glyphosate-degraded strain *Aspergillus oryzae* sp. A-F02 and its degradation characteristics. *Plant Dis. Pests* 1, 54–57.
- Xie, M., Liu, Z., Xu, Y., 2010. Removal of glyphosate in neutralization liquor from the glycine-dimethylphosphite process by nanofiltration. *J. Hazard. Mater.* 181, 975–980. <https://doi.org/10.1016/j.jhazmat.2010.05.109>
- Xing, B., Chen, H., Zhang, X., 2018. Efficient degradation of organic phosphorus in glyphosate wastewater by catalytic wet oxidation using modified activated carbon as a catalyst. *Environ. Technol.* 39, 749–758. <https://doi.org/10.1080/09593330.2017.1310935>
- Xing, B., Chen, H., Zhang, X., 2017. Removal of organic phosphorus and formaldehyde in glyphosate wastewater by CWO and the lime-catalyzed formose reaction. *Water Sci. Technol.* 75, 1390–1398. <https://doi.org/10.2166/wst.2017.006>
- Xue, W., Zhang, G., Xu, X., Yang, X., Liu, C., Xu, Y., 2011. Preparation of titania nanotubes doped with cerium and their photocatalytic activity for glyphosate. *Chem. Eng. J.* 167, 397–402. <https://doi.org/10.1016/j.cej.2011.01.007>
- Yang, Y., Deng, Q., Yan, W., Jing, C., Zhang, Y., 2018. Comparative study of glyphosate removal on goethite and magnetite: Adsorption and photo-degradation. *Chem. Eng. J.* 352, 581–589. <https://doi.org/10.1016/j.cej.2018.07.058>
- Yu, X.M., Yu, T., Yin, G.H., Dong, Q.L., An, M., Wang, H.R., Ai, C.X., 2015. Glyphosate biodegradation and potential soil bioremediation by *Bacillus subtilis* strain Bs-15. *Genet. Mol. Res.* 14, 14717–14730. <https://doi.org/10.4238/2015.November.18.37>

- Zhan, H., Feng, Y., Fan, X., Chen, S., 2018. Recent advances in glyphosate biodegradation. *Appl. Microbiol. Biotechnol.* 102, 5033–5043. <https://doi.org/10.1007/s00253-018-9035-0>
- Zhang, M.D., Wei, Y.F., Zhao, K., Mei, R.W., Huang, M., 2011. Glyphosate Degradation with Industrial Wastewater Effluent by Combined Adsorption Treatment and Advanced Oxidation Processes. *Adv. Mater. Res.* 233–235, 369–372. <https://doi.org/10.4028/www.scientific.net/AMR.233-235.369>
- Zhang, M.H., Dong, H., Zhao, L., Wang, D.X., Meng, D., 2019. A review on Fenton process for organic wastewater treatment based on optimization perspective. *Sci. Total Environ.* 670, 110–121. <https://doi.org/10.1016/j.scitotenv.2019.03.180>
- Zhang, Yaoyao, Zhang, Yi, Qu, Q., Wang, G., Wang, C., 2013. Determination of glyphosate and aminomethylphosphonic acid in soybean samples by high performance liquid chromatography using a novel fluorescent labeling reagent. *Anal. Methods* 5, 6465. <https://doi.org/10.1039/c3ay41166d>
- Zhao, H., Tao, K., Zhu, J., Liu, S., Gao, H., Zhou, X., 2015. Bioremediation potential of glyphosate-degrading *Pseudomonas* spp. strains isolated from contaminated soil. *J. Gen. Appl. Microbiol.* 61, 165–170. <https://doi.org/10.2323/jgam.61.165>
- Zhou, C.R., Li, G.P., Jiang, D.G., 2014. Study on behavior of alkalescent fiber FFA-1 adsorbing glyphosate from production wastewater of glyphosate. *Fluid Phase Equilibria* 362, 69–73. <https://doi.org/10.1016/j.fluid.2013.09.002>
- Zhou, J., Li, J., An, R., Yuan, H., Yu, F., 2012. Study on a New Synthesis Approach of Glyphosate. *J. Agric. Food Chem.* 60, 6279–6285. <https://doi.org/10.1021/jf301025p>

Traitement d'effluents complexes et de polluants émergents par couplage d'un procédé d'OVH et d'un procédé biologique

RESUME

Le couplage d'une oxydation en voie humide (OVH) et d'un traitement biologique a été étudié pour traiter les eaux usées (industrielles) contenant du glyphosate, un herbicide largement utilisé dans le monde. Afin d'évaluer les performances du procédé couplé, les performances de l'OVH seule puis du procédé biologique de traitement des eaux usées contenant du glyphosate ont été examinées. Tout d'abord, des expériences ont été menées pour évaluer l'hydrodynamique des bulles dans une colonne à bulles dans les conditions de l'OVH, afin de prédire le transfert de masse et de faciliter l'extrapolation du procédé. Deuxièmement, une étude cinétique a été réalisée pour déterminer les paramètres cinétiques de l'oxydation du glyphosate par le procédé OVH et une voie d'oxydation possible a été proposée. De plus, un dispositif microfluidique a été utilisé dans le procédé OVH pour traiter en continu les eaux usées contenant du glyphosate dans un système compact et efficace. En outre, afin d'améliorer la biodégradation du glyphosate par les boues activées, un processus d'acclimatation a été étudié et la cinétique de biodégradation du glyphosate par des boues activées acclimatées a été étudiée, ainsi que son éventuelle voie de biodégradation. Enfin, les effluents préoxydés ont ensuite été traités par les boues activées acclimatées afin de conclure à la faisabilité du procédé couplé.

Mot clefs

Polluants émergents, glyphosate, oxydation en voie humide, traitement biologique, voie de dégradation.

Treatment of complex effluents and emerging contaminants by a compact process coupling wet air oxidation with biological process

ABSTRACT

Coupling wet air oxidation (WAO) and biological treatment has been studied to treat (industrial) wastewater containing glyphosate, a most widely used herbicide in the world. In order to evaluate the performance of the combined process, the performance of the individual WAO process and biological process to treat glyphosate-containing wastewater have been investigated. First of all, some experiments have been conducted to evaluate bubble hydrodynamic in a bubble column under WAO conditions in order to predict mass transfer and scale-up WAO process. Secondly, a kinetic study has been done to determine the kinetic parameters of glyphosate oxidation by WAO process and a possible oxidation pathway has been proposed. As well, a microfluidic device was used for WAO process to continuously treat glyphosate-containing wastewater in a compact and efficient process. Furthermore, in order to improve the glyphosate biodegradation by activated sludge, an acclimation process has been studied and glyphosate biodegradation kinetics by acclimated activated sludge have been investigated, as well as its possible biodegradation pathway. Finally, the pre-oxidized effluent was further treated by the acclimated activated sludge in order to conclude on the feasibility of the coupled process.

Keywords

Emerging contaminants, glyphosate, wet air oxidation, biological treatment, degradation pathway.